TETRAMERIC PHOTOSYSTEM I: FROM INITIAL DISCOVERY AND CHARACTERIZATION IN CHROOCOCCIDIOPSIS SP. TS-821 TO EXPLORATION OF ITS DISTRIBUTION AND UNDERSTANDING OF ITS SIGNIFICANCE IN CYANOBACTERIA

A Dissertation Presented for the
Doctor of Philosophy
Degree
The University of Tennessee, Knoxville

Meng Li
December 2016

Copyright © 2016 by Meng Li
All rights reserved.

This dissertation is dedicated to
my parents
and
my wife
who provide endless support

ACKNOWLEDGEMENTS

I would like to thank all the friends I would like to thank. Some of the names may not be mentioned here but the appreciations are in my heart.

This journey would not be possible without Dr. Barry D. Bruce, who encouraged me to come to University of Tennessee and join his lab. I appreciate his great enthusiasm in photosynthesis research, both basic mechanisms and bioenergy studies. He is probably the most energetic man in his age I have ever met. His great enthusiasm brought me the cyanobacterium strain *Chroococcidiopsis* sp. TS-821, which is my favorite organism and the main species I studied as a graduate student. I also appreciate his generosity in training his students. Thanks to his hard work, I was able to attend numerous scientific meetings to get exposure in research communities to communicate with fellow scientists and most importantly to learn. At the same, the great collaborations Dr. Bruce brought to my research topic also helped. I am grateful to Dr. Bruce for his guidance as my mentor. I would like to thank my doctoral committee members, Dr. Brad M. Binder, Dr. Jerome Baudry, Dr. Engin H. Serpersu, and Dr. Paul D. Frymier for their time and support.

I would like to thank all the collaborators for their insights and efforts on this project. Particularly, Dr. Dmitry A. Semchonok, Dr. Gert T. Oostergetel, and Dr. Egbert J. Boekema at University of Groningen did most of the EM studies on the PSI tetramer; Dr. Alexandra Calteau at CEA / Institut de Génomique / Genoscope did the phylogenomic analysis cyanobacteria; Natalie Sasson and Dr. Muriel Gugger at Collection of Cyanobacteria, Institut Pasteur selected and

provided most materials of PCC strains involved in this study; Dr. Julian Whitelegge at University of California, Los Angeles did comparative proteomic analysis between the PSI trimer and PSI tetramer; Jesse Coe, Dr. Michael Vaughn, Dr. Liqing Chen and Dr. Petra Fromme at Arizona State University provided the protein crystallization facility and participated in the PSI tetramer initial crystallization screening.

I also would like to thank researchers who helped this study: Dr. John Dunlap for assistance with the initial PSI tetramer STEM imaging, Dr. Carlee McClintock for assistance with LC-MS/MS, Dr. Edward Wright for assistance with AUC, and Professor Yuwadee Peerapornpisal from Cheng Mai University for the generous gift of TS-821, Dr. Brad M Binder for providing some PCC strains for this study, Xiaofei Bai for assisting in PsaL antigen purification, Wilfredo F. Evangelista and Dr. Jerome Baudry for providing a powerful computer, Sisi Xiong for her assistance with code running and debugging.

I am grateful to the fun and helpful Bruce lab members. I would like to thank Dr. Prakitchai Chotewutmontri, Dr. Richard F. Simmerman, Dr. Kristen Holbrook, and Dr. Khoa Nguyen for providing helpful discussions and instructions with experiments. I am grateful to the lab technicians, Jenna Moe, Joshua R. Carter (Ridge), and Thomas A. Witt (Austin) who helped organizing the lab and made the lab enjoyable. I also appreciate the help from undergraduate students, Brian Moran, Stephen Richardson (Taylor), Melissa Lamicq, Genevieve Jeter and Jonathan T. Nguyen who worked with me. I thank Jonathan Nguyen and Jyotirmoy Mondal for reading my dissertation and providing helpful critiques.

ABSTRACT

Photosystem I (PSI) forms trimeric complexes in most characterized cyanobacteria. We had reported the tetrameric form of PSI in the unicellular cyanobacterium, *Chroococcidiopsis* sp. TS-821 (TS-821). Using Cryo-EM, a 3D model of the PSI tetramer structure at 11.5 [Angstrom] resolution was obtained and a 2D map within the membrane plane of at 6.1 [Angstrom]. In contrast to the three-fold symmetry in trimeric PSI crystal structure from *T. elongatus*, two different inter-monomer interactions involving PsaLs are found in the PSI tetramer. Phylogenetic analysis based on PsaL protein sequences shows that TS-821 is closely related to heterocyst-forming cyanobacteria. Additionally, this tetrameric form of PSI was closely correlated with a different genomic organization of the *psa* genes. Our results show that most heterocyst-forming cyanobacteria and close relatives have tetrameric or dimeric PSI, as distinguished from other cyanobacteria possessing mainly trimeric PSI. These cyanobacteria showed differential stability to detergent solubilization and ability to form tetrameric PSI. To investigate physiological influences on the formation of a tetrameric PSI, different environmental factors have been investigated. Our data show that nitrogen source, temperature, and salinity have little effect on the presence of tetrameric PSI. However, we observe that high light intensity tends to promote formation of the tetrameric PSI in at least three different cyanobacteria (TS-821, PCC 7414, and PCC 7428). Conversely, growth under low light promotes an increase in the trimer for strains that contain both oligomeric forms. In addition, preliminary spectral analysis indicates that the high light induced tetramer contains additional carotenoids. The evolutionary and physiological implications of multiple oligomeric forms of PSI will be discussed as well.

TABLE OF CONTENTS

CHAPTER ONE LITERATURE REVIEW 1
1.1 General Information about Photosynthesis and Light Reaction 2
1.2 General Function of Photosystem I 2
1.3 Cyanobacterial PSI Trimers 3
Observation/Occurrence 3
Crystal Structure and PSI Trimer Interface 4
Monomerization of Trimers 6
1.4 Plant PSI Monomer 7
1.5 Discovery of Tetrameric PSI in Cyanobacteria 8
Discovery in Cyanobacteria and Occurrence 8
Structure of PsaL 8
PSI Tetramer Stability and Physiology 9
1.6 Dynamics of Cyanobacterial PSI Complex 10
Overview 10
Effect of Light Intensity and Quality 10
Other Factors 11
1.7 Speculation on PSI Evolution 12
1.8 Summary and Research Background 15

CHAPTER TWO Materials and Methods 18
2.1 Growth of Cyanobacteria and Harvesting 19
Cyanobacteria Culture Media 19
General Maintenance of Cyanobacteria Liquid Culture 19
Special Culture Conditions 20
Purification of Cyanobacterial Culture 22
Harvesting of Cyanobacterial Cells 23
Cryopreservation for Cyanobacteria 25
2.2 Thylakoid Membrane Isolation 26
Cell Lysis 26
Thylakoid Membrane Pelleting and Resuspension 27
Chlorophyll Concentration Measurement 27
2.3 Biochemical Analyses of Photosynthetic Proteins 29
Blue Native PAGE 29
SDS-PAGE 30
Western Blot 31
2.4 Photosystem I Isolation and Characterization 32
Sucrose Density Gradient Isolation of PSI Oligomers 32
Characterization of TS-821 PSI 33
2.5 Structure Study of Tetrameric PSI 36
Electron Microscopy of Isolated PSI Oligomers and TS-821 Thylakoids 36
TS-821 PSI Tetramer Crystallization for Structure Determination 37
2.6 Antigen Design and Antibody Production 38
Antigen Design 38
Cloning and expression 39
Antigen Purification 41
Antibody production 42
2.7 *psaL* Gene Cloning and TS-821 Genome Sequencing 42
Genomic DNA Extraction 42

psaL Gene Cloning 43
Genome Sequencing of TS-821 46
2.8 Phylogenetic Analysis 46
Phylogenetic Analysis of PsaL 46
Phylogenomic Analysis of Sequenced Genomes 49
2.9 Genetic Engineering of *Synechocystis* sp. PCC 6803 49
Initial Attempt for *psaL* Substitution 49
Construction of *psaL* Mutants Using Codon Optimized DNA 51
Expressing PsaH/PsaL Using Broad-host Plasmid in *Synechocystis* 51
CHAPTER THREE Characterization of PSI Tetramer in *Chroococcidiopsis* sp. TS-821 55
3.1 Disclosure 56
3.2 Abstract 56
3.3 Introduction 57
3.4 Results 60
Native Organization of TS-821 Photosystems 60
TEM of Isolated PSI Particles 64
Single Particle Analysis of TS-821 PSI 66
TEM of Native Membranes Reveal PSI Tetramers 68
Characterization of Tetrameric PSI 68
Cloning of *psaL* Gene 77
Phylogenetic Analysis 81
3.5 Conclusions and Discussion 83
Tetrameric PSI Exists in *Chroococcidiopsis* sp. TS-821 83
Unique PsaL in TS-821 May be Responsible for the Formation of PSI Tetramer 86
Heterocyst-forming Cyanobacteria and Their Close Relatives May All Have Tetrameric PSI 88
Tetrameric PSI May be an Evolutionarily Advanced Form of PSI Oligomer 89
Tetrameric PSI Provides New Angle to Speculate Plastid Origin 93
CHAPTER FOUR Structure of Tetrameric PSI and PsaL 95
4.1 Disclosure 96
4.2 Abstract 96
4.3 Introduction 96
4.4 Cryo-EM Study of TS-821 PSI Tetramer 97
4.5 TS-821 PSI Tetramer Crystallization 106
Detergent screening 106
Crystallization 109
4.6 Comparison of PSI Oligomeric States in *Synechocystis* Expressing Different PsaL 111
The *psaL* Knockout Mutant Δ*psaL* 111
Expressing TS-821 PsaL in *Synechocystis* 115
Expressing *Arabidopsis* PsaL in *Synechocystis* 115
4.7 Discussion 122
CHAPTER FIVE Correlation of *psaL* Gene and Distribution of Tetrameric PSI Among Cyanobacteria 125
5.1 Disclosure 126
5.2 Abstract 126
5.3 Introduction 127
5.4 PSI Tetramer Distribution Among Cyanobacteria 128

Initial Hypothesis Test on PSI tetramer Distribution Among Heterocyst-forming Cyanobacteria 128
Investigation of PSI Tetramer Distribution in Cyanobacteria and Glaucophytes UTEX Strains. 138
Finding the Boundary of PSI Tetramer Distribution Among Cyanobacteria PCC Strains 177
5.5 Correlation of *psaL* genes and PSI Oligomeric States 214
Most Heterocyst-forming Cyanobacteria and Their Close Relatives Have Non-trimeric PSI as Their Major PSI Oligomer 214
The *psaL* Gene Genomic Location and PSI Oligomeric State 217
PsaL Structure and PSI Tetramer 220

CHAPTER SIX Physiological and Evolutionary Significance of PSI Tetramer: Tetrameric PSI May be a Primitive Adaptation to High Light Intensity 225
6.1 Disclosure 226
6.2 Abstract 226
6.3 The Effect of Nitrogen Source on PSI Tetramer 227
6.4 The Effect of Salinity on PSI Oligomeric States 230
6.5 The Effect of Temperature on Cyanobacterial PSI Oligomeric States 233
6.6 The Effect of Light Intensity on Cyanobacterial PSI Oligomeric States 237
More PSI Tetramer is Observed in TS-821 Under High Light 237
High Light Also Promotes PSI Tetramer Formation in PCC 7428 and 7414 242
Fine Tuning of PSI Oligomer Profile in TS-821 in Response Under Different Light Intensities 245
PSI Tetramer under High Light and Carotenoids between PSI Dimers 248
6.7 Speculation on PSI Oligomer Evolution and Plastid Origin from Cyanobacteria 254
Tetrameric PSI May be a Primitive Adaptation to High Light Intensity 254
PSI Monomerization in Plants and Green Algae May be a Result of PsaL Evolution Without Involving PsaH 254
Specific PsaL May Be Needed for the Introduction of PsaH 256

CHAPTER SEVEN Genome of *Chroococcidiopsis* sp. TS-821 and Proteomic Analyses of PSI Tetramer Versus PSI Trimer 257
7.1 Disclosure 258
7.2 Abstract 258
7.3 Genome Genome Assembly and Annotation 258
7.4 PsaL in PSI Tetramer and Trimer Are the Same 259
7.5 Discussion 261

CHAPTER EIGHT Conclusions and Future Directions 262
8.1 Conclusions 263
Tetrameric PSI Exists in TS-821 263
PsaL Diversity is a Key Reason for the Diversity of PSI Oligomers. 264
PSI in Most (If Not All) Heterocyst-forming Cyanobacteria and Their Close Relatives Form Tetramer or Dimer 265
PSI Tetramer, Compared with PSI Trimer, Is More Adapted to High Light 266
PSI Evolved from Trimeric to Tetrameric Oligomer *en route* to Monomeric in Plants and Green Algae 266
8.2 Future Directions 269

References **273**
Vita **283**

LIST OF TABLES

Table 2- 1 Culture conditions for Non-PCC source strains *21*
Table 2- 2 PCR primers and conditions for different psaL cloning *47*
Table 2- 3 Primer sequences used for psaL cloning *48*
Table 2- 4 Primers used for constructs in pSL1211 and pSLS vectors *54*

Table 5- 1 PSI oligomeric state in cyanobacteria studied *215*

Table 7- 1 Statistics of TS-821 genome de novo assembly *259*

LIST OF FIGURES

Figure 1- 1 Potential energy of interactions between PSI monomers in the PSI trimer 5

Figure 2- 1 Strain purity test examples. 24
Figure 2- 2 BN-PAGE of LB 1829 thylakoid membrane isolated from different centrifugal forces. 28
Figure 2- 3 $MgCl_2$ facilitates the disruption of trimeric PSI by OTG 34
Figure 2- 4 PsaL antigen design and epitope prediction 40
Figure 2- 5 Primer design for partial TS-821 psaL gene cloning 44
Figure 2- 6 Cloning and genomic organization of psaL genes 45
Figure 2- 7 Genetic complementation of Synechocystis psaL using TS-821 psaL. 50
Figure 2- 8 Schematic views of pSL1211-psaH and pSLS-psaH vectors 53

Figure 3- 1 Thylakoid membrane solubilization and photosystem identification 61
Figure 3- 2 Molecular weight estimation of TS-821 PSI using BN-PAGE. 63
Figure 3- 3 Isolation of TS-821 PSI tetramer and proof of tetramer presence 65
Figure 3- 4 SDS-PAGE of TS-821 PSI and T. elongatus PSI. 66
Figure 3- 5 Final two-dimensional maps of TS-821 PSI after single particle averaging with classification. 67
Figure 3- 6 Visualization of tetrameric PSI complexes in TS-821 thylakoid membrane 69
Figure 3- 7 Purified PSI Tetramer Dissociation upon Detergent Treatment. 70
Figure 3- 8 Properties of TS-821 PSI tetramer 72
Figure 3- 9 CD spectra of TS-821 PSI tetramer at different temperatures 76
Figure 3- 10 Alignment of selected PsaL sequences and phylogenetic tree based on PsaL protein sequences 79
Figure 3- 11 LC-MS/MS identification of subunits in TS-821 PSI tetramer 82
Figure 3- 12 PsaL alignment for phylogenetic analysis 87
Figure 3- 13 Photosystem I evolutionary model 92

Figure 4- 1 2D class averages of PSI tetramer projections from TS-821 99
Figure 4- 2 The 11.5 Å structure of TS-821 tetrameric PSI from TS-821 with each of the 4 monomers in a different color 100
Figure 4- 3 3D model of the TS-821 tetramer with the atomic structure of PSI from T. elongatus fitted in. 101
Figure 4- 4 Comparison of TS-821 inter-monomer spaces 103
Figure 4- 5 Comparison of trimeric interface of T. elongatus with interface type 1 of TS-821 105
Figure 4- 6 BN-PAGE of TS-821 thylakoid membrane solubilized in different detergents. 107
Figure 4- 7 BN-PAGE of TS-821 thylakoid membrane solubilized in different aliphatic maltosides 108
Figure 4- 8 TS-821 PSI tetramer crystallization 110
Figure 4- 9 BN-PAGE of solubilized thylakoid membranes from ΔpsaL mutant and CHpsaL mutant 112
Figure 4- 10 SDS-PAGE of ΔpsaL cell lysate and thylakoid membrane 113
Figure 4- 11 BN-PAGE of solubilized thylakoid membranes from Synechocystis expressing codon-optimized TS-821 psaL (SCHLLK). 116
Figure 4- 12 Western blot of SCHLLK-12 PSI from BN-PAGE gel 117
Figure 4- 13 BN-PAGE and SDS-PAGE analysis of PSI oligomers in SAtLLK 118
Figure 4- 14 Analysis of PSI oligomer in SSAtLLK-14 120

Figure 5- 1 BN-PAGE analysis of solubilized thylakoid from Nodularia spumigena PCC 73104 and Anabaena cylindrica PCC 7122 129
Figure 5- 2 SDS-PAGE of photosystems from PCC 73104 and PCC 7122 for PSI identification 130
Figure 5- 3 BN-PAGE of solubilized thylakoid membrane from PCC 7414 and PCC 7120 133
Figure 5- 4 SDS-PAGE of photosystems from PCC 7414 and PCC 7120 for PSI identification. 136
Figure 5- 5 SDS-PAGE of photosystems from LB 1829 for PSI identification..... 139
Figure 5- 6 BN-PAGE of solubilized thylakoid membrane from B 2349 and B 2660..... 141
Figure 5- 7 SDS-PAGE of photosystems from B 2349 and B 2660 for PSI identification 142
Figure 5- 8 BN-PAGE of solubilized thylakoid membranes and SDS-PAGE of photosystems from B 481 and LB 1920 for PSI identification..... 145
Figure 5- 9 BN-PAGE of solubilized thylakoid membranes and SDS-PAGE of photosystems from UTEX 1444 and LB 2558 for PSI identification 147
Figure 5- 10 BN-PAGE of solubilized thylakoid membrane from LB 1952, B 2965, and B 424 .. 149
Figure 5- 11 SDS-PAGE of photosystems from LB 1952, B 424, and B 2965 for PSI identification 151
Figure 5- 12 BN-PAGE of solubilized thylakoid membranes and SDS-PAGE of photosystems from B 2093 and B2963 for PSI identification 154
Figure 5- 13 BN-PAGE of solubilized thylakoid membranes and SDS-PAGE of photosystems from UTEX 1903 and LB 555 for PSI identification 157
Figure 5- 14 BN-PAGE of solubilized thylakoid membrane from LB 2766, B 379, B 381 and B 2014 160
Figure 5- 15 Characterization of Cyanophora PSI/II using sucrose density gradient ultracentrifugation, 77K fluorescence and PAGE analyses..... 162
Figure 5- 16 Confirming the monomeric PSI in B 379, B 381 and B 2014 by sucrose density gradient ultracentrifugation and SDS-PAGE. 165
Figure 5- 17 BN-PAGE and SDS-PAGE for B 482 and B 1830 PSI oligomer identification..... 167
Figure 5- 18 PAGE analysis of PSI oligomeric state in WH 7803 and LB 1556..... 170
Figure 5- 19 PAGE analysis of PSI oligomeric state in LB 1926, B SP48 in ASNIII, and WH 7803. 173
Figure 5- 20 PAGE analysis of PSI oligomeric state in SP25 and B SP48. 175
Figure 5- 21 PAGE analysis of PSI oligomeric state in LB 1598..... 178
Figure 5- 22 BN-PAGE of solubilized thylakoid membranes and SDS-PAGE of photosystems from PCC 7203 and PCC 6712 for PSI identification 180
Figure 5- 23 Structure analysis of PCC 6712 potential hexamer 182
Figure 5- 24 BN-PAGE of solubilized thylakoid membranes and SDS-PAGE of photosystems from PCC 6912 and PCC 7428 for PSI identification 184
Figure 5- 25 Detailed PAGE analysis of PSI complexes in PCC 6912 186
Figure 5- 26 BN-PAGE of solubilized thylakoid membranes and SDS-PAGE of photosystems from PCC 7509 and PCC 73102 for PSI identification 187
Figure 5- 27 PAGE analysis of PSI complexes in PCC 8926..... 190
Figure 5- 28 BN-PAGE of solubilized thylakoid membranes and SDS-PAGE of photosystems from PCC 9605 and PCC 7507 for PSI identification 193
Figure 5- 29 BN-PAGE of solubilized thylakoid membranes and SDS-PAGE of photosystems from PCC 9212 and PCC 7103 for PSI identification 195
Figure 5- 30 BN-PAGE of solubilized thylakoid membranes and SDS-PAGE of photosystems from PCC 7110, PCC 73103 and PCC 7367 for PSI identification 198
Figure 5- 31 BN-PAGE of solubilized thylakoid membranes and SDS-PAGE of photosystems from PCC 7430, PCC 7367, PCC 7107, PCC 7524, and 10914 for PSI identification..... 200
Figure 5- 32 BN-PAGE of solubilized thylakoid membranes from PCC 7107 and PCC 7524. ... 203
Figure 5- 33 BN-PAGE of solubilized thylakoid membrane from PCC 7336, PCC 9335, PCC 7502 and PCC 7704..... 204
Figure 5- 34 PAGE analysis of PSI complexes in PCC 7336, PCC 9335, PCC 7502, PCC 7704 and PCC 7104..... 205

Figure 5- 35 BN-PAGE of solubilized thylakoid membrane from PCC 7104, PCC 6406, PCC 7124 and PCC 7434 ..... *208*
Figure 5- 36 PAGE analysis of PSI complexes in PCC 6406, PCC 7124, PCC 7434, and PCC 7327 ..... *209*
Figure 5- 37 BN-PAGE of solubilized thylakoid membrane from PCC 7327, PCC 7806, PCC 10802 and PCC 6605 ..... *211*
Figure 5- 38 PAGE analysis of PSI complexes in PCC 7806, PCC 10802, and PCC 6605 ..... *213*
Figure 5- 39 PSI tetramer distribution and psaL gene location *219*
Figure 5- 40 Phylogenetic tree of PsaL *222*
Figure 5- 41 Alignment of PsaL loop insertion between second and third transmembrane helices *224*

Figure 6- 1 BN-PAGE of solubilized thylakoid membrane from PCC 7414 cultured with different nitrogen sources *228*
Figure 6- 2 BN-PAGE of solubilized thylakoid membrane from LB 1829 and PCC 7120 cultured with different nitrogen sources *229*
Figure 6- 3 BN-PAGE of solubilized thylakoid membrane from PCC 7122 and PCC 73104 cultured in different media *231*
Figure 6- 4 BN-PAGE of solubilized thylakoid membrane from B 2093 cultured in media with different salinity *232*
Figure 6- 5 BN-PAGE of solubilized thylakoid membrane from PCC 7414 cultured at different temperatures *234*
Figure 6- 6 BN-PAGE of solubilized thylakoid membrane from PCC 7203 and PCC 7428 cultured at different temperatures *235*
Figure 6- 7 BN-PAGE of solubilized thylakoid membrane from TS-821 cultured at different temperatures *236*
Figure 6- 8 Spectra analyses of TS-821 under different light intensities *238*
Figure 6- 9 Comparison of TS-821 PSI oligomeric profiles under different light intensities. *240*
Figure 6- 10 Comparison of PCC 7428 PSI oligomeric profiles under different light intensities. *243*
Figure 6- 11 Comparison of PC 7414 PSI oligomeric profiles under different light intensities. ... *244*
Figure 6- 12 Comparison of PCC 7203 PSI oligomeric profiles under different light intensities. *246*
Figure 6- 13 Comparison of SCHLLK-12 PSI oligomeric profiles under different light intensities. *247*
Figure 6- 14 Comparison of TS-821 PSI oligomeric profiles under different light intensities with same LED light source *249*
Figure 6- 15 Spectral changes of TS-821 PSI tetramer under high light *251*
Figure 6- 16 Spectral analysis of TS-821 PSI oligomers and inter-dimer carotenoids *253*
Figure 6- 17 Absorption spectra of PSI oligomers from PCC 7414 ..... *255*

CHAPTER ONE
LITERATURE REVIEW

1.1 General Information about Photosynthesis and Light Reaction

Photosynthesis is the process in photosynthetic organisms that converts light energy into chemical energy. Broadly speaking, photosynthesis includes anoxygenic and oxygenic photosynthesis (see review (*1*) for more information about the general evolution of photosynthesis). Most ongoing research on photosynthesis focus on oxygenic photosynthesis due to its direct impact on agriculture, climate change and energy. Oxygenic photosynthesis mainly is observed in cyanobacteria, algae, and plants. The process, using light energy, converts water and carbon dioxide into carbohydrates and oxygen molecules. The reaction dependent on light is called the light reaction, where ATP and reducing power, carried by ferredoxin and NADPH, are produced. To generate the reducing power, two photosystems drive the linear electron transfer from water to ferredoxin through a serial of electron carriers (*2*). While photosystem II (PSII) initiate the electron transfer by photo-oxidizing water molecules, photosystem I (PSI) catalyzes the last step of electron transfer to ferredoxin.

1.2 General Function of Photosystem I

Photosystem I, or PSI, is light dependent plastocyanin/cytochrome c: ferredoxin oxidoreductase. With light, PSI transfers an electron from its donor, plastocyanin or cytochrome c, to its acceptor, ferredoxin. In cyanobacteria, cytochrome c is commonly used as the electron donor, while plants have plastocyanin as the PSI electron donor (*3*). While linear electron transfer requires both PSI and PSII, PSI can also be involved in cyclic electron transfer independent from PSII. In this process, electron from ferredoxin is transferred

back to the PSI electron donor directly or indirectly through the cytochrome b_6f complex (*4*). This process generates proton gradient across the thylakoid membrane and eventually producing ATP by ATP synthase without producing net reducing power.

1.3 Cyanobacterial PSI Trimers

Observation/Occurrence

Cyanobacterial PSI has been reported as trimeric in most studies. The first study that directly showed the image of a PSI trimeric structure was done in *Synechococcus* (*5*). Later, the PSI trimer has also been observed in *Spirulina platensis*, showing special long wavelength Chl in the PSI trimer (*6, 7*). The trimeric PSI structure from the model cyanobacterium strain *Synechocystis* sp. PCC 6803 was confirmed by Kruip et al.(*8-10*). EM images of the PSI trimer were also obtained from *Synechococcus* sp. PCC 7002 (*11*). In the initial study of PSI from *Prochlorococcus* strains, the trimeric form was reported in MED4 and SS120 (*12*). A later study on *Prochlorococcus marinus* MIT 9313 showed that PSI trimer can also bind to additional antenna in the membrane (*13*). The PSI trimer in *Synechococcus* sp. PCC 7942 (PCC 7942) was reported in the PSI-IsiA supercomplex as well (*14*), even though earlier report had shown that PSI in PCC 7942, as well as in *Cyanothece* sp. ATCC 51142, is trimeric using non-denaturing gel electrophoresis (*15*). Interestingly, the most primitive known cyanobacterium, *Gloeobacter violaceus* PCC 7421, also has trimeric PSI (*16*). Meanwhile, crystallography studies of cyanobacterial PSI also showed trimeric PSI in cyanobacteria (*17, 18*), especially the high resolution structure of trimeric

PSI from *T. elongatus(18).* Due to the numerous studies and high consistency, cyanobacterial PSI was widely accepted as trimeric.

Until recently, the PSI tetramer was observed in cyanobacteria *Nostoc* sp. PCC 7120 (*19, 20*) and *Chroococcidiopsis* sp. TS-821 (TS-821) (*21*). Yet, due to the low number of examples, the PSI tetramer has not been viewed as a major oligomeric state in cyanobacteria.

Crystal Structure and PSI Trimer Interface

The crystal structure of the PSI trimer from *T. elongatus* revealed many details about how PSI forms a trimer (*18*). Based on the crystal structure, the calculated potential energy (Figure 1-1) due to the presence of PsaL (Photosystem I reaction center subunit XI), makes up more than two thirds of the inter-monomer interaction. Geometrically, PsaL sits in the center of the trimeric structure. These observations agree with early genetic studies on the function of PsaL in cyanobacteria, which showed that the deletion of the *psaL* gene results in the monomerization of PSI (*22-26*). PsaI also sits in the inter-monomer spaces and binds to PsaL. Potential energy calculation reveals that its interaction to neighboring PSI monomer is dependent on the presence of PsaL. This result is in line with the finding that PsaI-less PS I can form trimers but has fewer trimers. These trimers are more vulnerable to harsh detergent treatment(*25*). PsaM plays a similar role to PsaI in PSI trimer stabilization which was shown by a previous study, *psaM* knockout leading to less PSI trimer (*27*). Interestingly, nearly all inter-monomer interaction involving PsaM are mediated by the PsaM cofactor

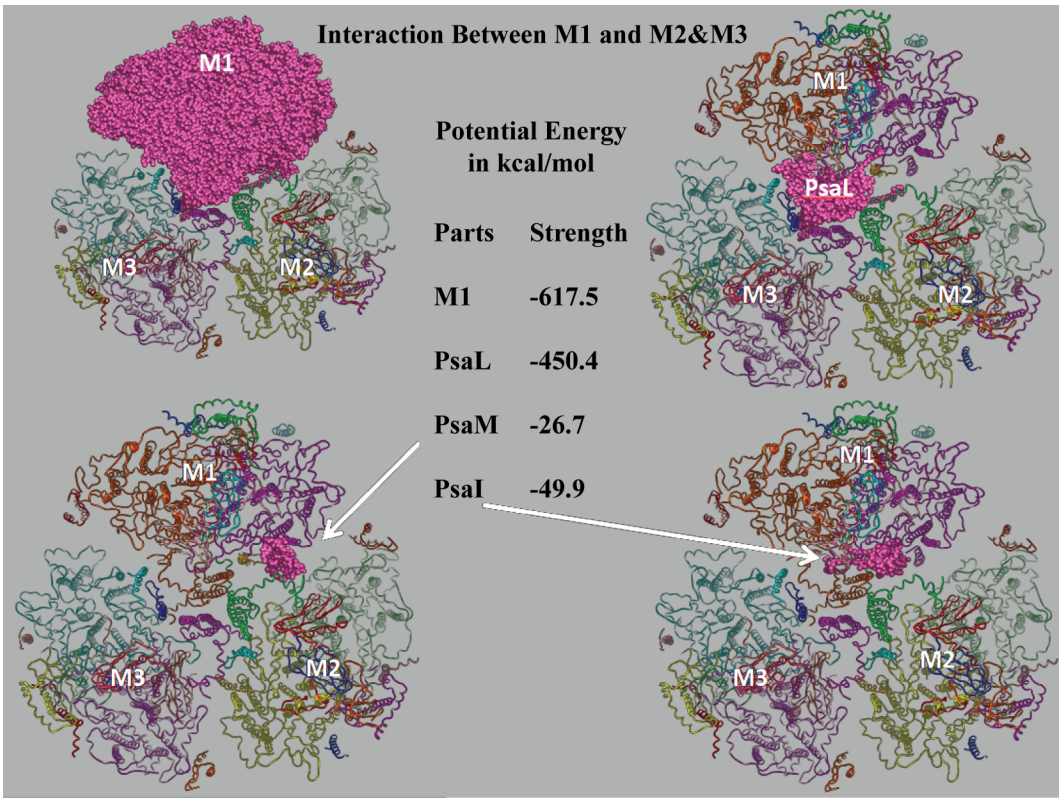

Figure 1- 1 Potential energy of interactions between PSI monomers in the PSI trimer

The total potential energy between one PSI monomer (M1) to the other two monomers (M2 and M3) was shown as M1 in the table. The contribution of M1 subunits (PsaL, PsaM, PsaI) to the M1 interaction with M2&M3 are listed as well. These subunits with their cofactors are highlighted separately in the PSI trimer structure and labeled or pointed out by arrows. Potential energy was calculated using PDB structure 1JB0 in MOE (Molecule Operating Environment) software (2010.10 version). "CHARMM27" force field was used for potential energy calculation after protonation. The protonation was operated under default settings with T=300, pH 7, etc. This work was done as a rotation project in Dr. Jerome Baudry's lab.

Monomerization of Trimers

PsaL is needed for PSI to form the trimeric structure in cyanobacteria. Multiple studies have shown that *psaL* knockout mutants only have monomeric PSI (*22-26*). Besides knocking out of *psaL,* adding a His-tag to the C-terminus of PsaL also results in the monomerization of PSI (*28*). This study indicates the importance of the C-terminus of PsaL in stabilizing the trimeric structure. In addition, the *Synechocystis pgsA* mutant with depletion of phosphatidylglycerol also has only monomeric PSI due to the inability of PsaL incorporation to PSI complex (*29*) Moreover, the *Synechocystis* knockout mutant of iron stress inducible protein, IsiA, also showed incapability of accumulating the PSI trimer (*30*). The deficiency of iron in the environment also can lead to the monomerization of PSI (*31, 32*). Besides mutagenesis, environmental stress can also lead to the monomerization of PSI in cyanobacteria. High light intensity can induce PSI monomerization, with the monomerization being mitigated by high light inducible polypeptides (HLIP) (*33*). In addition to high light induced monomerization of PSI in cyanobacteria, far-red light also induced the PSI monomer in *Leptolyngbya* sp. JSC-1, which involves a far-red light inducible *psaL* gene expression (*34*). Besides light conditions, excess sulfite stress can also induce PSI monomerization in *Synechococcus elongatus* PCC 7942 (*35*). Moreover, low temperature can also lead to more PSI monomers in the model strain *Synechocystis* sp. PCC 6803 (*36*).

1.4 Plant PSI Monomer

In contrast to the PSI trimer reported in cyanobacteria, algal PSI and plant PSI have been reported as monomeric (*19, 37-40*). The crystal structure of plant PSI monomer has been solved (*39*) and refined several times (*41-44*). One of the major significances of this structure is revealing the structural differences between cyanobacterial PSI trimer and plant PSI monomer. In the crystal structure of plant PSI, PsaH binds to PsaL, which leads to the speculation that PsaH blocks PSI trimerization in plant (*45-48*) considering the absence of PsaH in cyanobacteria. In addition to the difference in PsaH, multiple light harvesting complex I (LHCI) proteins are bound to PSI monomer in plant. Moreover, PsaG, PsaN are PSI subunits in plant PSI but not present in cyanobacterial PSI trimer. The cyanobacterial PsaM and PsaX were not found in the crystal structure of plant PSI monomer. Putatively, PsaM is present in pine trees, such as UniProt protein P41601.

Even though it seems reasonable to speculate that PSI monomerization may have involved PsaH, the structural changes of PsaL in plant PSI is noticeable. First, the C-terminus is shorter in plant PsaL, compared with that in *T. elongatus* PsaL. Second, the loop sequence between second and third transmembrane helices is longer in plant PsaL (*21*). This loop insertion later was resolved in the conformation binding PsaH N-terminus (*41*), indicating PsaL may have evolved to optimize PsaH binding. A different theory of PSI monomerization without involving PsaH was proposed based on these observations (*21*).

1.5 Discovery of Tetrameric PSI in Cyanobacteria

Discovery in Cyanobacteria and Occurrence

The first report of a cyanobacterial PSI tetramer was found in the heterocyst-forming cyanobacterium, *Nostoc* sp. PCC 7120 (or *Anabaena* sp. PCC 7120) (*19*). In addition to the PSI tetramer in cyanobacterium, the tetrameric structure was also observed in the glaucophyte *Cyanophora paradoxa* NIES 547 (*19*). In this study, PSI tetramer structure was inferred from the data obtained from BN-PAGE and sucrose density gradient centrifugation. This publication did not change the broadly accepted view of PSI trimer in cyanobacteria. Later, with further study on *Nostoc* sp. PCC 7120, the EM images of the PSI tetramer clearly presented the tetrameric structure, with new discovery of direct phycobilisome attachment to the PSI tetramer (*20*). Around the same time, tetrameric PSI from a unicellular cyanobacterium *Chroococcidiopsis* sp. TS-821 was reported as well, with more detailed biophysical characterization and evolutionary speculation (*21*). In addition to the two cyanobacteria with directly reported PSI tetramer, the PSI study in *Nostoc punctiforme* PCC 73102 (ATCC 29133) (*49*) was also later interpreted as tetrameric (*19*). Even though it has been speculated that all heterocyst-forming cyanobacteria and their close relatives have tetrameric PSI (*21*), no further evidence have been shown to test this hypothesis.

Structure of PsaL

Compared with PsaL in the PSI trimer, PsaL of known tetrameric PSI has a shorter C-terminus sequence and a longer loop insertion between second and third transmembrane helices (*21*). The C-terminus of PsaL was speculated to

stabilize the trimeric PSI, with evidence that the C-terminus His-tag PsaL does not form trimeric PSI (*28*). Later Cryo-EM structure study of the PSI tetramer from TS-821 showed that the PsaL in trimeric PSI *from T. elongatus* does not fit in the tetrameric PSI electron density map (*50*), indicating the difference of the PsaL C-terminus is one of the key factors determining PSI oligomeric states. The PsaL in plants also showed similar short C-termini (*21*) and the C-terminal structural difference has been revealed in crystal structures (*41-44*).

The loop insertion between second and third transmembrane helices in TS-821 PsaL appears to be the intermediate of that in *T. elongatus* and plant (*21*). It was speculated that this loop insertion region may bind to PsaH in plant PSI, and later refined PSI crystal structure supported this speculation (*41, 44*). This PsaH-PsaL interaction indicates important role this loop insertion played in PSI evolution.

PSI Tetramer Stability and Physiology

Cyanobacterial PSI tetramer is not as stable as the PSI trimer. When the thylakoid membrane is solubilized with excess amount of mild detergent DDM, or the isolated PSI tetramer complex is treated with additional detergent, the tetrameric PSI can dissociate easily to PSI dimers and monomers (*19, 21*). This leads to the speculation that tetrameric PSI may be able to respond fast to environmental changes potentially with a faster state transition rate (*21*). In the study of *Nostoc* sp. PCC 7120 PSI tetramer, phycobilisome was observed directly binding to PSI, indicating that the PSI tetramer can have higher optical cross section under low light compared with the PSI trimer (*20*). Meanwhile,

based on the observation that tetrameric PSI has low cooperativity in photo-excitation (*21*), it was also speculated that the PSI tetramer may be the result of adaptation to high light intensity (*50*). The high light stress experiment showed that abundance and stability of PSI tetramer increases under high light while trimeric PSI is enriched under low light (*50*). This experiment supports the theory that PSI tetramer is a primitive adaptation to high light.

1.6 Dynamics of Cyanobacterial PSI Complex

Overview

Even though the PSI trimer has been reported in most studied cyanobacteria, the quantity of PSI trimer, the components and structures of the PSI complex is neither uniform nor static. In different cyanobacteria, the observed relative amount of PSI trimer and PSI monomer are different. In the same cyanobacteria, the trimeric PSI abundance can be affected by light intensity (*33*), light quality (*34*), temperature (*36*) and other stresses (*35*). In addition to the simple PSI trimer, the PSI-IsiA complex can also form under various stresses in cyanobacteria (*13, 14, 51-53*). After discovery of PSI tetramer, the dynamics of PSI structure in response to light intensity was also observed (*50*).

Effect of Light Intensity and Quality

The PSI trimer is more abundant in cyanobacteria under low light. In the study of high light stress for *Synechocystis*, the relative amount of trimeric PSI is higher under lower light (*33*). This result indicates that trimeric PSI is more stable

under low light and more adaptive to low light. In line with this study, the *psaL* knockout mutant also showed slower growth under green light (*25*). The IsiA protein, binding the PSI trimer for photoprotection, is needed for PSI trimerization in *Synechocystis (30)*, also indicating that the PSI trimer is not well adapted to high light. In the cyanobacterium TS-821, which has both trimeric PSI and tetrameric PSI, the abundance of trimeric PSI is also higher under low light intensity (*50*). Low light promotes the formation of PSI trimer. The cooperativity among the PSI monomers in trimeric PSI (*54, 55*) may guarantee the efficiency under low light.

In addition to light intensity tuning the abundance of trimeric PSI, cyanobacterial photosynthesis under far-red light also involves PSI oligomer remodeling (*34*). Under far-red light, the only PSI oligomer observed in *Leptolyngbya* sp. JSC-1 was monomeric, which involves the expression of a *psaL* gene expressed only under far-red (*34*). Bioinformatics analysis showed that similar far-red responsive genes are also present in several heterocyst-forming cyanobacteria (*34*). This study clearly showed that PSI monomerization does not need PsaH and suggests that two copies of *psaL* gene in some heterocyst-forming cyanobacteria may be related to their ability utilizing far-red light.

Other Factors

Many cyanobacterial PSI can associate with IsiA (Iron stress-induced chlorophyll-binding protein A) protein to form supercomplexes under iron depleted conditions (*13, 14, 51, 56*). Usually this supercomplex involves a ring

structure of 18 IsiA surrounding a PSI trimer (*13, 14, 51*). When PsaL is absent, IsiA protein can still bind to PSI monomers with different ring structures (*57*). Prolonged starvation of iron for cyanobacteria can also lead to PSI monomerization and similar PSI-IsiA supercomplexes in *psaL* knockout mutant (*32*). Even though PsaL is not required for forming PSI-IsiA supercomplexes, IsiA is needed for PSI to form trimeric structure (*30*). While PsaF and PsaJ are absent, the PSI-IsiA supercomplex forms with a smaller ring structure of 17 IsiA (*58*). Other organizations of the PSI-IsiA supercomplex were also observed in WT cyanobacteria (*56*). Even though most IsiA related studies were done by depleting iron in the growth media, oxidative stress and salt stress can also induce the expression of *isiA* gene (*52, 53*). Interestingly, IsiA is also needed for *Synechocystis* to survive high light (*59*). The general role of the IsiA is probably protecting photosystems from photo-oxidative stress.

In addition to IsiA related stress, other factors also affect PSI complex structures. A recent study showed that higher temperature favors the formation of PSI trimer in *Synechocystis (36)*. Moreover, PSI monomerization was observed when *Synechococcus* was stressed with excess sulfite, which was proposed to repress reactive oxygen species (*35*).

1.7 Speculation on PSI Evolution

Modern plastids share the same cyanobacterial ancestor. Understanding how PSI evolved from cyanobacteria to plants may help identify where plastid came from among various diversified cyanobacteria. Several reviews have discussed about the PSI evolution assuming that cyanobacterial PSI is trimeric

and plant monomeric PSI evolved directly from trimeric PSI by introducing the novel PsaH subunit (*45-48*). The discovery of tetrameric PSI in cyanobacteria and glaucophyte (*19-21*) provides the foundation for rethinking about the question of PSI evolution.

Trimeric PSI is the primitive form of PSI compared with tetrameric PSI. Before the discovery of tetrameric PSI, all PSI in cyanobacteria had been reported as PSI trimers. Among all the known cyanobacterial PSI oligomers, trimeric PSI was observed in the most primitive cyanobacterium *Gloeobacter violaceus* PCC 7421 (*16*). This study supports that trimeric PSI is the primitive form of the PSI oligomers in cyanobacteria. The PSI tetramer may have evolved from trimeric PSI due to the structural changes in PsaL (*21*), even though this theory needs to be tested. First, the observation of tetrameric PSI has only been confirmed in two strains of cyanobacteria. Whether this special form of PSI is universal to heterocyst-forming cyanobacteria and their close relatives still needs to be verified. This study will present the results on testing this hypothesis on PSI tetramer distribution. Tetrameric PSI has been observed in many different cyanobacteria.

PSI monomerization does not need PsaH. As discussed in PSI trimer monomerization section, many environmental factors can affect the relative amount of PSI trimer and PSI monomer in cyanobacteria that have mainly trimeric PSI. Only monomeric PSI was observed in the cyanobacterium *Leptolyngbya* sp. JSC-1 under far-red light, with PsaL expressed (*34*). This example indicates that PSI monomerization probably is independent of PsaH. In

this manuscript, more examples of exclusive monomeric PSI without the involvement of PsaH will be given. Now, the PSI evolution question is: where did the plant PSI monomer come from, the PSI trimer or tetramer?

The PSI monomer evolved more likely from the PSI tetramer than the PSI trimer. Initial hypothesis originated the observation that PsaL sequence in tetrameric PSI looks like the intermediate structure between PsaL trimeric PSI and PsaL in plant monomeric PSI (*21*). At the same time, the observation of the PSI tetramer in glaucophyte supported making such assumption (*19*). Moreover, the *in vitro* PSI tetramer is in equilibrium with PSI dimers and monomers, further suggesting that the PSI tetramer is closer to a monomeric PSI (*21*). Along with reporting the PSI tetramer Cryo-EM structure, TS-821 was shown to have more tetrameric PSI under high light while the PSI trimer is more abundant under low light (*50*). This observation provided more insight in PSI evolution and further supports the theory that PSI monomer in plants evolved from PSI tetramer. Together with the observation that the PSI tetramer has low cooperativity compared with PSI trimer (*21, 54, 55*), one can conclude that tetrameric PSI is more adapted to high light, while PSI trimer is more suitable for low light environment. To confirm the tuning of PSI oligomer is not a special case for TS-821, more cyanobacteria were tested for this manuscript. A careful study of TS-821 responding to different light intensities also supported the initial observation and conclusion of more PSI tetramer under high light. Considering its better adaptation to high light, tetrameric PSI may have provided early endosymbionts

better competitiveness under high light. This is reasonable since most modern plants compete for the brightest sunlight.

1.8 Summary and Research Background

PSI, as one of the key protein complexes in oxygenic photosynthesis, has been well characterized for it biochemical and biophysical properties. PSI has also been used bioenergy studies such as hydrogen production (*54*) and bio-solar cells (*55*). The crystal structures of *T. elongatus* trimeric PSI (*18*) and *P sativum* monomeric PSI (*43*) seemed to make the story of PSI structure almost complete. With hope of getting a more stable PSI from TS-821, a strain isolated from a hot spring in northern Thailand, for bioenergy application, this study originally aimed to characterize the PSI from TS-821. Initial attempt of isolating the PSI from TS-821 using sucrose density gradient centrifugation as described in established protocol for *T. elongatus* (*54*) was not successful. This led to the careful analysis of thylakoid membrane solubilization and the discovery of tetrameric PSI in TS-821 (*21*). Chapter three summarizes the initial discovery and characterization of the PSI tetramer in TS-821.

After initial discovery of the tetrameric PSI in TS-821, the question about why TS-821 form PSI tetramers was asked. To understand the biochemical reason for PSI tetramer formation, structural studies using Cryo-EM were done in collaboration with Dr. Boekema's group in University of Groningen. Recently, attempt of crystallization of tetrameric PSI showed some encouraging results, done by collaborating with Dr. Fromme's group in Arizona State University. In

addition, genetics work was done, testing the role of PsaL in determining the oligomeric state of PSI. All those work are summarized in Chapter four.

In the initial publication about tetrameric PSI in TS-821, we also hypothesized that heterocyst-forming cyanobacteria and their close relatives may all have tetrameric PSI. To test this hypothesis, multiple species of heterocyst-forming cyanobacteria were cultured and tested for their PSI oligomeric states. With encouraging results showing most heterocyst-forming cyanobacteria have tetrameric PSI, a more comprehensive study was followed, done in collaboration with Dr. Gugger's group in Institut Pasteur and Dr. Calteau in CEA/Genoscope. These studies showed that tetrameric PSI can be found in most heterocyst-forming cyanobacteria as well as their close relatives. The correlation between PsaL and PSI oligomeric state was investigated as well. The results are summarized in Chapter five.

With all the information about the PSI tetramer in heterocyst-forming cyanobacteria and their close relatives, the evolutionary and physiological significance was investigated. After testing multiple environmental factors, the light intensity turned out to be affecting the stability and quantity of PSI tetramer versus PSI trimer. The initial discovery of this phenomenon was published with the PSI tetramer Cryo-EM structure paper (*50*). Later, more strains were tested to see if the tuning of PSI oligomer by light intensity is unique to TS-821. Meanwhile, a careful study of TS-821 responding to different light intensities was done to confirm that the observation of shifting PSI oligomers is due to the change in light intensities. These results of physiological studies are summarized

in Chapter six. Moreover, to understand if the tuning of PSI oligomers is related to differential expression of different PsaLs, genome of TS-821 was sequenced and comparative protein analysis between trimeric and tetrameric PSI was done in collaboration with Dr. Whitelegge in UCLA. These results are summarized in Chapter seven.

In summary, this manuscript describes our studies on tetrameric PSI in cyanobacteria. The studies include the initial discovery and characterization in TS-821, the structural study attempts for understanding biochemical base of tetrameric PSI formation, extensive investigation on tetrameric PSI distribution in cyanobacteria, as well as understanding the physiological significance of the PSI tetramer in cyanobacteria. Altogether, the knowledge gained from these studies refreshes the view of PSI structure and evolution.

CHAPTER TWO

Materials and Methods

2.1 Growth of Cyanobacteria and Harvesting

Cyanobacteria Culture Media

Most cyanobacteria grow in BG-11 media. BG-11_0 (or BG-11 -N), which contains no $NaNO_3$ compared with regular BG-11 media, is used for some heterocyst-forming cyanobacteria cultures. Marine cyanobacteria usually grow faster in modified ASN III media. It contains BG-11 medium with addition of ASNIII media major salts (25 g/L NaCl, 3.5g/L $MgSO_4$ x $7H_2O$, 2.0g/L $MgCl_2$ x $6H_2O$, 0.5 g/L KCl).

Media were autoclaved and cooled down before cell inoculation. For plate culture, 1.5% (w/v) agar was added before autoclave. Some *Synechocystis* mutant are selected and maintained on 50 μg/mL Kanamycin and/or up to 5 μg/mL gentamycin plates.

General Maintenance of Cyanobacteria Liquid Culture

Chroococcidiopsis sp. TS-821 (TS-821) and *Thermosynechococcus elongatus* BP-1 (*T. elongatus*) were maintained in two-liter glass culture bottle with aeration at 45°C, with continuous white fluorescent light as lighting source. At the same time, *Synechocystis* sp. PCC 6803 was cultured at 24 °C. The light intensity at the surface of the culture bottle, in most cases, is ~ 40 μmol/m^2/s. Cells were harvested at late log phase. The wet cell mass harvested from a two-liter bottle culture is usually 3~4 grams.

Other cyanobacteria from UTEX were maintained as recommended by the culture collection center at University of Texas, Austin. To achieve sufficient cell mass for PSI oligomer identification, all cyanobacteria have been cultured in BG-

11 media to test their viability and their preference of light intensity in the range of 20~100 μmol/m^2/s (Table 2-1). Most cyanobacteria can grow fast in BG-11 media with proper light intensity, except some strains isolated from marine environment which grow better in modified ASN III media. Other thermophilic cyanobacteria were cultured at 37 °C

Cyanobacteria from Pasteur Institute, most PCC strains, are received as harvested cell pellets; some of which are recovered on BG-11 plates and then cultured in liquid BG-11 media for PSI tetramer physiological significance studies.

Special Culture Conditions

To study the physiological significance of PSI tetramer in cyanobacteria, non-standard culture conditions were tested. To investigate the effect of nitrogen sources, cyanobacteria (see Chapter Six for strain details) are cultured separately in BG-11, BG-11_0 or BG-11 supplemented with 1 mM NH_4Cl two days before cell harvesting. To test the effect of temperature, some thermophilic cyanobacteria were cultured at 45 °C versus 37 °C. In addition, a culture of *Fischerella muscicola* PCC 7414 grown at 37 °C was incubated at 24 °C before harvesting. To investigate the effect of salinity, some marine cyanobacteria were cultured in both BG-11 and modified ASNIII media.

To investigate the physiological significance of tetrameric PSI in cyanobacteria, high light conditions were tested for several strains: TS-821, PCC 7414, PCC 7428, PCC 7203, and *Synechocystis* expressing TS-821 PsaL (SCHLLK-12). Intial test was done with TS-821 dense liquid culture (2 L) under continuous low light (LL, 40 μmol/m^2/s). The culture was split into two halves and

Table 2- 1 Culture conditions for Non-PCC source strains

Strains	Source	Media	Temperature (°C)	Light intensity (μmol/m^2/s)	Also known as
Fremyella diplosiphon B 481[a]	UTEX	BG-11	20	100	PCC 7601
Nodularia harveyana B 2093	UTEX	ASNIII	24	20	
Scytonematopsis contorta 2963	UTEX	BG-11	24	50	
Spirirestis rafaelensis B 2660	UTEX	BG-11	24	30	
Anabaena flos-aquae B 1444	UTEX	BG-11	24	20	ATCC 29413
Scytonema hofmanni B 2349	UTEX	BG-11	24	30	PCC 9009
Fischerella muscicola LB 1829	UTEX	BG-11	37	40	PCC 9339
Fischerella ambigua 1903	UTEX	BG-11	37	40	
Anabaena flos-aquae LB 2558	UTEX	BG-11	24	50	
Calothrix parietina LB 1952	UTEX	BG-11	24	50	
Gloeotrichia ghosi LB 1920	UTEX	BG-11	24	20	
Mastigocladus sp B2965	UTEX	BG-11	37	40	
Tolypothrix distorta B 424	UTEX	BG-11	24	50	
Scytonema crispum LB 1556[b]	UTEX	BG-11	24	20~50	
Fischerella sp. PCC 7414	Binder[c]	BG-11	37	40	
Nodularia sp. PCC 73104	Binder	BG-11	24	20	
Anabaena sp. PCC 7122	Binder	BG-11	24	30	
Nostoc sp. PCC 7120	Binder	BG-11	24	20	
Hapalosiphon welwitschii B 1830	UTEX	BG-11	37	40	PCC 9431
Gloeocapsa alpicola LB 1598	UTEX	BG-11	24	20~50	PCC 6308
Aphanothece sp. SP25	UTEX	BG-11	24	20~50	
Plectonema boryanum B 482	UTEX	BG-11	24	20~50	PCC 6306
Pseudanabaena sp B SP48	UTEX	ASNIII	24	20~50	
Spirulina platensis LB 1926	UTEX	ASNIII	24	20~50	
Calothrix membranacea B 379	UTEX	BG-11	24	50	
Cylindrospermum licheniforme B 2014	UTEX	BG-11	24	20	
Anabaena inaequalis B 381	UTEX	BG-11	24	20	
Cyanophora biloba LB 2766	UTEX	Bold1NV	24	30	
Cyanophora paradoxa LB 555	UTEX	Bold3N	24	50	
Synechococcus sp. WH 7803	Bruce[d]	ASNIII	24	20	

[a] B 481 was cultured in flask on orbital shaker shaking at 120 rpm with 14-hour light 10-hour dark cycle.
[b] LB 1556 was cultured up to 6 months before harvesting
[c] Strains denoted with “Binder” as source are from Binder lab as described in previous study (*60*).
[d] WH 7803 was maintained in Bruce lab

supplemented with BG-11 medium for a two-day continuous growth under different light intensities before harvesting. For low light condition, the culture was maintained in a 2 L bottle while the high light (HL, 800 μmol/m^2/s) growth was carried out in a 25 L photobioreactor (Photon Systems Instruments, Czech Republic). For other cyanobacteria tested for high light response, cultures at late log phase were split into two halves and transferred to fresh BG-11 or BG-11_0 (PCC 7414) media. Then the two halves were cultured for two days, as described for initial TS-821 experiment (*50*).

To eliminate the potential stress from cell culture density and/or difference from lighting sources, a systematic analysis of how TS-821 respond to different level of light intensity was done by culturing similar inoculum in photobioreactor for two days under 5 light conditions (50 μmol/m^2/s, 100 μmol/m^2/s, 200 μmol/m^2/s, 400 μmol/m^2/s and 800 μmol/m^2/s). For each light condition, half of the light intensity is provided by white LED light and the other half is from red LED. The 2 L mid-log phase TS-821 cell (OD680 0.6-0.8) culture under white light fluorescent light were inoculated to the 25 L bioreactor to starting OD 680 at 0.04 (measured by equipped fluorometer probe from Photon Systems Instruments, lab spectrometer reading at ~0.13) before turning on the bioreactor lights. Cells are harvested and kept in -20 °C before PSI oligomer analysis.

Purification of Cyanobacterial Culture

Most UTEX cultures studied are xenic cultures. At the same time, prolonged cultures will limit the growth of cyanobacteria and favor the growth of heterotrophic microbes. To eliminate the contaminant strains, cyanobacterial

culture cleaning was done as described by Rippka *et al*. (*61, 62*). Cyanobacterial cell cultures from plate or liquid media were transferred into BG-11 supplemented with 0.1% casamino acids (casein enzymatic hydrolysate), 0.5% glucose, 50 μg/mL cycloheximide and 1mg/mL ampicillin. The cells were incubated in normal growth conditions in the dark. After 12 hours, 24 hours and 48 hours, aliquots were taken and plated on growth media by streaking to select single colonies. The purified cultures were tested on nutrient agar as well as BG-11 supplemented with 0.05% casamino acids and 0.5% glucose in dark. Autoclaving for 50 minutes is necessary for nutrient agar plates to avoid internal contamination from media or agar.

The purification results of *Spirirestis rafaelensis* B 2660, *Chroococcidiopsis* sp. TS-821 were shown in Figure 2-1, compared with impure *Synechocystis psaL* knockout mutant (Δ*psaL*). The M3 micropore tape (Nexcare™) has been tested to prevent contamination from growth chamber air based on the fact that 2~3 week incubation of the testing plates does result in any visible microbial colonies.

Harvesting of Cyanobacterial Cells

Most cyanobacterial cultures were harvested by centrifugation at 10, 000 g for 5 min, followed by resuspension in water. The resuspension works easiest on an orbital shaker even though vortexing was used as well. The cell resuspensions were then pelleted by another centrifugation in 50 mL falcon tubes, 10,000 g for 5 min. Cell pellets were weighed with empty a falcon tube as reference. Cell pellets were stored at -20°C.

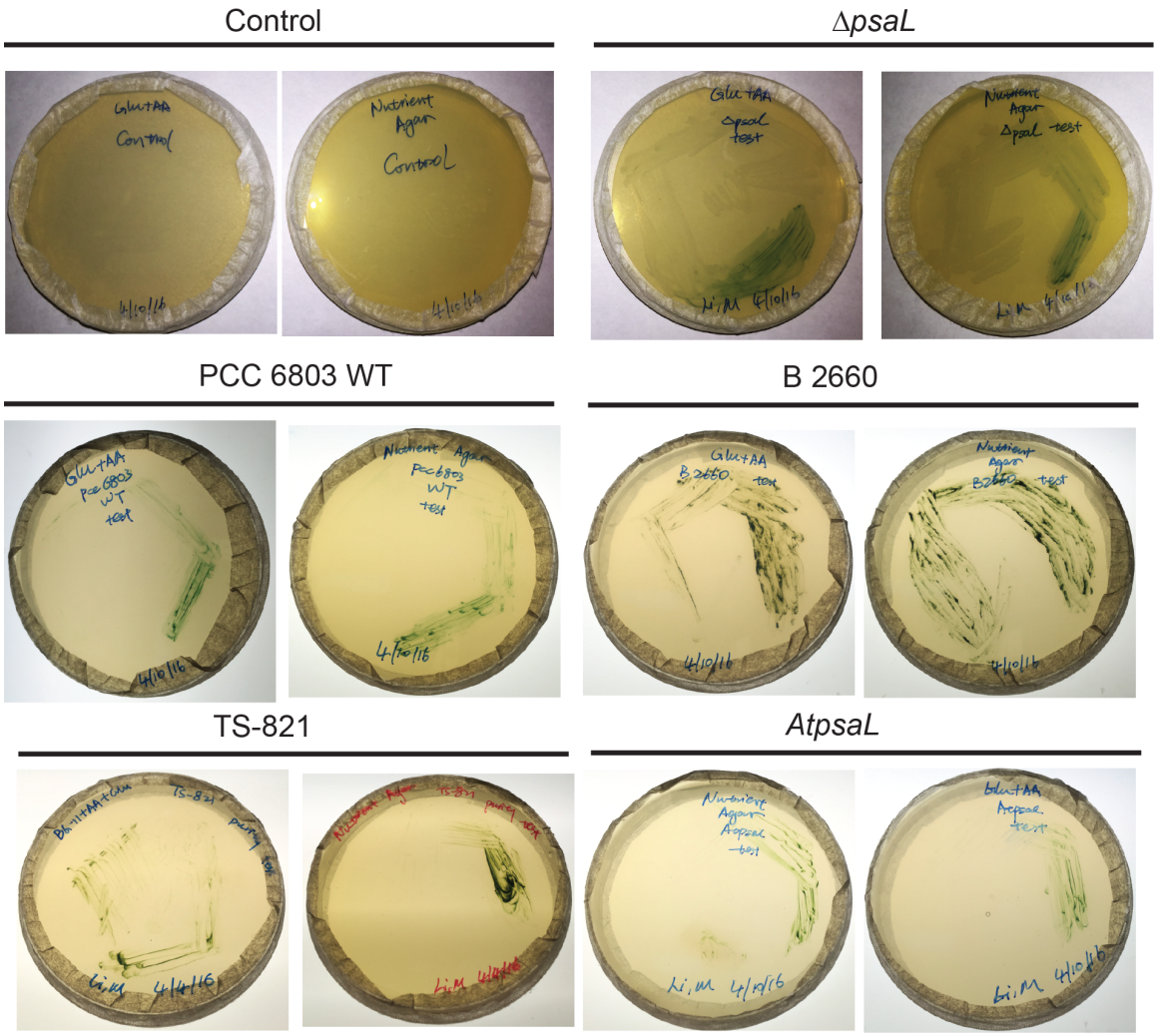

Figure 2- 1 Strain purity test examples.

Control plates have no inoculum. Clean cyanobacterial culture should show no heterotrophic colonies as shown in PCC 6803 WT, B 2660, TS-821 and *Synechocystis* mutant expressing *Arabidopsis* PsaL (*AtpsaL*). Contaminated cyanobacterial culture will show heterotrophic microbial colonies outgrowing, as shown in Δ*psaL*.

Some heterocyst-forming cyanobacteria form microbial mats, such as *Fischerella muscicola* PCC 7414, can be alternatively harvested by filtration.

Cryopreservation for Cyanobacteria

The cryopreservation of cyanobacteria was done mainly by referring to the guidelines from UTEX culture collection center(*63*). In practice, cyanobacterial liquid cultures were spun down on a table top centrifuge at top speed for 2 min and resuspended in 1 mL cryoprotectant: 50% BG-11 + 5% methanol or 8% DMSO, with 50% BG-11 + 8% DMSO used for most cultures. Alternatively, cyanobacteria grown on agar plates can be transferred directly into the cryoprotectant solutions. Some of the marine cyanobacteria or strains isolated from brackish environments were preserved in saline media with 8% DMSO. The resuspended cells were transferred to cryovials if necessary. Even though original publication suggested a slow freezing process before plunging into liquid nitrogen(*63*), direct freezing in liquid nitrogen or -80 °C seemed to work as well.

To recover the culture cultures from cryopreservation, quickly thaw the frozen vials in 35 °C or room temperature water bath. Then the cells were should be spun down before being resuspended in growth media. After resuspension, the cells should be incubated in dark for one day with caps loosened for gas exchange before plating and culturing in liquid media.

2.2 Thylakoid Membrane Isolation

Cell Lysis

For thylakoid membrane preparation, cells are lysed either by beater beading or French Press. Before cell disruption, cell pellets were washed in buffer A (50 mM MES-NaOH, pH 6.5, 5 mM $CaCl_2$, 10 mM $MgCl_2$)(*64*) and then pelleted by centrifugation at 10,000 g for 5 min. After pelleting the cell suspension, cell pellets were resuspended in buffer A containing 25% glycerol for bead beating or in buffer A + 0.5 M sorbitol for French Press. Cell resuspensions were homogenized before lysis. Among the cyanobacteria we studied, *Scytonema crispum* LB 1556 shows large hairy cell aggregates, which do not dissociate upon vortexing or homogenizing. Cell aggregates were broken into small fragments by grinding in liquid nitrogen before resuspension in lysis buffer and homogenization.

For initial study of TS-821 (Chapter Three), cell lysis was done as described in Watanabe *et al.* (*64*) with slight modifications. Bead beating was carried out on bead beater (MP FastPrep®-24) 20 times with each time shaking at 4m/s for 10 s and followed by incubation on ice for 2 min. After removing unbroken cells and beads by centrifugation, cell lysate was used for thylakoid isolation.

In later extensive study of PSI tetramer distribution, the French Press method was used. Homogenized cell suspensions were passed through the French Press three times at 1500 or 2000 psi (10 to 14 MPa), unbroken cells were removed by pelleting at 10,000 g for 5 min. In some cases, large membrane

fragments were pelleted without this step due to the low amount of unbroken cells and/or direct membrane pelleting observed at 10, 000g.

Thylakoid Membrane Pelleting and Resuspension

Thylakoid membranes were pelleted by spinning down cell lysate at 180,000 g (TLA 55 rotor, Beckman) for 1 hour in original study (*21*). The pellets were resuspended in buffer A containing 25% glycerol and stored at -20°C or -80 °C. In most cases, membrane pelleting from cell lysate was done by centrifugation at 40,000 rpm (193,000 g Type 50.2 Ti, Beckman) for 30 min at 4 °C. Thylakoid membrane pellets were resuspended in buffer A + 12.5% glycerol and homogenized before storing at -20 °C or -80 °C. For high light versus low light experiments, thylakoids were washed in buffer A once and pelleted at 193,000 g for 15 min before final resuspension. In some special cases where cell mass is low and large membrane fragments are ready to be pelleted at lower g-force, thylakoids were resuspended after spinning at 10,000 g for 5 min. One example was given in Figure 2-2 showing the larger membrane has similar PSI components to fine membranes isolated at higher g force (40,000g for 45 min).

Chlorophyll Concentration Measurement

Chlorophyll (Chl) concentration was determined as described previously (*65*). In this study, we measured the Chl concentration without considering other chlorophyll besides chlorophyll a (Chl a). 5 to 15 µL (V µL) sample were added to 90% methanol to a final volume at 1 mL and heat treated at 65 °C for more than 2 min. Then the solution is spun down at 21,000 g for 2 min. The absorption at

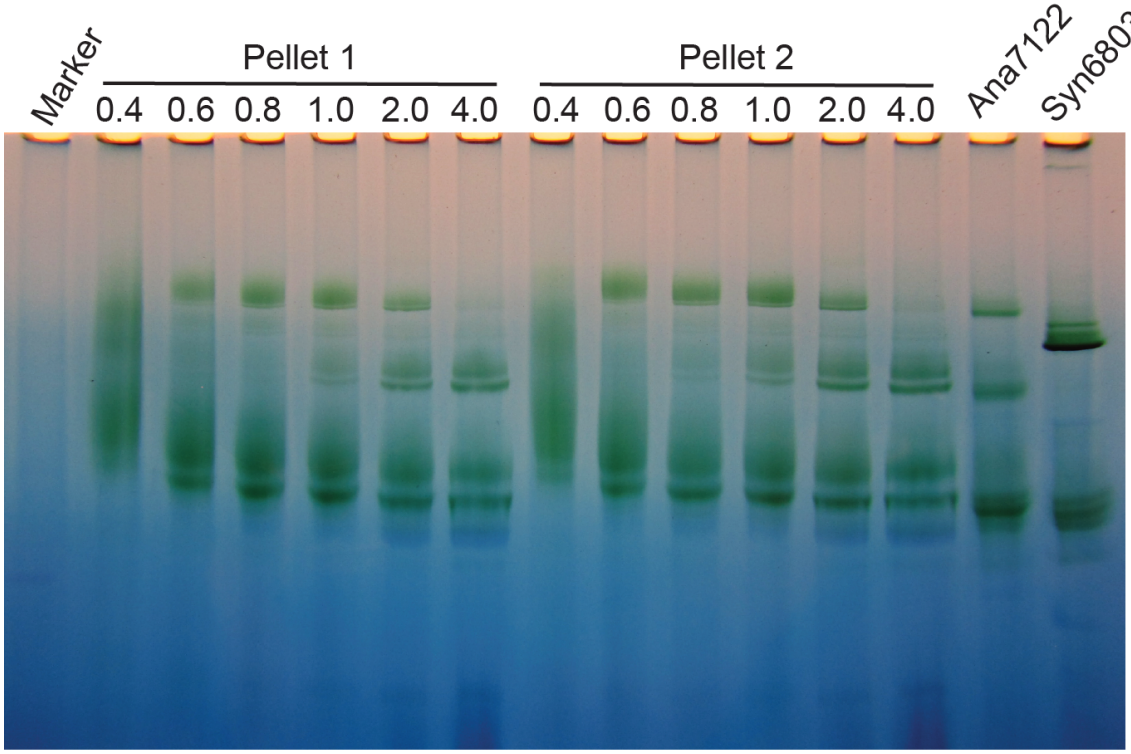

Figure 2- 2 BN-PAGE of LB 1829 thylakoid membrane isolated from different centrifugal forces.

Pellet 1 and pellet 2 are isolated from 10,000 g 5 min and 40,000 g 45 min spinning respectively. Membrane containing 0.4 mg/mL Chl was solubilized in different concentration of DDM (w/v, %). ~ 2 µg Chl were loaded for each lane. Thylakoid membrane from *Anabaena* sp. PCC 7122 (Ana7122) and *Synechocystis* sp. PCC 6803 (Syn6803) solubilized in 1% DDM were used as controls to identify PSI oligomers.

665 nm (A_{665}) was measured. At least three repeats were done for Chl concentration calculation using following equation:

$$\text{Concentration of } Chl \text{ /(mg/mL)} = A_{665} \times 13.9 / V$$

2.3 Biochemical Analyses of Photosynthetic Proteins

Blue Native PAGE

4-16% BN-PAGE gels (Invitrogen) were used to analyze solubilized thylakoids or isolated photosystems according to the user manual and references (*66, 67*). 3-12% gels were only used at the beginning of this study to determine which system works better for analyzing solubilized membranes. In addition, some of the BN-PAGE gels were homemade using a gradient mixer. Homemade gels are good in analyzing large amount of samples, however, it also suffers from relative low repeatability especially for minor protein species.

To analyze PSI oligomeric states, thylakoid membranes were solubilized in different concentration of detergent n-dodecyl-β-maltoside (DDM) (Glycon, Germany) at 25°C for 1.5 h. Some other detergents were also tested for the purpose of crystallization of PSI. Insoluble material was removed by by centrifuging 180,000 g for 5 min or 98, 000 g for 10 min at 4 °C. Supernatants were taken out for analysis on Blue Native PAGE (BN-PAGE) of PSI isolation. The solubilized thylakoid membrane can be stored at -20 °C for a few days for analysis or repetition of an experiment.

As a general rule, membrane protein samples as mixed solubilized membrane or isolated samples were mixed with a 5x loading solution, containing 0.05% Ponceau S, 25% glycerol and appropriate amount of Coomassie Brilliant

Blue G-250 (G-250), to 1x. The final sample loading mix should have a G-250 to detergent mass ratio in the range of 1/10~1/4 as described in reference(*66*). For any sample having a detergent concentration lower than 0.05% (w/v), the final G-250 concentration in the sample was 0.005%.

To run the BN-PAGE, G-250 in the cathode is necessary and 0.02% G-250 in running buffer was used as cathode in this study. Most BN-PAGE gels were run with 150 V constant voltage for 105 min or till the bands of interest resolved for the homemade gels. Gel images were taken before fixation and staining to identify the green bands for photosystems. After staining, gel images are taken using UVP transilluminator (Upland, CA) to visualize proteins with lower abundance and for quantification using VisionWorks®LS analysis software (UVP, Upland, CA).

SDS-PAGE

Tris-Tricine SDS-PAGE (*68*) was used exclusively in this study. In most cases, the 0.75 mm Biorad Mini-PROTEAN® spacer plates were used. 30% T (29:1) acrylamide was used as a stock to make 10% gels. Electrophoresis was carried out by constant voltage 150 V for 40~45 min after 30 V for 15 min for a typical 10% gel. In big gel (18 x 16 cm plates, Hoefer®, Holliston, MA) settings, electrophoresis was done in similar fashion with extended running time till the front dye reaches the lower edge of the gel. For photosystem identification, 10% acrylamide gel was used as described previously (*68*) and silver stain was carried out using fast stain method (*69*). Known photosystem subunits PsaA/B, PsaF, PsaL and PsaD are used for PSI identification. For individual PSI subunits

identification, bands of interest were sliced out after Coomassie Brilliant Blue stain and subsequently treated with trypsin for LC-MS/MS (*21*).

Western Blot

After SDS-PAGE, polyacrylamide gels were carefully transferred into blotting cassette (idEA, Minneapolis, MN*)*. Protein bands were transferred to a 0.45 µm PVDF membrane (Millipore) under 12 or 24 V for at least 1 hour at room temperature in transfer buffer (25 mM Tris + 5% methanol) considering high pKa of interested proteins. Bjerrum Buffer (50 mM Tris, 39 mM glycine) was also tested, which showed better transfer efficiency but was used only for PsaH related work. Membranes were blocked using TBS-T buffer (25 mM Tris-HCl pH 8.0, 137 mM NaCl, 3 mM KCl, 0.1% Tween-20) + 3% NFM (non-fat milk powder) at room temperature for 1 hour. Primary antibody antisera were diluted from 1:2,5000 to 1: 5000 in TBS-T + 3% NFM depending on the efficiency of antisera before treating the blocked membranes overnight at 4 °C. The membranes were then washed using TBS-T + 3% NFM three times for 15 min each time at room temperature. Secondary antibody (goat anti-rabbit) conjugated to HRP was diluted in TBS-T + 3% NFM down to 1:50,000 before treating the washed membranes for 1 hour at room temperature. Following the secondary antibody treatment, the membranes were washed in TBS-T three times for 10 min each time at room temperature. The targeted proteins were then detected using chemiluminsence HRP substrate (Millipore) with signal recorded using ChemiDoc XDS system (Bio-Rad).

2.4 Photosystem I Isolation and Characterization

Sucrose Density Gradient Isolation of PSI Oligomers

For initial study of PSI tetramer in TS-821 (Chapter Three), TS-821 thylakoid membrane containing 0.4 mg/ml Chl were solubilized in 0.4% DDM as described above. The solubilized membrane solution was loaded on a 10-30% sucrose gradient containing buffer A and 0.01% DDM. To isolate pure tetrameric PSI, sucrose gradient ultracentrifugation was done twice at 4°C. First centrifugation was done using SW-32Ti rotor at 28,000 rpm for 16 hours. The bottom green fraction was taken out and dialyzed against buffer A containing 0.01% DDM. Dialyzed PSI tetramer was concentrated using centrifugal concentrator (Millipore Centriplus). Then the concentrated tetramer was loaded on another 10-30% sucrose gradient and centrifuged at 28,000 rpm for 24 hours. Each green fraction from the second gradient was taken out for dialysis and analysis.

In later stage of this study, we slightly adjusted the protocol for sucrose density gradient centrifugation to study PSI oligomeric states as well as isolate tetrameric PSI. To study PSI oligomeric states, as a parallel or complementary experiment to BN-PAGE profiling, thylakoid membranes containing 0.4 mg/mL Chl were solubilized in 0.6~1% DDM. After removing insoluble fragments, the solubilized membranes containing 1 mg Chl were loaded on 10-30% sucrose density gradient in buffer A containing 0.01% DDM. Centrifugation was done using the SW32Ti rotor spinning at 30,000 rpm for 24 hours once. This method showed comparable result with BN-PAGE analysis. For large loading of

solubilized membrane (containing 1~3 mg Chl) on a sucrose density gradient, centrifugation was done twice with the first 20-hour spin followed by dialysis and another 24-hour spin. Lower ionic strength such as 0.4 x buffer A in sucrose density gradient for PCC 7414 PSI oligomers was tried and showed no observable difference for PSI profiles. The 0.01% DDM in sucrose is very close to the reported CMC 0.009% so that it will have minimal interference with PSI tetramer, which is sensitive to higher concentration detergent.

The TS-821 PSI dimer for single particle analysis was made by incubating isolated PSI tetramer with 5% DDM for at least one hour at room temperature. Then the PSI dimer was isolated using SDGC and dialyzed before analysis. The *T. elongatus* PSI monomer was made by adding 0.375% n-octyl-β-D-thioglucoside (Anatrace) into HPLC purified PSI trimer, with Chl concentration at 0.11 mg/ml, and followed by eighteen “heat-freeze” cycles inspired by *El-Mohsnawy* et al (*70*) and described in previous study (*55*). The disruption of trimer is facilitated by magnesium ions in the HPLC purified PSI, because the dialyzed sample did not show as good dissociation of PSI trimer (Figure 2-3).

Characterization of TS-821 PSI

To confirm the conversion of PSI tetramer to dimer and monomer, purified TS-821 PSI tetramer in 0.01% DDM with Chl concentration at 0.30 mg/ml was diluted into Chl concentration at 0.15 mg/ml using different concentration of DDM. After 1.5h incubation at room temperature, treated PSI tetramer samples were analyzed using BN-PAGE.

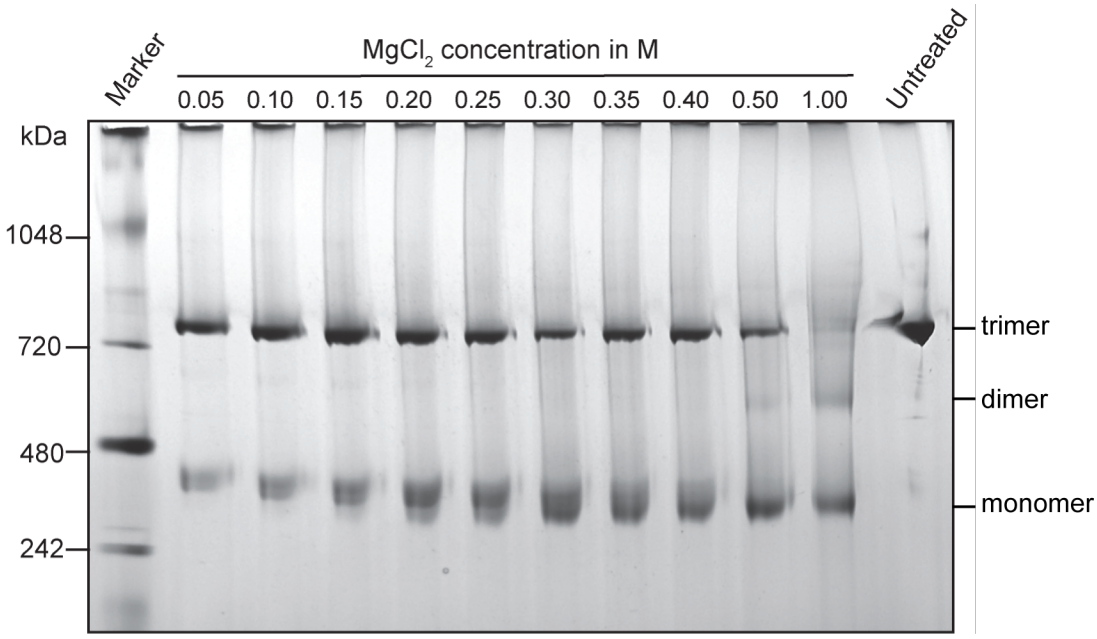

Figure 2- 3 $MgCl_2$ facilitates the disruption of trimeric PSI by OTG

PSI trimer isolated from *T. elongatus* (0.11 mg/mL Chl) was treated in 0.375% OTG with different concentration of $MgCl_2$. Higher concentration of $MgCl_2$ results in more PSI trimer dissociation. The molecular weights of protein markers (NativeMark™) and bands corresponding to PSI trimer, dimer, monomer are denoted.

Analytical Ultracentrifugation (AUC) and 77 K fluorescence spectra were analyzed and acquired as described before (*54*). CD spectra were scanned from 350-760 nm under different temperatures, 15-90°C, with 5°C steps and three minutes temperature equilibrations. Thermostability was inferred from graphing the peak value of ~ 510 nm and at ~705 nm versus temperature. For comparison of low temperature fluorescence, we isolated both the monomer and trimer form of PSI from *T. elongates* BP-1.

PSI P_{700} photo-oxidation and kinetics of re-reduction experiment was carried out using Joliot Type Spectrometer (JTS-10) (BioLogics USA, Knoxville, TN). *T. elongatus* cyt c_6 expressed in *E. coli* and isolated via IMAC (*54*) was used to reduce the photo-oxidized P_{700} in the presence of 0.1 mM methyl viologen and 0.1 mM ascorbic acid in buffer A containing 0.01% DDM. Kinetics were determined with PSI tetramer at 3 µg/mL Chl *a* and cyt c_6/P_{700} ratios were varied from 0, 10, 20, and 40 for comparison. The kinetics was fit using a single exponential decay using GraphPad Prism 6. For light-intensity dependent photo-oxidation, PSI containing 1ug/mL Chl *a* were photo-oxidized using actinic light of 10 ms duration. The maximum ΔAbs_{705nm} was plotted against light intensity and fit to the allosteric sigmoidal curve.

Absorption spectra (200-800 nm) of isolated proteins and pigments were taken using Cary 300 UV-Vis spectrometer (Agilent). The Sample buffers were used as blanks. For PSI oligomer absorption spectra comparisons, A_{680} was adjusted close to 0.5 or 1. The PSI absorption differences were calculated after normalizing the data at A_{680}.

2.5 Structure Study of Tetrameric PSI

Electron Microscopy of Isolated PSI Oligomers and TS-821 Thylakoids

Microscopic images of the various PSI preps were acquired using both scanning transmission electron microscopy (STEM) and transmission electron microscopy (TEM). For the STEM, 5 µL sample was placed on a freshly glow discharged carbon film supported by a 400 mesh Cu grid (Electron Microscopy Sciences). After 1 minute, excess sample was removed and the grid with sample was stained for 1 minute with either 0.5% phosphotungstic acid or 1% uranyl. After drying, the sample was imaged with a Zeiss Auriga (Carl Zeiss Microscopy) operating at 30KV in STEM mode. This allowed direct comparison of the *T. elongatus* trimer, a detergent disrupted *T. elongatus* PSI monomer and the isolated TS-821 tetramer.

For single particle analysis, supercomplexes were negatively stained with 2% uranyl acetate for electron microscopy carbon-coated copper grids. Imaging and image processing were performed on as described in previous studies (*20, 71, 72*). For the final class-sums the best 10% of the projections were used. To visualize TS-821 native thylakoids, TEM was performed. The isolated thylakoid membrane was washed using 0.05% DDM with 0.5 mg/mL Chl for 15 minutes to remove phycobilisomes. The thylakoid membrane was pelleted by centrifugation at 15, 600 g for 15 min. The pellets were then washed again in buffer A and spun down. The washed thylakoid membrane was suspended and diluted in buffer A before TEM analysis. TEM images were obtained and analyzed as described

previously (*73*). Our collaborators in University of Groningen also did Cryo-EM to acquire 3D structure of tetrameric PSI.

TS-821 PSI Tetramer Crystallization for Structure Determination

A 2 L TS-821 purified culture was used as an inoculum to a 120 L large-scale culture in bioreactor with light intensity ranging from 40-200 μmol/m^2/s for 2 weeks. Cells were harvested by centrifugation at 10,000 g for 3 min. Cell lysis and membrane preparation were done using French Press method. Membrane final resuspension in buffer A + 12.5% glycerol was done after washing with buffer A once. Thylakoid membrane containing 1 mg/mL Chl was solubilized in 1% DDM in a total volume of 15 mL at 25 °C for 1.5 hours. The insoluble fraction was pelleted at 193, 000 g for 15 min before loading onto a buffer free 10-30% sucrose gradient containing 0.01% DDM. Ultracentrifugation was done as described in PSI isolation section. Isolated PSI was dialyzed against 0.1 x buffer A + 0.01% DDM at room temperature. Dialyzed PSI was then concentrated using Amicon® 100 K MWCO concentrators (Millipore). To remove large aggregates and particulates, concentrated PSI was filtered through a 0.22 μm Olympus syringe filter (Genesee) before setting up for crystallization. Concentrators and 0.22 μm filters were equilibrated using dialysis buffer before concentration and filtration.

A preparation of PSI tetramer from TS-821 thylakoid membrane containing 120 mg Chl yielded 5.36 mg Chl of PSI. A stock of PSI containing 2.69 mg/mL Chl was used for crystallization condition screening. The stock PSI tetramer concentration is ~ 7 μmol/L assuming that Chl makes up ¼ of the protein

complex and that PSI tetramer has a molecular weight at 1.5 MDa. For crystallization screening, commercial kits MembFac, Index, and PEG/ION (Hampton Research) were used. Automatic sample mixing was done using Phoenix drop setter (Rigaku). Crystallization temperature was set at 20 °C. To screen and identify crystal formation, images were taken automatically in the incubation chamber. SONNIC (*74*) imaging (Formulatrix) was done after 3 days of incubation to confirm potential crystal formations. After initial screening, further optimization was done by varying precipitant concentration and protein to precipitant ratios.

In the meantime, desalting condition was tested as well by dropping $MgCl_2$ and $CaCl_2$ concentrations to half of the stock and increasing PSI concentration to 14, 21, 28 µmol/L. Samples were placed in 4 °C for the crystallization experiment. This experiment was done by dilution of ~5 µmol/L PSI tetramer to 2.5 µmol/L using 0.5 mM MES, pH 6.4 + 0.01% DDM, followed by concentrating in 100 K MWCO concentrators.

2.6 Antigen Design and Antibody Production

Antigen Design

PsaL sequences are not well conserved for antigen design from a single consensus sequence. To achieve one antigen for all PsaL of interest in this study, i.e. *Chroococcidiopsis* sp. TS-821, *Arabidopsis*, *Thermosynechococcus elongatus* BP-1, and *Synechocystis* sp. PCC 6803, a fused protein, CATSPsaL containing fragments of different PsaL was designed to achieve epitopes matching those fragments. To predict the epitopes, Kolaskar & Tongaonkar

Antigenicity's methods (*75*) on IEDB Analysis Resource (http://tools.immuneepitope.org/tools/bcell/iedb_input) and ABCpred (*76*) (http://www.imtech.res.in/raghava/abcpred/index.html) were used. The antigen sequence is aligned against different PsaL fragments and its predicted antigen to ensure the high probability of getting antibody for each PsaL (Figure 2-4). In addition to the N-terminal fragments, the loop insertion between second and third trans-membrane helices of TS-821 PsaL was also used to achieve high antigenicity for TS-821.

For PsaH, the N-terminus of *Arabidopsis* PsaH was used as an antigen to generate antibody.

Cloning and expression

Synthetic plasmid pBSK-CATSpsaL (IDT, San Jose, CA) and pTYB2 (NEB) were digested in XmaI and NdeI restriction enzymes. The digested products were separated by electrophoresis in 1% agarose in TAE buffer at 100 V constant voltage for 1 hour. The insert and digested pTYB2 plasmid was sliced out after ethydium bromide staining and imaging on a UV light plate. The isolated DNA fragments were then extracted from agarose gel using QIAGEN kit. Ligation was done using LigaFast™ rapid DNA ligation system (Promega). The ligation product was then transformed into *E. coli* GC5™ competent cells for plasmid propagation and sequence check later. 100 µg/mL Ampicillin (Amp) was used for selection. Miniprep of plasmid DNA was done using the QIAGEN miniprep kit. Isolated plasmid DNA was then transformed into *E. coli* ER2566 for antigen expression after sequencing the ligation product. Small DNA fragment sequencing in this study is done using Sanger sequencing at UT Genomics Core.

A

>CATSPsaL(Antigen)
MAQAIDASKNRPSDPRNQQVVQPINGDPFIGSLETPISDSGLVKTFIGNLPAYRKGLSPILRGLEV
GMAHGYSLYAATDPPKPVATVTVPNPPDTFDTTEG

B

```
Antigen   MAQAIDASKNRPSDPRNQQVVQPINGDPFIGSLETPISDSGLVKTFIGNLPAYRKGLSPILRGLEVGMAHGYSLYAATD--PPKP--VATVTVPNPP-DT--FDTTEG
At        ---------AVKSDKTTFQVVQPINGDPFIGSLETPVTSSPLIAWYLSNLPGYRTAVNPLLRGVEVGLAHGFTIYGISSFKEGEPSIAPSLTLTGRKKQPDQLQTADG
T.e.      ---------------MAEELVKPYNGDPFVGHLSTPISDSGLVKTFIGNLPAYRQGLSPILRGLEVGMAHGYAAYGLVSFQKGGS-----------SSDP--LKTSEG
Syn6803   -------------MAESNQVVQAYNGDPFVGHLSTPISDSAFTRTFIGNLPAYRKGLSPILRGLEVGMAHGYSSYGLVTFQGEQG-----------SGDT--LQTADG
TS-821    MAQAIDASKNRPSDPRNQEVVYPSRRDPQIGNLETPINNSSLVKWFINNLPAYRPGITPLRRGLEVGMAHGYSLYAATD--PPKP--VATVTVPNPP-DT--FDTTEG
0.95      ------------------------------------------------------------------------LYAATD--PPKP--VATVTV---------------
0.93      ------------------------------------------------------------------------------------VATVTVPNPP-DT--FDTT--
0.90      --------------------VQPINGDPFIGSLETP-------------------------------------------------------------------------
0.89      ---------------------------------------------KTFIGNLPAYRKGLSP-------------------------------------------------
0.87      ------------------------------------------------------------VGMAHGYSLYAATD--PP-------------------------------
0.86      -----DASKNRPSDPRNQQVV---------------------------------------------------------------------------------------
0.75      ------------------------------------------------YRKGLSPILRGLEVGM-----------------------------------------
0.74      ----------------------------------TPISDSGLVKTFIGNL-------------------------------------------------------------
0.68      -------------DPRNQQVVQPINGDPF-------------------------------------------------------------------------------
```

C

```
Antigen   MAQAIDASKNRPSDPRNQQVVQPINGDPFIGSLETPISDSGLVKTFIGNLPAYRKGLSPILRGLEVGMAHGYSLYAATD--PPKP--VATVTVPNPP-DT--FDTTEG
At        ---------AVKSDKTTFQVVQPINGDPFIGSLETPVTSSPLIAWYLSNLPGYRTAVNPLLRGVEVGLAHGFTIYGISSFKEGEPSIAPSLTLTGRKKQPDQLQTADG
T.e.      ---------------MAEELVKPYNGDPFVGHLSTPISDGGLVKTFIGNLPAYRQGLSPILRGLEVGMAHGYAAYGLVSFQKGGS-----------SSDP--LKTSEG
Syn6803   -------------MAESNQVVQAYNGDPFVGHLSTPISDSAFTRTFIGNLPAYRKGLSPILRGLEVGMAHGYSSYGLVTFQGEQG-----------SGDT--LQTADG
TS-821    MAQAIDASKNRPSDPRNQEVVYPSRRDPQIGNLETPINNSSLVKWFINNLPAYRPGITPLRRGLEVGMAHGYSLYAATD--PPKP--VATVTVPNPP-DT--FDTTEG
```

Figure 2- 4 PsaL antigen design and epitope prediction

(A) PsaL antigen sequence in fasta format is shown. (B) Alignment of CATSPsaL with PsaL N-termini and loop insertions from *Arabidopsis* (At), *T. elongatus* (T.e.), *Synechocystis* sp. PCC 6803 (Syn6803), and TS-821. First three amino acid residues of loop insertions are in bold format for clarity. The ABCpred epitopes with different scores are aligned as well. Identical fragments to antigen are highlighted in green, and predicted epitopes are underlined. (C) The predicted epitopes using Kolaskar & Tongaonkar method are colored in red.

The pTYB2-AtH plasmid was cloned in a similar way from pBSK-AtH and pTYB2 for PsaH antigen production. Colonies of transformed *E. coli* ER2566 cells were checked by colony PCR to verify the presence of the expression vector. Multiple colonies were cultured in liquid LB + Amp media for induction screening using IPTG. Parallel cultures without induction were used for large volume culture for antigen purification. The cells expressing CATSPsaL was induced at OD_{600nm} 0.3~0.6, 20 °C or 15 °C, with 0.5~1 mM IPTG for 16 hours. The expression of PsaH antigen was induced at 15 °C for 16 hours from OD_{600nm} 0.7, with 0.5 mM IPTG. Induced cells were harvested by centrifugation, 10,000 g for 5 min or 5000 g for 10 min.

Antigen Purification

IMPACT™ Chitin Resin (NEB) was used as column matrix for antigen purification. Cell pellets were suspended in ice cold lysis buffer (column buffer + 0.2mM PMSF+1μM Leupeptin+ 1 μM Pepstatin) and homogenized before cell lysis using sonication. Usually, a 2 L culture pellet was suspended in 30 mL lysis buffer. Sonication was done with 15 s on and 45 s off cycle with total sonication time ranging from 3 to 10 min depending on the volume of total cell suspension. Containers of cell suspension were kept on ice during sonication. Unbroken cells and cell membrane were pelleted and removed by centrifugation at 30,000 g or 193,000 g for 30 min. Supernatant was used for antigen purification on a chitin beads column. The purification process of antigen on the column was carried out following manufacture's guide (NEB) with cleavage at room temperature for 16~24 hours.

The elution was analyzed using SDS-PAGE to check the purity of antigens. Usually further clean up using concentrators (Millipore) with 30 K MWCO or 10 K MWCO was necessary to remove chitin-binding domain from antigens. Dialysis against 0.1 x PBS was done followed by concentration using Millipore concentrators. Final antigen concentration was determined using Pierce™ BCA protein assay kit.

Antibody production

Antibody was produced at Pocono Rabbit Farm (Canadensis, PA) using the 91-day protocol on two rabbits. For PsaL antibody production, the purified 1 mg/mL antigen was used as inoculum. For PsaH antibody production, KLH (keyhole limpet hemocyanin, Pierce) was crosslinked with purified antigen. The AtH-KLH crosslinked product was used as inoculum.

2.7 *psaL* Gene Cloning and TS-821 Genome Sequencing

Genomic DNA Extraction

Most cyanobacterial DNA was extracted for *psaL* cloning are done using following protocol. The cyanobacterial cells were washed 3 times using sterile water before DNA extraction. These cells were further washed 3 times using TE buffer (1 mM EDTA, 10 mM Tris-HCl pH 7.4) containing 0.6% SDS. Cells were then broken in TE buffer using beads-beater with 0.1 mm silica beads (MP FastPrep®-24) and the following process was described previously by Billi *et al.* (*77*). TS-821 DNA for genome sequencing as well as some cyanobacterial DNA for *psaL* cloning was extracted using the NucleoBond® DNA isolation kit.

psaL Gene Cloning

The following protocol was used for initial TS-821 *psaL* cloning (Chapter Three). According to Fewer *et al.* (*78*), *Chroococcidiopsis* is closely related to heterocyst-forming cyanobacteria. Multiple heterocyst-forming cyanobacterial *psaL* gene sequences (Figure 2-5) and its 5 kb flanking region on both sides were acquired from GenBank and aligned in Megalign (Lasergene DNAStar, Madison, WI). This alignment identified highly conserved regions that were used to amplify the *psaL* gene in TS-821. Primer 5'-GCACCACCAATVCCRCC-3' and 5'-GGGAACTTRGAAACVCC-3' were used to amplify a ~400 bp fragment within *psaL*. The PCR products were ligated into pGEM T-easy vector (Promega) for sequencing. After acquiring the sequence of the partial *psaL* gene, two other primers based on the known partial sequence, 5'-ATAACCTGCCAGCATATC-3' and 5'-CAAATTAAGAAGCCACTCGC-3', combined with several different putative primers outside the *psaL* coding region, were used to obtain the whole *psaL* gene sequence. The result showed that each of the primer independently is capable of amplifying a fragment containing the *psaL* flanking region. Primers based on the sequencing results of flanking regions, 5'-AGATTCTGCTGATGCGATCG-3' and 5'-GCTTTCTGGGGAATTAGTTGC-3', were used to amplify the whole sequence of *psaL* and its flanking regions and verify the presence of single *psaL*. BlastX (http://blast.ncbi.nlm.nih.gov) was used to infer the translated protein products. The gene structure is shown in Figure 2-6A with the primers used for amplification shown. Alignment of the genomic organization of *psaL* with adjacent genes is shown in Figure 2-6B. Genomic data

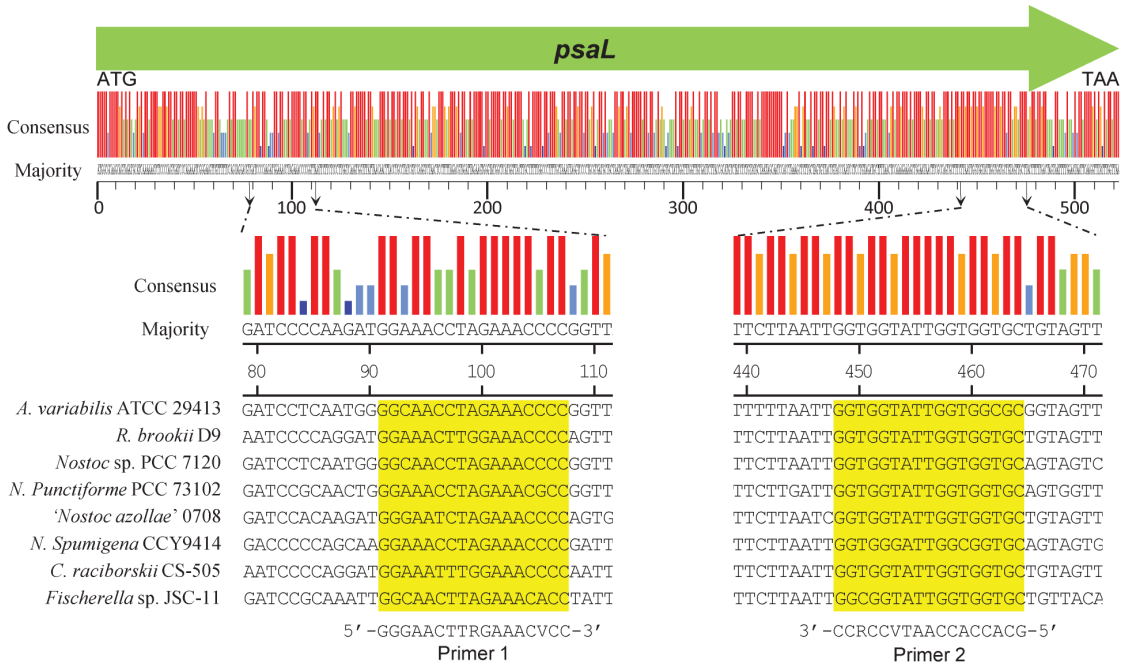

Figure 2- 5 Primer design for partial TS-821 *psaL* gene cloning

Multiple heterocyst-forming cyanobacterial *psaL* gene coding sequences were aligned in Megalign (Lasergene DNAStar, Madison, WI), conserved regions were picked to design a pair of degenerative primers to clone partial TS-821 *psaL* gene. Figure was used for earlier publication.

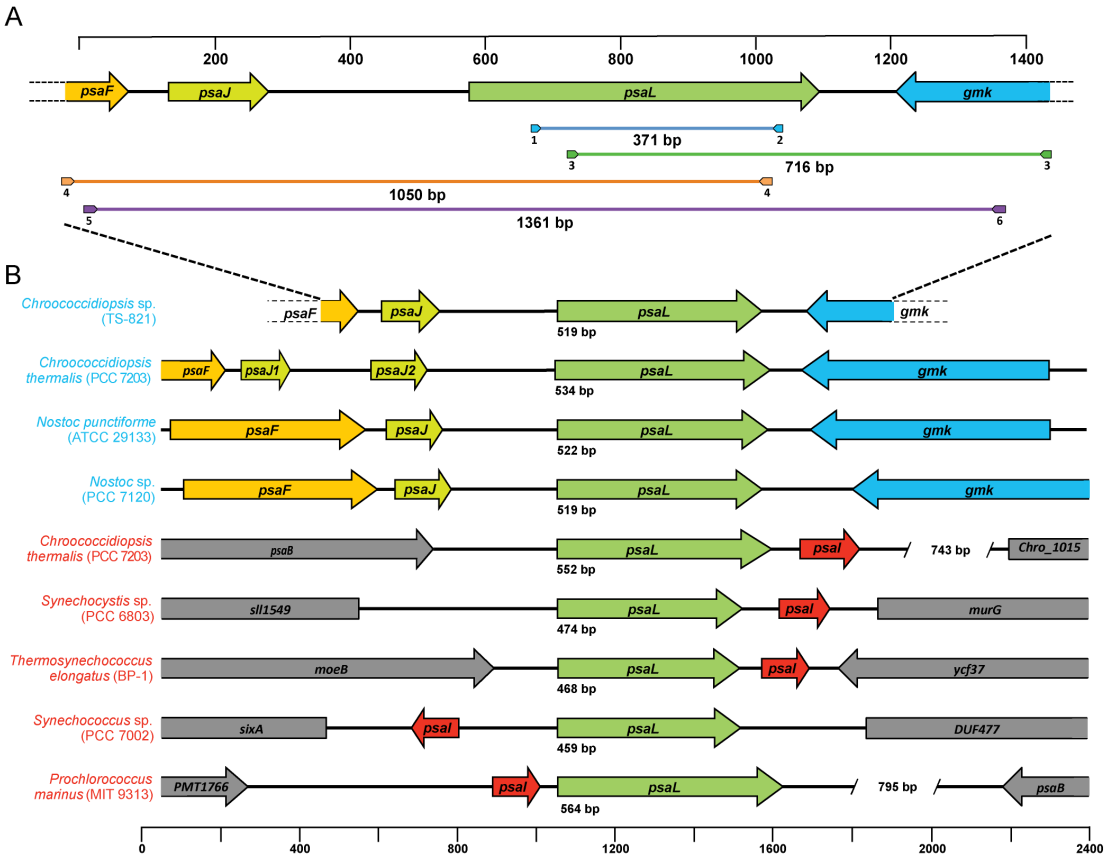

Figure 2- 6 Cloning and genomic organization of *psaL* genes

(A) Cloning of TS-821 *psaL* gene was achieved through several steps. First, partial *psaL* sequence was amplified using primers (1 and 2) derived from conserved consensus in heterocyst-forming cyanobacteria *psaL* genes (see Methods for details). With known sequences inside TS-821 *psaL* gene, primer 3 and primer 4 were designed, both of which independently amplified a flanking region of *psaL*. Primer 5 and primer 6 were designed to confirm the presence of a single *psaL*. The genes were identified using translated DNA sequences.

(B) Cyanobacterial *psaL* genomic locus comparison. Most cyanobacterial psaL genes locate either adjacent to *psaF*, *psaJ* and *gmk* (heterocyst-forming cyanobacteria or related) or adjacent to psaI (other groups). *psaF*, *pasJ*, *psaL*, *psaI* and *gmk* genes are shown in orange, yellow, green, red and blue respectively. Other genes are shown in grey. Rulers are shown separately for A and B, in units of bp.

was taken from NCBI and the JGI Integrated Microbial Genomes site (https://img.jgi.doe.gov/).

For *psaL* cloning of other heterocyst-forming cyanobacteria, different primer sets (Table 2-2 and Table 2-3) from *psaF* and *gmk* genes were used to amplify the *psaL* gene and its flanking region. The cyanobacteria of interests were classified using their known DNA seuquences or genus names to pick primer pairs. PCR products were ligated into pJET vectors using CloneJET™ PCR cloning kit.

Genome Sequencing of TS-821

TS-821 DNA for genome sequencing was isolated from purified TS-821 culture. The DNA was submitted to UT Genomic Core for sequencing using Illumina® MiSeq Kit V2 with 2 x 250 bp read length. The resulted FASTQ files were analyzed using ABySS (version 1.9.0) (*79*), SPAdes (version 3.7.1) (*80*), and A5-miseq (*81*). The assembly quality was assessed using QUAST (*82*). The assembled contigs were submitted to PATRIC (*83*) for annotation, which uses the RAST (*84*) system.

2.8 Phylogenetic Analysis

Phylogenetic Analysis of PsaL

The following method was used for Chapter Three. In addition to TS-821 PsaL, other PsaL protein sequences from cyanobacteria, red algae, green algae and plants were obtained from the Integrated Microbial Genomes (https://img.jgi.doe.gov/) and Uniprot (http://www.uniprot.org/). For identical

Table 2- 2 PCR primers and conditions for different *psaL* cloning

Strain	Primers	Annealing
Mastigocladus sp. B 2965	PsaF156/gmkB1A	43 °C
Calothrix parietina LB 1952	PsaF156/gmkB1C	52.3 °C
Scytonematopsis contorta 2963	PsaF156/gmkB2	52 °C
Spirirestis rafaelensis B 2660	PsaF156/gmkB2	52 °C
Anabaena flos-aquae LB 2558	PsaF156/gmkB2	52 °C
Nodularia spumigena PCC 73104	PsaF156/gmkB2	47 °C
Cylindrospermum licheniforme B 2014	PsaF156/gmkB2	52 °C
Anabaena inaequalis B 381	PsaF156/gmkB2	52 °C
Tolypothrix distorta B 424	PsaFB3/gmkB2	54.6 °C
Scytonema crispum LB 1556	PsaFB3/gmkrB2	57.5 °C
Fischerella ambigua 1903	PsaFFisch/gmkFisch	52 °C
Nodularia harveyana B 2093	PsaFr156/gmkB2	52 °C
Calothrix membranacea B 379	PsaFr156/gmkrB2	52 °C
Gloeotrichia ghosi LB 1920	PsaF156/gmkB2	52 °C

Table 2- 3 Primer sequences used for *psaL* cloning

Primer name	Sequence 5' to 3'
PsaF156	ATG MSW MGA TTG TT GCT TTG
PsaFB3	TGG ATT GGY TGG GTM GG
PsaFFisch	TGC AAA CAA TCA AAA AGC ARG
PsaFr156	TGG ATH GGY TGG GTH GG
gmkB1A	GGT AAR GGH ACT TTA ATG
gmkB1C	GAR TGG GCW GAR TTT GC
gmkB2	GAR TGG GCV GAA TTT GCK GG
gmkFisch	AAA GGB ACT TTA ATG CGA TCG

sequences, only representative sequences were used for the phylogenetic tree building. The sequences were aligned using ClustalW within MEGA 5 (*85*) to truncate the first methionine, signal peptides in plant and green algae, and N-terminal gap region. The rest of the sequences were submitted to EBI T-Coffee Multiple Sequence alignment (http://www.ebi.ac.uk/Tools/msa/tcoffee/) for a better alignment (*86*). After manually optimizing alignment, phylogenetic analysis with T-Coffee alignment was done with MEGA version 5 (*85*). The suggested best model, rtREV+G+I+F, was used for maximum likelihood tree building with 5 discrete gamma categories, 1000 bootstrap replicates and 95% site coverage cutoff for gap partial deletion. Neighbor-joining tree was also built using MEGA version 5 using Poisson model with the same setting as in maximum likelihood tree. The final tree was a condensed tree with a 50% cutoff.

Phylogenomic Analysis of Sequenced Genomes

Dr. Alexandra Calteau in Genoscope did the phylogemoic analysis. The detailed methods will be available in manuscript.

2.9 Genetic Engineering of *Synechocystis* sp. PCC 6803

Initial Attempt for *psaL* Substitution

Primers 5′-AACCGGTTAGCCCATTTCATCAGC-3′ and 5′-CCGGGGTACCAAGGTCGTCTCC-3′, annealing to the flanking region of wild-type psaL, were used to clone the wild-type genomic sequence into pCR 2.1-TOPO vector (Invitrogen) for subsequent clone constructions (Figure 2-7). Site-directed mutagenesis was done to create an NdeI restriction site at the wild-type

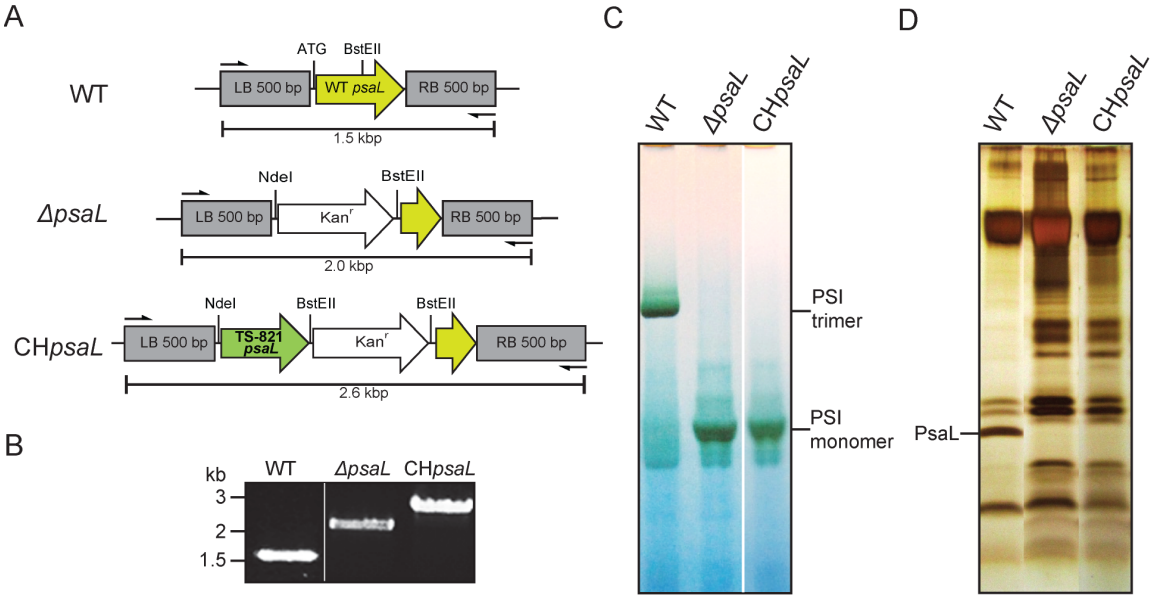

Figure 2- 7 Genetic complementation of *Synechocystis psaL* using TS-821 *psaL*.

(A) Constructs of *psaL* knockout and complementation. *Synechocystis psaL* knockout mutant (*ΔpsaL*) was constructed by replacing wild type (WT) *psaL* first 300 bp coding sequence with kanamycin resistant gene (Kan^r). TS-821 *psaL* expressing mutant (CH*psaL*) was constructed by replacing WT *psaL* first 300 bp coding sequence with TS-821 *psaL* and Kan^r open reading frame. NdeI restriction site was created by site directed mutagenesis and used with BstEII to make the constructs. Primers, shown as arrows, binding in WT *psaL* flanking region, at left bound (LB) 500 bp and right bound (RB) 500 bp, were used to identify the transformants.

(B) Identification of homozygous mutants using PCR. Expected fragment sizes of different genetic background are shown in panel (A).

(C) BN-PAGE of solubilized thylakoids of *Synechocystis* WT and mutants. Thylakoids of 0.4mg/mL Chl were solubilized in 1% DDM. PSI trimer and monomer are denoted.

(D) SDS-PAGE of WT PSI trimer and mutants PSI monomers. The band corresponding to PsaL is denoted. Silver stain was used for visualization.

psaL start codon. The open reading frame of the kanamycin resistance gene PcpcC:kmTe as described in a previous study (*87*) was cloned using primers 5′-GGTTACCCTCGATATTT AGGAG-3′ and 5′-GGTAACCTAAAAGGGAATGCGt-3′, containing BstEII restriction sites. The TS-821 psaL gene was cloned using primers: 5′-GGTAACCTTACTTGAAAATGTTTTG-3′ and 5′-CATATGGCGCAAGCAATAGA TGC-3′. Knockout mutant of psaL (ΔpsaL) and replacing Synechocystis psaL with TS-821 psaL mutant (CH*psaL*) were constructed as shown in Figure 2-7A. Transformation was done using optimum natural transformation conditions as described previously when the cell culture density OD730 was ~0.8 (*88*). Kanamycin (60 μg/mL) was used for selection on agar plates and for subsequent liquid culture.

Construction of *psaL* Mutants Using Codon Optimized DNA

To improve the expression level of exogenous PsaLs, the codon optimized synthetic *psaL* DNAs in pBSK vector were obtained from IDT (San Jose, CA). Similar methods were used for cloning and *Synechocystis* transformation. Multiple lines of mutants were tested by western blot before PSI oligomeric state analysis. The mutants are named as Synthetic *Chroococcidiopsis* sp. TS-821/*Arabidopsis thaliana psaL* replacing *Synechocystis psaL* with Kanamycin resistant gene, followed by colony number. For example, SCHLLK-12 means the *Synechocystis* mutant line 12 expressing synthetic TS-821 *psaL*.

Expressing PsaH/PsaL Using Broad-host Plasmid in *Synechocystis*

To investigate if PsaH preferentially bind to specific PsaL, synthetic *Arabidopsis psaH2* gene (IDT, San Jose, CA) was cloned to pSL1211 plasmid

(*89*). The expression of His-tagged PsaH is under control of the lac promoter and induced by IPTG. To express PsaH without His-tag, pSLS was constructed by removing the His-tag coding region from pSL1211 through SDM (site directed mutagenesis). The cloned vectors pSL1211-PsaH, pSLS-PsaH (Figure 2-8), were transformed into *E. coli* S17-1 (a gift from Alexandra Lab) strain before biparental conjugation. *E. coli* transformants were selected using LB media containing 5 μg/mL gentamycin and confirmed by colony PCR using rrBseq and M13Rseq primers (Table 2-4). The confirmed S17-1 cells were subcultured in liquid LB media with gentamycin selection till the OD_{600} at 0.4~0.6. In the meantime, the *Synechocystis* cultures were at a density OD_{730} 0.6~0.8. 5 mL of the S17-1 cells and 20~40 mL of the *Synechocystis* were spun down for conjugation. Cell pellets were gently resuspended and mixed in liquid media containing 50% LB and 50% BG-11, total volume ~ 1 mL. The mixed cell resuspension was dropped on a BG-11 agar plate and incubated in the *Synechocystis* growth chamber for 16-hour conjugation and following 24-hour recovery with cells spread out on the plate. Selection was done by transferring the cell lawn mixtures to BG-11 + 5 μg/mL gentamycin plates after recovery. The selection plates also contain 50 μg/mL kanamycin if *Synechocystis* have PsaL mutation background. Positive colonies were confirmed by colony PCR to detect the presence of the plasmids. Large volume, 1~2 L, culture was done in static flask with LB supplemented with 0.5 μg/mL gentamycin after unsuccessful culture in bubbling bottle. His-tagged PsaL expressing vectors are also constructed: pSL1211-SynpsaL (WT *psaL*), pSL1211-CHpsaL, and pSL1211-AtpsaL.

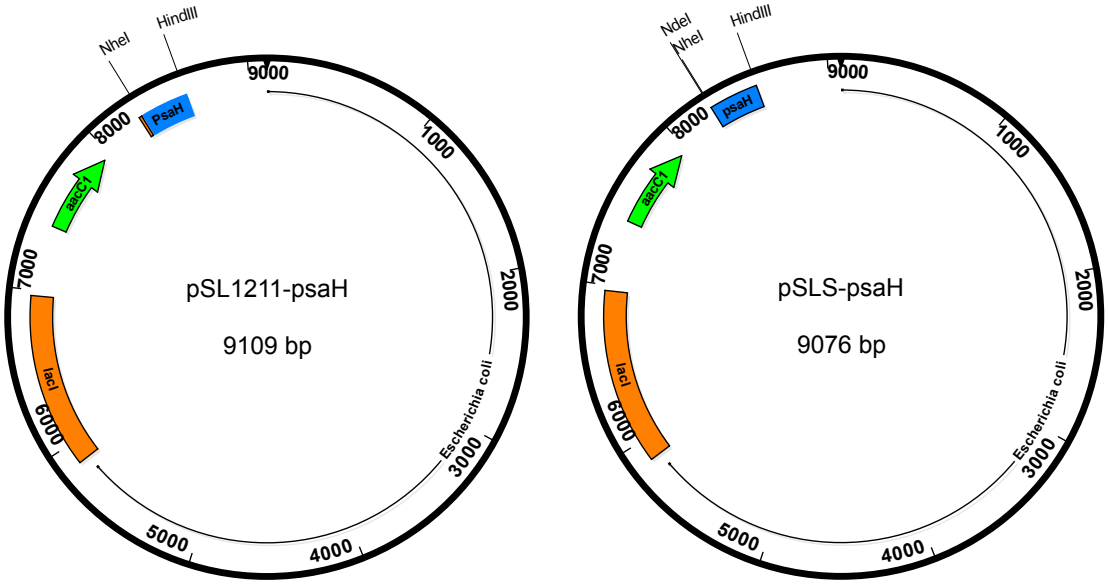

Figure 2- 8 Schematic views of pSL1211-psaH and pSLS-psaH vectors

Synthetic *psaH* gene and *psaL* genes were cloned to pSL1211 (containing His-tag) and pSLS vectors. For pSL1211-psaH, NheI and HindIII restriction sites were used. NdeI and HindIII were used for pSLS-psaH construct. Plasmids for His-PsaL expression, pSL1211-SynpsaL pSL1211-CHpsaL, and pSL1211-AtpsaL, were constructed in similar way to pSL1211-psaH.

Table 2- 4 Primers used for constructs in pSL1211 and pSLS vectors

Primer name	Sequence 5' to 3'	Template/function
SL1211SDM2fwd	CGATTAAATAAGGAGGAATAACATATGGCT AGCATGACTGGTGGAC	pSL1211 SDM
SL1211SDM2rvs	GTCCACCAGTCATGCTAGCCATATGTTATT CCTCCTTATTTAATCG	pSL1211 SDM
rrBseq	GCTACGGCGTTTCACTTCTG	Sequencing
M13Rseq	AGCGGATAACAATTTCACACAGG	Sequencing
NheI SynpsaL up	GCT AGC GCT GAA TCT AAC C	*Synechocystis psaL*
HindIII SynpsaL dn	AAG CTT AGT TAA ATA GAC CCC	*Synechocystis psaL*
NheI SChL up	GCTAGCGCCCAAGCCATTGATGC	TS-821 *psaL*
HindIII SChL dn	AAGCTTATTTAAAAATGTTCTGAATC	TS-821 *psaL*
NheI SAtL up	GCT AGC GCC GTG AAA TCC G	*Arabidopsis psaL*
HindIII SAtL dn	AAG CTT ATT TCA CAA AGT AGG G	*Arabidopsis psaL*

CHAPTER THREE

Characterization of PSI Tetramer in *Chroococcidiopsis* sp. TS-821

3.1 Disclosure

This chapter has been published in the journal Plant Cell in 2014 (*21*). Copyright belongs to American Society of Plant Biologists (www.plantcell.org). The materials and methods are included in Chapter Two. Single particle analysis was done by our collaborators; all the results are included for integrity.

3.2 Abstract

Photosystem I (PSI) is a Type I reaction center associated with oxygenic photosynthesis. It is found in a wide range of organisms including cyanobacteria, algae, non-vascular, and vascular plants. Unlike the monomeric reaction centers found in green and purple non-oxygenic bacteria, PSI forms trimeric complexes in most cyanobacteria with a three-fold rotational symmetry that is primarily stabilized via non-covalent interactions between adjacent PsaL subunits. In plants and algae, however, PSI is monomericIn this study, we have discovered a new, tetrameric form of PSI in the thermophilic cyanobacterium, *Chroococcidiopsis* sp. TS-821 (TS-821). In TS-821, PSI forms tetrameric and dimeric species. We have investigated these species by BN-PAGE, sucrose density gradient centrifugation, 77 K fluorescence, CD, and single particle analysis. TEM analysis of native membranes confirms the presence of the tetrameric PSI structure prior to detergent solubilization. To investigate why TS-821 forms tetramers instead of trimers, we have cloned and analyzedits *psaL* gene. Interestingly, this gene product contains a short insert between the second and third predicted trans-membrane helices. Phylogenetic analysis based on PsaL protein sequences shows that TS-821 is closely related to heterocyst-

forming cyanobacteria, some of which also have a tetrameric form of PSI. In light of the presence of tetrameric PSI in glaucophytes and the close phylogenetic placement of chloroplasts to heterocyst-forming cyanobacteria, we propose that PSI evolved from a trimeric to tetrameric oligomer *en route* to becoming monomeric in green algae and plants.

3.3 Introduction

Photosynthetic reaction centers are chlorophyll (Chl) pigment-protein complexes capable of converting light energy into a stable charge separation. In oxygenic photosynthesis, Photosystem II (PSII) and Photosystem I (PSI) work in series to couple the splitting of water with the reduction of ferredoxin (*90*). Whereas PSII has evolved to have a strong oxidizing potential, PSI has evolved to have a low potential acceptor that is capable of reducing $NADP^+$ via the soluble Fe/S protein ferredoxin. Interestingly, unlike the non-oxygenic, monomeric bacterial reaction centers, photosynthetic reaction centers in oxygenic organisms are found as monomers (plant PSI), dimers (all PSII) or trimers (cyanobacterial PSI). Cyanobacterial PSI trimers have been reported in many published works (*5, 8-17, 91*), and the only existing crystal structure of a cyanobacterial PSI, from *Thermosynechococcus elongatus* BP-1 (*T. elongatus*) (*18*), suggests that cyanobacteria PSI preferentially forms a trimer. Although there have been reports of trimeric forms of PSI in higher plants (*40, 92*), it is now widely accepted that plant PSI forms only monomeric complexes (*40, 93*). Furthermore, it is known that PSI is a monomer in green and red algae (*37*) as well as in diatoms (*38*).

Cyanobacterial PSI trimers have been reported in almost every subclass of cyanobacteria. The most well characterized PSI trimers are from *Synechocystis*, *Synechococcus*, and *Thermosynechococcus*, and PsaL is needed for PSI trimerization in these cyanobacteria (*22, 25, 26*). In contrast, plant PSI is monomeric in the presence of PsaL, possibly due to interaction with the PsaH subunit that is not found in cyanobacteria (*45-47*). However, both PSI tetramer and dimer were reported in the heterocyst-forming cyanobacterium, *Nostoc* sp. PCC 7120 (*19, 20*). A similar tetrameric PSI was also observed in the glaucophyte, *Cyanophora paradoxa,* using Blue Native PAGE (BN-PAGE) and sucrose density gradient centrifugation (SDGC), but was not characterized in detail (*19*).

In the current study, we have identified a third organism, the unicellular cyanobacterium *Chroococcidiopsis* sp. TS-821 (TS-821), that contains tetrameric PSI complex. TS-821 is a thermophilic cyanobacterium isolated from a hot spring in Thailand (*94*). It was originally identified as a member of the *Chroococcidiopsis* genus according to the physiological and morphological properties described by Stainer and Waterbury (*95*). *Chroococcidiopsis* is classified as a class II cyanobacterium because of its 'multi-fission' property, but a recent classification study based on 16S rRNA sequences showed that *Chroococcidiopsis* is a close relative to heterocyst-forming cyanobacteria (*78*). Thus, the prior classification of *Chroococcidiopsis* may require reconsideration. TS-821 and other related cyanobacteria are remarkable thermophilic cyanobacteria capable of surviving various extreme environments (*94*). This extreme environmental tolerance and

the ability to grow to high cellular density (*96*) makes TS-821 an attractive source for large-scale production of thermostable photosynthetic complexes.

In TS-821, PSI forms tetrameric and dimeric species, which we have characterized using BN-PAGE, SDGC, 77 K fluorescence, circular dichroism (CD), analytical ultracentrifugation (AUC), electron microscopy (EM), and single particle analysis. To investigate why TS-821 forms tetramers/dimers instead of trimers, the *psaL* gene in TS-821 was cloned and analyzed, revealing that the gene product contains a short insert between the second and third predicted trans-membrane helices. Furthermore, phylogenetic analysis based on PsaL protein sequences revealed that TS-821 is closely related to heterocyst-forming cyanobacteria, some of which also have a tetrameric form of PSI.

The evolutionary process by which PSI evolved from a monomeric Type I reaction center in green bacteria into a trimeric complex found in most cyanobacteria is poorly understood (*47*). Neither the mechanism nor evolutionary pressure that drove the cyanobacterial trimeric form back to a monomeric form in plants and algae has been determined. However, our work indicates that structural changes in PsaL may be a widespread evolutionary event and provides additional insight about PSI evolution from cyanobacteria to chloroplasts. Additionally, the significance of PSI tetramer in PSI evolution and endosymbiotic origin of chloroplasts is discussed.

3.4 Results

Native Organization of TS-821 Photosystems

The robust and highly efficient nature of PSI (*48*) makes it very attractive for solar energy applications such as hydrogen production and photovoltaics (*97-99*). Therefore, we sought to isolate and characterize PSI from TS-821 for potential utilization in these applications. To identify the pigment-protein complexes in the thylakoids of TS-821, we used BN-PAGE as a rapid method for identification with a minimum potential for disruption or denaturation (*66*). TS-821 thylakoid membranes were solubilized in different concentrations of detergent dodecyl-maltoside (DDM) and analyzed via BN-PAGE. A similar analysis was performed on solubilized thylakoid membranes from the well-characterized thermophilic cyanobacteria *T. elongatus* as a control (Figure 3-1A). When the thylakoids were solubilized in low DDM concentrations (0.6 - 1.0% w/v), three major green bands and six other faint bands were observed. At a higher detergent concentration, the top green band disappeared, while the middle major green band increased. This result suggests a possible inter-conversion; however, in agreement with previous studies (*19, 64*), a similar solubilization of the *T. elongatus* thylakoids revealed predominantly PSI trimer, PSII dimer, and PSII monomer by BN-PAGE. The PSI trimer was smaller than the largest green band observed in TS-821 and was not affected by increasing the detergent concentration used for solubilization. Using the actual molecular weights of the *T. elongatus* photosystems (PSII monomer, 350 kDa; PSII dimer, 700 kDa; PSI trimer, 1068 kDa) (*18, 100*) as sizing standards in this gel system, the apparent

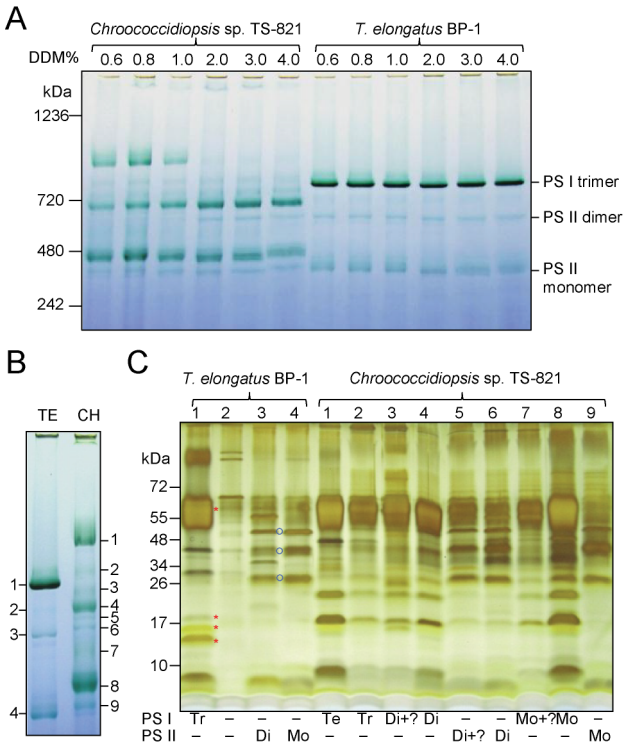

Figure 3- 1 Thylakoid membrane solubilization and photosystem identification

(A) BN-PAGE of solubilized thylakoid membranes from *Chroococcidiopsis* sp. strain TS-821 (CH) and *T. elongatus* BP-1 (TE). Thylakoid membranes containing 0.2 mg/ml Chl were solubilized in detergent DDM with different concentrations and loaded on a 4-16% BN-PAGE gel. The numbers above each lane indicate the concentration of DDM (w/v %). Soluble protein marker positions are indicated on left.

(B) BN-PAGE of 1% DDM solubilized thylakoid membranes (0.2 mg/ml Chl) from TE and CH. Visible bands before staining, as labeled, were cut out and denatured in SDS-PAGE sample solubilization buffer for following SDS-PAGE.

(C) SDS-PAGE of proteins from BN-PAGE. Characteristic subunit bands for PSI (red asterisks) and PSII (blue circles) from TE are used to identify photosystems in CH. The identification results are shown underneath each lane with the inference of monomer (Mo), dimer (Di), trimer (Tr), tetramer (Te) and uncertainty (?) indicated. Silver stain was used to visualize SDS-PAGE bands.

molecular weights of the three large green bands in TS-821 were ~400 kDa, ~800 kDa and ~1600 kDa (Figure 3-2). These values suggest a size distribution for monomer, dimer and tetramer forms of PSI, respectively. Furthermore, there is no prominent band corresponding to the trimer as was observed in the membranes from *T. elongatus.*

To further characterize and confirm the identity of each of the green bands observed by BN-PAGE, a second dimensional analysis using SDS-PAGE was performed. The BN-PAGE was repeated using 1.0% DDM solubilized thylakoid membranes (Figure 3-1B). Individual TS-821 green bands were carefully excised from the BN-PAGE and solubilized in SDS-PAGE sample buffer (*68*) and subsequently analyzed using SDS-PAGE with silver stain. For comparison, a similar treatment was applied to solubilized thylakoid membranes of *T. elongatus (*Figure 3-1C). The identity of the green bands corresponding to PSI and PSII was confirmed by the presence of characteristic subunit bands (PsaA/PsaB, PsaD, PsaF, D1/D2, CP47, and CP43) in the silver-stained SDS-PAGE gel. According to the individual subunit composition and apparent molecular weights of the different green bands, the oligomeric forms were identified as indicated at the bottom of each lane. This analysis verified that the three large green bands corresponded to PSI, and their native molecular weights indicate that they exist natively in monomeric, dimeric and tetrameric forms. Monomeric and dimeric PSII are identified in remaining green bands.

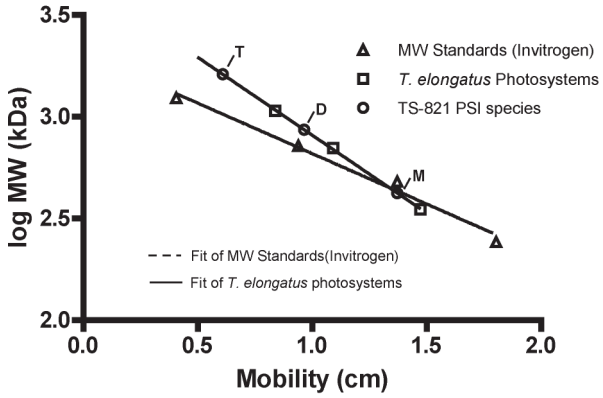

Figure 3- 2 Molecular weight estimation of TS-821 PSI using BN-PAGE.

Protein MW standards (Invitrogen) were initially used for molecular weights estimation. According to the fit (dash line) and the reported known photosystem crystal structures, the calculated molecular weights for *T. elongatus* PSI trimer and PSII dimer were underestimated. To estimate the molecular weights of TS-821 PSI, the photosystems from *T. elongatus* were used as molecular weight standards. The R^2 values of linear fits using protein MW standards (dash line) and *T. elongatus* photosystems (solid line) are 0.985 and 0.999 respectively. The calculated molecular weights for the three major green bands (Figure 3-1A) are 400 kDa, 800 kDa, and 1600 kDa, which represent the PSI monomer (M), dimer (D), and tetramer (T) respectively.

PSI Tetramer Isolation

To confirm the presence of PSI tetramer observed by BN-PAGE, a two-step SDGC fractionation similar to what has been reported for isolation of the *T. elongatus* PSI trimer was developed (*54*). After first SDGC, the tetramer was readily detected and collected (Figure 3-3A). The isolated PSI tetramer was analyzed by BN-PAGE (Figure 3-3C), which showed some contaminating proteins. This crude tetramer was loaded on a second sucrose gradient after dialysis and concentration. Four distinct green bands were observed following centrifugation, suggesting that the tetrameric PSI can disassemble into monomer and dimer, while the trimer may be from the first SDGC which did not separate the trimer from tetramer (Figure 3-3B). The oligomeric statuses of these four bands were confirmed by BN-PAGE (Figure 3-3C). The SDS-PAGE analysis of all four green bands from the second SDGC (Figure 3-4A) confirms that they are all TS-821 PSI complexes in different oligomeric states, possibly monomer, dimer, trimer, and tetramer.

TEM of Isolated PSI Particles

Upon isolation of the resolved tetrameric PSI particles by SDGC, their organization was investigated by STEM and TEM. Unlike the organization of the PSI trimer from *T. elongatus* (Figure 3-3D), the tetramer from TS-821 clearly reveals each of the four monomers organized in a somewhat “four-leaf clover” arrangement (Figure 3-3F). In comparison, the *T. elongatus* monomeric PSI isolated from dissociated PSI trimer tend to form chain structures or amorphous

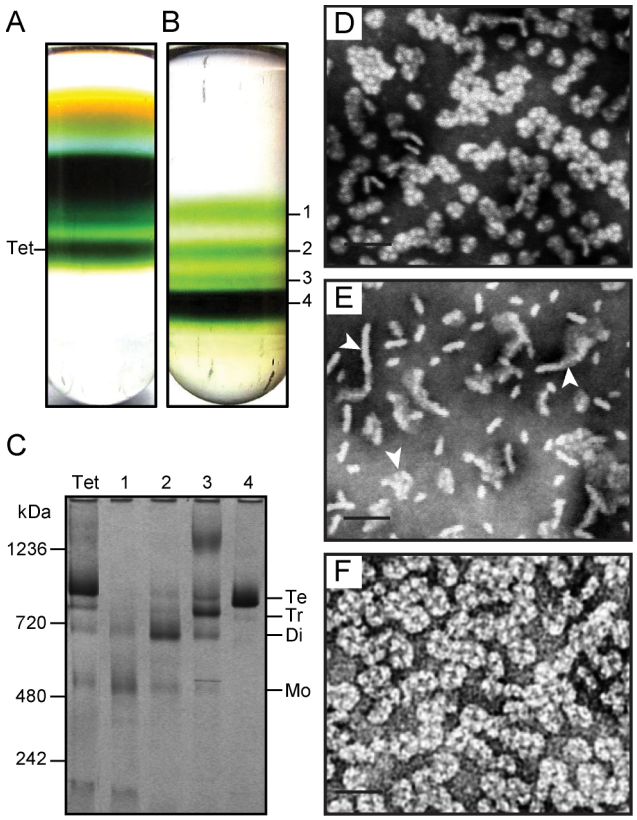

Figure 3- 3 Isolation of TS-821 PSI tetramer and proof of tetramer presence

(A) PSI tetramer (Tet) isolation from solubilized TS-821 thylakoid membrane using sucrose gradient ultracentrifugation.

(B) PSI separation in sucrose gradient after second ultracentrifugation. Tetramer isolated from thylakoid membranes was dialyzed and loaded on a second sucrose gradient to further purify the tetramer. Four bands as labeled were isolated and loaded on BN-PAGE for analysis.

(C) BN-PAGE analysis of PSI oligomers isolated from sucrose gradient ultracentrifugation. Image was taken after Coomassie Blue staining.

(D) STEM image of isolated *T. elongatus* PSI trimer.

(E) STEM image of isolated *T.elongatus* PSI monomer. Arrowheads point at examples of monomeric PSI aggregation.

(F) TEM image of isolated TS-821 PSI tetramer. Scale bars equal 50 nm.

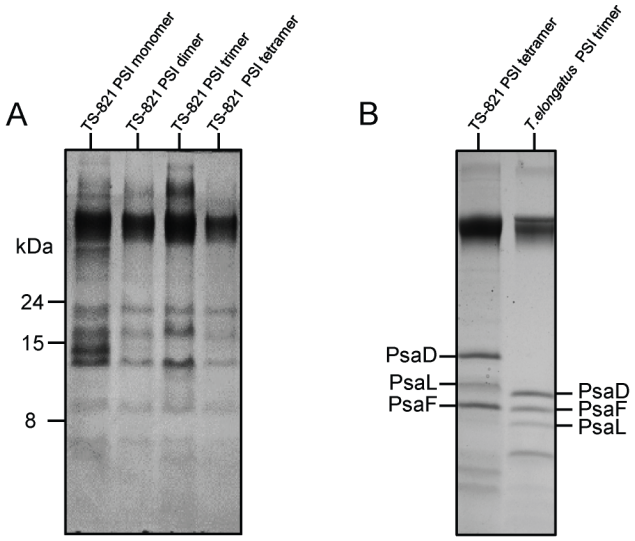

Figure 3- 4 SDS-PAGE of TS-821 PSI and *T. elongatus* PSI.

(A) SDS-PAGE of isolated TS-821 PSI monomer, dimer, trimer, and tetramer from second SDGC (Figure 2B).
(B) SDS-PAGE of isolated TS-821 PSI tetramer and *T. elongatus* PSI trimer. The PsaD, PsaF and PsaL subunits are labeled.

structures, as shown in Figure 3-3E. This result suggests that the TS-821 tetrameric PSI is unlikely resulted from monomeric PSI aggregation

Single Particle Analysis of TS-821 PSI

Upon isolation and staining with uranyl acetate we performed a TEM analysis of the single particles. Electron microscopy showed the presence of exclusively tetrameric PSI particles in different orientations on the carbon support film. Classification of projections showed that about 5,000 projections were more or less representing non-tilted views (Figure 3-5A), showing a two-fold symmetry. A two-fold rotational symmetry was also imposed on the 2D after processing

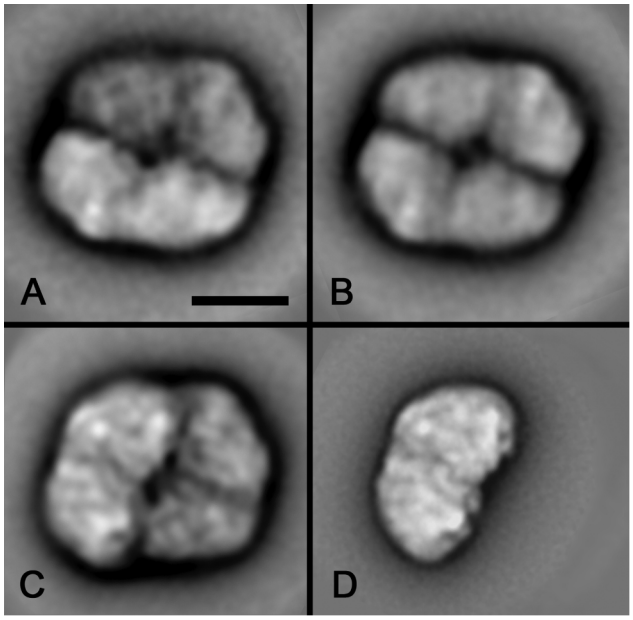

Figure 3- 5 Final two-dimensional maps of TS-821 PSI after single particle averaging with classification.

(A) Close-to non-tilted map of tetramers, best 1024 particles out 5,000.

(B) Map of frame A, with 2-fold rotational symmetry imposed.

(C) A typical tilted map of 2048 summed particles from a homogeneous class of in total 10,000 projections.

(D) Map of biochemically isolated PSI dimer, best 2048 particles out 8,000. Scale bar equals 10 nm.

This figure was generated by our collaborators in Dr. Boekema's group at University of Groningen.

(Figure 3-5B). The majority of 25,000 particles were substantially tilted on the support film (Figure 3-5C). The maps indicate that although the complex is clearly composed from 4 PSI monomers, the association of these monomers is in such a way that it creates a pseudo-tetramer with just two-fold rotation symmetry, which is compatible to a situation in with two PSI dimers associate into a tetramer. The averaged image of biochemically isolated TS-821 PSI dimers (Figure 3-5D) is also consistent with the PSI tetramer being composed of a dimer of dimers, yet the precise orientation and assembly interface is not clear from this analysis.

TEM of Native Membranes Reveal PSI Tetramers

To investigate if PSI tetramer exists in native thylakoid membrane, the TEM images of TS-821 thylakoids were acquired (Figure 3-6A). The particles with right size according to isolated PSI tetramer (Figure 3-5) were picked and analyzed (Figure 3-6B). The averaged image (Figure 3-6C and D) of those particles showed high similarity to isolated PSI tetramer. This indicates the presence of PSI tetramer in the native thylakoid membrane of TS-821.

Characterization of Tetrameric PSI

Both BN-PAGE and SDGC showed that TS-821 PSI exists as a tetramer, with significant amounts of dimeric and monomeric forms, and very little trimer. The dimeric forms could reflect intermediates during tetramer assembly or possibly be the result of disassembly due to detergent disruption. To test the latter possibility, the purified tetramer was treated with increasing concentration of DDM, which resulted in decreased amount of tetramer and increased amount of dimer and monomer (Figure 3-7A). Quantification of the different oligomeric

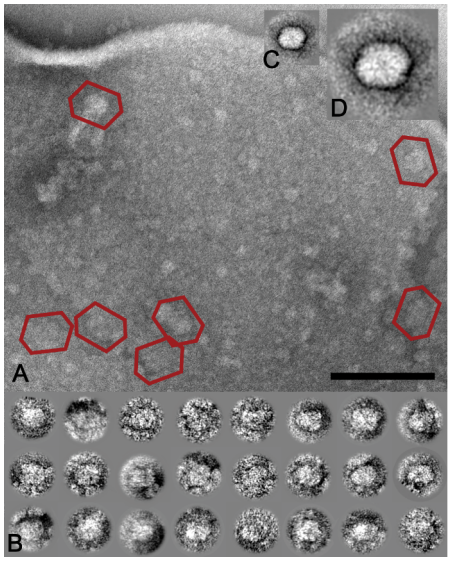

Figure 3- 6 Visualization of tetrameric PSI complexes in TS-821 thylakoid membrane

(A) Overview of a part of a double thylakoid membrane depicted in a thick layer of negative stain (2% uranyl acetate). Some visible tetrameric PSI particles are marked by red boxes.

(B) A gallery of 24 particles, selected from a series of membranes.

(C) An average of the best 47 projections (out of 150 selected), presented on the same scale as the membrane.

(D) Same average as in C, magnified 2x. Scale bar for A,B and C equals 100 nm.

This figure was generated by our collaborators in Dr. Boekema's group at University of Groningen.

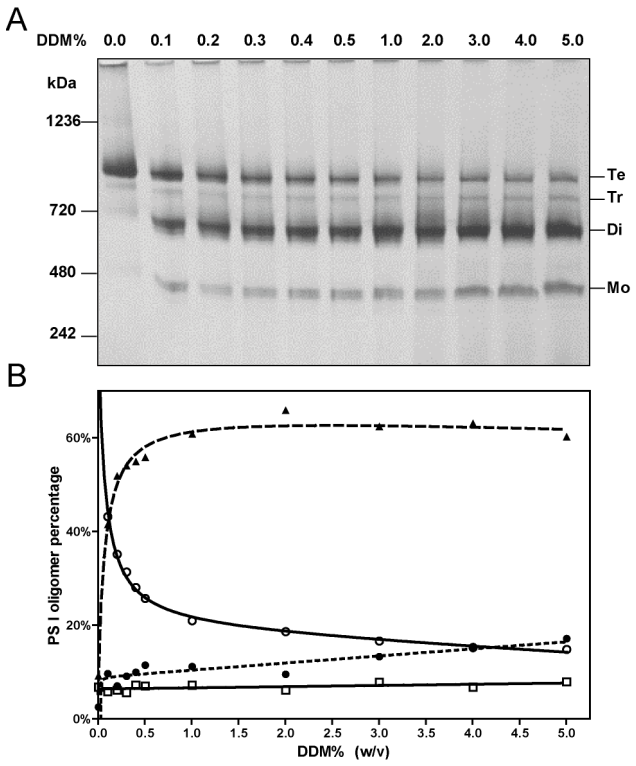

Figure 3- 7 Purified PSI Tetramer Dissociation upon Detergent Treatment.

(A) BN-PAGE analysis of purified PSI tetramer treated using different amount of detergent DDM. The final concentrations of DDM (w/v %) are shown on top of each lane. The final concentration of Chl for each lane is 0.15 mg/ml.

(B) Percentages of PSI oligomers under different DDM concentration. The percentages of TS-821 PSI Monomer (filled circle, ●), dimer (filled triangle, ▲), trimer (open square, □), and tetramer (open circle, ○) under different concentrations of DDM are shown.

forms (Figure 3-7B) suggested that the tetramer disassembles into the dimer directly, which appears quite stable since it only partially disassembled into the monomer. This can be explained by the structural features of TS-821 PSI tetramer and dimer: a tetrameric PSI has two PSI dimers associated together with inter-dimer gaps while the PSI dimer is composed of two tightly tethered PSI monomers (Figure 3-5). Interestingly, the amount of trimer remained low and did not change as a function DDM concentration. This correlation would suggest that the trimeric form is not only a minor component in thylakoids based on BN-PAGE, but is unable to form a stable intermediate or undergo inter-conversion with the other oligomeric forms. The different oligomeric forms of many cyanobacterial PSI display altered emission peaks in low temperature fluorescence (77 K). The *Spirulina platensis* and *T. elongates* PSI trimer have an emission peak at ~730 nm with the monomer emission blue-shifted to ~715-725 nm (*70, 101*). The 77 K fluorescence showed that TS-821 PSI monomer, dimer, and tetramer share a common emission peak at 715 nm (Figure 3-8A); however, similar analysis of the isolated monomers and trimers from *T. elongatus* display different peak emissions, in agreement with previously published values of <725 nm and ~730 nm, respectively (Figure 3-8A). The blue shift in the 77 K fluorescence to the lower value of 715 nm suggests that the Chl emission in all three forms of the TS-821 PSI complex share a similar environment and lack the far-red form that is associated with the trimeric form of other cyanobacterial PSI complexes.

Consequently, some of the tetrameric Chls could experience a “monomeric-like” environment. Interestingly, the organization of the tetramer as

Figure 3- 8 Properties of TS-821 PSI tetramer

(A) Low temperature fluorescence of TS-821 PSI monomer (M), dimer (D) and tetramer (Tet), compared with *T. elongatus* (TE) PSI trimer and monomer.
(B) Low temperature fluorescence of TS-821 whole cell and isolated PSI compared with those from *T. elongatus*.
(C) AUC analysis of TS-821 PSI tetramer. The dashed line denotes previously published S value of the PSI trimer from *T. elongatus* (Iwuchukwu et al., 2010).
(D) Thermostability of PSI tetramer inferred from the CD spectra. Triangles indicate the maximum absorbance around 515 nm and circles show those around 705 nm.
(E) PSI tetramer reduction using *T. elongatus* cyt c_6. Different concentrations of cytochrome were used. Circle, square, triangle and upside down triangle show the cytochrome c to PSI ratio of 0, 10, 20 and 40 respectively.
(F) Photo-oxidation of TS-821 PSI monomer, dimer and tetramer with different light intensities. The same graph with linear light intensity axis is shown in the embedded panel which shows the saturation of the oxidation.

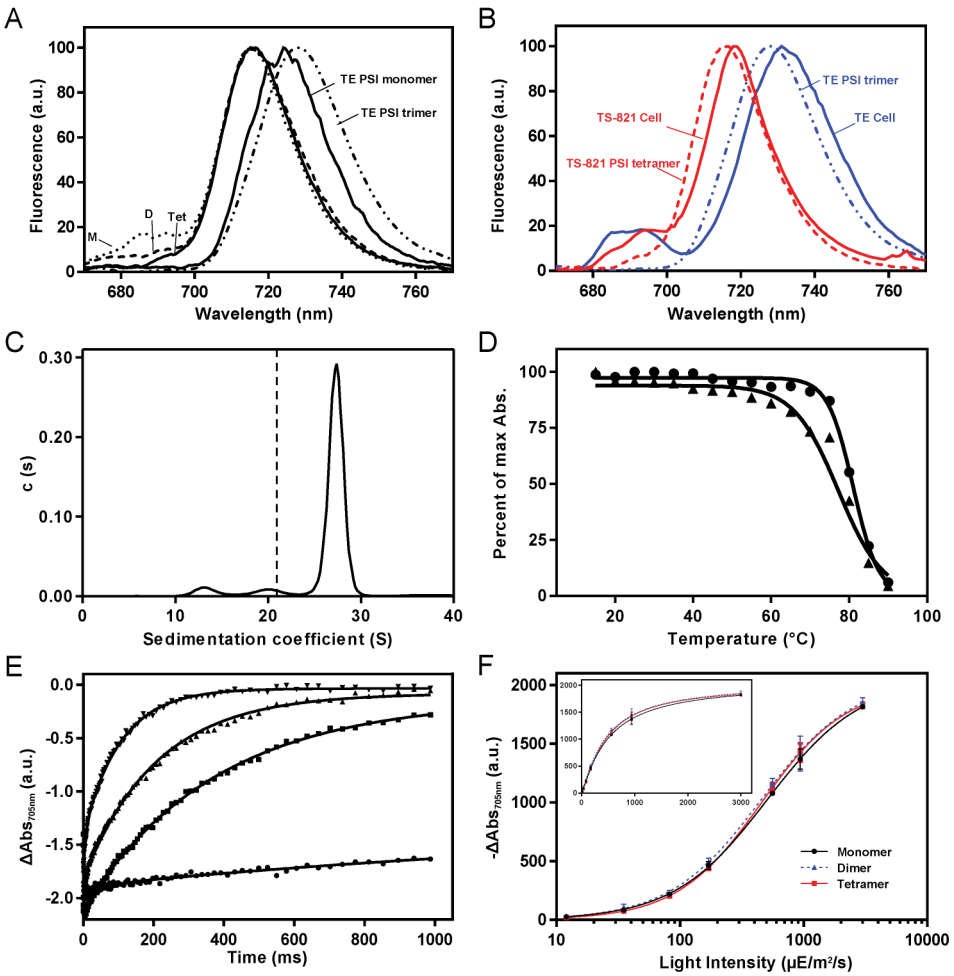

Figure 3-8 continued

reveled from the single particle analysis reveals a central cavity of low electron density (shown most clearly in Figure 3-5B). This is contrast to a more uniform density that exists between the individual monomers observed in the TEM of the trimeric structures (*10, 51*). Although we do not know the chemical composition of this central cavity, it is clearly different than observed in trimeric PSI preps and most likely is filled with lipids and/or detergent molecules. This may provide a similar environment to the far-red chlorophyll molecules as observed in monomeric PSI isolated from native or salt and heat treated thylakoid membrane (*70, 101*). To confirm that the characteristic emission of isolated TS-821 PSI is in its native form, the whole cell emission spectrum was obtained as well (Figure 3-8B). The comparison of whole cell emission at 77K and that from isolated PSI reveals a 3 nm blue shift of the emission peak of PSI upon isolation; this 3 nm blue shift is also observed in *T. elongatus* PSI (Figure 3-8B). This indicates that the TS-821 PSI is present in a tetramer/dimeric/monomeric form in thylakoid membranes.

Since BN-PAGE can be influenced by variations in anionic lipid composition and/or variations in binding of the negatively charged dye Coomassie brilliant blue, which individually or together could alter electrophoretic mobility, an independent means of assessing the size of the tetramer was needed to confirm the results from BN-PAGE. Therefore, AUC was performed using velocity sedimentation. This assay allowed the determination of the sedimentation coefficient of the TS-821 PSI tetramer while also allowing direct comparison to the monomer and trimer forms of *T. elongatus* PSI. The TS-821

PSI tetramer has a sedimentation coefficient value of 28S (Figure 3-8C). These values contrast with those of the isolated *T. elongatus* PSI trimer and monomer, which are 21S (dashed line in Figure 3-8C) and 12S, respectively (*54*). These AUC results clearly support the identity of the larger species as a tetramer.

To investigate the thermostability of the PSI complex, the decrease in circular dichroism signal of the Chl molecules was monitored with respect to increasing temperature. This approach has been shown to differentiate the thermostability of the bulk antenna Chl as well as the special pair associated with P_{700}. This assay can differentiate the thermostability of PSI complexes from mesophilic cyanobacteria and thermophilic cyanobacteria (*54*). The CD spectra of *Chroococcidiopsis* PSI tetramer (Figure 3-9) showed a similar pattern to that of *T. elongatus* PSI trimer as described in the previous study (*54*). Based on the peak values from antenna Chl (509-515 nm) and P_{700} (701-707 nm), the denaturing profile was shown in Figure 3-8D. The curve was fit using Boltzmann sigmoidal distribution, and the estimated T_m values for antenna Chl and P_{700} were 77°C and 81°C respectively (Figure 3-8D).

To confirm the photochemical activity of the PSI tetramer, we investigated both the photo-oxidation at 705 nm and its re-reduction using a recombinant cyt c_6 from *T. elongatus* expressed in *E. coli.* The ability of photo-bleached P_{700} to recover was dependent on the presence of cyt c_6. As the molar ratio of cyt c_6/PSI was increased the rate of re-reduction increased, yet it did not saturate at the highest level (cyt c_6/PSI=40) tested (Figure 3-8E). This suggests that PSI in TS-821 is similar to *T. elongatus* PSI in using c-type cytochrome as its electron

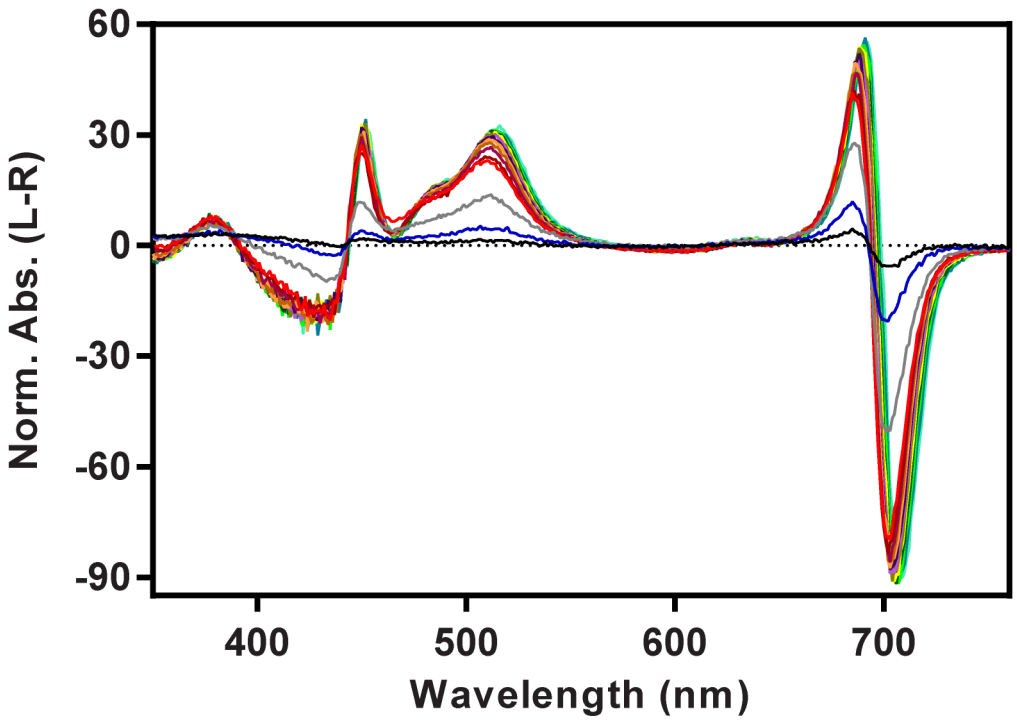

Figure 3- 9 CD spectra of TS-821 PSI tetramer at different temperatures

As temperature goes up from 15˚C to 90˚C by 5˚C steps, the peak values decrease.

donor. A previous study showed the different light-intensity dependent photo-oxidation profiles between *T. elongatus* PSI trimer and monomer (*55*). A similar experiment was carried out to compare the photo-oxidation properties among TS-821 PSI monomer, dimer and tetramer (Figure 3-8F). In contrast to the significant cooperativity in *T. elongatus* PSI trimer, with a Hill coefficient at 1.4 (*55*), our results showed the hill coefficients for TS-821 PSI monomer, dimer, and tetramer are 1.15±0.08, 1.17±0.15, and 1.26±0.09. This indicates the PSI tetramer and dimer have very low, if any, cooperativity.

Cloning of *psaL* Gene

Based on the crystal structure and gene deletions, PsaL has been reported as important for PSI trimerization in most cyanobacteria, and its absence results in the loss of the trimer (*22, 25, 26*); therefore it is of interest to compare the PsaL proteins associated with this tetramer with those PsaL proteins from cyanobacteria that form trimers. The PsaL subunit in TS-821 was suspected to be larger as indicated by comparison of subunits of purified PSI tetramer and purified *T. elongatus* PSI trimer via SDS-PAGE (Figure 3-4B). A band corresponding to PsaL in *T. elongatus* PSI trimer was not obvious in the tetramer, yet an additional subunit in the tetramer was observed with an apparent molecular weight of ~20 kDa that was not present in *T. elongatus* PSI trimer. The difference in PsaL gene products may explain the differences in PSI oligomeric state.

In order to identify the possible structural reason for why TS-821 PSI forms tetramers and not trimers, the *psaL* gene from TS-821 was cloned and

sequenced. The TS-821 *psaL* gene was cloned initially using conserved region of *psaL* gene among heterocyst-forming cyanobacteria as described in material and methods. The full-length gene and some flanking sequences were cloned using primers that were taken from the known sequence after first partial *psaL* cloning (Figure 2-6A). Sequencing of this larger genomic fragment allowed the general organization to be of determined. Comparison of this genomic structure to other cyanobacteria is shown in Figure 2-6B. It is clear that the TS-821 *psaL* gene has both *psaF* and *psaJ* genes upstream and the *gmk* gene downstream, which is similar to the gene arrangement in heterocyst-forming cyanobacteria. Most of the other cyanobacterial *psaL* genes are located adjacent to *psaI* gene. This PsaI subunit has also been reported to stabilize the PSI trimer (*24, 25*). Interestingly, some hetero-cyst-forming cyanobacteria as well as close relatives (highlighted species in clade III in Figure 3-10B), such as *Chroococcidiopsis thermalis* PCC 7203, have two different copies of *psaL*. Moreover these two genes are also organized differently in their genomes. One organization, mostly having tetrameric PSI, is quite conserved with *psaL* positioned adjacent to *psaF*, *psaJ*, and *gmk* and the other organization, mostly PSI trimer, has the *psaL* gene placed close to *psaI*, which is often flanked by different unrelated genes (Figure 2-6B).

TS-821 *psaL* encodes a 172 a.a. protein with a molecular weight of 18.5 kDa. To verify the identity of this *psaL* gene product, LC-MS/MS was done using both the intact PSI tetramer complex and the individual subunits upon separation by SDS-PAGE and gel band excision. This proteomic analysis was conducted

Figure 3- 10 Alignment of selected PsaL sequences and phylogenetic tree based on PsaL protein sequences

(A) Alignment of TS-821 PsaL (TS-821, sequence acquired in this study) with other PsaL sequences from *T. elongatus* BP-1 (TE), *Synechocystis*, *Chlamydomonas*, and *Arabidopsis*. Putative trans-membrane helices are highlighted according to the available structure in PDB, 1JB0. The major differences of PsaL sequences among different species are underlined.
(B) Phylogenetic tree of cyanobacteria and plastids based on PsaL protein sequences. Heterocyst-forming cyanobacteria are denoted with filled diamonds (◆) while other filamentous cyanobacteria are labeled with open diamonds (◇). Cyanobacteria that have two different PsaL sequences in this alignment are highlighted. Known PSI trimers (▲) and tetramers (□) are labeled at the end of the species' names. Species having two different PsaL sequences are highlighted. Bootstrap values of Maximum Likelihood and Neighbor Joining method are shown at each branch point, upper and lower respectively. Viridiplantae and Rhodoplantae are denoted as V and R respectively in circles. Three major cyanobacterial clades are numbered as I, II, III in circles as well.

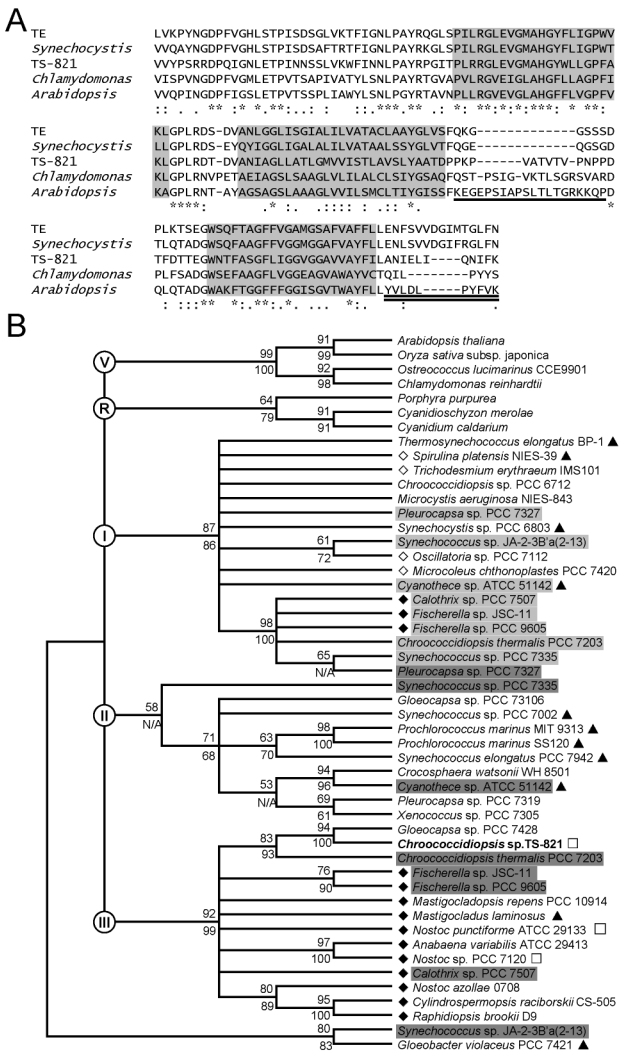

Figure 3-10 continued

using the genomes from closely related cyanobacteria yet still convincingly showed that the ~20 kDa subunit is PsaD and the following smaller band is PsaL (Figure 3-4B and Figure 3-11). Compared with *T. elongatus* and *Synechocystis* PsaL, the PsaL proteins in TS-821, *Chlamydomonas* and *Arabidopsis* have shorter C-termini but contain longer loop insertions between trans-membrane helices 2 and 3 (Figure 3-10A). Our proteomic results confirmed that the TS-821 PsaL is derived from our cloned gene and contains a longer insertion compared with *T. elongatus* and *Synechocystis* PsaL; however, the insertion is still shorter than in green algae and plants (Figure 3-10A) which have monomeric PSI.

Phylogenetic Analysis

To understand the evolutionary significance between PSI tetramer and PsaL, a phylogenetic tree was built based on PsaL protein sequences of cyanobacteria, rhodophyta, chlorophyta, and plants (Figure 3-10B). The un-rooted tree was re-rooted using *Gloeobacter* and its close relative as an outside group. Cyanobacteria basically fall into three clades: *Thermosynechococcus* related clade, *Prochlorococcus* related clade, and heterocyst-forming cyanobacteria clade (denoted as clade I, II, and III respectively in Figure 3-10B). TS-821 falls in clade III, which indicates its close relationship to heterocyst-forming cyanobacteria. PSI tetramer has only been reported in this cyanobacterial clade (*19, 20*). Many cyanobacteria have two different copies of *psaL* gene (highlighted in Figure 3-10B). For instance, some heterocyst-forming cyanobacteria in clade III such as *Fischerella* sp. JSC-11 also have a second PsaL-encoding gene that belongs to the *Thermosynechococcus* related clade I.

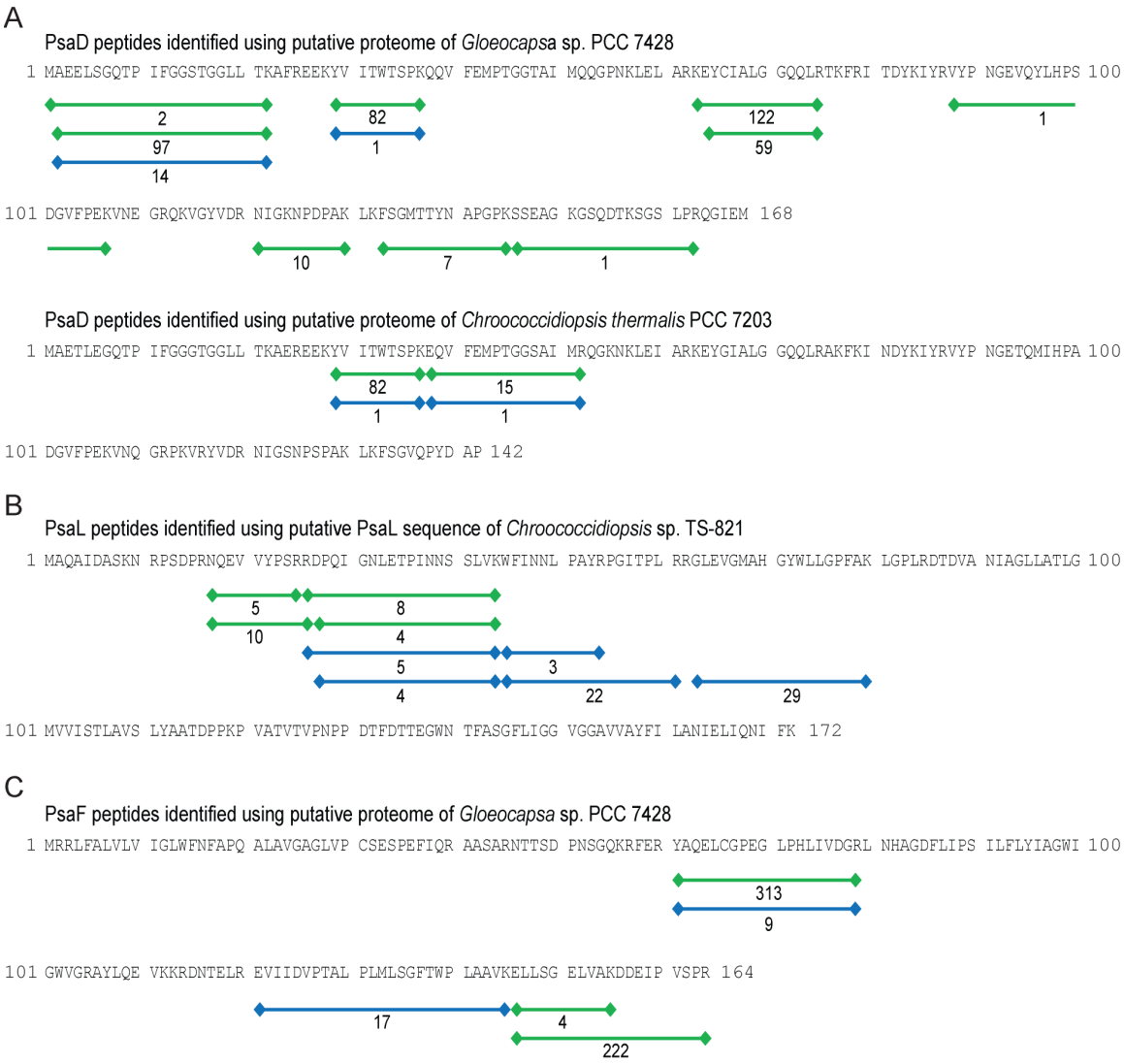

Figure 3- 11 LC-MS/MS identification of subunits in TS-821 PSI tetramer

(A) TS-821 PsaD peptides identified by searching against proteomes of *Gloeocapsa* sp. PCC 7428 and *Chroococcidiopsis thermalis* PCC 7203.

(B) TS-821 PsaL peptides identified by searching against TS-821 PsaL sequence.

(C) TS-821 PsaF peptides identified by searching against proteome of *Gloeocapsa* sp. PCC 7428.

Distinct peptides identified using PSI tetramer whole protein complex and separated bands after SDS-PAGE (Figure 3-4B) are denoted using green and blue bars respectively. The number of filtered spectra for each distinct peptide is shown under the bar.

It would be interesting to see if PSI in these cyanobacteria forms both a tetramer and a trimer. According to the phylogenetic analysis based on PsaL sequences, eukaryotes do not belong to any modern cyanobacterial clade studied, indicating the deep evolutionary origin of eukaryotic PsaL, shown as clade V and R for Viridiplantae and Rhodoplantae respectively (Figure 3-10B).

3.5 Conclusions and Discussion

Tetrameric PSI Exists in *Chroococcidiopsis* sp. TS-821

Using very similar conditions that have been developed for other thermophilic cyanobacteria (*17, 19, 54*), we have verified the presence of PSI tetramer in TS-821. BN-PAGE and SDS-PAGE analysis of thylakoids showed the majority of TS-821 PSI is present in the membrane as either a tetramer or dimer with a significant amount of monomer (Figure 3-1). Similar analysis of thylakoids from *T. elongatus* revealed predominantly trimeric form of PSI. Interestingly, the thylakoids of TS-821 show very small amounts of a green band with a similar molecular weight to a PSI trimer (Figure 3-1B). The presence of multiple forms of PSI suggest that there may be some equilibrium between the monomer, dimer, and tetramer and may suggest a step-wise process of assembly.

The PSI tetramer, with a sedimentation coefficient of 28S (Figure 3-8F), can be isolated using SDGC for further analysis. The electron micrograph showed the organization of the PSI tetramer comprising four monomers that are somewhat loosely tethered in the center, forming a dimer of dimers (Figure 3-3F and Figure 3). Noticeably, there is a cavity in the center of the PSI tetramer, not observed in the native membrane, which may harbor some cofactors or lipids

that are washed away during preparation. This four-leaf clover structure allows considerable more solvent access to each monomer than what is observed in the relatively tightly organized trimer that has been observed for the *T. elongatus* trimer in this work and others (*54*). In addition, careful TEM analysis also rule out the possibility that the larger PSI complex observed was larger due to the association with additional antennae complexes, such as IsiA as has been observed in some iron-stressed cyanobacteria (*51, 102-105*).

The fact that we observe this tetramer in native membranes prior to detergent solubilization confirms that this tetrameric PSI is not an artifact that results from aggregation on monomers or some other membrane protein complex (Figure 3-6). A second argument against and artifactual self-assembly is the failure of *T. elongatus* monomers to reassembly into a tetrameric structure following their monomerization (Figure 3-3E). These monomers form larger aggregates that may result from hydrophobic interactions, similar to what has been observed for plant PSI preparations (*40*). Analysis of the isolated TS-821 tetramer by BN-PAGE indicates that this high molecular weight species remains even when high levels of detergent are added (5% DDM) (Figure 3-7), suggesting the tetramer is unlikely an artifact arising from insufficient detergent solubilization. Furthermore, the 77K fluorescence emission spectra of TS-821 whole cell and PSI (Figure 3-8B) confirm the presence of tetrameric PSI in the thylakoid membrane before isolation and solubilization.

Due to the novel size and organization of the PSI tetramer, we wanted to further investigate the functional properties of this new form of PSI. One of the

features of trimeric PSI observed in most cyanobacteria is the presence of a low temperature, far-red fluorescent species. This species is lost when the complex is denatured, dried, or exposed to high levels of detergent (*106*). This shift in emission wavelength between the PSI monomer and trimer forms has been observed in various cyanobacteria (*70, 101, 107, 108*) with the PSI trimer containing more far-red Chls. It has been observed that in *T. elongatus* this far-red species is lost or significantly shifted to the blue in the monomeric form (*70*). Interestingly, in TS-821, the tetrameric PSI does not contain a prominent far-red fluorescent species. As shown in Figure 3-8A, the emission spectra of the TS-821 PSI monomer, dimer and tetramer preparations are nearly the same. According to a previous study, some far-red Chls are located in the interfaces between trimeric PSI monomers (*70*). In contrast to the PSI trimers, TS-821 PSI tetramer showed almost no difference from dimer and monomer in low-temperature fluorescence emission. These results suggest a model that four PSI monomers interact with each other without the involvement of interfacial Chls, which, in contrast, are key components of PSI trimer in *T. elongatus* (*18*). This model is consistent with the TEM images showing that two PSI monomers assemble at a 180-degree angle (Figure 3-5) instead of 120 degree in PSI trimer as viewed from the stromal or lumen side. Whether the far-red Chl molecules are simply missing in TS-821 or alternatively their emission properties reflect a different chemical environment is not known.

Unique PsaL in TS-821 May be Responsible for the Formation of PSI Tetramer

PsaL probably plays an important role in PSI tetramerization in TS-821 as well as in trimerization in other cyanobacteria. Using an alignment of several *psaL* sequences we were able to design primers to enable the PCR amplification of the TS-821 *psaL* gene. Proteomic analysis identified 9 different peptides (covering 37% of the coding sequence as shown in Figure 3-11) that confirmed that this protein is encoded by the *psaL* gene that we cloned (Figure 2-6A). Based on this gene sequence and proteomic data, the TS-821 PsaL has a shorter C-terminus and a longer insertion between trans-membrane helices 2 and 3 than PsaL in *Synechocystis* PCC 6803 and *T. elongatus* (Figure 3-10A). The distinct features of PsaL in TS-821 tetramer are also present in PsaL from the organisms shown in Clade III of Figure 3-10B, and the sequences are shown in Figure 3-12. Interestingly, this clade includes *Nostoc* sp. PCC 7120 which also has been shown to contain a tetrameric form of PSI (*19, 20*). While the longer insertion in TS-821 can make PsaL more flexible for conformational changes, the C-terminus of PsaL is believed to stabilize the PSI trimer (*45*). Collectively, this data suggests that the structural differences in PsaL are responsible for the different oligomeric forms of PSI. To test this hypothesis, we have replaced the *psaL* in *Synechocystis* with TS-821 *psaL* using homologous recombination. Although we were successful in replacing this gene, the result was congruent to deleting the entire *psaL* gene because both formed exclusively monomeric PSI lacking PsaL (Figure 2-7). This result suggests that the TS-821 PsaL protein is

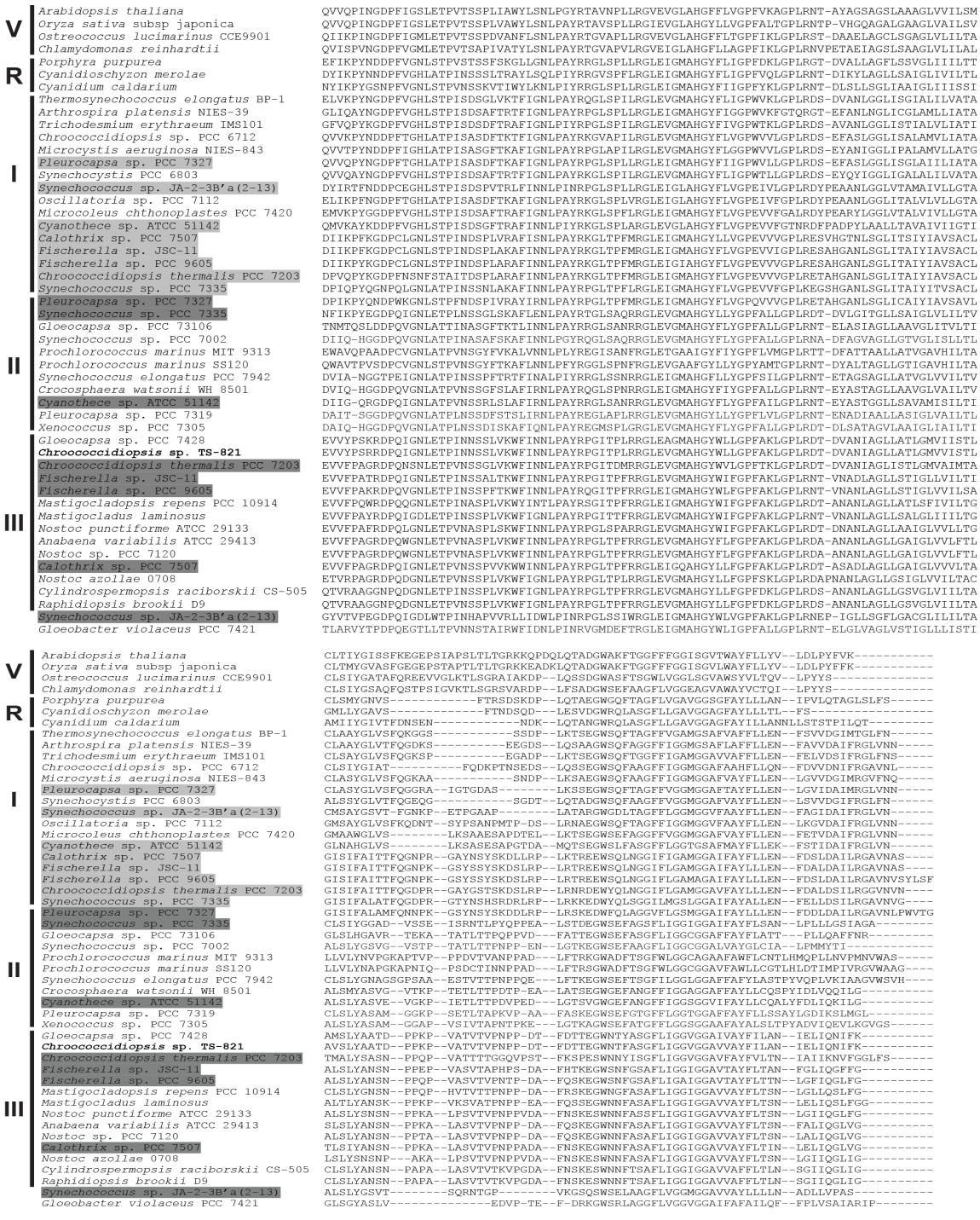

Figure 3- 12 PsaL alignment for phylogenetic analysis

Strains that have two different PsaL sequences are highlighted in accordance with Figure 3-10.

not expressed or possibly not correctly inserted into the thylakoids. One possible explanation is the different codon usage between *Synechocystis* and TS-821. The TS-821 *psaL* gene has a Codon Adaptation Index (CAI) of 0.41 vs. 0.69 for the native *Synechocystis psaL* gene. Although the relationship between the difference of PsaL and tetrameric PSI formation is not proven, numerous studies have shown that PsaL is needed for cyanobacterial PSI monomers to form trimers (*22, 25, 26*). Based on the crystal structure of the *T. elongatus* PSI, it is clear that PsaL forms the organizational center of the trimer (*18*). In addition to a significant structural role in known PSI trimers, the PsaL sequence has the highest diversity among all the cyanobacterial PSI subunits (*109*). The variation suggests that PsaL differences may explain the diversity in PSI oligomeric forms.

Heterocyst-forming Cyanobacteria and Their Close Relatives May All Have Tetrameric PSI

Based on the phylogenetic analysis of the PsaL sequences we can place TS-821 in the clade III that includes heterocyst-forming cyanobacteria such as *Fischerella* and *Mastigocladus*. However, TS-821 was initially characterized and named according to its morphological and physiological properties (*94*). Fewer *et al*. reported that *Chroococcidiopsis* is a close relative to heterocyst-forming cyanobacteria based on the cyanobacterial 16S RNA sequences (*78*). Our phylogenetic analysis based on PsaL protein sequences (Figure 3-10B), as well as the genomic organization of the *psaL* gene (Figure 2-6B), also places TS-821 very close to the heterocyst-forming group of cyanobacteria (Figure 3-10B). Similar to what we discovered in TS-821, tetrameric PSI has been reported in

heterocyst-forming cyanobacterium *Nostoc* sp. PCC 7120 (*19, 20*). The heterocyst PSI in *Nostoc punctiforme* shown on BN-PAGE by Cardona *et al*. (*49*) was interpreted as a tetramer by Watanabe *et al.* (*19*). All these data, along with our phylogenetic tree suggest that all cyanobacteria in Clade III may have tetrameric PSI. Even though PSI trimer in heterocyst-forming cyanobacterium *Mastigocladus laminosus* was reported (*17*), this conclusion does not rule out the possible presence of PSI tetramer in *M. laminosus* because of the different PSI purification method used. Some of the heterocyst-forming cyanobacterial genomes (for example, *Fischerella* and *Calothrix*) contain two *psaL* genes, one of which falls into the trimer forming Clade I and the second aligns with the tetrameric forming Clade III (Figure 3-10B). It is quite plausible that some cyanobacteria in Clade III have both trimeric and tetrameric PSI either in different cells types or possibly in response to different environmental or physiological conditions. More studies on PSI organization from other heterocyst-forming cyanobacteria are needed to verify this possibility. Unlike the heterocyst-forming cyanobacteria (clade III), almost all other cyanobacteria have trimeric PSI and their PsaL is phylogenetically clustered into either clade I or II (Figure 3-10B).

The tetrameric PSI, in equilibrium with dimeric and monomeric PSI, can represent a more versatile form of PSI oligomer, compared with tightly associated trimeric PSI.

Tetrameric PSI May be an Evolutionarily Advanced Form of PSI Oligomer

As shown in previous study, the trimeric PSI has a higher cross section compared with monomeric PSI (*55*), which indicates the trimeric PSI is a more

efficient form especially under low light intensity. This agrees with the earlier finding that *Synechococcus psaL* knockout mutant grows slower than wild type under green light (*25*). In contrast to the disadvantage of having a monomeric PSI, the *psaL* mutants of *Synechocystis* and *Synechococcus* showed faster growth rates than wild-type cells when DCMU was added with glucose supplement (*22, 25*). These results indicate somewhat advantages of having a monomeric PSI, which is supported by later observation that both *Synechocystis* and *Synechococcus* downregulate the expression level of PsaL and make more monomeric PSI lacking PsaL under iron deficiency stress (*31*). In summary, PSI monomer is favored when cyanobacteria deal with stresses possibly including high light intensity. With tetrameric PSI, which is more readily to dissociate into monomers, TS-821 and other cyanobacteria in Clade III can potentially respond to stress or environmental changes faster. Even though the tetrameric PSI does not possess similar high cooperativity to PSI trimer (*55*), the direct attachment of phycobilisome to tetrameric PSI in *Nostoc* sp. PCC 7120, in favor of cyclic electron transfer and ATP production in heterocyst, was shown (*20*). This indicates that tetrameric PSI has a higher absorption cross section *in vivo* and hence higher light energy conversion efficiency (*20*). Therefore, the tetrameric form of PSI, attaching to phycobilisome and interconverting with monomeric PSI, may represent a more versatile and advantageous form of PSI in clade III cyanobacteria.

Tetrameric PSI can be the transition form in evolution from cyanobacterial trimeric PSI to plant monomeric PSI. While most cyanobacterial PSI have been

isolated as trimers, PSI from plants are monomeric (*39*). According to our phylogenetic analysis, PSI can be grouped into three categories: exclusively monomeric (Clade R and V), predominantly trimeric (Clade I and II), and tetrameric (Clade III) (Figure 3-10B). PSI organization in *Gloeobacter violaceus,* a very primitive cyanobacteria (*110*), is also a trimer (*16*), which indicates that trimeric PSI is ancestral to both the tetrameric and monomeric PSI. Besides the discovery of PSI tetramer in TS-821 and *Nostoc*, tetrameric PSI has also been observed in glaucophyte *C. paradoxa* (*19*). Glaucophytes, green algae and land plants share the same plastid ancestor, while glaucophytes are considered to be more primitive (*111*). All those data combined, suggest that PSI evolved from a stable trimer to a metastable tetramer before becoming exclusively monomeric in plants. A model of this evolutionary transition is shown in Figure 3-13. Some reviews have pointed out that the modification of PsaL C-terminus and the emergence of PsaH in plant PSI led to the monomeric form of PSI in plants (*45-47*). In plant PSI monomer, according to the available crystal structure (*42*), the longer insertion between trans-membrane helix 2 and trans-membrane helix 3 in PsaL is in close vicinity of PsaH, which indicates their potential interaction that stabilizes the monomeric form of PSI. This insertion, along with short C-terminus, is also found in PsaL of tetrameric PSI (Figure 3-10 and Figure 3-12), which further indicates that tetrameric PSI may be an intermediate form during the evolution of the PSI in higher plants and green algae.

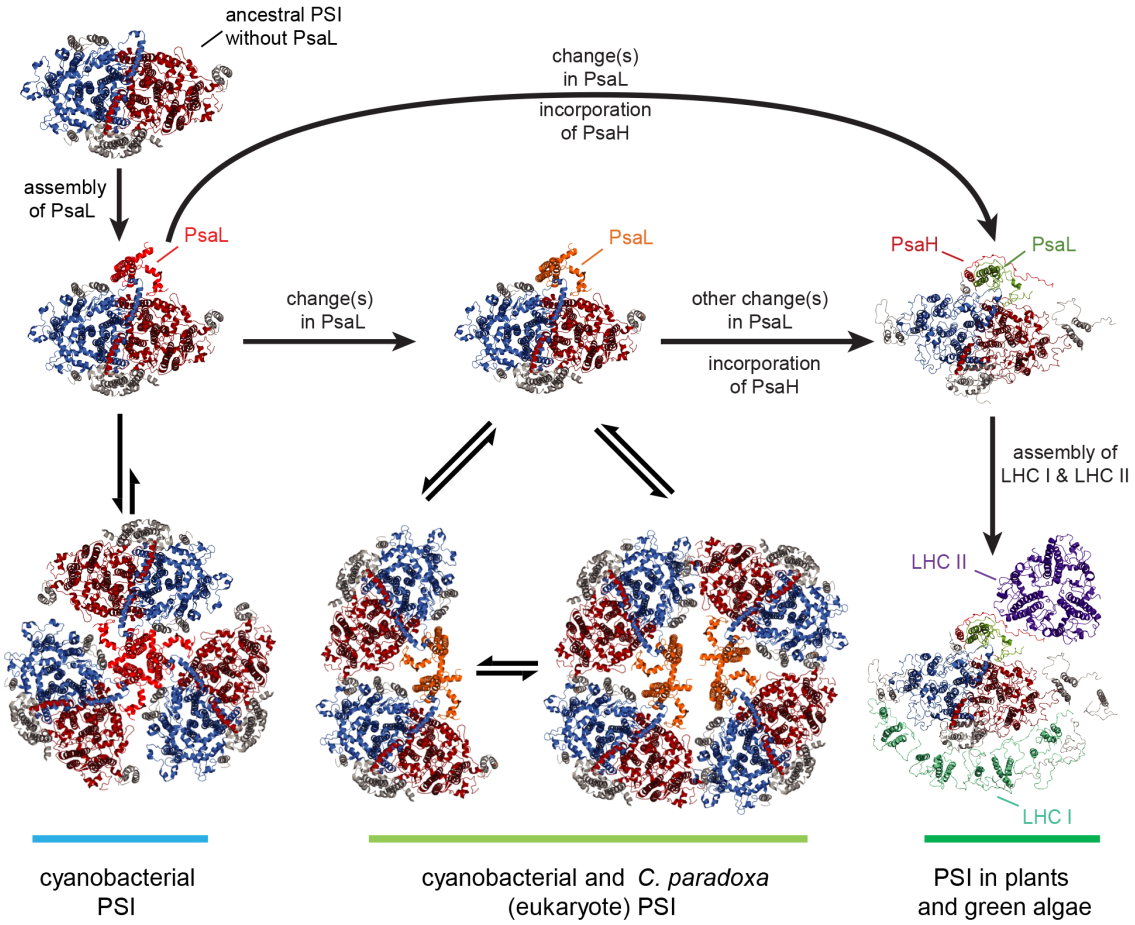

Figure 3- 13 Photosystem I evolutionary model

Cyanobacterial PSI was evolved from the ancestral PSI without PsaL. The advent of PsaL in cyanobacteria promotes the trimerization of PSI while the PSI trimer dissociation is not favored. As PsaL evolved with structural modification, PSI trimer becomes less favorable. PSI monomers form dimers and tetramers which in turn dissociate into monomers. This PSI equilibrium is possessed by *C. paradoxa* (eukaryote) as well as cyanobacteria, which indicates the possibility of plastids ancestor has a tetrameric form of PSI. With further PsaL modification and PsaH emergence, the monomeric PSI is exclusively favored in green algae and plants. Alternatively, the monomeric PSI becomes exclusive with one step which involves both PsaL modification and PsaH emergence. Images of PSI and LHC-II are derived from available crystal structures in PDB, 1JB0, 3LW5 and 2BHW.

Tetrameric PSI Provides New Angle to Speculate Plastid Origin

What is the role or position of *Chroococcidiopsis* in the evolutionary transition from cyanobacteria to plastids? Deusch *et al.* point out that heterocyst-forming cyanobacteria are the origin of plant plastids by comparing cyanobacterial and plant genomes (*112*). However, the placement of heterocyst-forming cyanobacteria as a likely progenitor to the plastid was questioned by Falcón *et al.* pointing out the insufficient coverage of cyanobacterial genome (*113*). Instead, Falcón *et al.* conclude that unicellular nitrogen-fixing cyanobacteria (subsection I) are the closest relative to plastids according to the phylogenetic trees built based on 16S RNA and *rbcL* sequences (*113*), while other studies support the idea that plastids originated from nitrogen-fixing cyanobacteria (*114-117*). One should keep in mind that the phylogenetic trees favoring subsection I being the plastid ancestor are based on one or two sequences. A recent study by Shih *et al*., using 25 protein sequences and covering more cyanobacteria genome, tried to explore the common ancestor of plastid, but this study does not support either of those two positions above (*118*). Shih *et al*. also observed the PsaL-like C-terminus extension in some Chl binding proteins (*118*), which indicates that *psaL* derived gene sequences could have been involved in enabling dynamic interaction with antennae complexes during evolution. At the same time, Gupta showed the importance and accuracy of using conserved insertions and deletions when studying cyanobacterial phylogenetics (*115*). After comparing the sequences of PsaL (shown in Figure 3-10A) as well as the general genomic organization of *psaL* and its surrounding genes (Figure

2-6B) it would appear that the diazotrophic TS-821, as well as heterocyst-forming cyanobacteria, has a PsaL that is more closely related to those found in plants and green algae. This structural similarity suggests the possibility that PSI tetramer is evolutionarily closer to the PSI monomer found in most plants and green algae. In addition, the versatility of PSI tetramer may also grant the early endosymbionts high adaptability to constantly change environmental conditions. We speculate that *Chroococcidiopsis* or its close relative is the ancestral origin of plastids considering the existence of tetrameric PSI in glaucophyte *C. paradoxa*, which supports the conclusion of Deusch (*112*).

In summary, we suspect that *Chroococcidiopsis* may be the closest relative to plastids considering its special characteristics. Possibly the tetrameric form of PSI is a common feature shared during cyanobacterial PSI evolution allowing heterocyst formation and further PSI evolution after endosymbiosis by eukaryotes. To test this hypothesis and find out the ancestral cyanobacteria for plastids, more phylogenomic analyses are needed with more genomic data from some special groups such as *Chroococcidiopsis* and *Cyanophora*.

CHAPTER FOUR

Structure of Tetrameric PSI and PsaL

4.1 Disclosure

This chapter contains published and unpublished data of structural studies of TS-821 PSI tetramer. Our collaborators in University of Gronigen did the Cryo-EM analysis. Crystallization work was done in collaboration with Fromme group in Arizona State University. The Cryo-EM structure study has been published in BBA-Bioenergetics recently (*50*). These results are presented here for comprehensive view of the current status of understanding tetrameric PSI structure.

4.2 Abstract

To understand how PSI form tetramer in TS-821 and gain insight how PSI evolved to a tetrameric structure, the structure study of tetrameric PSI is needed. In this chapter, the results of a Cryo-EM study and early stage effort for crystallography are presented and discussed. The Cryo-EM study revealed the special inter-monomer interaction in tetrameric PSI. Also it showed that the modification of PsaL C-terminus is important for PSI tetramer formation. It has been speculated that PsaL is the main reason for PSI oligomeric state diversity. One approach to test this hypothesis and evolutionary speculation is expressing different PsaL from different PSI oligomers in *Synechocystis* to see if it results in different oligomers in the transgenic strains. The preliminary results of this approach are presented.

4.3 Introduction

Multiple techniques can be used to study and verify the PSI tetrameric structure, as shown in Chapter Three. However, to gain insight into the

biochemical components and special organization in tetrameric PSI, three-dimension structural studies are necessary. The three-dimension structure can also help elucidating the biochemical/genetic reason of forming tetrameric PSI in cyanobacteria.

It has been more than a decade since the first high-resolution cyanobacterial trimer PSI structure was solved (*18*). Since then, the cyanobacterial PSI have been widely perceived as trimeric in all cyanobacteria, or mostly trimeric even after reports of tetrameric PSI in two species of cyanobacteria (*19, 21*). Later, the plant PSI structure was solved and improved several times with further details resolved (*41*). The PSI structural evolution from PSI trimer to monomer in eukaryotic organisms was speculated as a result of introduction of PsaH subunit (*46-48*). In contrast, we proposed that PSI evolved from preferentially trimeric to tetrameric/dimeric before becoming exclusive monomeric due to the structural change in PsaL subunit (*21*). The latest plant PSI structure (*41*) actually support our speculation that the loop between second and third transmembrane helices of PsaL in plant PSI interacts with PsaH. This indicates the evolution of PsaL provides the platform for PsaH binding, instead of PsaH disrupting the trimeric form of PSI in plants and green algae.

4.4 Cryo-EM Study of TS-821 PSI Tetramer

To obtain structural insight into the *Chroococcidiopsis* PSI tetramer we used a large cryo-EM data set, which was first classified using RELION applying standard procedures and routines, including phase contrast transfer correction and particle alignments. The 12 most populated classes show 2D maps of intact

tetramers in different orientations, including top-views and side-views (Figure 4-1). Collectively, these 12 classes contained about 47% of the initial data set and were used for getting an initial 3D model. The remaining 53% of the particles were either poorly focused, aggregated or in some other way low-quality and were discarded. In the next step, 3D classification was performed for which an initial reference with imposed C2 symmetry was used. As a result, twenty 3D classes were obtained that in total included 157,845 particles. Among them, one 3D class, which had the highest resolution, included 23,145 particles. This most consistent 3D class was further refined and post-processed with B-factor sharpening. The resulting 3D structure had an overall resolution of 11.5 Å by the "gold standard" Fourier shell correlation (FSC) = 0.143 criterion (Figure 4-2). The best non-symmetrized 2D map of the tetramer, almost in the plane of the membrane, showed ~6.1 Å resolution and included 45,901 particles (Figure 4-1).

The obtained 3D volume confirms that photosystem I from TS-821 is a tetramer with C2 type of symmetry (Figure 4-2). This means that the tetramer is a dimer of dimers (red-blue and green-yellow, resp.) and that the monomer can take two different non-equivalent positions (A and B in Figure 4-3) in the assembly. Neighboring monomers are related by a rotation of 114° and 66°, respectively, resulting in two different monomer interfaces, annotated as type 1 and type 2 (Figure 4-3). To get further insight into the orientation and interaction of the monomers in the tetrameric PSI complex from TS-821, the crystal structure of the *T. elongatus* monomer (PDB entry: 1JB0) was fitted into the 3D density, initially as a rigid body. The overall fit suggests that there is no major

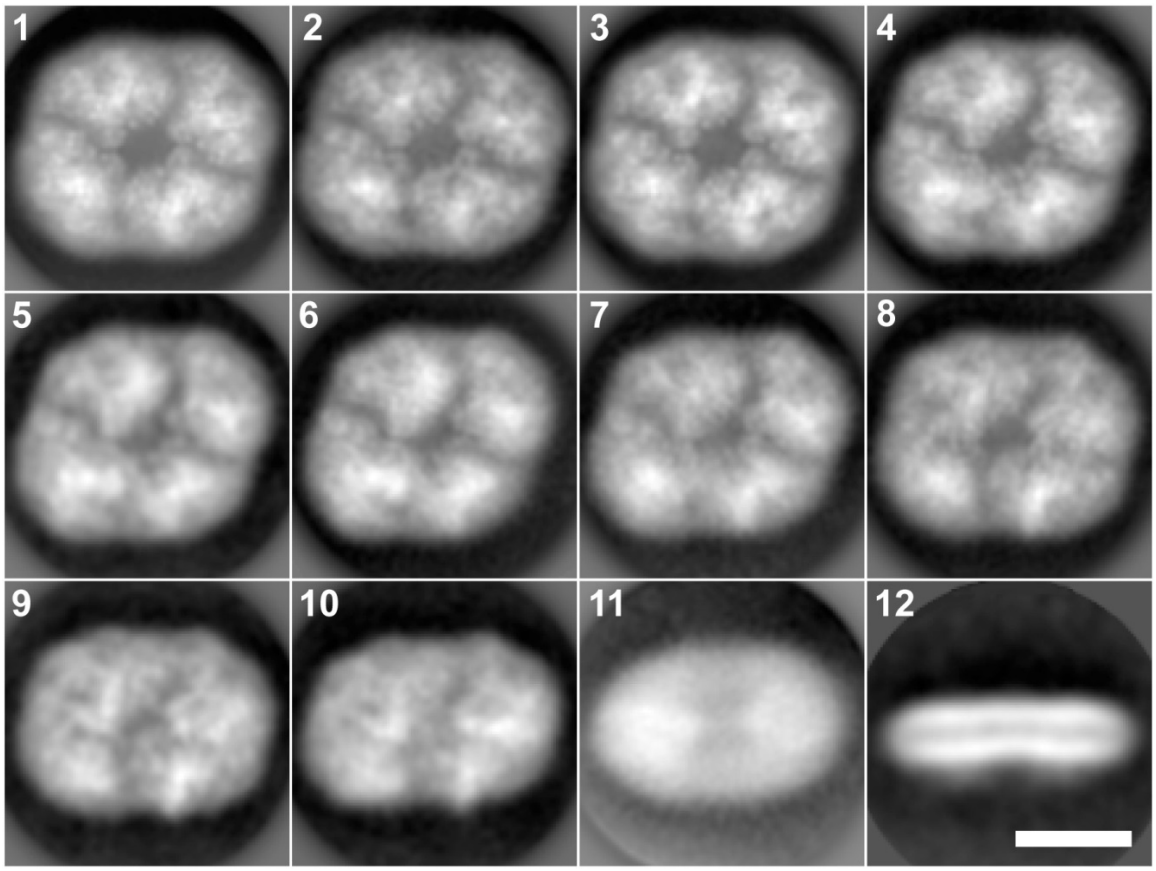

Figure 4- 1 2D class averages of PSI tetramer projections from TS-821

Some classes represent top-views, with PSI seen as in the membrane plane (1-3), some others show the complex in side-view position (12), whereas others represent particles in views intermediate between top- and side-views (in particular frame 11). Scale bar is 100 Å.

This figure was generated by our collaborators in Dr. Boekema's group at University of Groningen.

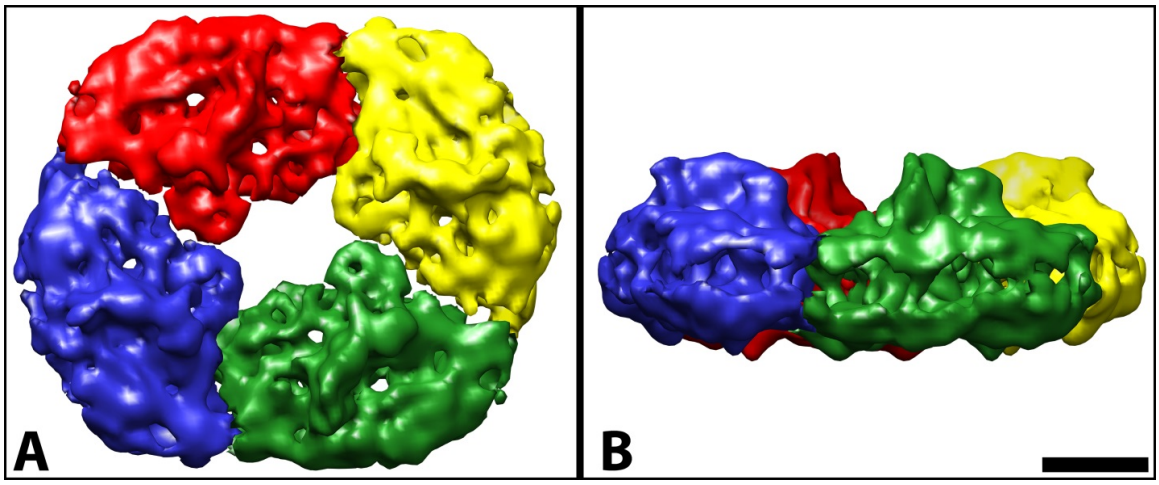

Figure 4- 2 The 11.5 Å structure of TS-821 tetrameric PSI from TS-821 with each of the 4 monomers in a different color

(A) The PSI tetramer, as seen from the stromal side of the membrane. The tetramer is comprised of two equal dimers: red-blue and green-yellow.

(B) View of the tetramer parallel to the membrane plane. Scale bar is 50 Å.

This figure was generated by our collaborators in Dr. Boekema's group at University of Groningen.

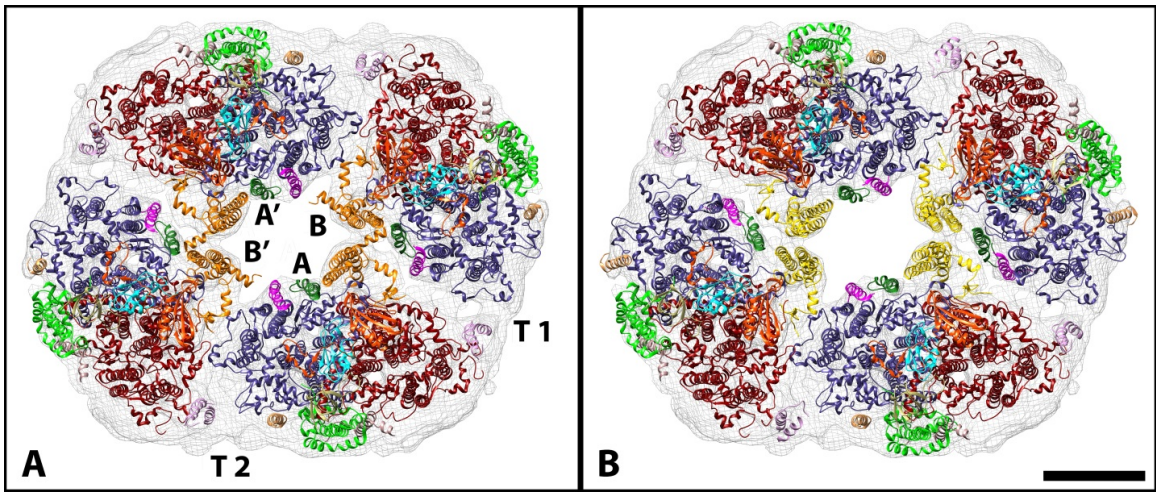

Figure 4- 3 3D model of the TS-821 tetramer with the atomic structure of PSI from *T. elongatus* fitted in.

(A) Model with the crystal structure of *T. elongatus* fitted as a rigid body inside the 3D volume map of TS-821, shown as a mesh.

(B) Model with the subunits of the crystal structure of *T. elongatus* fitted separately into the 3D volume.

The PsaL subunit is the modeled structure for TS-821 based on the a.a. sequence and PsaL from *P. sativum* as a template. The four monomers inside the TS-821 tetramer are named A, B, A', B' and the two interface types between monomers T 1 and T 2. The models show a view from the stromal side. Pigments haven been omitted. 3D volume map is shown as a mesh. Scale bar is 50 Å.

This figure was generated by our collaborators in Dr. Boekema's group at University of Groningen.

rearrangement of the subunits comprising the monomer. The main discrepancy was an absence of density for the PsaL subunit in the C-terminal region (Figure 4-4 A and B region marked with asterix). Therefore, it was decided to try to model PsaL based on the known primary structure and homology with the pea *Pisum sativum* PsaL structure, and subsequently fit all individual subunits into the TS-821 3D density.

Based on the known amino acid sequence (*21*), the PsaL subunit of TS-821 was modeled using PsaL subunit of *P. sativum* as a template (PDB entry: 4Y28.L). The modeled PsaL subunit of TS-821 was used to substitute the existing PsaL subunit in crystal structure of *T. elongatus* (Figure 4-3 B) and most of the subunits from the crystal structure of *T. elongatus* were fitted separately into the 3D volume map of TS-821 (Figure 4-3 B and Figure 4-4 C, D). The densities for PsaX in monomer A and PsaC and PsaF in monomer B were not sufficiently well defined to allow individual subunit fitting. They were placed based on the rigid body PSI monomer fit.

The modified PsaL fits much better in the experimental 3D density than the homologous *T. elongatus* structure (Figure 4-4). The main difference is in the C-terminal PsaL-h helix in *T. elongatus* (marked with an asterisk in Figure 4-4 A, B), which is absent in TS-821. A consequence of the 2-fold rotational symmetry in the TS-821 PSI tetramer is the presence of 2 different types of interfaces between the monomers: type 1 between monomers A and B, and type 2 between monomers A and B' (Figure 4-3). Figure 4-4 shows a closer look at the two interfaces for both the *T. elongatus* crystal structure fitted as a rigid body and the

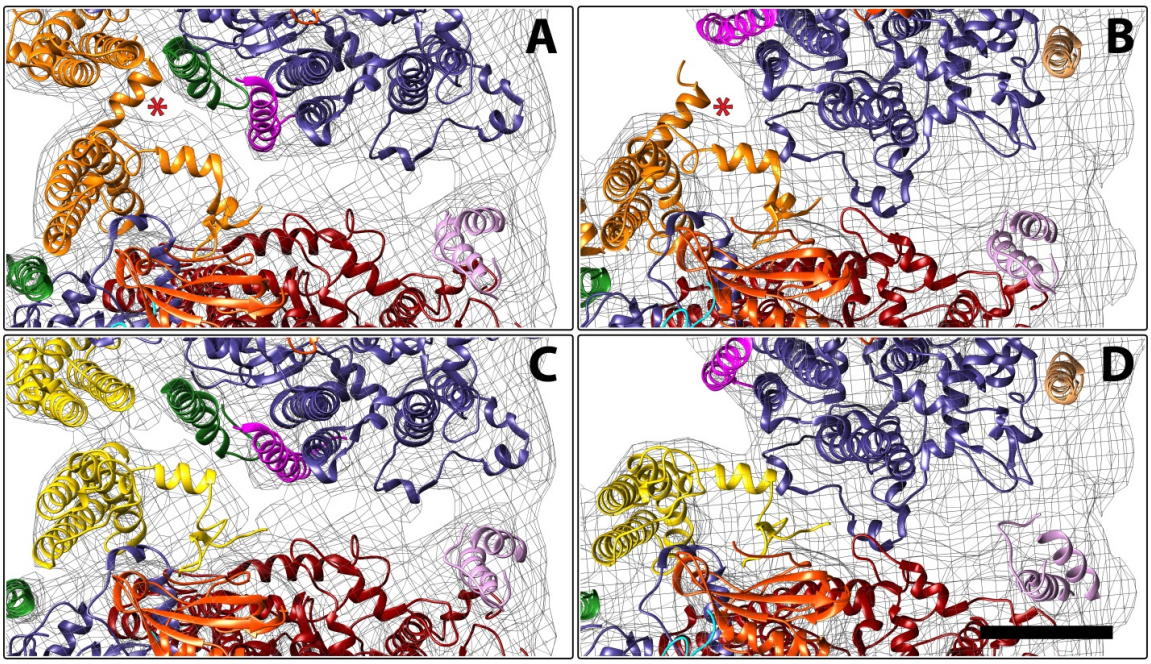

Figure 4- 4 Comparison of TS-821 inter-monomer spaces

(A) Interface type 1 with the crystal structure of *T. elongatus* fitted as a rigid body into the 3D volume map of TS-821.

(B) Interface type 2 with the crystal structure of *T. elongatus* fitted as a rigid body.

(C) Interface type 1 with the crystal structure of *T. elongatus* fitted into the 3D volume map of TS-821. The subunits were fitted separately and PsaL is substituted by the modeled one from TS-821.

(D) Same as in C. for interface type 2.

Colors of the subunits: PsaA – dark red; PsaB – dark slate blue; PsaD – orange red; PsaL (original) – orange; PsaL (modeled) – gold; PsaI – forest green; PsaM – magenta; PsaK – plumb; PsaX – sandy brown. Scale bar is 50 Å.

This figure was generated by our collaborators in Dr. Boekema's group at University of Groningen.

T. elongatus crystal structure with substituted TS-821 PsaL subunit and with each subunit fitted separately.

The type 1 interface for the rigid body fitted structure revealed contacts between subunits PsaL- PsaB, PsaL – PsaI, PsaL – PsaL, PsaL – PsaM, PsaA – PsaB, and PsaA – PsaM. After replacing PsaL with the TS-821 modeled version and fitting all subunits individually only contacts between subunits PsaL – PsaI, PsaL – PsaL, PsaA – PsaB, and PsaA – PsaM were apparent.

The type 2 interface after fitting the crystal structure as a rigid body revealed only contacts between subunits PsaA and PsaB. After modifying PsaL and individual fitting, an additional contact between PsaL and PsaB was observed.

The type 1 interface in TS-821 is similar to the monomer interface in the trimeric PSI from *T. elongatus*, in which all monomers are related by a 120° rotation (Figure 4-5) instead of 114°. The main difference is near the center of the complex, where PsaL in *T. elongatus* makes contact with subunits PsaA, PsaB, and PsaM in the neighboring subunit, in addition to the contacts found in the TS-821 model. The more extended contacts near the center in *T. elongatus* PSI is a consequence of the different relative monomer orientation and also of the α-helical extension at the C-terminus of the subunit, which penetrates into the neighboring monomer.

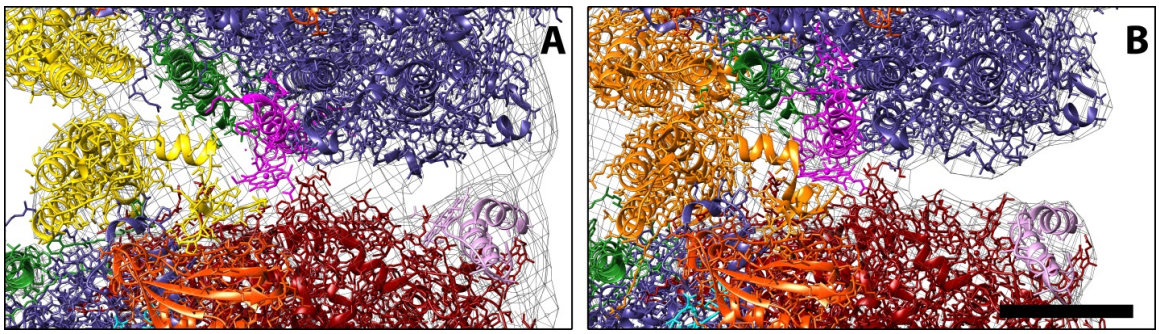

Figure 4- 5 Comparison of trimeric interface of *T. elongatus* with interface type 1 of TS-821

(A) Interface type 1 with the crystal structure of *T. elongatus* fitted into the 3D volume map of TS-821 where the subunits were fitted individually and PsaL subunit is substituted by the modeled one from TS-821. All atoms and bonds, including those from the pigments, are shown.

(B) Interface of the trimeric PSI crystal structure fitted into the same 3D volume density map of *T. elongatus* at 11.5 Å. Subunits colored the same as on previous figures. Scale bar is 50 Å.

This figure was generated by our collaborators in Dr. Boekema's group at University of Groningen.

4.5 TS-821 PSI Tetramer Crystallization

Detergent screening

Considering the fact that PSI tetramer dissociates into dimers upon high DDM treatment, a search for better detergent than DDM was done by solubilizing TS-821 thylakoid membrane in different detergents.

CYMAL-5, CYMAL-6, and CYMAL-7 showed similar effect on thylakoid membrane solubilization (Figure 4-6.). Also, PSI tetramer is more sensitive to CYMAL treatment than to DDM treatment. MEGA-8, MEGA-9, and MEGA-10 showed poor ability to maintain tetrameric PSI structure (Figure 4-6). In contrast, tetradecyl maltoside (TDM) seems to be milder than DDM, with PSI tetramer. A further screening was done among aliphatic maltosides: DDM, TDM and α-DDM (Figure 4-7). In general, TDM is the best in terms of preserving PSI tetramer structure; however, TDM has the lowest ability of solubilizing thylakoid membrane. α-DDM showed the harshest property disrupting PSI structure at higher concentration. To achieve high yield of PSI tetramer, TDM has been selected for PSI purification. Later observation found that TDM is easy to precipitate. Heating in water bath is usually necessary to dissolve TDM in water at higher concentration such as 10%. As a result, final crystallization involved the PSI tetramer isolated using DDM as the detergent considering its high efficiency in solubilizing the thylakoid membrane and relative mildness in preserving the tetrameric structure of PSI.

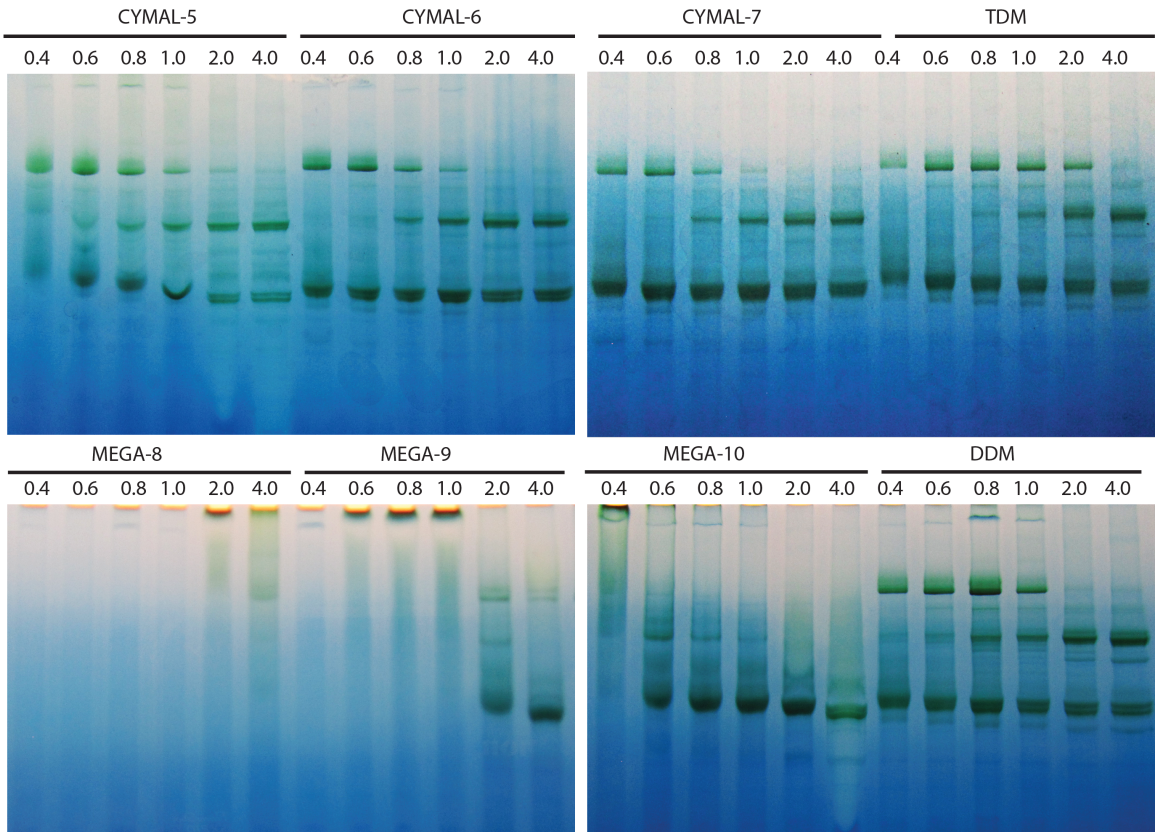

Figure 4- 6 BN-PAGE of TS-821 thylakoid membrane solubilized in different detergents.

TS-821 thylakoid membrane containing 0.4 mg/mL Chl was solubilized in different detergents with different concentrations (w/v, %), denoted as numbers above each lane. CYMAL-5, 5-Cyclohexyl-1-Hexyl-β-D-Maltoside; CYMAL-6, 6-Cyclohexyl-1-Hexyl-β-D-Maltoside; CYMAL-7, 7-Cyclohexyl-1-Hexyl-β-D-Maltoside; MEGA-8, n-Octanoyl-N-methyl-D-glucamine; MEGA-9, n-Nonanoyl-N-methyl-D-glucamide; MEGA-10, n-Decanoyl-N-methyl-D-glucamide.

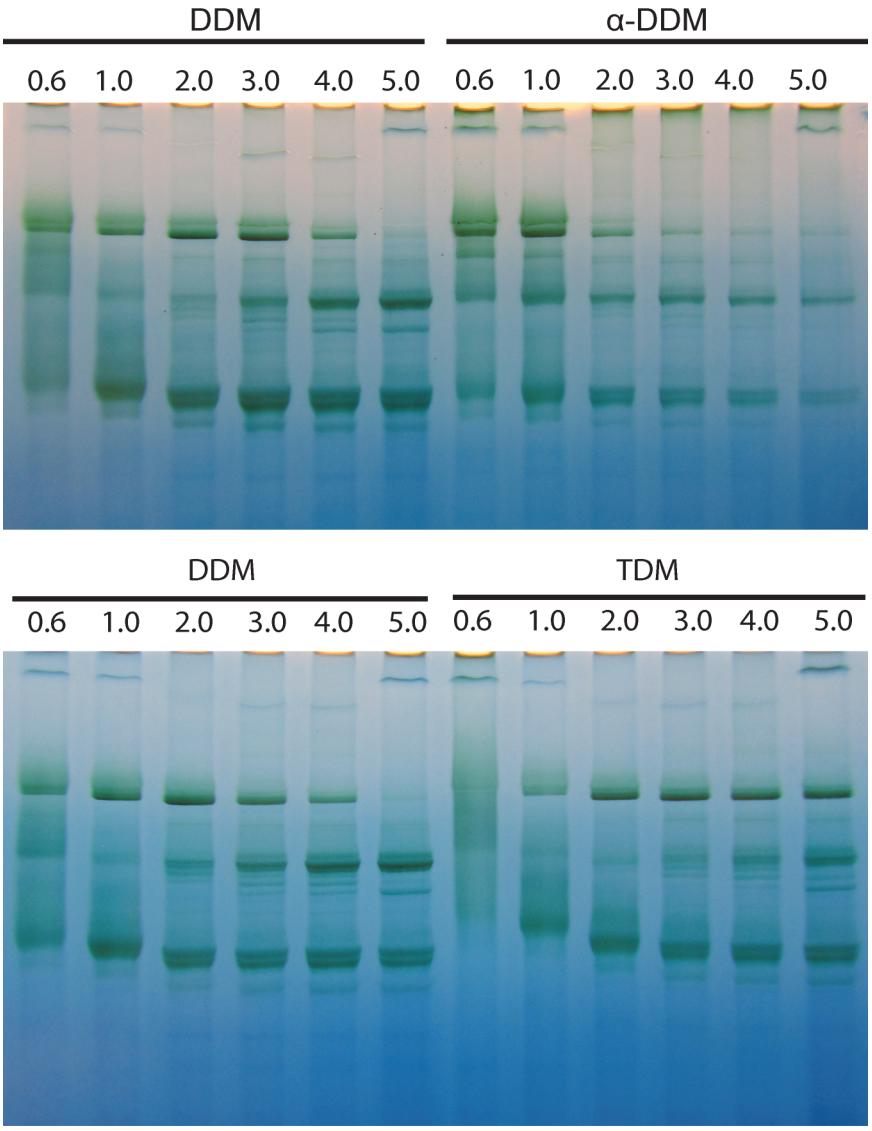

Figure 4- 7 BN-PAGE of TS-821 thylakoid membrane solubilized in different aliphatic maltosides

TS-821 thylakoid membrane containing 1 mg/mL Chl was solubilized in different aliphatic maltosides with different concentrations (w/v, %), denoted as numbers above each lane. ~2 µg Chl for each lane were loaded.

Crystallization

TS-821 PSI purification and initial crystallization were set up as described in Materials and Methods. Two days after initial screening in 3 x 96 well conditions, crystals showed up in some conditions. Notably, many conditions with 2-Methyl-2,4-pentanediol (MPD) resulted in crystals as well as a condition with isopropanol. Among all conditions that showed potential PSI crystals, one in MemFac, D1.2 well, showed needle crystals at day 2. Further optimization was done for several conditions.

Conditions with MPD showed orange crystals (Figure 4-8 A), which could be the result of PSI denaturation since the dark green precipitations do not show birefringent effect. The orange color may be from the carotenoids crystal. The crystal formed in condition containing isopropanol may have a similar mechanism of denaturing PSI tetramer and forming carotenoids crystals.

The condition of “0.6 M MgSO4, 0.1 M HEPES pH 7.5 4% PEG 400” generate needle crystals after two days (Figure 4-8 B). However, longer incubation resulted in dissolving of the PSI crystals. These results indicate that PEG 400 may be a good precipitant for PSI tetramer crystallization and that high MgSO4 concentration may result in the re-dissolve of PSI crystals. As a result, PEG 400 with different concentration and low MgSO4 concentration are being tested for further optimization.

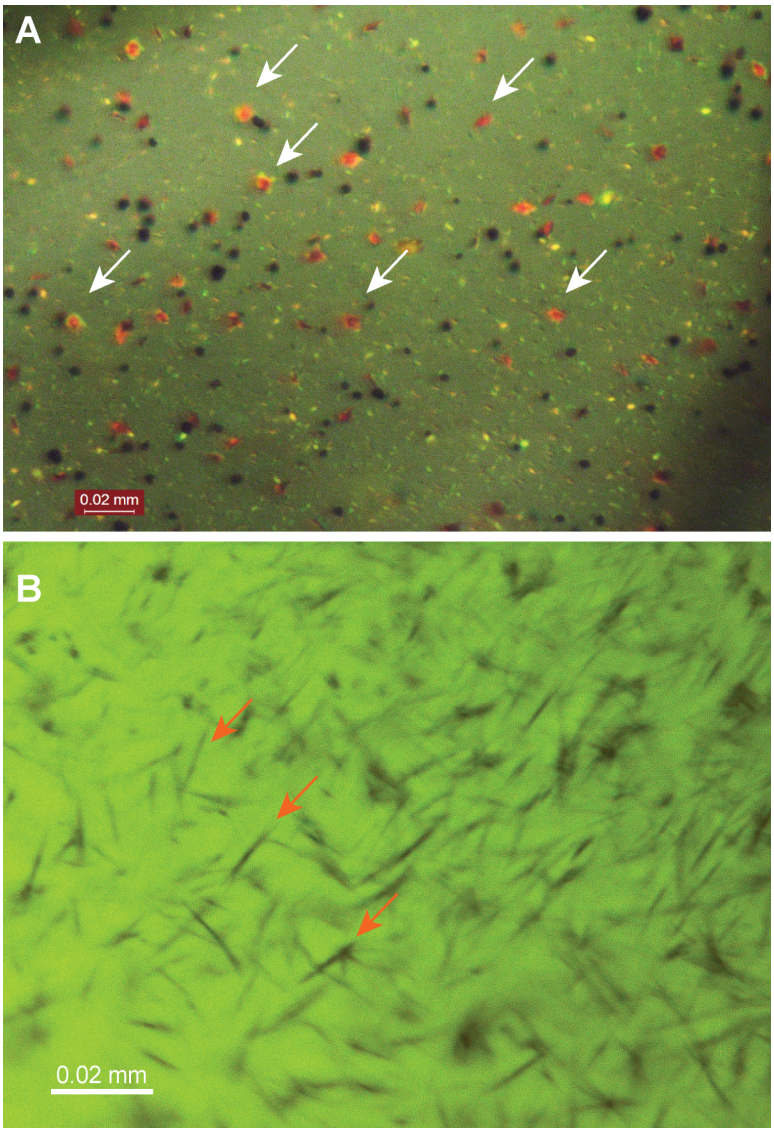

Figure 4- 8 TS-821 PSI tetramer crystallization

(A) Image of PSI tetramer incubated with MPD under polarized light source. Examples of potential carotenoids crystals are pointed out.

(B) Image of PSI tetramer needle crystals incubated with PEG 400 under non-polarized light. Examples are pointed out by arrows even though numerous crystals are easy to see.

4.6 Comparison of PSI Oligomeric States in *Synechocystis* Expressing Different PsaL

The *psaL* Knockout Mutant Δ*psaL*

The *Synechocystis* Δ*psaL* mutant was constructed as described in the materials and method. The main phenotype of Δ*psaL* is that PSI is exclusively monomeric (Figure 4-9), consistent with earlier studies about cyanobacterial Δ*psaL* mutants (*22, 24, 25, 103, 119*). In addition to the monomeric PSI feature in Δ*psaL* mutants, Δ*psaL* also showed slower growth under green light but higher tolerance to DCMU treatment (*25*). Moreover, the Δ*psaL* mutants treated under high light express the high light induced protein, HliA, binding with PsaD (*119*) and PsaL is needed for *Synechocystis* to survive high light intensity (400 μmol/m^2/s)(*33*). All these results indicate that PsaL is probably involved in response to light intensities. As speculated in Chapter Three, PSI monomer may be better oligomeric state than trimeric PSI for the growth under high light(*21*).

We were curious to know if the knockout of PsaL induces other responses, the thylakoid and cytosolic proteins were analyzed using SDS-PAGE (Figure 4-10). The preliminary result clearly shows protein differences between WT and Δ*psaL* mutant. A detailed protein profiling is needed to see what proteins are up-regulated or down-regulated, which may help elucidate the role of PSI trimer or PsaL and explain the observed phenotypes in addition to monomeric PSI.

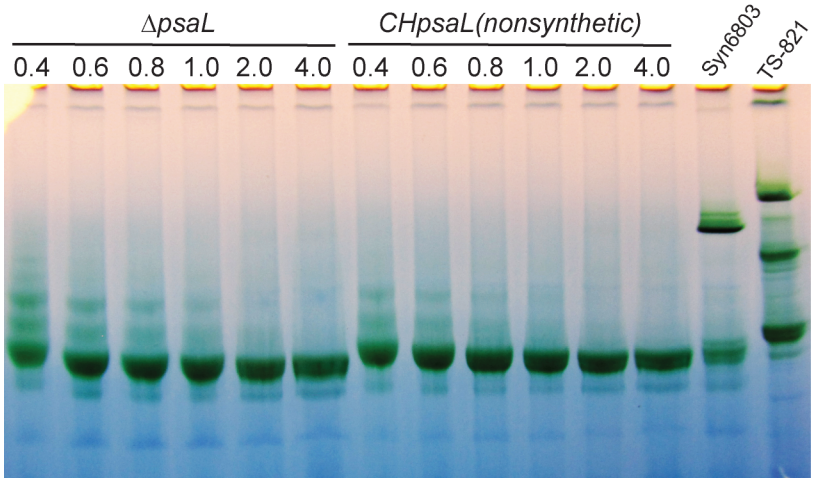

Figure 4- 9 BN-PAGE of solubilized thylakoid membranes from Δ*psaL* mutant and *CHpsaL* mutant

Thylakoid membranes from *Synechocystis* mutants, Δ*psaL* and *CHpsaL*, were solubilized in different concentrations of DDM with 0.4 mg/mL Chl. Concentrations of DDM (w/v, %) are labeled on top of each lane. Thylakoid membranes from *Synechocystis* WT (Syn6803) and TS-821 solubilized in 1% DDM with 0.4 mg/mL Chl were used as controls. For each lane, ~ 2 µg Chl were loaded.

Figure 4- 10 SDS-PAGE of Δ*psaL* cell lysate and thylakoid membrane

(A) SDS-PAGE of *Synechocystis ΔpsaL* and *CHpsaL* thylakoid membranes (mbr). Two lines of *CHpsaL* mutants were analyzed. Major differences in protein components were denoted using green arrows. TS-821 PSI tetramer (tet) and *T. elongatus* PSI trimer (tri) were used as control to denote PsaL (red arrows), which is not present in Δ*psaL* and *CHpsaL*. Two different loading amounts adjusted by Chl concentration were tested to confirm the observed differences.
(B) SDS-PAGE of *Synechocystis ΔpsaL* and *CHpsaL* cell lysate. The same lines of cells were used as in (A). Two different protein amounts were used to clarify the differences between WT and *ΔpsaL*. Protein concetration was estimated by A_{280nm}, with 1 unit of absorbance equals 1 mg/mL protein. These gels further confirm that *CHpsaL* (codon unoptimized) mutants look like *ΔpsaL.*

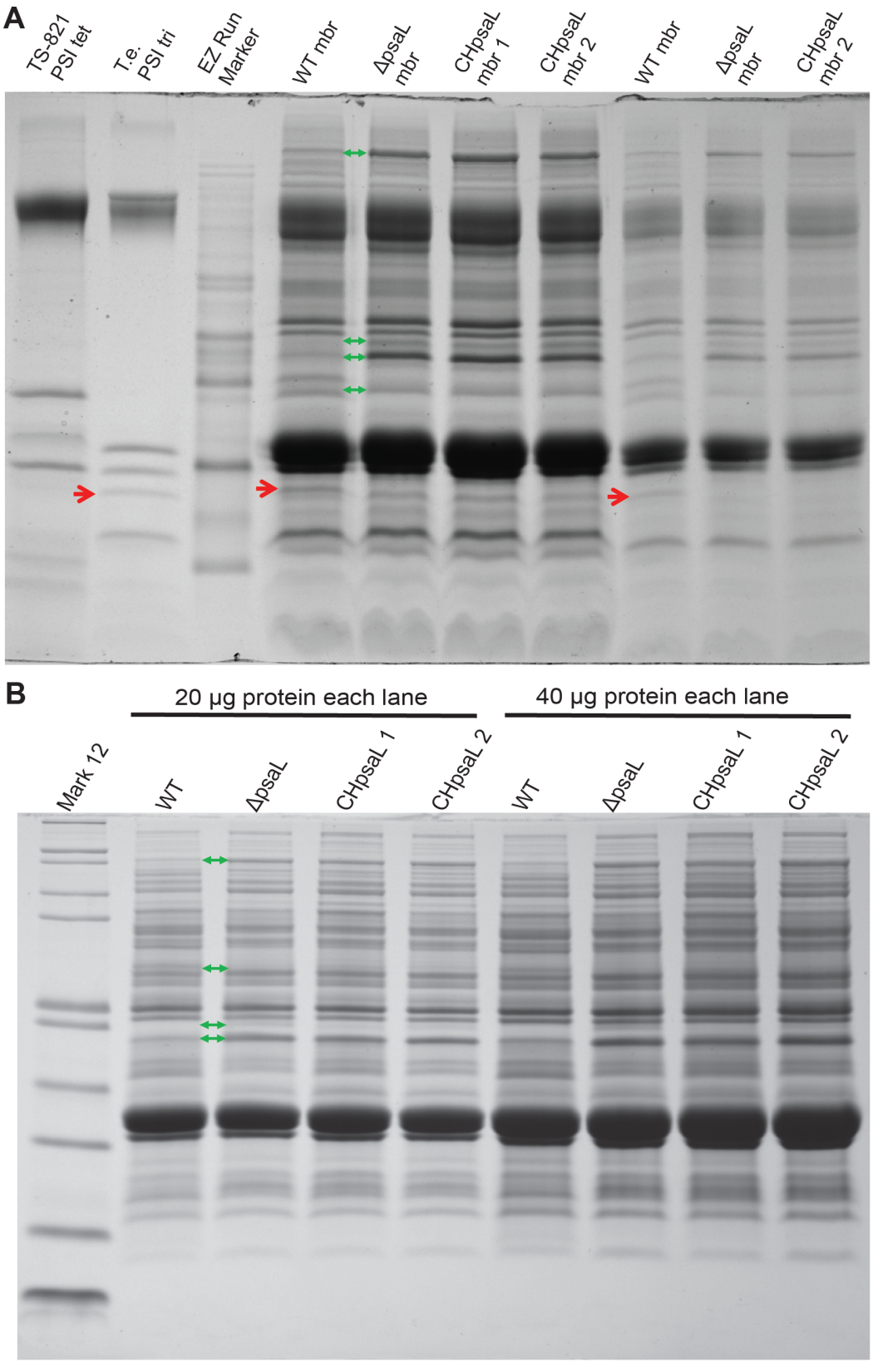

Figure 4-10 continued

Expressing TS-821 PsaL in *Synechocystis*

After initial attempts to express TS-821 PsaL in *Synechocystis(21)*, the codon optimized *psaL* was used with similar design. All the tested mutant lines showed PSI monomers exclusively (Figure 4-11). To rule out this monomerization of PSI is due to the absence of PsaL as described in Chapter Three. Western blot analysis was carried out to detect the presence of PsaL in PSI monomer in the SCHLLK-12 mutant line (Figure 4-12). With a total 16 μg Chl loading on one lane, a faint green band from the mutant showed bigger molecular weight than the TS-821 and *Synechocystis* PSI trimer with TS-821 PsaL incorporated (Figure 4-12). Due to the low quantity, the large PSI complex in SCHLLK-12 was not isolated for further identification. It is clear to see that TS-821 PsaL in *Synechocystis* mainly made PSI monomers.

Expressing *Arabidopsis* PsaL in *Synechocystis*

To see if *Arabidopsis* PsaL (Uniprot: Q9SUI4) supports PSI trimer formation, *Synechocystis psaL* was replaced with *Arabidopsis psaL* coding sequencing with the transit peptide removed. Similar to what was observed in *Synechocystis* expressing TS-821 PsaL, SAtLLK mutants expressing *Arabidopsis* PsaL all showed monomeric PSI (Figure 4-13 A and Figure 4-14 A). SDS-PAGE and silver staining showed that the major green bands are PSI (Figure 4-13 C and Figure 4-14 B). The western blot of SSAtLLK-14 showed the presence of PsaL in PSI monomer in the mutant expressing *Arabidopsis* PsaL (Figure 4-14 C and D). This indicates that *Arabidopsis* PsaL does not support the PSI trimeric structure in *Synechocystis.*

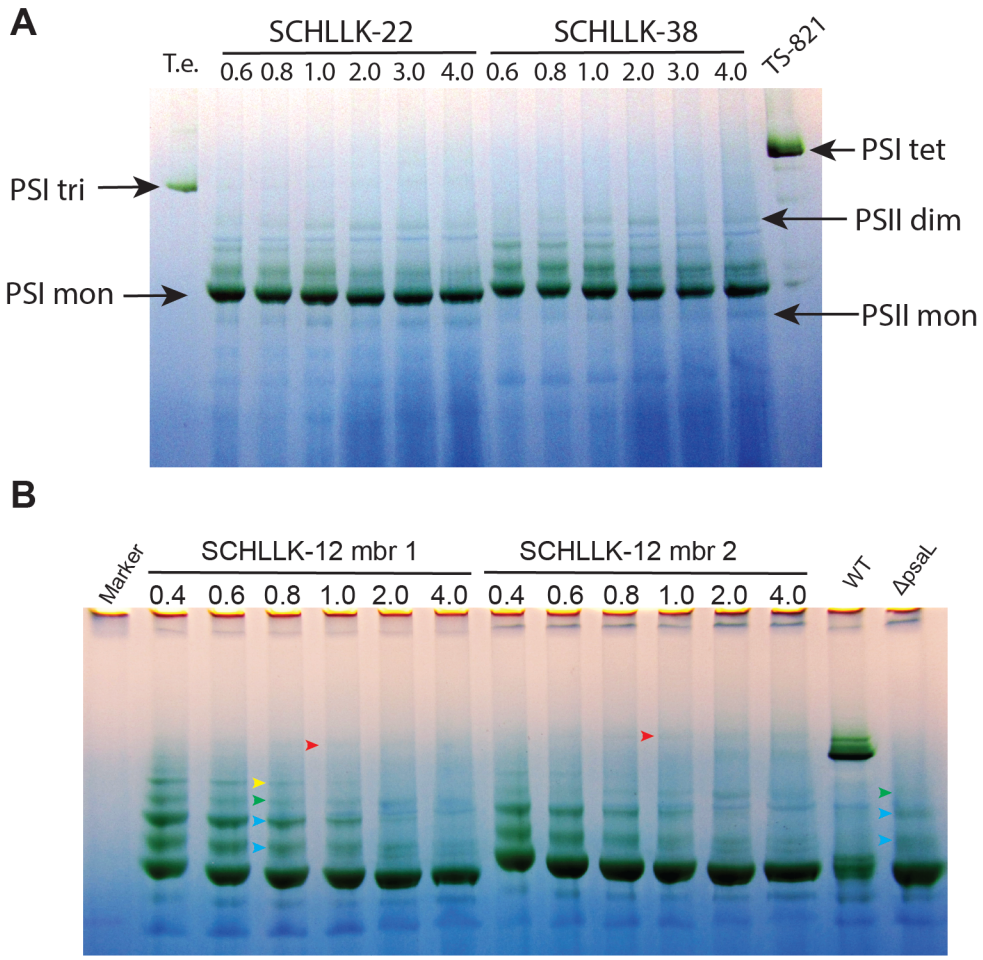

Figure 4- 11 BN-PAGE of solubilized thylakoid membranes from *Synechocystis* expressing codon-optimized TS-821 *psaL* (SCHLLK).

(A) BN-PAGE analysis of PSI oligomeric state of SCHLLK-22 and SCHLLK-38. Isolated *T. elongatus* (T.e.) PSI trimer (tri) and TS-821 PSI tetramer (tet) were used as controls.

(B) BN-PAGE analysis of PSI oligomeric state of SCHLLK-12. WT and *ΔpsaL* thylakoid membrane with 0.4 mg/mL Chl in 1% DDM were used as controls. Two different membrane (mbr) pelleting methods were tested. Potential unique green bands are pointed out by red and yellow arrows while similar green bands shared by SHLLK-12 and *ΔpsaL* are pointed out using green and blue arrows.

For each solubilization condition, ~2 µg Chl were loaded. Different concentrations of DDM (w/v, %) were denoted on top of each lane.

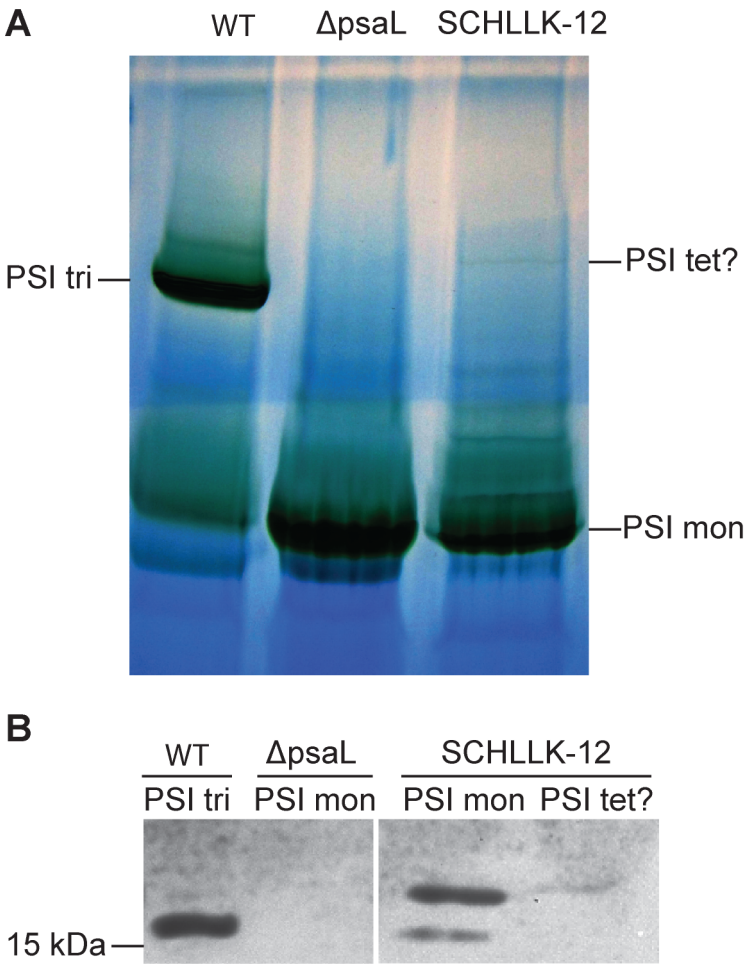

Figure 4- 12 Western blot of SCHLLK-12 PSI from BN-PAGE gel

(A) BN-PAGE of solubilized thylakoid membranes from *Synechocystis* WT, *ΔpsaL*, and SCHLLK-12. PSI samples were sliced out for from the gel for following SDS-PAGE and western blot to detect the presence of PsaL. Each lane was loaded with solubilized membrane containing 16 µg Chl.

(B) Western blot of the PSI samples from BN-PAGE. PSI trimer (tri) from WT, PSI monomers (mon) from *ΔpsaL* and SCHLLK-12, as well as potential PSI tetramer (tet?) were analyzed.

Figure 4- 13 BN-PAGE and SDS-PAGE analysis of PSI oligomers in SAtLLK

(A) BN-PAGE analysis of PSI oligomeric state of *Synechocystis* SAtLLK mutants (two lines SAtLLK-3 and SAtLLK-4) expressing *Arabidopsis* PsaL. Thylakoid membranes with 0.4 mg/mL Chl were solubilized in different concentrations of DDM (w/v, %), labeled on top of each lane. WT and *ΔpsaL* thylakoid membrane with 0.4 mg/mL Chl in 1% DDM were used as controls. ~ 2 µg Chl were loaded for each lane.
(B) BN-PAGE gel show the green bands sliced out for subsequent SDS-PAGE and photosystem identification.
(C) SDS-PAGE of green bands from BN-PAGE gel (B) and PSI identification in SAtLLK mutants. WT PSI trimer (tri), *ΔpsaL* PSI monomer (mon) were used as controls. The identification of photosystems is denoted on top of each lane.

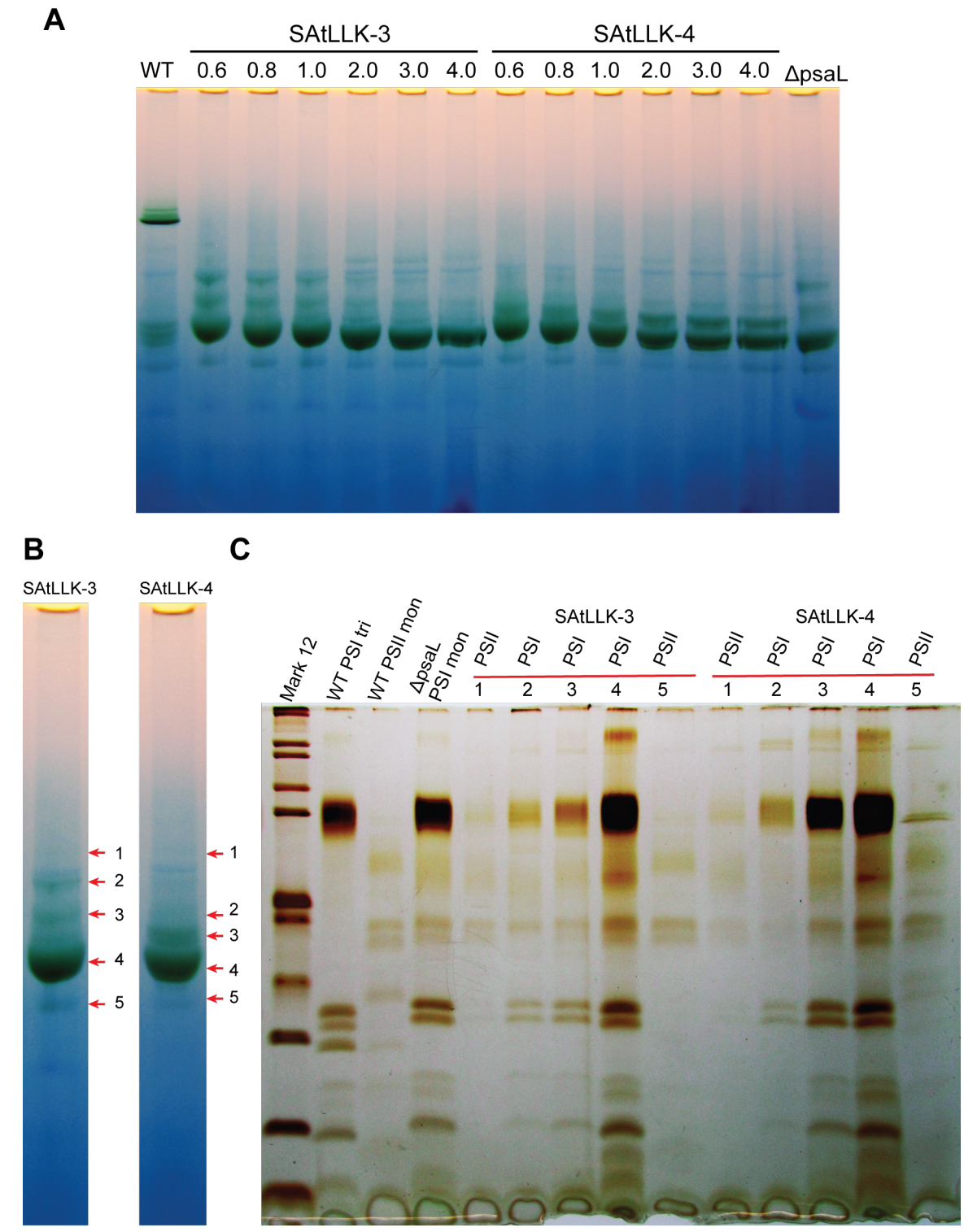

Figure 4-13 continued

Figure 4- 14 Analysis of PSI oligomer in SSAtLLK-14

(A) BN-PAGE of solubilized thylakoid membrane from *Synechocystis* SSAtLLK-14 expressing *Arabidopsis* PsaL. Thylakoid membranes with 0.4 mg/mL Chl were solubilized in different concentrations of DDM (w/v, %), labeled on top of each lane. WT thylakoid membrane with 0.4 mg/mL Chl in 1% DDM was used as controls. ~ 2 µg Chl were loaded for each lane. Numbered arrows point at green bands for subsequent SDS-PAGE analysis. Solubilization condition at 1% DDM was used.

(B) SDS-PAGE of bands sliced out from BN-PAGE gel (A). Silver stain was used to visualize the bands. The identification of photosystem is denoted on top of the band number.

(C) BN-PAGE of SSAtLLK-14 before western blot to detect the presence of PsaL. The homemade BN-PAGE gel was used. Bands sliced out for subsequent experiment are pointed by arrows. ~8 µg Chl were loaded for each lane.

(D) Western blot of PSI bands isolated from BN-PAGE gel (C). *Arabidopsis* seedling whole cell extract was used as a control.

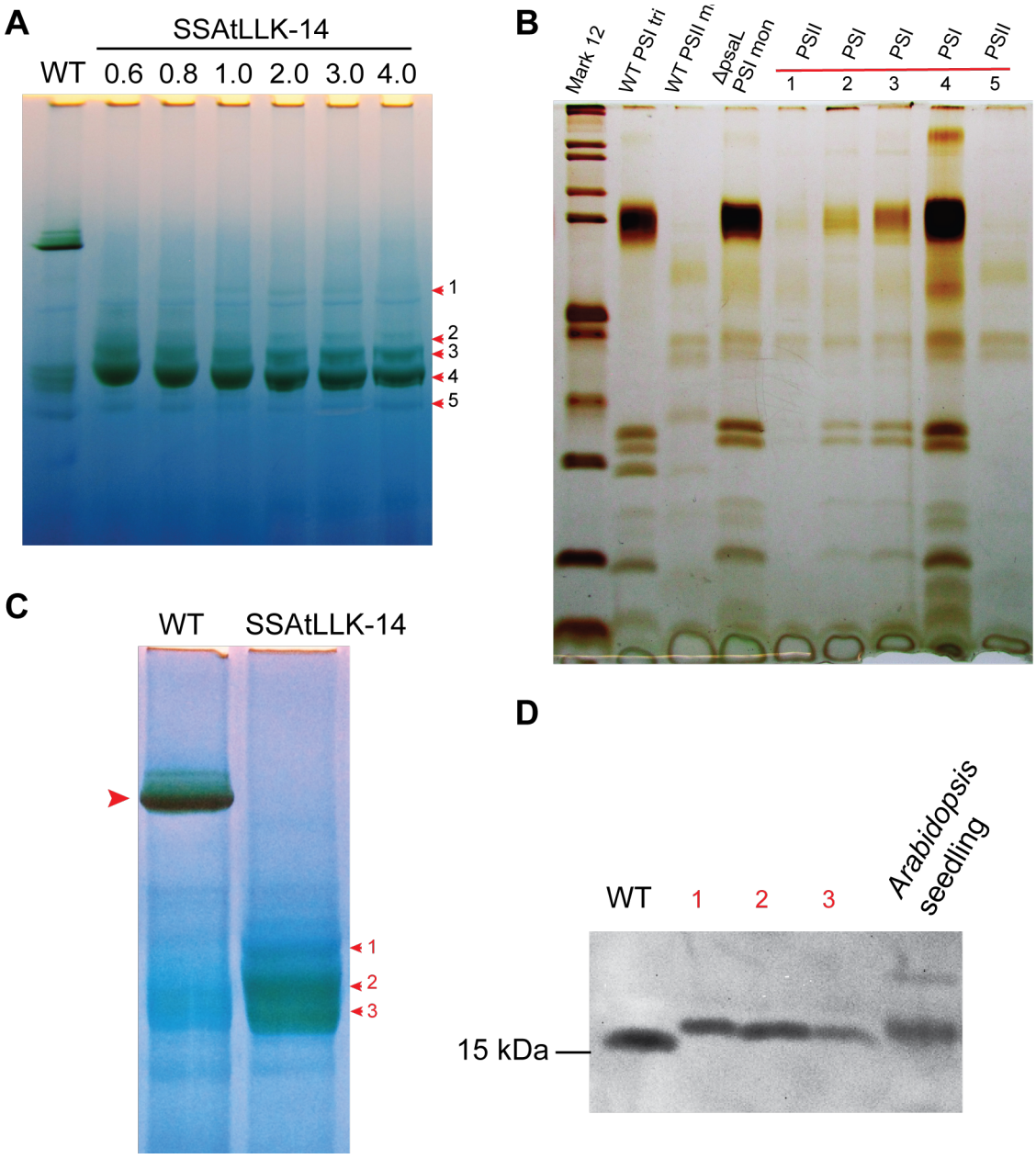

Figure 4-14 continued

4.7 Discussion

Our Cryo-EM results confirm that the PSI supercomplex of TS-821 has a tetrameric organization with C2 symmetry. The absence of 4-fold rotational symmetry leads to two different, non-equivalent, monomer positions in the tetramer and to the existence of two different monomer interfaces. One interface (type 1) is similar to that in trimeric PSI from *T. elongatus*. The second interface is quite different in the contacts between subunits. In preparations of TS-821 PSI, dimers have been observed in addition to the tetramers. These dimers were exclusively built from monomers (A and B, Figure 4-3A) connected by a type I interface. This suggests that the type 1 interaction is stronger than the type 2, and that the tetramer can be considered a dimer of (A-B) dimers.

To get more insight into the binding interactions in the two interfaces, a homologous high-resolution X-ray structure of PSI from *T. elongatus* was fitted into our density map for TS-821. Initially as a rigid body fit at the monomer level, but the position and orientation of most subunits could be refined individually. Interactions could be described at the level of secondary structure elements. The current resolution of 11.5 Å is not sufficient to draw more detailed conclusions about interactions at the amino acid level and the location of pigments that play an important role in the transfer of energy.

Because the PsaL subunit from the crystal structure of *T. elongatus* did not fit well inside the experimentally obtained 3D density map, the PsaL from TS-821 was modeled based on the amino acid sequence using the *P. sativum* crystal structure as a template. This gave a much better fit, but also shows the

less close interaction between PsaL subunits from neighboring monomers due to the absence of the C-terminal L-h helix from *T. elongatus*. PsaL plays a central role in the trimer formation of *T. elongatus* PSI (*120*). The absence of the C-terminal L-h helix in TS-821 may explain the formation of tetramers, because of a weaker binding between L subunits over the type 1 interface, allowing for a second type of interaction via the type 2 interface.

Even though current Cryo-EM structure of PSI tetramer revealed the how PSI tetramer differs from PSI trimer in terms of inter-monomer interfaces involving PsaL, further improvement on the resolution of PSI tetramer structure is needed to elucidate how PsaL and other subunits associate within the tetrameric PSI. Currently, further improvement of the resolution of tetrameric PSI structure using Cryo-EM is ongoing, while crystallography study is also promising. The preliminary data on TS-821 PSI crystallization provides the foundation for further improvement in crystallization conditions and future structure solvation.

Before the publication of high resolution structure of the PSI trimer from *T. elongatus* (*18*), multiple studies had shown that PsaL is necessary for PSI to form trimer(*22, 24, 25*). Those studies and the crystal structure of PSI (PDB 1JB0) confirmed the annotation for PsaL as required for PSI trimerization (*18*). However, the fact that Δ*psaL* mutants showed different phenotypes compared with wild type in response to light quantity and quality (*25, 33, 119*) has not been studied in details for its mechanism. Our preliminary results showed that the knockout of *psaL* actually induced differential protein expression pattern in the cytosol and thylakoid membrane (Figure 4-10). A detailed study on how Δ*psaL* mutants

respond to different light intensities or colors will elucidate what additional roles PsaL plays other than stabilizing the trimeric PSI.

Since plant PSI is monomeric with the presence of PsaL and PsaH which binds to PsaL (*39, 41*), this led to the speculation that PsaH is responsible for keeping plant PSI from forming trimeric PSI (*46-48*). However, the study of plant PsaH mutants did not show that the structure of PSI is trimeric (*121*). The fact we observed tetrameric PSI in equilibrium with dimer and monomer cast a doubt on this theory of PSI evolution (*21*). Here we have shown that plant (*Arabidopsis*) PsaL does not support the trimeric PSI, which indicates that PSI monomerization in green algae and land plants is independent from PsaH. This monomerization may only depend on the structural change of PsaL. Later Chapters will show more examples of PSI monomerization without PsaH.

CHAPTER FIVE

Correlation of *psaL* Gene and Distribution of Tetrameric PSI Among Cyanobacteria

5.1 Disclosure

This Chapter contains results that are not published but in preparation for a manuscript, which includes unpublished data from other chapters as well. The phylogenomic analysis and extensive PsaL phylogenetic analysis were done by Dr. Alexandra Calteau. Most PCC strains were selected and provided by Natalie Sasson and Dr. Muriel Gugger. My major contribution is culturing UTEX strains and the biochemistry work on PSI tetramer identification. The cloning of cyanobacterial *psaL* sequencing from strains with unknown genomes were obtained with assistance from Thomas A. Witt. EM image was acquired by Dr. Dmitry A. Semchonok.

5.2 Abstract

PSI tetramer have been reported in two cyanobacteria species and one glaucophyte species. Whether or not this tetrameric PSI is unique to a few cyanobacteria is not known. We have speculated that all heterocyst-forming cyanobacteria ant their close relatives have tetrameric PSI. In this chapter, the PSI oligomeric states of 61 strains of cyanobacteria are presented, with 39 classified in the heterocyst-forming cyanobacteria and close relatives' clade. Not all but most cyanobacteria in this clade have tetrameric or dimeric PSI. Some of which have both tetrameric and trimeric PSI. Most cyanobacteria outside this clade have trimeric PSI as their major PSI oligomer while special cases with potential PSI dimer and tetramer were observed too. Investigation on the glaucophytes species revealed monomeric PSI in two *Cyanophora* species. The correlation of PSI oligomeric states and PsaL structures are discussed.

5.3 Introduction

Upon our first publication about tetrameric PSI in TS-821 (*21*), we noticed that PSI tetramer is present in another cyanobacterium, *Nostoc* sp. PCC 7120 (*19, 20*). After literature review, we found that the PSI oligomeric states in heterocyst-forming cyanobacteria had been poorly studied. Based on the fact that TS-821 is closely related to heterocyst-forming cyanobacteria and the observation that all cyanobacteria in clade III have a *psaL* gene located adjacent to *psaF* and *psaJ,* we proposed that PSI in this clade are probably all tetrameric (*21*). In the meantime, we noticed that TS-821 has trimeric PSI and that some cyanobacteria have two copies of *psaL* genes, which may explain why TS-821 has both trimeric PSI and tetrameric PSI (*21*). This observation led us to further speculate that cyanobacteria possessing two different copies of *psaL* gene in Clade III may have two forms of PSI oligomer (*21*).

Despite all the new ideas about the PSI oligomer in cyanobacteria, experiments testing those hypotheses were needed. This Chapter focuses on the experiments testing PSI oligomeric states among cyanobacteria and its correlation with *psaL* genes. After testing more than 50 different cyanobacteria strains, including 39 strains belonging to Clade III (heterocyst-forming cyanobacteria and close relatives), we found that most cyanobacteria in Clade III have tetrameric or dimeric PSI, with three having exclusive monomeric PSI. In contrast, other cyanobacteria mostly have trimeric PSI, while special cases may have some dimeric PSI or tetrameric PSI, and even potential hexameric PSI. How PsaL correlates to the PSI oligomeric state will be discussed in this Chapter.

5.4 PSI Tetramer Distribution Among Cyanobacteria

Initial Hypothesis Test on PSI tetramer Distribution Among Heterocyst-forming Cyanobacteria

To test the hypothesis that all heterocyst-forming cyanobacteria and their close relatives have tetrameric PSI (*21*) (Chapter Three), the strains from the previous study (*60*) were cultured as described in materials and methods. The results support this hypothesis. Details are described for each strain.

Nodularia spumigena PCC 73104

Nodularia spumigena PCC 73104 (PCC 73104) was a strain isolated from Spotted Lake in Canada (*61, 122*), it was used as a standard strain to identify the genus *Nodularia* (*61*).It does not produce toxin nodularin (*122*). In agreement with the previous study (*61*), PCC 73104 does not grow well under aerobic nitrogen fixing conditions.

Harvested from BG-11 media, PCC 73104 was analyzed using BN-PAGE to characterize their PSI oligomeric state as described in materials and methods. As shown in Figure 5-1, the solubilized thylakoid membranes from PCC 73104 showed three major green bands on a BN-PAGE gel. Under solubilization conditions with higher concentration of DDM, the amount of green bands with the highest molecular weights, corresponding to a potential PSI tetramer, is lower. This indicates that PCC 73104 have tetrameric PSI, in equilibrium with the PSI monomer and dimer. The SDS-PAGE and silver staining results clearly showed that those green bands of interest are PSI (Figure 5-2).

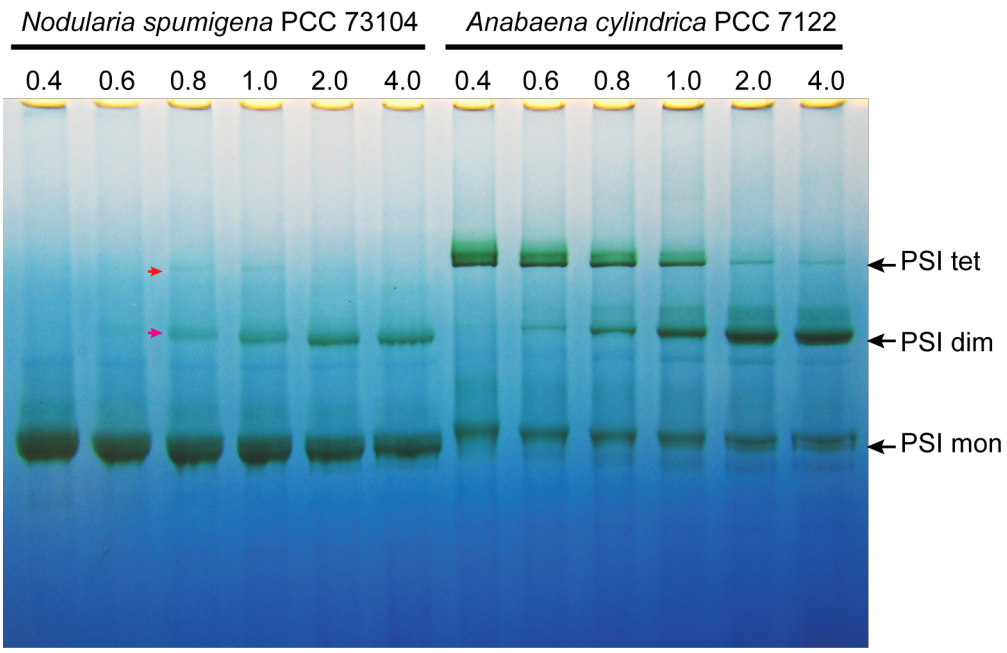

Figure 5- 1 BN-PAGE analysis of solubilized thylakoid from *Nodularia spumigena* PCC 73104 and *Anabaena cylindrica* PCC 7122

Thylakoid membranes from PCC 73104 and PCC 7122 with 0.4 mg/mL Chl were solubilized in different concentrations of DDM (w/v, %), labeled on top of each lane. ~ 2 µg Chl were loaded for each condition. The potential PSI monomer (mon), dimer (dim), and tetramer (tet) are denoted by arrows. The three letter code, mon, dim, tri, and tet for monomer, dimer, trimer and tetramer respectively, will be used in other figures as well.

Figure 5- 2 SDS-PAGE of photosystems from PCC 73104 and PCC 7122 for PSI identification

(A) BN-PAGE of solubilized thylakoid membrane from PCC 73104 and PCC 7122 with 0.4 mg/mL Chl in 1% DDM. TS-821 and *T. elongatus* (TE) were used as controls. The bands that were sliced out for PSI identification were numbered.
(B) SDS-PAGE of green bands isolated from BN-PAGE gel of PCC 73104 solubilized thylakoid membrane.
(C) SDS-PAGE of green bands isolated from BN-PAGE gel of PCC 7122 solubilized thylakoid membrane.
PSI and PSII bands from TE and TS-821 were used as controls. The CP47, CP43 and D1/2 proteins are pointed out for clear comparison. The identification of photosystems is labeled on top of each lane, with band numbers in (B) and (C) corresponding to the bands labeled in (A). The oligomeric states of photosystems are denoted as well. Some oligomeric states are not clear with one "+" sign labeled following an oligomeric state interpretation, indicating their bigger size compared to corresponding oligomers.

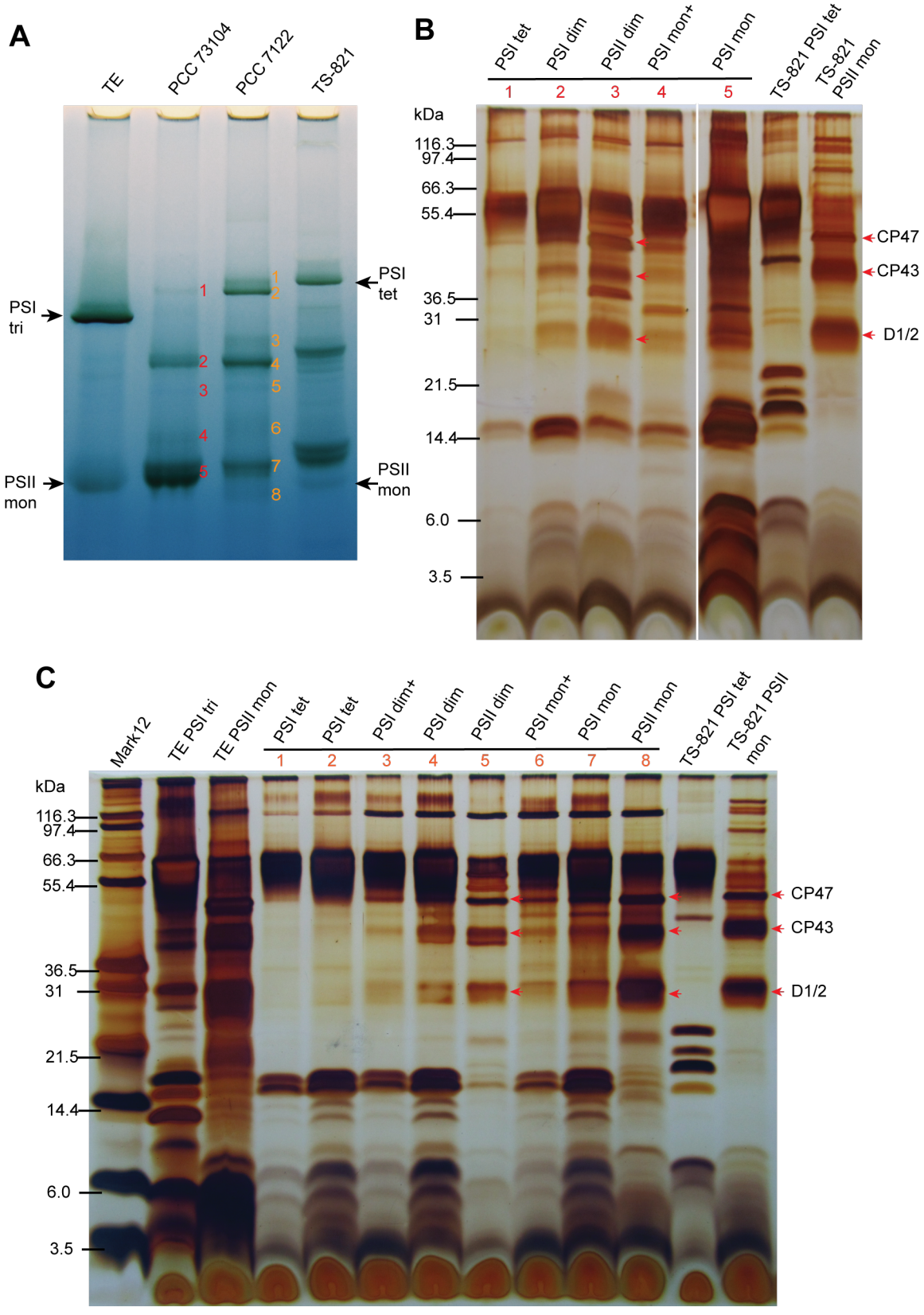

Figure 5-2 continued

One interesting observation is that PCC 73104 PSI tetramer was not shown at 0.4% DDM (Figure 5-1), which can be a result of insufficient solubilization.

Anabaena cylindrica PCC 7122

Anabaena cylindrica PCC 7122 (PCC 7122) is also used as a reference strain for the genus *Anabaena (61).* As shown in Figure 5-1 and Figure 5-2, PCC 7122 also has PSI monomer, dimer, and tetramer. With 0.4% DDM, PCC 7122 showed mostly tetrameric PSI and little PSI dimer (Figure 5-1), which may indicate that the observation of PSI dimer can be a solubilization effect.

Fischerella muscicola PCC 7414 and *Nostoc* sp. PCC 7120

Fischerella muscicola PCC 7414 (PCC 7414) was originally isolated from a hot spring in New Zealand and used as a reference strain for the genus *Fischerella* (*61*). The genome of PCC 7414 was sequenced and it was speculated that cyanobacteria in Subsection V are the closest relatives to plastid ancestor (*123*). To our interest, PCC 7414 has two different copies of *psaL* gene, as similar to some of other strains of *Fischerella* such as PCC 9605. Gan, F et al. observed these copies of *psaL* gene in PCC 7414 and speculated that they may be expressed under different light conditions, one in response to far-red light (*34*). Here we show that PCC 7414 has tetrameric PSI and a more detailed study about this strain will be presented in Chapter six.

As shown in Figure 5-3A, after BN-PAGE, three major green bands representing potential PSI tetramer, dimer, monomer are shown. The relative quantity distribution of those three green bands under different solubilization conditions show similar pattern to that of TS-821, with the potential PSI tetramer

Figure 5- 3 BN-PAGE of solubilized thylakoid membrane from PCC 7414 and PCC 7120

(A) Thylakoid membranes with 0.4 mg/mL Chl from PCC 7414 cultured in BG-11_0 and BG-11 were solubilized in different concentrations of DDM (w/v, %), labeled on top of each lane. ~ 2 µg Chl were loaded for each condition. The potential extra-large potential PSI.bands are pointed out by arrows.
(B) Thylakoid membranes with 0.4 mg/mL Chl from PCC 7120 cultured in BG-11 were solubilized in different concentrations of DDM (w/v, %), labeled on top of each lane.TS-821 thylakoid membrane solubilized in 1% DDM was used as a control. ~ 2 µg Chl were loaded for each condition.
(C) BN-PAGE (homemade gel) of solubilized thylakoid membrane from PCC 7414 and PCC 7120 with 0.4 mg/mL Chl in 1% DDM. TS-821 was used as a control. The bands that were sliced out for PSI identification were numbered or pointed as “extra”. For each lane ~ 8 µg Chl were loaded.

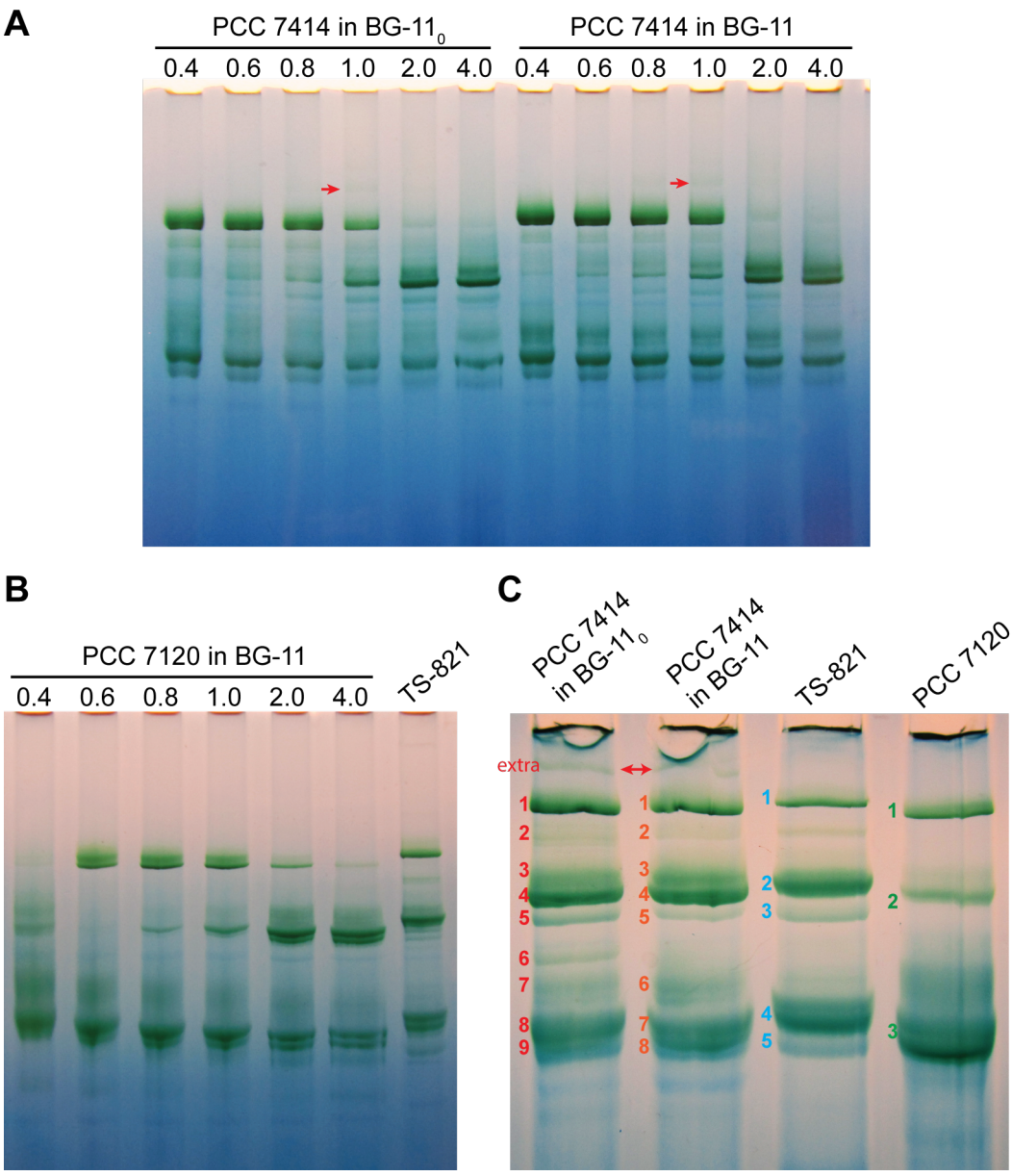

Figure 5-3 continued

dissociating into dimers under high detergent concentration. Interestingly, an extra-large faint green band is shown at several conditions of solubilization (red arrows, Figure 5-3 A and C). The growth media (BG-11 vs BG-11_0) do not seem to affect the PSI tetramer except that an additional green band, No. 6 under PCC 7414 in BG-11_0, is shown when PCC 7414 was cultured in nitrogen fixation conditions (Figure 5-3C). Confirmed by second dimension SDS-PAGE (Figure 5-4), PCC 7414 has PSI tetramer, along with PSI trimer, dimer, and monomer.

In PCC 7414, the extra-large band of PSI may correspond to PSI-phycobilisome supercomplex similar to what has been observed in PCC 7120 (*20*). At the same time, PCC 7414 shows an additional PSI monomer species (No. 6 under PCC 7414 in BG-11_0, Figure 5-3C and Figure 5-4B) under nitrogen fixation conditions. Those two observations are interesting, which can be further studied. In this study understanding the distribution of the PSI tetramer and physiological significance is the main focus. The impact of nitrogen source on the PSI tetramer was studied more extensively and comprehensively, as shown in Chapter Six.

<u>*Nostoc* sp. PCC 7120</u>

Nostoc sp. PCC 7120 (PCC 7120) was classified in the genus of *Anabaena (61)*, however, *Nostoc* was still widely used as the genus name for the strain PCC 7120. Previous studies have studied PCC 7120 for its PSI oligomeric state and the first report of PSI tetramer in cyanobacteria was also in PCC 7120 (*19, 20*). In addition to the discovery of PSI tetramer in PCC 7120, the direct attachment of PSI to phycobilisome was also reported (*20*). In this study, we

Figure 5- 4 SDS-PAGE of photosystems from PCC 7414 and PCC 7120 for PSI identification.

(A) SDS-PAGE of green bands isolated from BN-PAGE gel of solubilized thylakoid membrane from PCC 7414 cultured in BG-11. TS-821 photosystem bands were used as controls.
(B) SDS-PAGE of green bands isolated from BN-PAGE gel of solubilized thylakoid membrane from PCC 7414 cultured in BG-11_0 and from PCC 7120 cultured in BG-11. TS-821 PSI monomer was used as a control for PSII identification. Some PSII major subunits are pointed out by arrows.
The identification of photosystems is labeled on top of each lane, with band numbers corresponding to the bands labeled in Figure 5-3C. The oligomeric states of photosystems are denoted as well. Some oligomeric states are not clear with one or two "+" sign labeled following an oligomeric state interpretation, indicating their bigger sizes compared to corresponding oligomers.

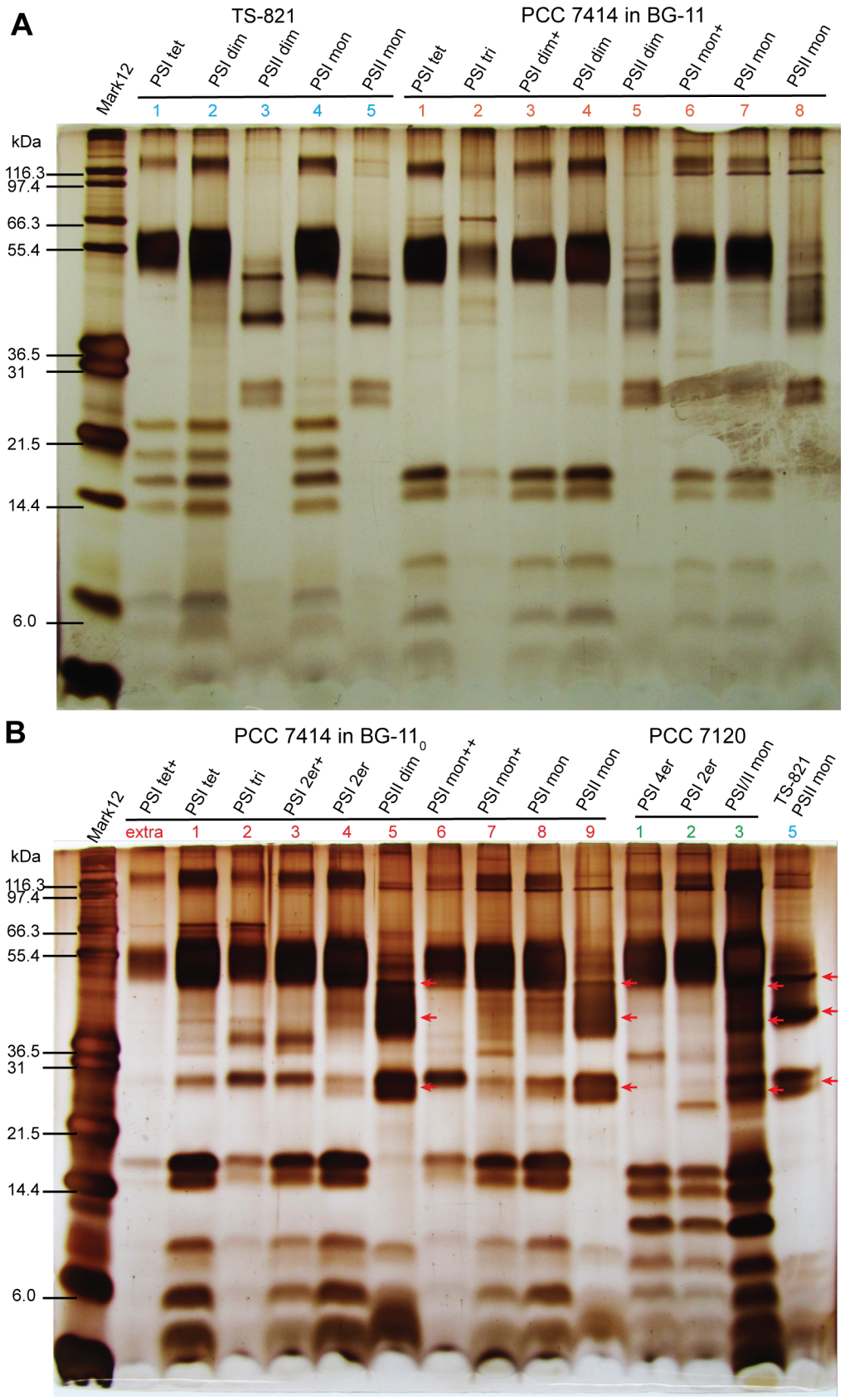

Figure 5-4 continued

used PCC 7120 as a control and confirmed the observation of previous study. At the same time, some physiological conditions were tested using PCC 7120 to explore the reason of forming tetrameric PSI in cyanobacteria. The results for PCC 7120 confirms the observation made by Watanabe et al. (*19*).

Investigation of PSI Tetramer Distribution in Cyanobacteria and Glaucophytes UTEX Strains.

After initial confirmation that more heterocyst-forming cyanobacteria have tetrameric PSI, we decided to extensively investigate the distribution of PSI tetramer among cyanobacteria. Tetrameric PSI was expected to be present in all heterocyst-forming cyanobacteria, however, the results support that most heterocyst-forming cyanobacteria form tetrameric PSI but there are some special strains that only possess monomeric PSI. Detailed results are presented for each strain investigated.

Fischerella muscicola UTEX LB 1829

Fischerella muscicola UTEX LB 1829 (LB 1829) is also known as *Fischerella* sp. PCC 9339, which has been sequenced for its genome (*118*). As shown in Figure 2-2, the membrane solubilized pattern for LB 1829 is quite similar to what was observed in PCC 7414 with major green bands being potentially PSI tetramer, dimer and monomer. There is also a minor portion of potential PSI trimer. The SDS-PAGE of major green bands indicates the presence of PSI tetramer in LB1829 (Figure 5-5).

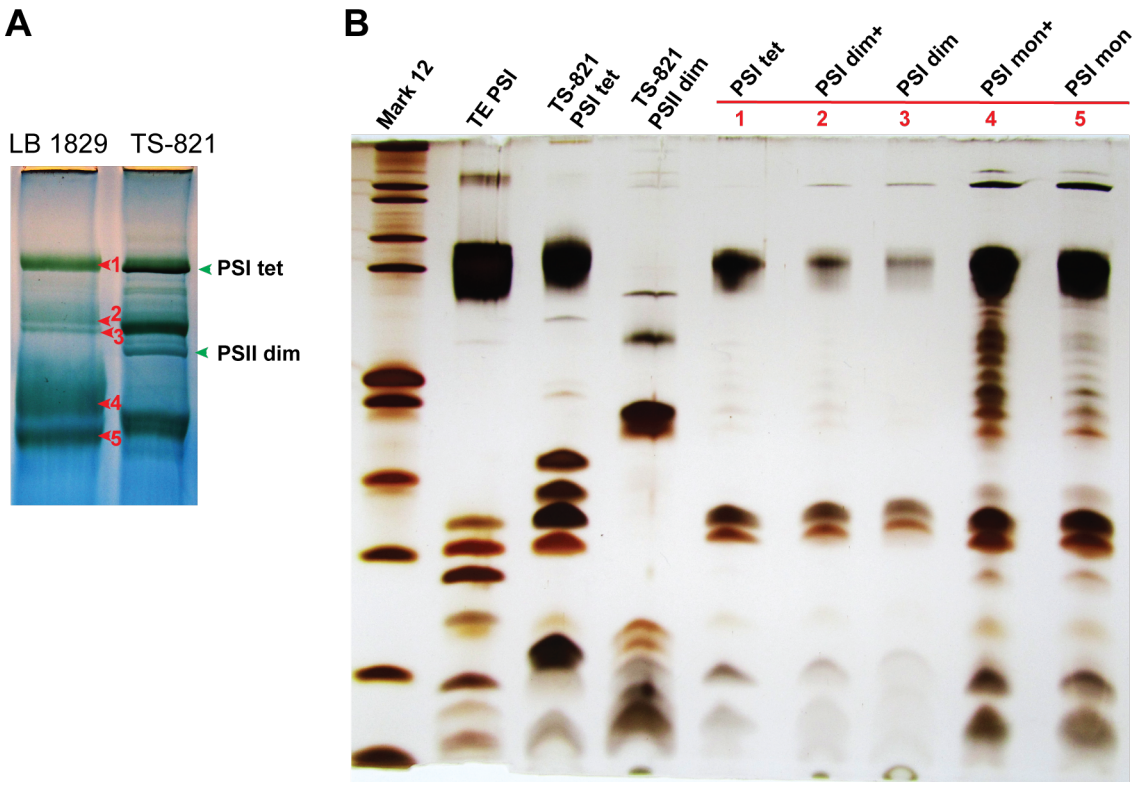

Figure 5- 5 SDS-PAGE of photosystems from LB 1829 for PSI identification

(A) BN-PAGE (homemade gel) of solubilized thylakoid membrane with 0.4 mg/mL Chl in 1% DDM from LB 1829, with TS-821 as a control. Bands of interest are labeled and isolated for following SDS-PAGE.

(B) SDS-PAGE of green bands isolated from BN-PAGE gel (A). Protein standards Mark12 was used. Purified TE PSI (trimer), TS-821 PSI and PSII from BN-PAGE gel (A) were used as control for PSI identification. Numbered lanes correspond to numbered bands in (A) from LB 1829. PSI oligomeric state interpretations were denoted on top of each lane as well.

Scytonema hofmanni UTEX B 2349 and *Spirirestis rafaelensis* UTEX B 2660

Scytonema hofmanni UTEX B 2349 (B 2349), also known as *Tolypothrix* sp. PCC 9009, has been sequenced for its genome (118). *Spirirestis rafaelensis* UTEX B 2660 (B 2660) is a novel cyanobacterium species isolated recently from San Rafael Sell in Utah, US (*124*). The closest strain for B 2660 outside the genus *Spirirestis* is in the genus *Tolypothrix* (*124*).

As shown in Figure 5-6, B 2349 and B 2660 showed very similar population of green bands after BN-PAGE analysis. At lower concentration of DDM, 0.4%, the membranes are not solubilized very well. Clearly, the abundance of potential PSI dimer species increases as the DDM concentration increases, with the decreases of potential tetrameric PSI. SDS-PAGE analysis (Figure 5-7) of the green bands confirmed that both B 2349 and B 2660 have tetrameric PSI as well as trimeric PSI. The close membrane solubilization pattern may indicate that they are close relatives.

Fremyella diplosiphon UTEX B 481 and *Gloeotrichia ghosi* UTEX LB 1920

Fremyella diplosiphon UTEX B 481 (B 481), also known as *Tolypothrix* sp. PCC 7601, is famous for its fine tuning of the light harvesting complex in response to different light colors (*125*). In contrast to well characterized light harvesting characteristics, the photosystems of B 481 have not been characterized. *Gloeotrichia ghosi* UTEX LB 1920 (LB 1920) was not characterized for its photosystem either. During thylakoid membrane preparation, the cell lysates of both LB 1920 and B 481 show purple/pink color, which indicates the presence of phycoerythrin in both strains.

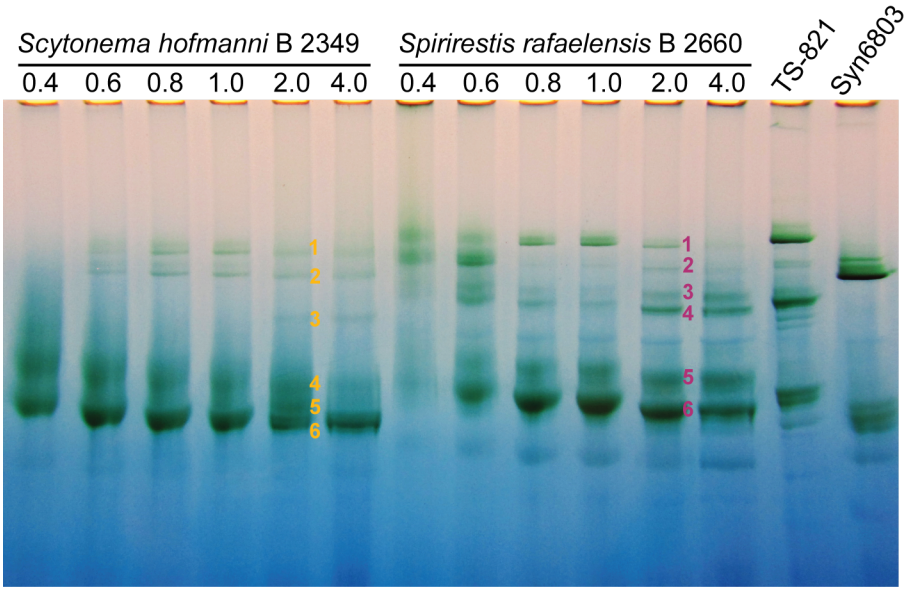

Figure 5- 6 BN-PAGE of solubilized thylakoid membrane from B 2349 and B 2660

Thylakoid membranes with 0.4 mg/mL Chl from B 2349 and B 2660 were solubilized in different concentrations of DDM (w/v, %), labeled on top of each lane. Solubilized thylakoid membranes from TS-821 and *Synechocystis* sp. PCC 6803 (Syn6803) with 0.4 mg/mL Chl in 1% DDM were loaded as controls. ~ 2 µg Chl were loaded for each condition. The green bands sliced out for second dimension SDS-PAGE (Figure 5-7) and PSI identification are numbered on the right side of each band.

Figure 5- 7 SDS-PAGE of photosystems from B 2349 and B 2660 for PSI identification

(A) SDS-PAGE of green bands isolated from B 2349 BN-PAGE gel (Figure 5-6).

(B) SDS-PAGE of green bands isolated from B 2660 BN-PAGE gel (Figure 5-6)

Purified TE PSI (trimer), TS-821 PSI and PSII from BN-PAGE gel were used as control for PSI identification. Numbered lanes correspond to numbered bands in Figure 5-6. PSI oligomeric state interpretations were denoted on top of each lane as well.

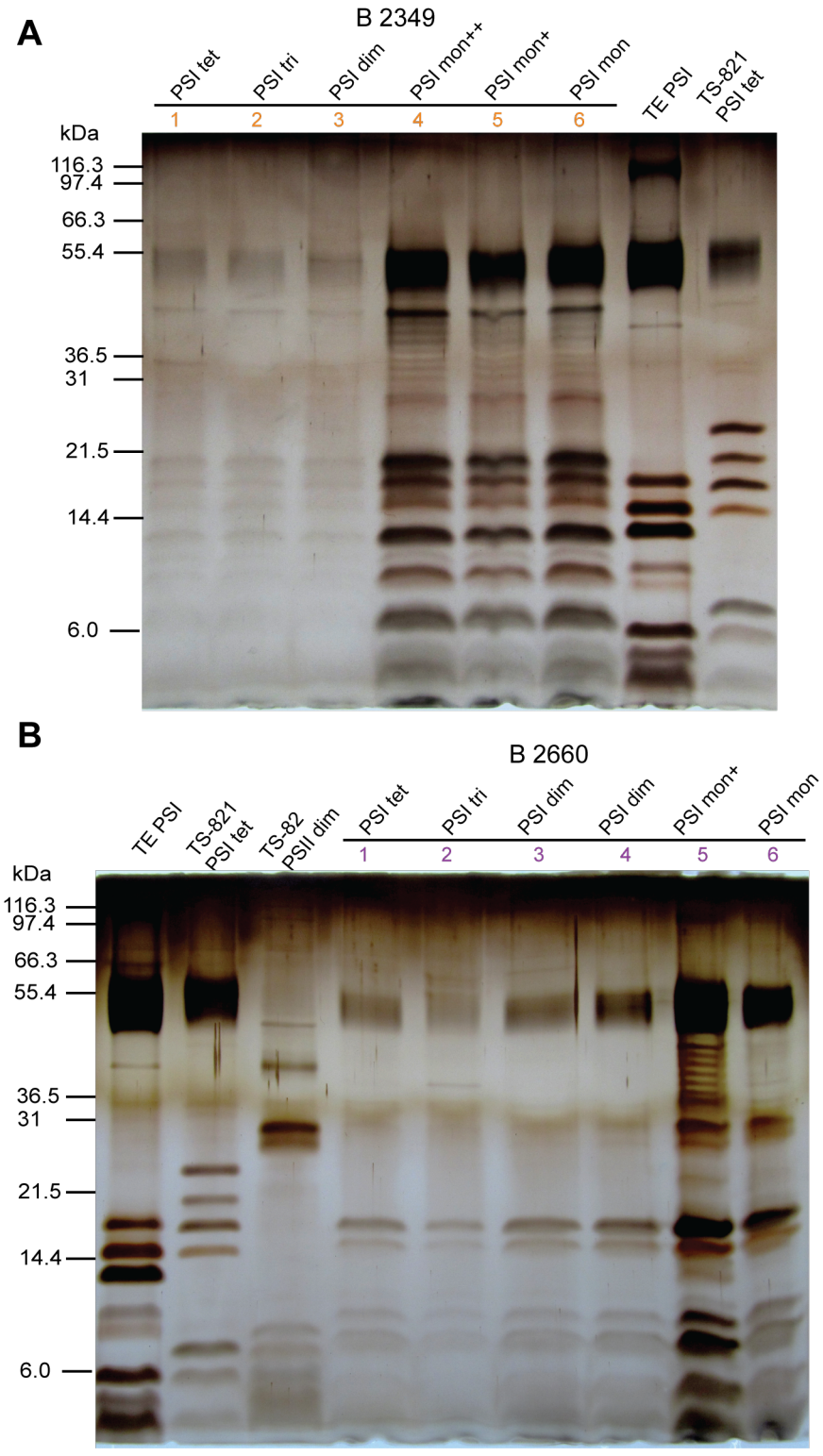

Figure 5-7 continued

The BN-PAGE and SDS-PAGE analyses showed that both B 481 and LB 1920 have tetrameric PSI (Figure 5-8). The tetrameric PSI dissociate into PSI dimers under solubilization conditions with high % DDM (Figure 5-8). No PSI trimer was observed in B 481 and LB 1920 (Figure 5-8), in contrast to what have been observed in B 2349, and B 2660 (Figure 5-6). What cause this difference will be discussed but the reason may need further studies.

Anabaena flos-aquae UTEX 1444 and *Anabaena flos-aquae* UTEX LB 2558

Anabaena flos-aquae UTEX 1444 (UTEX 1444), also known as *Anabaena variabilis* ATCC 29413 with known genome sequence, was predicted to have tetrameric PSI (*21*). *Anabaena flos-aquae* UTEX LB 2558 (LB 2558), classified as the same species as UTEX 1444, has not been studied for its genome or photosystems. The analysis of the PSI oligomeric state using BN-PAGE and SDS-PAGE showed that both UTEX 1444 and LB 2558 have tetrameric PSI (Figure 5-9). The membrane solubilized pattern for these two s trains look similar to that of B 481 and B 1920 (Figure 5-8), without obvious PSI trimer present.

Calothrix parietina UTEX LB 1952, *Tolypothrix distorta var. symplocoides* UTEX B 424

Calothrix parietina UTEX LB 1952 (LB 1952) and *Tolypotrhix distorta var. symplocoides* UTEX B 424 (B 424) are not well-studied strains. As heterocyst-forming cyanobacteria with little information available, they are good candidates for testing if the PSI tetramer exist in heterocyst-forming cyanobacteria. As shown in Figure 5-10 and Figure 5-11, both LB 1952 and B 424 have tetrameric PSI, which dissociates into dimers upon high concentration of detergent

Figure 5- 8 BN-PAGE of solubilized thylakoid membranes and SDS-PAGE of photosystems from B 481 and LB 1920 for PSI identification

(A) BN-PAGE of solubilized thylakoid membrane from B 481 and LB 1920. Thylakoid membranes with 0.4 mg/mL Chl from B 481 and LB 1920 were solubilized in different concentrations of DDM (w/v, %), labeled on top of each lane. Solubilized thylakoid membranes from TS-821 and *Synechocystis* sp. PCC 6803 (Syn6803) with 0.4 mg/mL Chl in 1% DDM were loaded as controls. ~ 2 µg Chl were loaded for each condition. The green bands sliced out for second dimension SDS-PAGE (B) and PSI identification are numbered on the right side of each band.

(B) SDS-PAGE of photosystems from B 481 and LB 1920 for PSI identification. Purified TE PSI (trimer), TS-821 PSI and PSII from BN-PAGE gel were used as control for PSI identification. Numbered lanes correspond to numbered bands in (A). PSI oligomeric state interpretations were denoted on top of each lane as well.

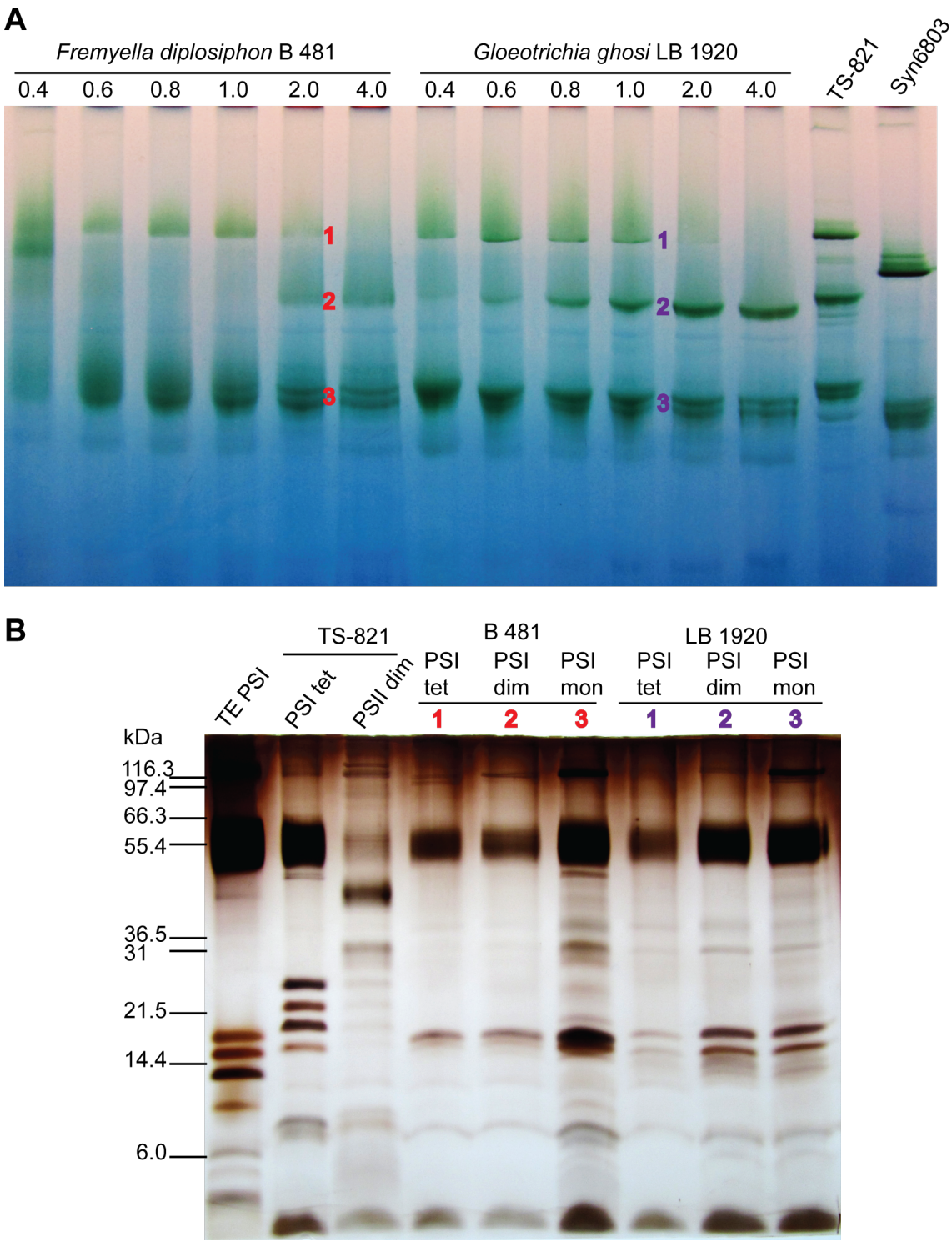

Figure 5-8 continued

Figure 5- 9 BN-PAGE of solubilized thylakoid membranes and SDS-PAGE of photosystems from UTEX 1444 and LB 2558 for PSI identification

(A) BN-PAGE of solubilized thylakoid membrane from UTEX 1444 and LB 2558. Thylakoid membranes with 0.4 mg/mL Chl from UTEX 1444 and LB 2558 were solubilized in different concentrations of DDM (w/v, %), labeled on top of each lane. Solubilized thylakoid membranes from TS-821 and Synechocystis sp. PCC 6803 (Syn6803) with 0.4 mg/mL Chl in 1% DDM were loaded as controls. ~ 2 µg Chl were loaded for each condition.

(B) BN-PAGE (homemade gel) of solubilized thylakoid membranes of UTEX 1444 and LB 2558 for following SDS-PAGE (C) The green bands sliced out for second dimension SDS-PAGE (C) and PSI identification are numbered. TS-821 PSI (tet) and PSII (dim) are pointed out and used as controls

(C) SDS-PAGE of photosystems from UTEX 1444 and LB 2558 for PSI identification. Purified TE PSI (trimer), TS-821 PSI and PSII from BN-PAGE gel were used as control for PSI identification. Numbered lanes correspond to numbered bands in (B). PSI oligomeric state interpretations were denoted on top of each lane as well.

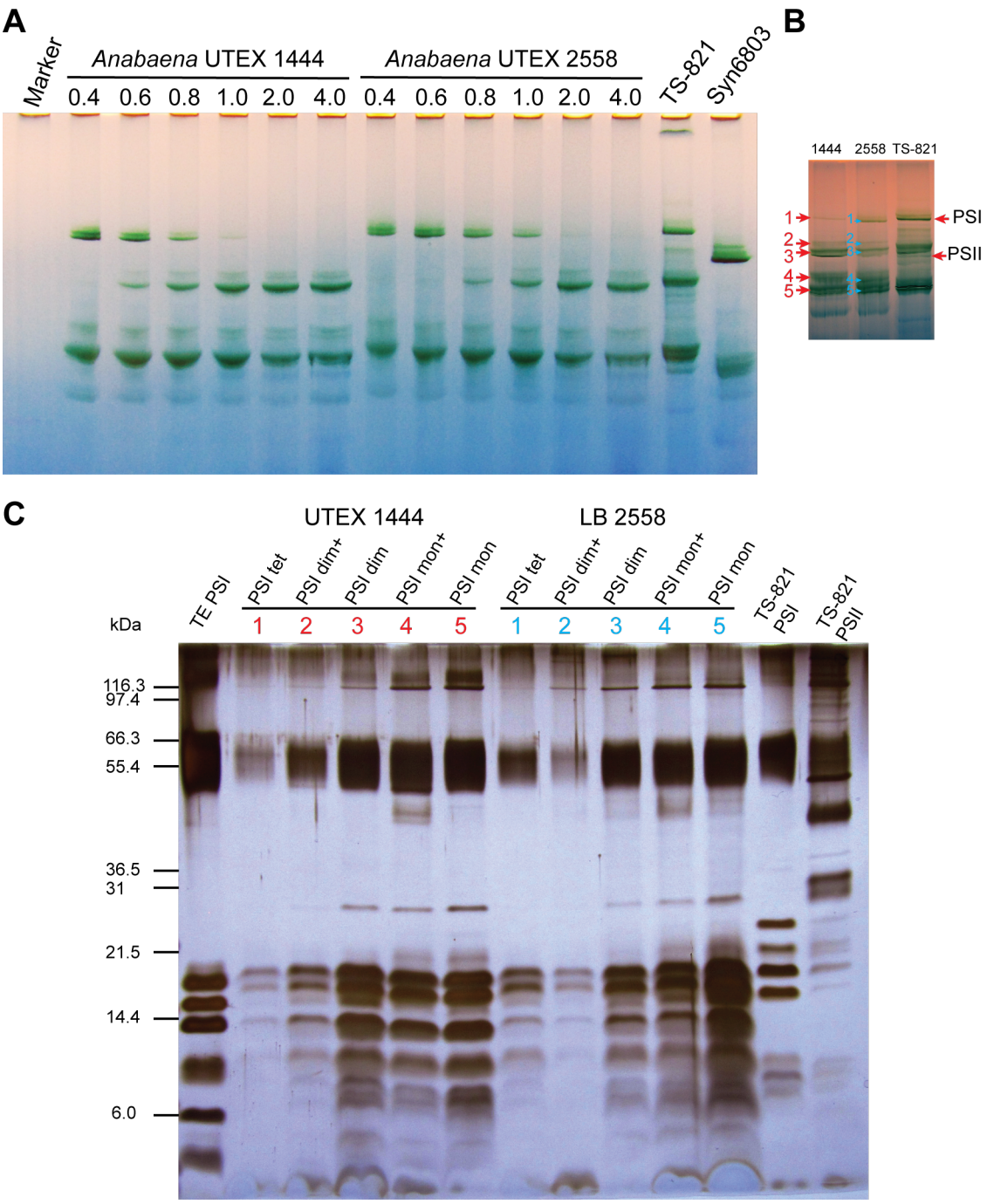

Figure 5-9 continued

Figure 5- 10 BN-PAGE of solubilized thylakoid membrane from LB 1952, B 2965, and B 424

(A) BN-PAGE of solubilized thylakoid membrane from LB 1952 and B 2965. Thylakoid membranes with 0.4 mg/mL Chl from three strains were solubilized in different concentrations of DDM (w/v, %), labeled on top of each lane. Solubilized thylakoid membranes from TS-821 and *Synechocystis* sp. PCC 6803 (Syn6803) with 0.4 mg/mL Chl in 1% DDM were loaded as controls. ~ 2 µg Chl were loaded for each condition for both (A) and (B).
(B) BN-PAGE of solubilized thylakoid membrane from B 424.
(C) BN-PAGE (homemade gel) of solubilized thylakoid membrane from LB 1952 and B 424 for following SDS-PAGE and PSI identification (Figure 5-11). The green bands (C) sliced out for second dimension SDS-PAGE and PSI identification are numbered. Solubilization condition in 1% DDM was used. TS-821 PSI (tet) and PSII (dim) are pointed out and used as controls. ~ 8 µg Chl were loaded for each lane.

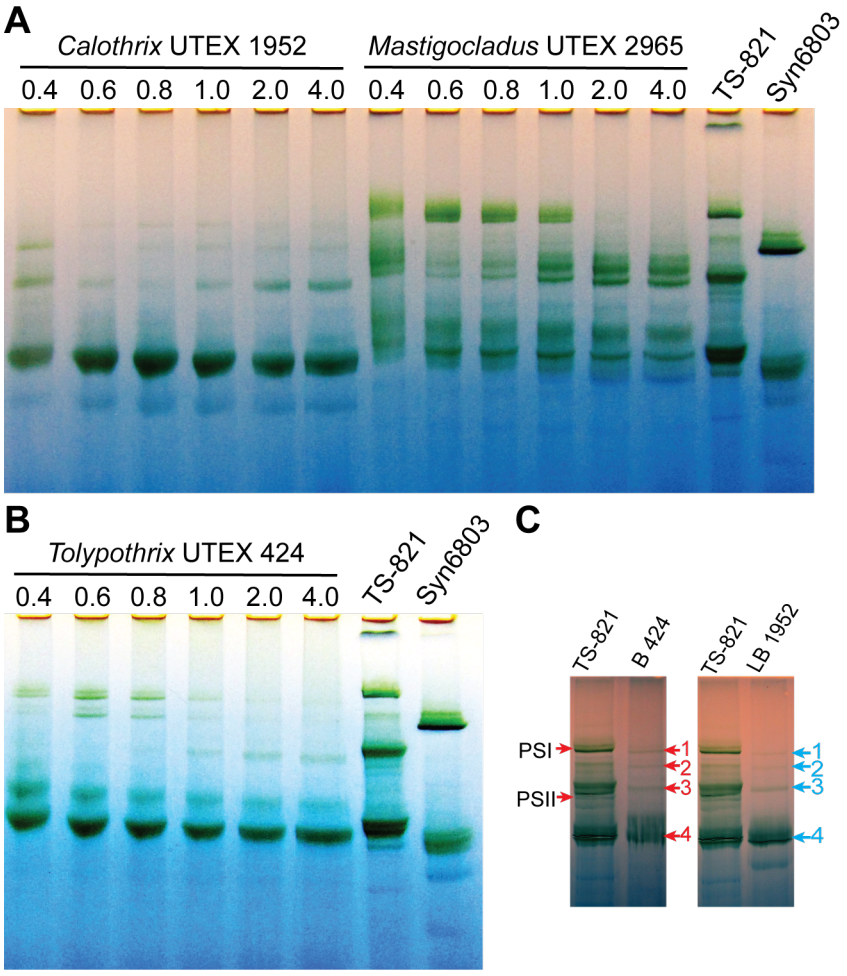

Figure 5-10 continued

Figure 5- 11 SDS-PAGE of photosystems from LB 1952, B 424, and B 2965 for PSI identification

(A) SDS-PAGE of photosystems from LB 1952 and B 424 for PSI identification. Purified TE PSI (trimer), TS-821 PSI and PSII from BN-PAGE gel were used as control for PSI identification. Numbered lanes correspond to numbered bands in Figure 5-10. PSI oligomeric state interpretations were denoted on top of each lane as well.

(B) BN-PAGE (homemade gel) of solubilized thylakoid membrane from B 2965 for following SDS-PAGE and PSI identification (C). Solubilization condition in 1% DDM was used. ~ 8 µg Chl were loaded for each lane.

(C) SDS-PAGE of photosystems from B 2965 for PSI identification. Purified TE PSI (trimer), TS-821 PSI and PSII from BN-PAGE gel were used as control for PSI identification. Numbered lanes correspond to numbered bands in (B). PSI oligomeric state interpretations were denoted on top of each lane as well.

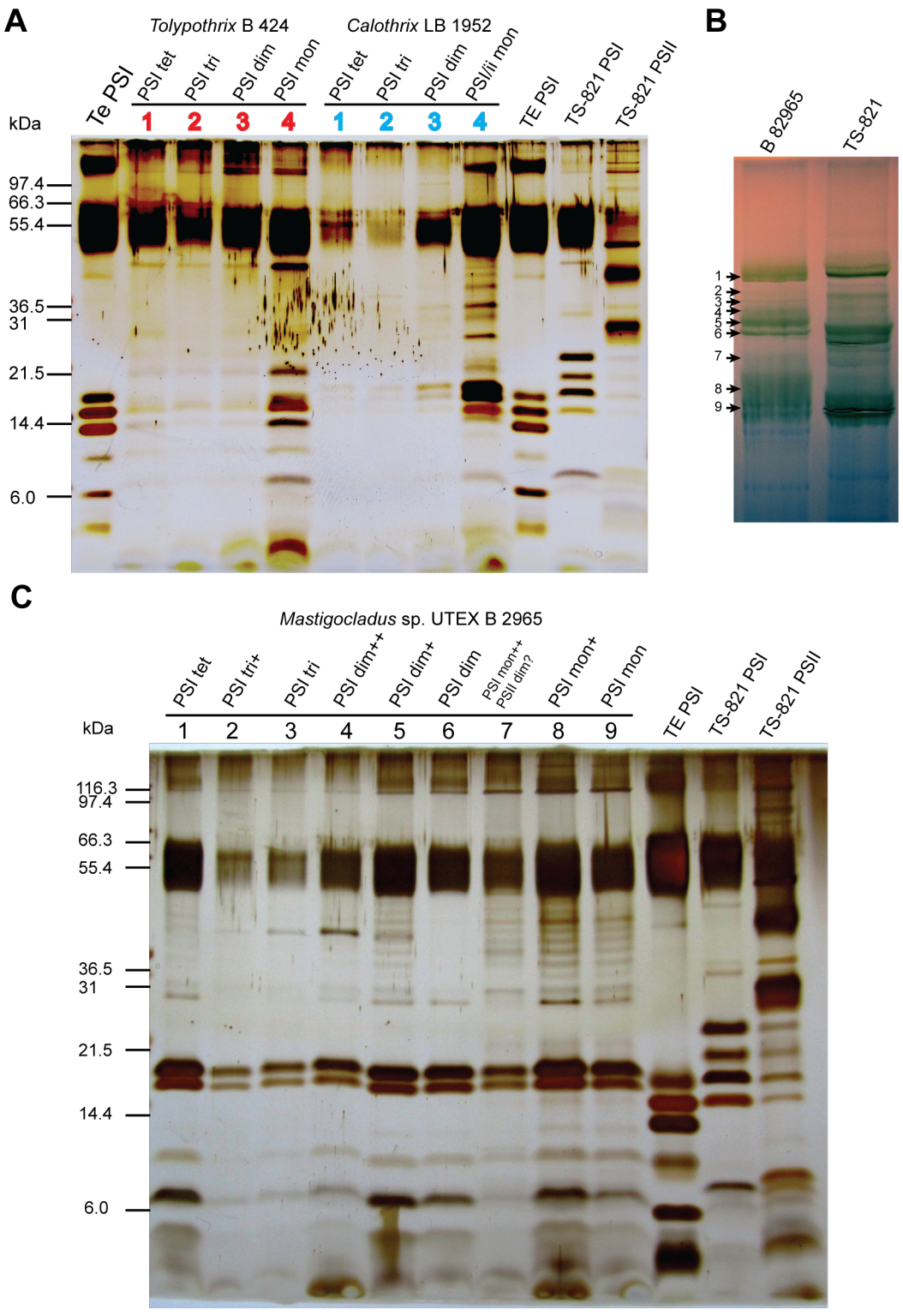

Figure 5-11 continued

treatment. Both strains also have trimeric PSI, which is more as predominant as tetrameric PSI. Considering that PSI tetramer can dissociate into dimers and monomers, PSI trimer in LB 1952 and B 424 can be considered as minor species.

Mastigocladus sp. UTEX B 2965

Mastigocladus sp. UTEX B 2965 (B 2965) is a thermophilic strain which can survive but grow slow at 20 °C. As shown in Figure 5-10 and Figure 5-11, the PSI oligomeric species are quite similar to what have been described in *Fischerella* species (PCC 7414 and LB 1829), indicating B 2965 is close related to *Fischerella*.

Nodularia harveyana UTEX B 2093

Nodularia harveyana UTEX B 2093 (B 2093) was isolated from coastal pond with salinity 1.8% in San de Fuca, WA (*126*). The suggested medium for culturing this strain from UTEX is BG-11. However, B 2093 grow faster in modified ASNIII media than in BG-11. As shown in Figure 5-12, B 2093 has tetrameric PSI and trimeric PSI. The tetrameric PSI in B 2093 is very stable considering its relative high abundance even under in high concentration of DDM (Figure 5-12A). This is in contrast to what was observed in *Nodularia spumigena* PCC 73104 (Figure 5-1 and Figure 5-2), even though both strains are classified as *Nodularia*.

Scytonematopsis contorta sp. nov. UTEX B 2963

Scytonematopsis contorta sp. nov. UTEX B 2963 (B 2963) was isolated recently from Hawaii, little was studied about this strain except the original characterization (*127*). B 2963 does not show abundant PSI tetramer except

Figure 5- 12 BN-PAGE of solubilized thylakoid membranes and SDS-PAGE of photosystems from B 2093 and B2963 for PSI identification

(A) BN-PAGE of solubilized thylakoid membrane from B 2093 and B2963. Thylakoid membranes with 0.4 mg/mL Chl from B 2093 and B 2963 were solubilized in different concentrations of DDM (w/v, %), labeled on top of each lane. Solubilized thylakoid membranes from TS-821 and Synechocystis sp. PCC 6803 (Syn6803) with 0.4 mg/mL Chl in 1% DDM were loaded as controls. ~ 2 µg Chl were loaded for each condition. A potential PSI tetramer band is pointed out by an arrow.

(B) BN-PAGE (homemade gel) of solubilized thylakoid membranes of B 2093 (1% DDM) and B 2963 (2% DDM) for following SDS-PAGE (C) The green bands sliced out for second dimension SDS-PAGE (C) and PSI identification are numbered. TS-821 PSI (tet) and PSII (dim) are pointed out and used as controls. ~ 8 µg Chl were loaded for each lane.

(C) SDS-PAGE of photosystems from B 2093 and B 2963 for PSI identification. Purified TE PSI (trimer), TS-821 PSI and PSII from BN-PAGE gel were used as control for PSI identification. Numbered lanes correspond to numbered bands in (B). PSI oligomeric state interpretations were denoted on top of each lane as well.

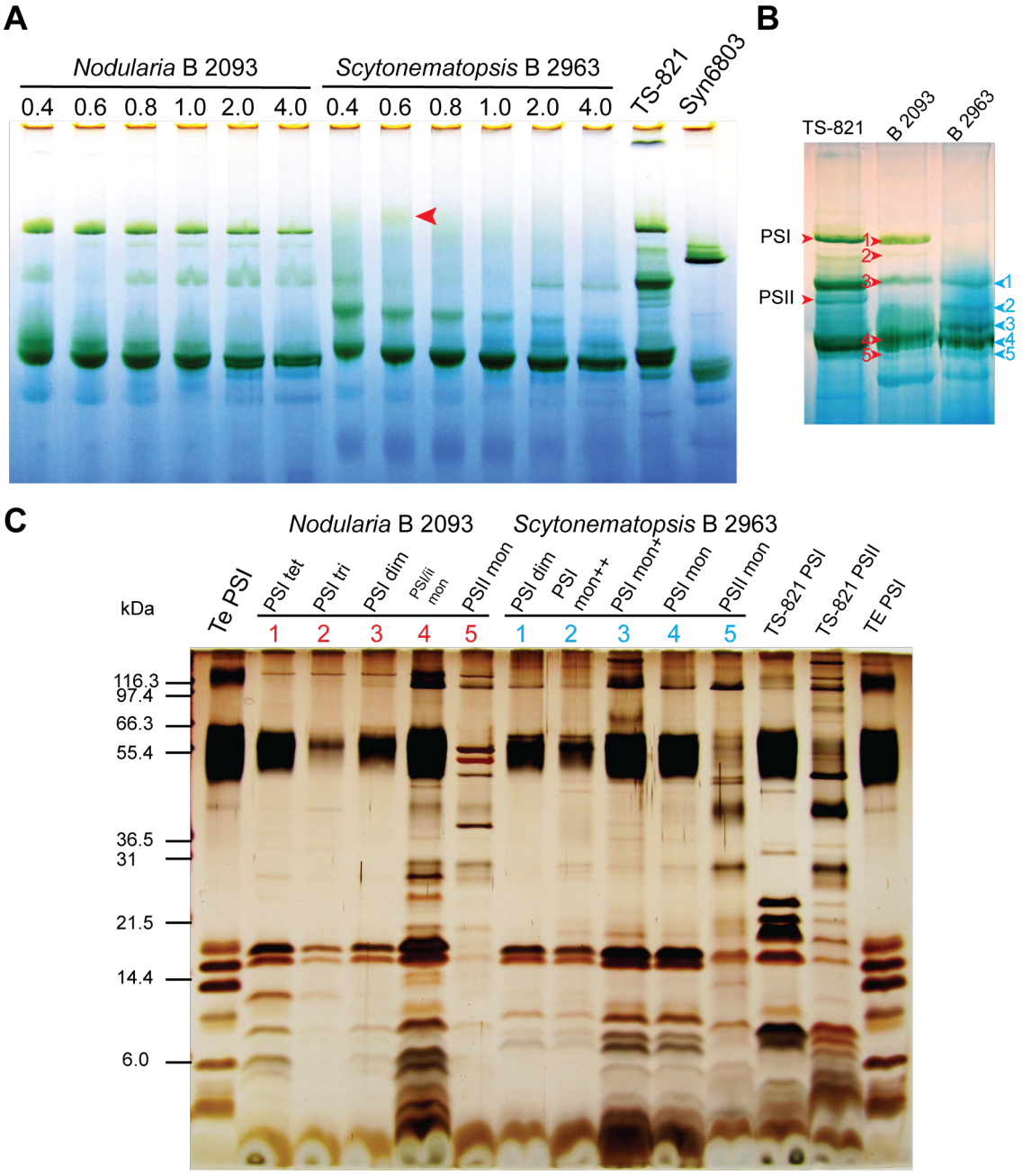

Figure 5-12 continued

some faint bands (arrow, Figure 5-12A) look like PSI tetramer. Due to its low abundance and poor uniformity, it is impractical to test if it is tetrameric PSI using BN-PAGE and SDS-PAGE. With the observed PSI dimer (Figure 5-12), we do not rule out the possibility of the presence of PSI tetramer in B 2963.

Fischerella ambigua UTEX 1903

Fischerella ambigua UTEX 1903 (UTEX 1903) is also known as *Mastigocladus laminosus*, according to UniProt (Taxon identifier 83541). The PSI in *Mastigocladus laminosus* was reported as trimeric (*17*). Since the strain was not denoted as any culture collection center strain, it is hard to verify this original result. We included the *Mastigocladus laminosus* PCC 7605 in the phylogenetic analysis of PsaL and denoted it as having PSI trimer (*21*). By studying UTEX 1903, we can verify whether or not *Mastigocladus laminosus* has tetrameric PSI. The results showed that UTEX 1903 does have tetrameric PSI, the membrane solubilization results analyzed using BN-PAGE look similar to other *Fischerella* species (Figure 5-13).

Glaucophytes *Cyanophora*

It has been reported that the glaucophyte *Cyanophora paradoxa* has tetrameric PSI (*19*). To further verify this observation, *Cyanophora paradoxa* UTEX LB 555 (LB 555) and *Cyanophora biloba* UTEX LB 2766 (LB 2766), were cultured. As shown in Figure 5-13, LB 555 only has monomeric PSI with the thylakoid membrane thoroughly solubilized when DDM concentration reaches 2%. This can be a result of a relatively low fraction of the membrane being thylakoid. As for LB 2766, it showed similar results to LB 555, with the PSI monomer being

Figure 5- 13 BN-PAGE of solubilized thylakoid membranes and SDS-PAGE of photosystems from UTEX 1903 and LB 555 for PSI identification

(A) BN-PAGE of solubilized thylakoid membrane from UTEX 1903 and LB 555. Thylakoid membranes with 0.4 mg/mL Chl from UTEX 1903 and LB 555 were solubilized in different concentrations of DDM (w/v, %), labeled on top of each lane. Solubilized thylakoid membranes from TS-821 and Synechocystis sp. PCC 6803 (Syn6803) with 0.4 mg/mL Chl in 1% DDM were loaded as controls. ~ 2 µg Chl were loaded for each condition.
(B) BN-PAGE (homemade gel) of solubilized thylakoid membranes of UTEX 1903 and LB 555 (2% DDM) for following SDS-PAGE (C) The green bands sliced out for second dimension SDS-PAGE (C) and PSI identification are numbered. TS-821 PSI (tet) and PSII (dim) are pointed out and used as controls. ~ 8 µg Chl were loaded for each lane.
(C) SDS-PAGE of photosystems from UTEX 1903 and LB 555 for PSI identification. Purified TE PSI (trimer), TS-821 PSI and PSII from BN-PAGE gel were used as control for PSI identification. Numbered lanes correspond to numbered bands in (B). PSI oligomeric state interpretations were denoted on top of each lane as well.

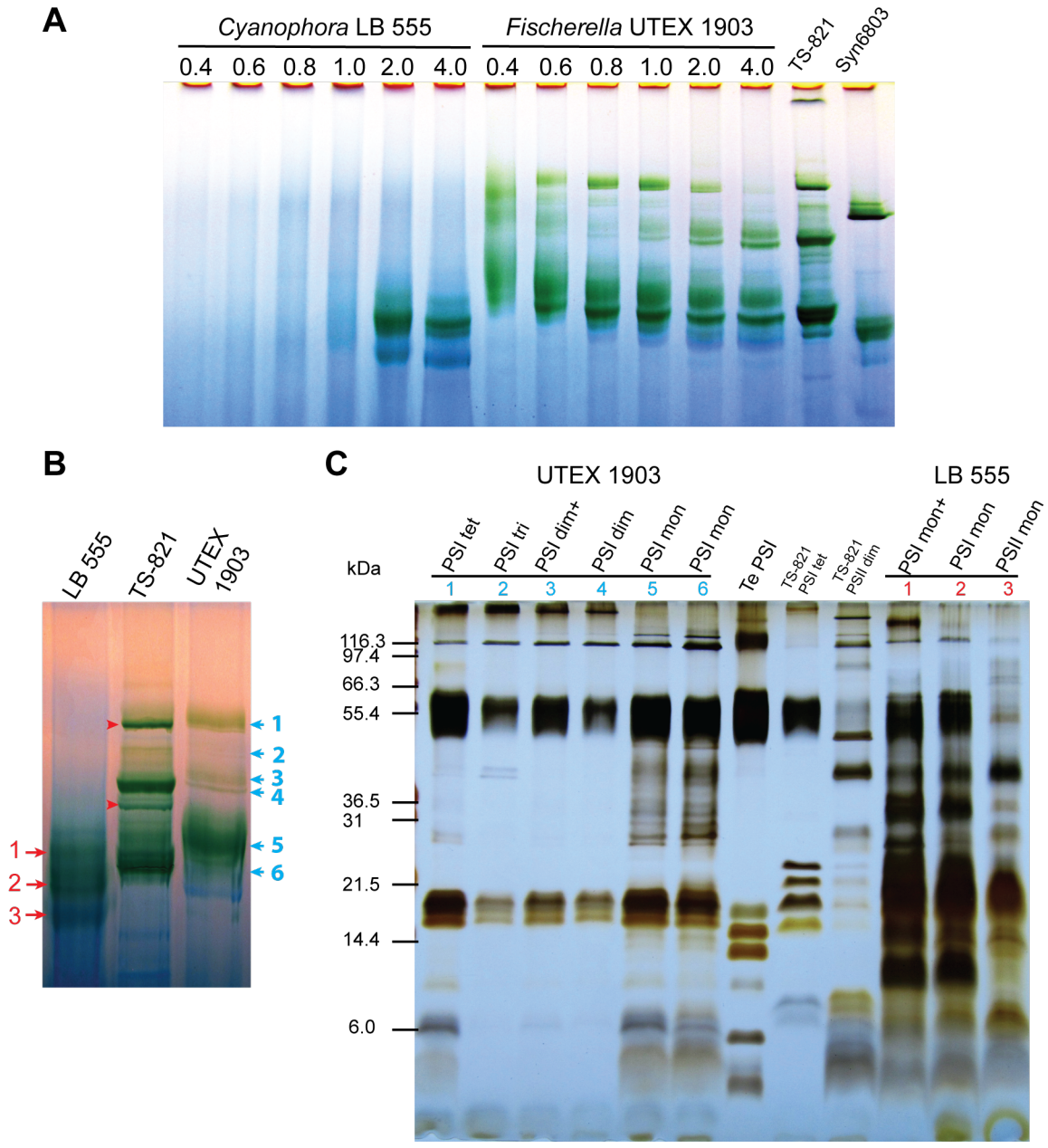

Figure 5-13 continued

the exclusive form of PSI oligomer (Figure 5-14A). To further confirm that two strains of *Cyanophora* studied here possess monomeric PSI, solubilized membranes were analyzed using sucrose density gradient ultracentrifugation. Only one green band corresponding to photosystems was resolved for both LB 555 and LB 2766 (Figure 5-15A). 77K fluorescence emission spectra of the green band showed peaks around 690 nm and 720 nm (Figure 5-15B), corresponding to peaks for PSII and PSI respectively. BN-PAGE analysis showed that both green bands from the sucrose density gradient have mainly two Chl containing proteins (Figure 5-15C), possibly PSI monomer and PSII monomer. The SDS-PAGE analysis of those protein complexes from BN-PAGE gel (Figure 5-15D) does not clearly identify the PSI monomer, which can be a result of the presence of other proteins or PSI in *Cyanophora* being unique in its composition.

Calothrix membranacea UTEX B 379*, Anabaena inaequalis* UTEX B 381 and *Cylindrospermum licheniforme* UTEX B 2014

Calothrix membranacea UTEX B 379 (B 379), *Anabaena inaequalis* UTEX B 381 (B 381) and *Cylindrospermum licheniforme* UTEX B 2014 (B 2014) are all heterocyst-forming cyanobacteria. There were no molecular studies that analyzes all those three strains together. Even though PSI tetramer was expected in all those three strains according to our earlier hypothesis, the results of BN-PAGE analysis of solubilized thylakoid membrane were surprising. All three strains have exclusively monomeric PSI, without any other obvious oligomeric forms showing on a BN-PAGE gel (Figure 5-14 B and C). The

Figure 5- 14 BN-PAGE of solubilized thylakoid membrane from LB 2766, B 379, B 381 and B 2014

(A) BN-PAGE of solubilized thylakoid membrane from LB 2766. Solubilized thylakoid membranes from TS-821 and *Synechocystis* sp. PCC 6803 (Syn6803) with 0.4 mg/mL Chl in 1% DDM were loaded as controls.
(B) BN-PAGE of solubilized thylakoid membrane from B379.
(C) BN-PAGE of solubilized thylakoid membrane from B 381 and B 2014.
Thylakoid membranes with 0.4 mg/mL Chl from three strains were solubilized in different concentrations of DDM (w/v, %), labeled on top of each lane. For B 381, B 379 and B 2014, solubilized membrane was centrifuged for 20 min at 54, 000 rpm before loading. TS-821 solubilized membrane with same treatment was used as control. ~ 2 µg Chl were loaded for each condition.

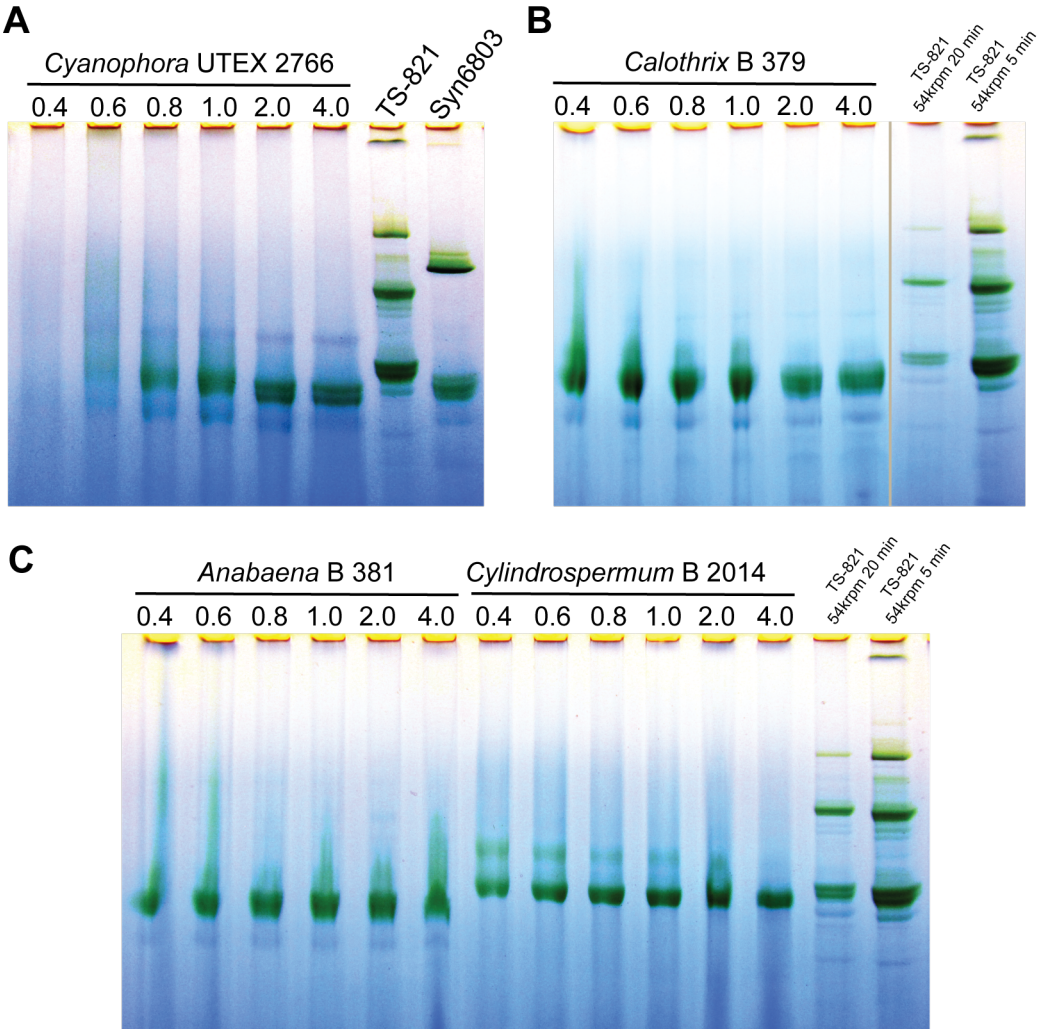

Figure 5-14 continued

Figure 5- 15 Characterization of *Cyanophora* PSI/II using sucrose density gradient ultracentrifugation, 77K fluorescence and PAGE analyses.

(A) Sucrose density gradient ultracentrifugation of solubilized thylakoid membrane from LB 555 and LB 2766. Membranes containing 0.2 mg/mL Chl were solubilized in 0.6% DDM before being loaded. Centrifugation was done using the SW32 Ti Rotor spinning at 30,000 rpm for 24 hours. The green bands corresponding to PSI/PSII are pointed out by arrows and used for following analyses.
(B) 77K fluorescence emission spectra of PSI/PSII samples isolated from sucrose density gradient (A). Spectra were normalized to maximum emission.
(C) BN-PAGE of PSI/PSII samples isolated from sucrose density gradient (A). TE PSI (trimer) was used as a control. Green bands sliced out for SDS-PAGE are pointed out and numbered.
(D) SDS-PAGE of *Cyanophora* PSI/PSII isolated from BN-PAGE gel (C). Interpretations of PSI/PSII were labeled on top of each lane with uncertainty, denoted with “?”.

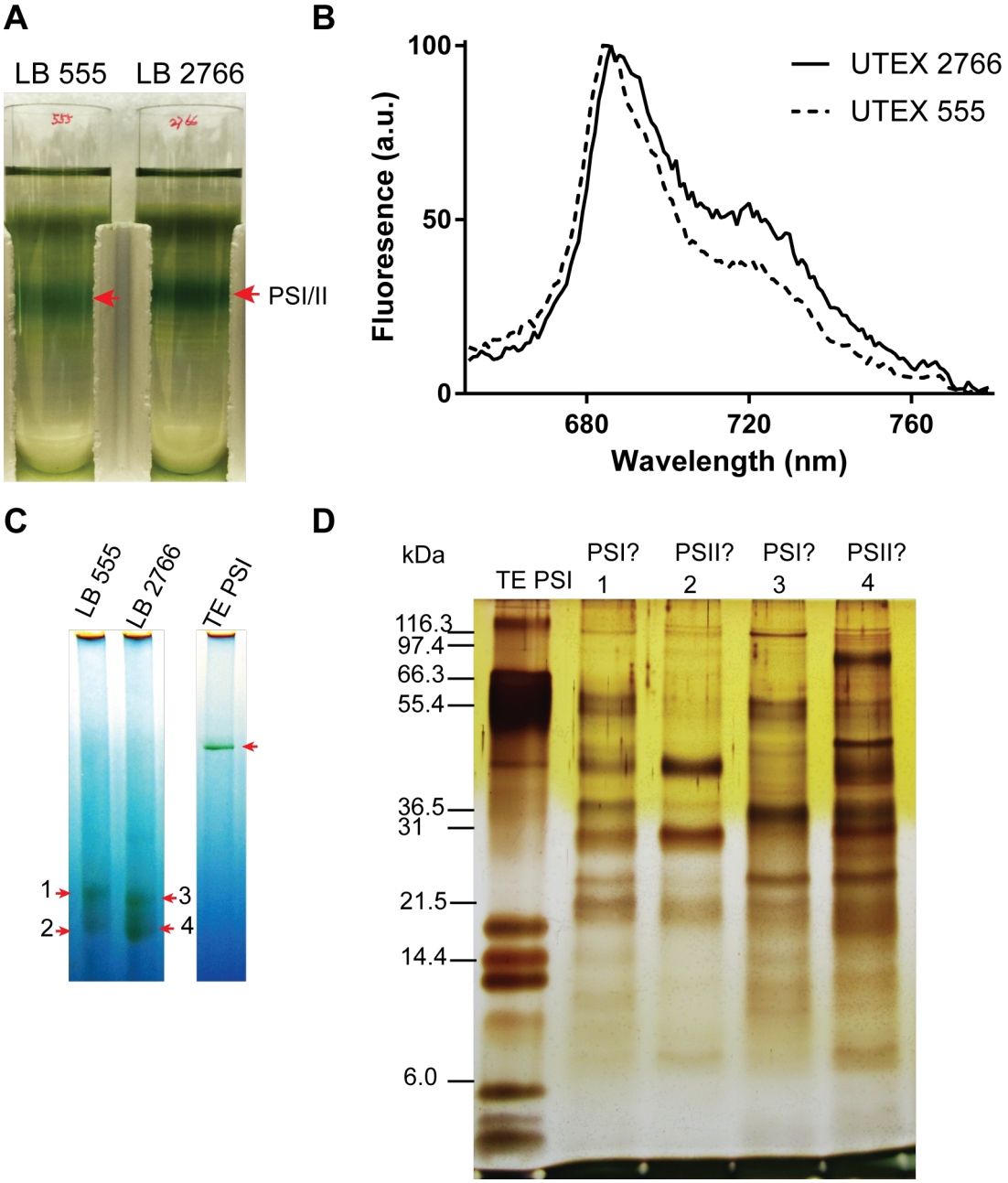

Figure 5-15 continued

solubilized membrane was centrifuged with prolonged time (20 min instead of 5 min) to pellet large particles interfering BN-PAGE analysis. To confirm this observation using BN-PAGE, sucrose density gradient ultracentrifugation was done to analyze the PSI oligomeric state in those three strains (Figure 5-16).

The results agree with the observation that B 379, B 381, and B 2014 all have little, if any, other PSI oligomers than monomeric PSI. A green band with density close to a tetrameric PSI was resolved for B 2014 (Figure 5-16A), however, the SDS-PAGE analysis of this potential PSI tetramer showed that it is not pure PSI (Figure 5-16B). This indicates that B 2014 may have exclusively monomeric PSI, with as minor species being other proteins associated with PSI subunits as a complex or an assembly intermediate.

Plectonema boryanum UTEX B 482

Plectonema boryanum UTEX B 482 (B 482), also known as *Leptolyngbya boryana* PCC 6306, has been sequenced for its genome. It is a filamentous strain of cyanobacteria but does not produce heterocyst. It was expected to possess trimeric PSI. The BN-PAGE analysis of the solubilized thylakoid membranes showed the presence of trimeric PSI in B 482 (Figure 5-17A). The PSI bands were confirmed by second dimension SDS-PAGE (Figure 5-17B).

Hapalosiphon welwitschii B 1830

Hapalosiphon welwitschii B 1830 (B 1830), also known as *Fischerella* sp. PCC 9431, has also been sequenced for its genome. It was expected to have tetrameric PSI. The BN-PAGE and SDS-PAGE analysis showed the presence of PSI tetramer (Figure 5-17). Even though B 1830 is closely related to other

Figure 5- 16 Confirming the monomeric PSI in B 379, B 381 and B 2014 by sucrose density gradient ultracentrifugation and SDS-PAGE.

(A) Sucrose density gradient ultracentrifugation analysis of solubilized thylakoid membrane from B 379, B 381 and B 2014. Membrane containing 0.4 mg/mL Chl was solubilized in 0.6% DMM and centrifuged for 24 hours at 30,000 rpm using the SW 32 Ti rotor. Solubilized TS-821 thylakoid membrane was used as control. The PSI oligomer position in in gradient was pointed out for TS-821. Green bands isolated from B 379, B 381 and B 2014 for SDS-PAGE analysis are pointed out by arrows too. Potential PSI tetramer in B 2014 is labeled as “tet?”.
(B) SDS-PAGE of fractions isolated from the sucrose density gradient (A). Purified TE PSI trimer was used as control. Strain number and PSI oligomeric state are denoted on top of each lane.

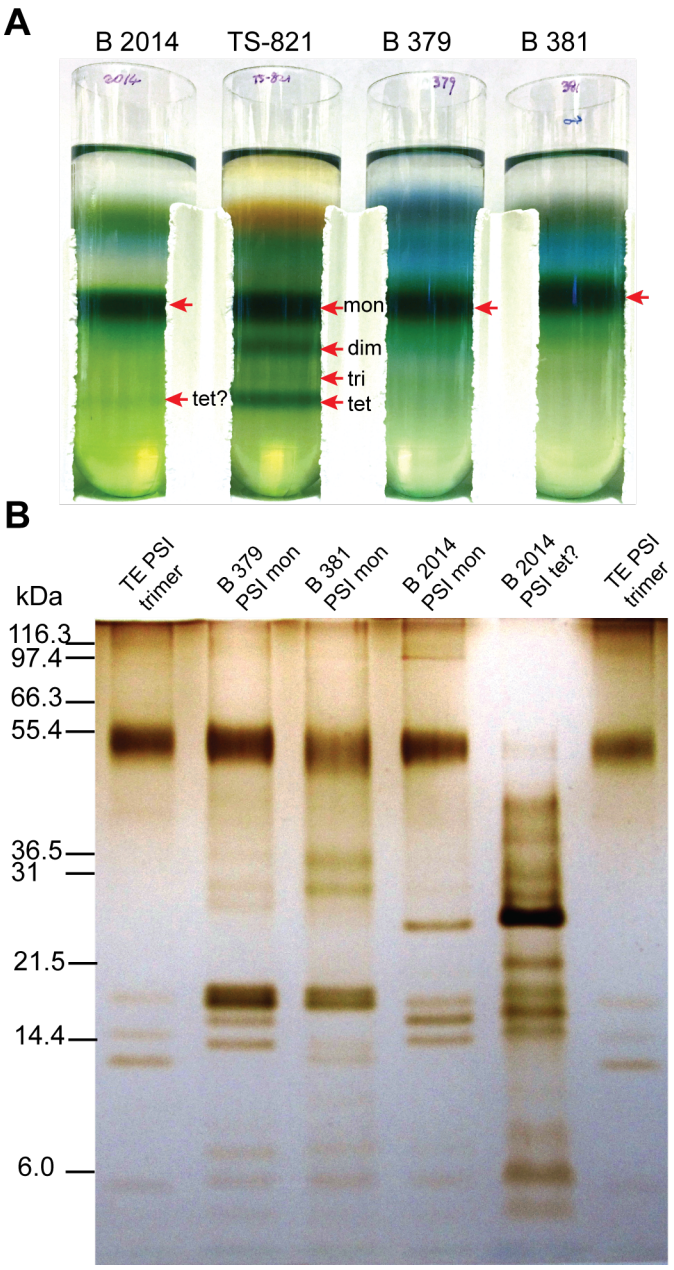

Figure 5-16 continued

Figure 5- 17 BN-PAGE and SDS-PAGE for B 482 and B 1830 PSI oligomer identification

(A) BN-PAGE of solubilized thylakoid membrane from B 482 and B1830. Thylakoid membranes with 0.4 mg/mL Chl from B 482 and B1830 were solubilized in different concentrations of DDM (w/v, %), labeled on top of each lane. Solubilized thylakoid membranes from TS-821 and *Synechocystis* sp. PCC 6803 (Syn6803) with 0.4 mg/mL Chl in 1% DDM were loaded as controls. ~ 2 µg Chl were loaded for each condition. The green bands sliced out for second dimension SDS-PAGE (B) and PSI identification are numbered on the left side of each band.
(B) SDS-PAGE of photosystems from B 482 and B1830 for PSI identification. Syn6803 PSI (tri), TS-821 PSI (tet) and PSII (dim) from BN-PAGE gel were used as control for PSI identification. Numbered lanes correspond to numbered bands in (A). PSI oligomeric state interpretations were denoted on top of each lane as well.

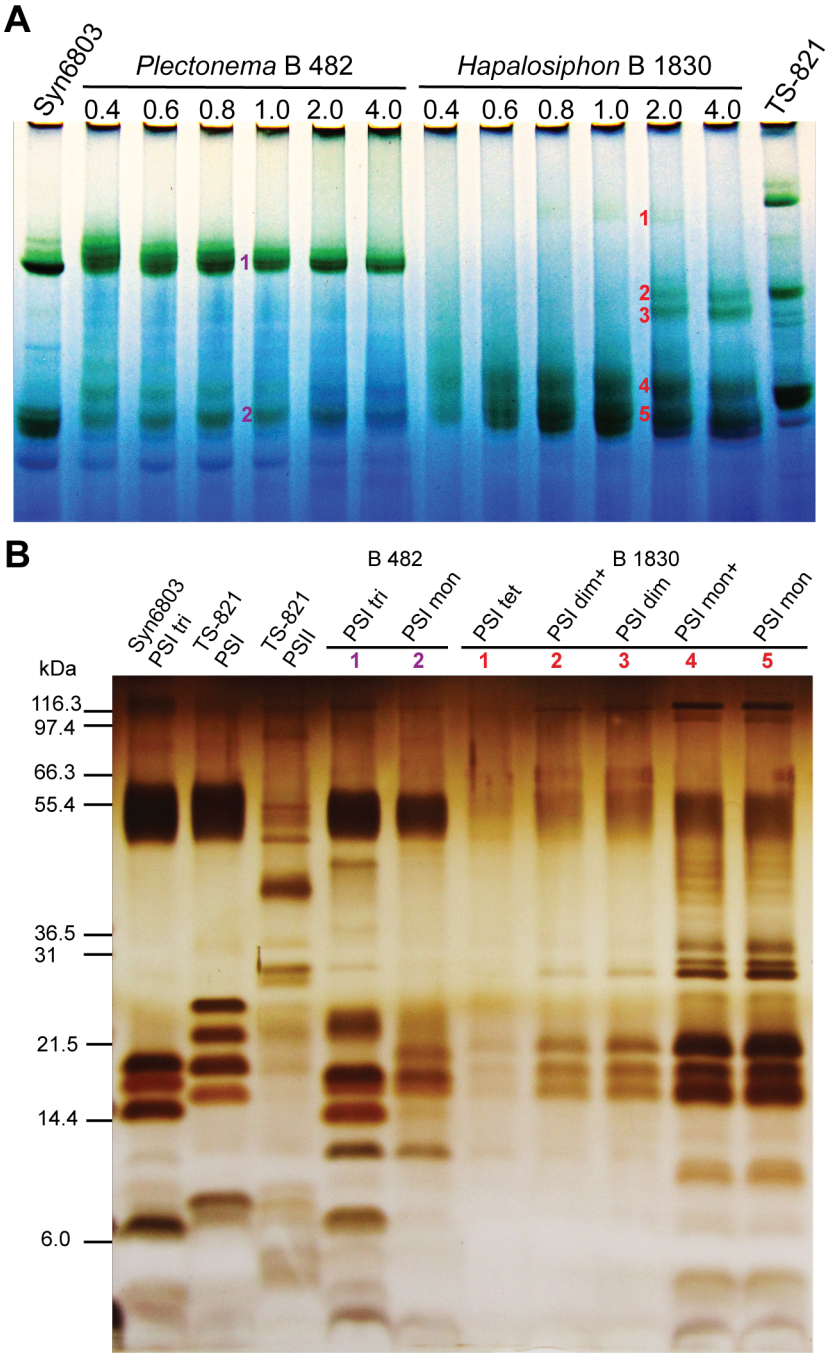

Figure 5-17 continued

Fischerella strains, the abundance of tetrameric PSI is relatively lower than other *Fischerella* strains.

Synechococcus sp. WH 7803

Synechococcus sp. WH 7803 (WH 7803) is a marine cyanobacterium known for its phycoerythrin production, with red cellular color. It should have trimeric PSI based on the hypothesis of tetrameric PSI distribution. The BN-PAGE analysis showed that very likely WH 7803 has trimeric PSI, which migrates further on the BN-PAGE gel under higher concentration of DDM (Figure 5-18). SDS-PGAE showed that the major green band in WH 7803 is PSI (Figure 5-19B).

Scytonema crispum UTEX LB 1556

Scytonema crispum UTEX LB 1556 (LB 1556) is a heterocyst-forming cyanobacterium that grows extremely slow, with most cells (filaments) intertwined together forming an “algae ball”. LB 1556 has tetrameric PSI and trimeric PSI (Figure 5-18A). The speculations were confirmed by the SDS-PAGE analysis (Figure 5-18B). The abundance of PSI tetramer in LB 1556 is relatively low, but significant amount of PSI dimer was observed.

Spirulina platensis UTEX LB 1926

Spirulina platensis UTEX LB 1926 (LB 1926), also known as *Arthrospira platensis* PCC 7345, was not studied for this photosystem properties. The same species bur a different strain, *Spirulina platensis*, was reported to have trimeric PSI and monomeric PSI with the trimeric PSI possessing long wavelength Chl (*6, 9*). Here we confirmed the observation that LB 1926 has trimeric PSI as the

Figure 5- 18 PAGE analysis of PSI oligomeric state in WH 7803 and LB 1556

(A) BN-PAGE of solubilized thylakoid membrane from WH 7803 and LB 1556. Thylakoid membranes with 0.4 mg/mL Chl from WH 7803 and LB 1556 were solubilized in different concentrations of DDM (w/v, %), labeled on top of each lane. Solubilized thylakoid membranes from TS-821 and *Synechocystis* sp. PCC 6803 (Syn6803) with 0.4 mg/mL Chl in 1% DDM were loaded as controls. ~ 2 µg Chl were loaded for each condition. The LB 1556 green bands sliced out for second dimension SDS-PAGE (B) and PSI identification are numbered on the left side of each band. The potential PSI trimer from WH 7803 is pointed out by an arrow.

(B) SDS-PAGE of photosystems from LB 1556 for PSI identification. Syn6803 PSI (tri), TS-821 PSI (dim) and PSII (dim) from BN-PAGE gel were used as control for PSI identification. Numbered lanes correspond to numbered bands in (A). PSI oligomeric state interpretations were denoted on top of each lane as well.

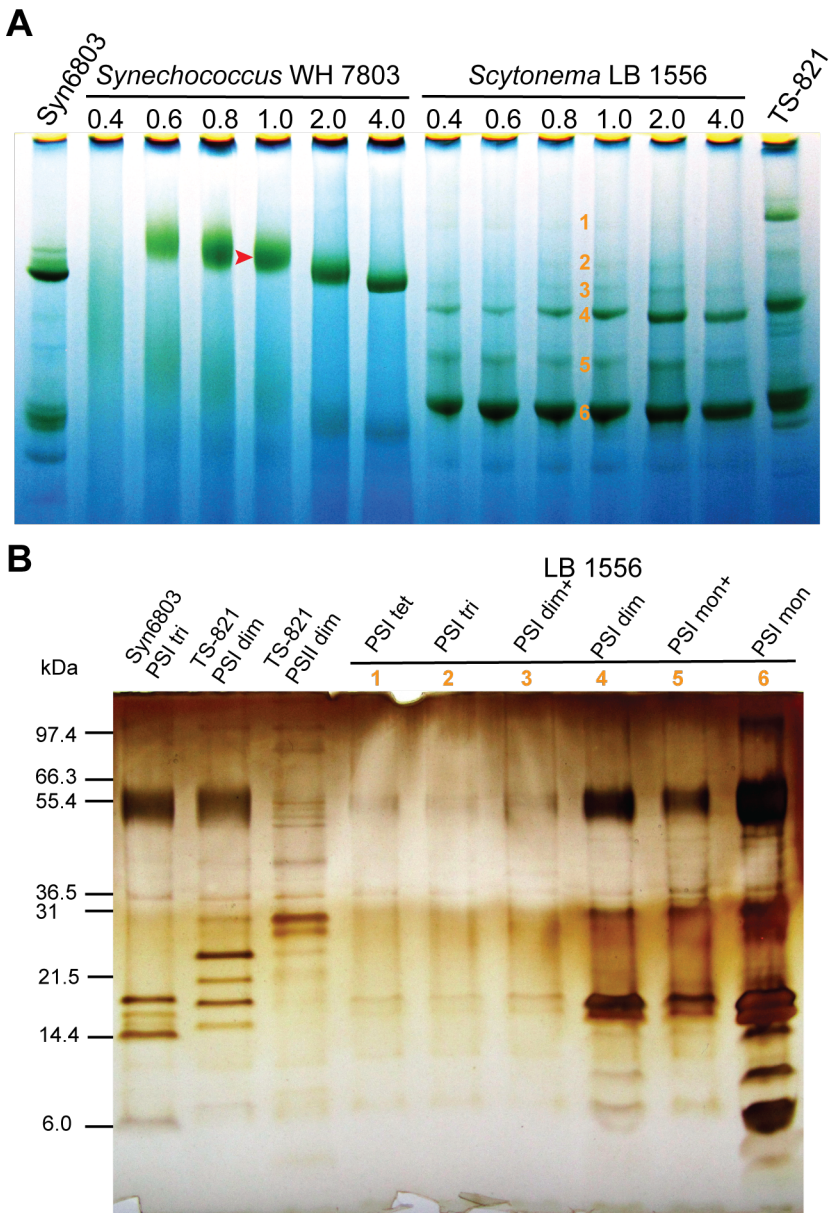

Figure 5-18 continued

major oligomeric form of PSI with significant amount of PSI monomers (Figure 5-19). Interestingly, besides the major species monomer and trimer, PSI in LB 1926 seems to form dimeric and some other super complexes (Figure 5-19). Even though not studied in details, this observation agrees with earlier study that an additional peak of Chl containing protein (potentially PSI dimer) was observed when the solubilized thylakoid membrane was analyzed by size exclusion chromatography (*6*).

Aphanothece sp. UTEX SP25

Aphanothece sp. UTEX SP25 (SP25) is a unicellular strain of cyanobacteria. It is a strain not closely related to heterocyst-forming cyanobacteria, isolated from Great Salt Plains, Oklahoma, USA (*128*). It has been shown that SP 25 is salt tolerant but prefer fresh water environment (*128*). PSI trimer was expected for this strain. The BN-PAGE and SDS-PAGE analysis showed that trimeric PSI is its major PSI oligomers (Figure 5-20). Similar to LB 1926, SP25 has some PSI super complexes as minor species (Figure 5-20). Significant amount of PSI monomer was also observed in SP25 (Figure 5-20).

Pseudanabaena sp. UTEX B SP48

Pseudanabaena sp. UTEX B SP48 (B SP48) is filamentous but does not possess heterocyst. B SP48 was also isolated from Great Salt Plains, Oklahoma, USA and halotolerant (*128*). *Pseudanabaena* are considered as very basal cyanobacteria that branched early before endosymbiosis (*118*). B SP48 was shown closely related to *Prochlorococcus (128)*, indicating possible trimeric psi in B SP48. As shown in Figure 5-20, B SP48 has trimeric PSI as its major PSI

Figure 5- 19 PAGE analysis of PSI oligomeric state in LB 1926, B SP48 in ASNIII, and WH 7803.

(A) BN-PAGE of solubilized thylakoid membrane from LB 1926, B SP48 in ASNIII. Thylakoid membranes with 0.4 mg/mL Chl from LB 1926, B SP48 cultured in ASNIII medium were solubilized in different concentrations of DDM (w/v, %), labeled on top of each lane. Solubilized thylakoid membranes from TS-821 and *Synechocystis* sp. PCC 6803 (Syn6803) with 0.4 mg/mL Chl in 1% DDM were loaded as controls. ~ 2 µg Chl were loaded for each condition. The LB 1926 green bands sliced out for second dimension SDS-PAGE (B) and PSI identification are numbered on the left side of each band.
(B) SDS-PAGE of photosystems from LB 1926 and WH 7803 for PSI identification. WH 7803 potential trimer was isolated from BN-PAGE gel (Figure 5-18A). Syn6803 PSI (tri), TS-821 PSI (dim) and PSII (dim) from BN-PAGE gel were used as control for PSI identification. Numbered lanes correspond to numbered bands in (A). PSI oligomeric state interpretations were denoted on top of each lane as well.

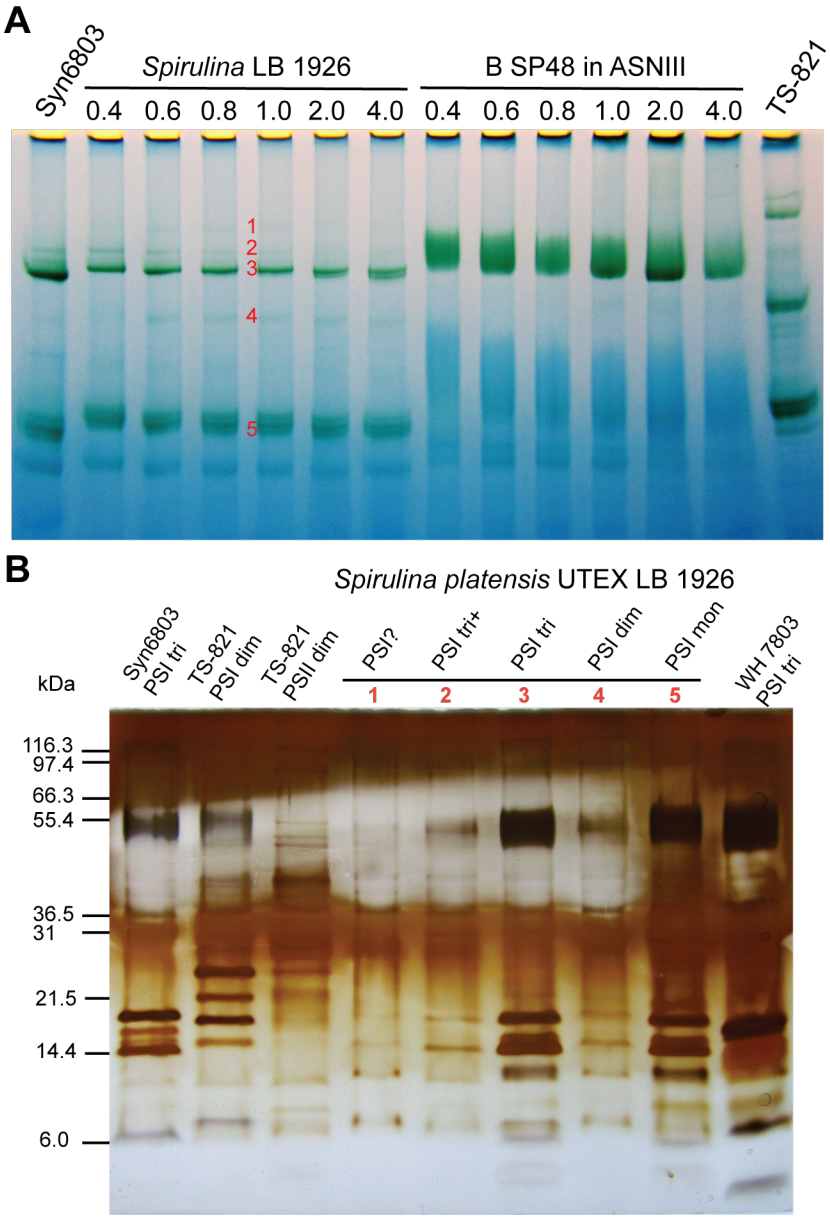

Figure 5-19 continued

Figure 5- 20 PAGE analysis of PSI oligomeric state in SP25 and B SP48.

(A) BN-PAGE of solubilized thylakoid membrane from SP25 and B SP48. Thylakoid membranes with 0.4 mg/mL Chl from SP25 and B SP48 cultured in BG-11 medium were solubilized in different concentrations of DDM (w/v, %), labeled on top of each lane. Solubilized thylakoid membranes from TS-821 and *Synechocystis* sp. PCC 6803 (Syn6803) with 0.4 mg/mL Chl in 1% DDM were loaded as controls. ~ 2 µg Chl were loaded for each condition. The green bands sliced out for second dimension SDS-PAGE (B) and PSI identification are numbered on the left side of each band.

(B) SDS-PAGE of photosystems from SP25 and B SP48 for PSI identification. Syn6803 PSI (tri), TS-821 PSI (tet) and PSII (dim) from BN-PAGE gel were used as control for PSI identification. Numbered lanes correspond to numbered bands in (A). PSI oligomeric state interpretations were denoted on top of each lane as well.

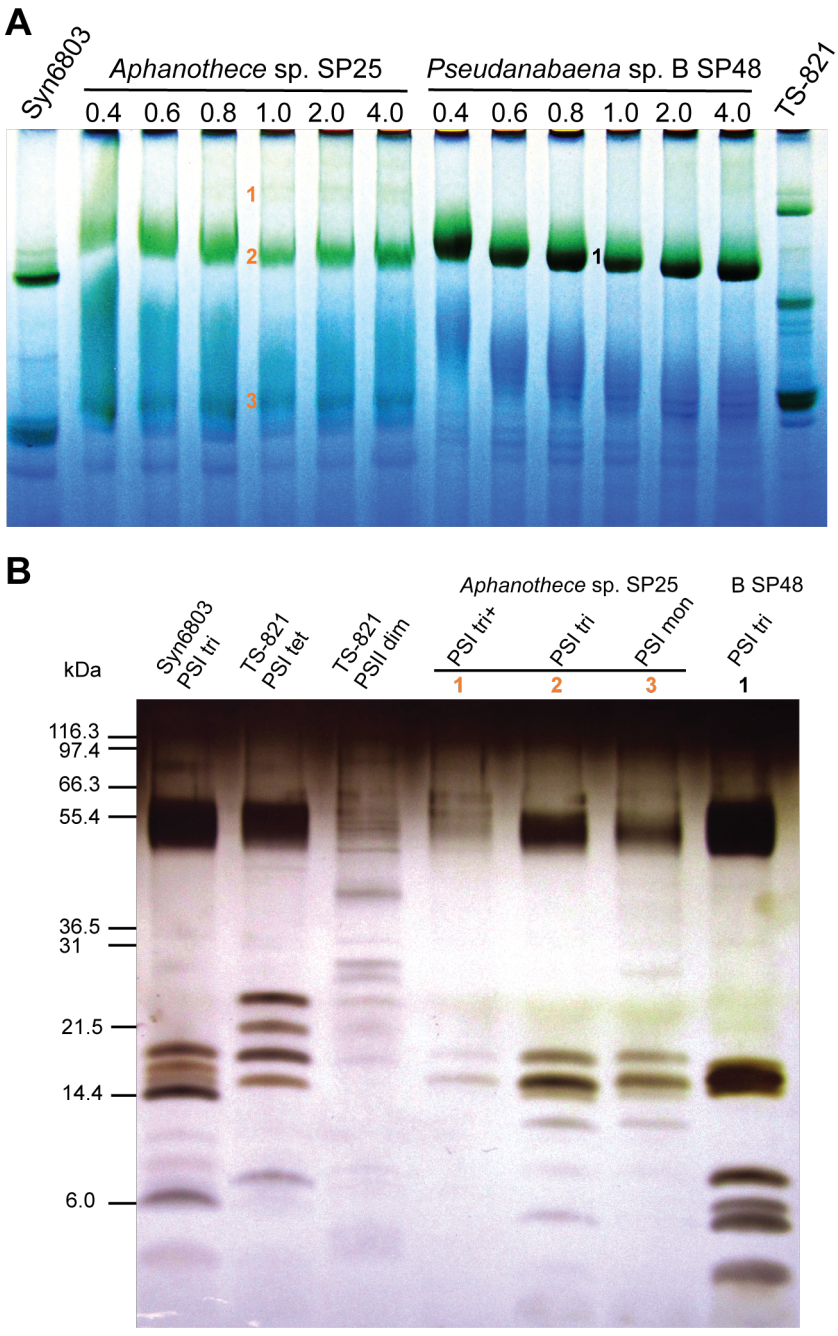

Figure 5-20 continued

oligomer. Compared with SP25, PSI monomer in B SP48 is less abundant. Growth media (salinity difference) do not seem to affect the formation of PSI trimer in B SP48 (Figure 5-19A and Figure 5-20A).

Gloeocapsa alpicola UTEX LB 1598

Gloeocapsa alpicola UTEX LB 1598 (LB 1598), also known as *Geminocystis herdmanii* PCC 6308 or *Synechocystis* sp. PCC 6308, is a unicellular cyanobacterium with sequenced genome. As expected, it has trimeric PSI as its major PSI oligomer (Figure 5-21).

Finding the Boundary of PSI Tetramer Distribution Among Cyanobacteria PCC Strains

Through the initial test and investigation on UTEX strains, one can conclude that most heterocyst-forming cyanobacteria have tetrameric PS and that some have monomeric PSI. Since most of the UTEX strains studied here have no known genome sequences. To understand evolutionarily where and when cyanobacteria evolved to have tetrameric PSI, a more extensive investigation was done by adding 30 cyanobacteria PCC strains with most of their genomes sequenced. While it is true that most of the heterocyst-forming cyanobacteria and their close relatives have tetrameric PSI, some of the cyanobacteria in this group have mainly monomeric PSI with some dimeric PSI. Also, potential dimeric PSI, tetrameric PSI, even hexameric species of PSI has been observed outside this group. Moreover, the PSI in *Chamaesiphon minutus* PCC 6605, a strain outside the predicted tetrameric PSI group, is mainly monomeric, even though a small fraction of PSI trimer and potential dimeric PSI

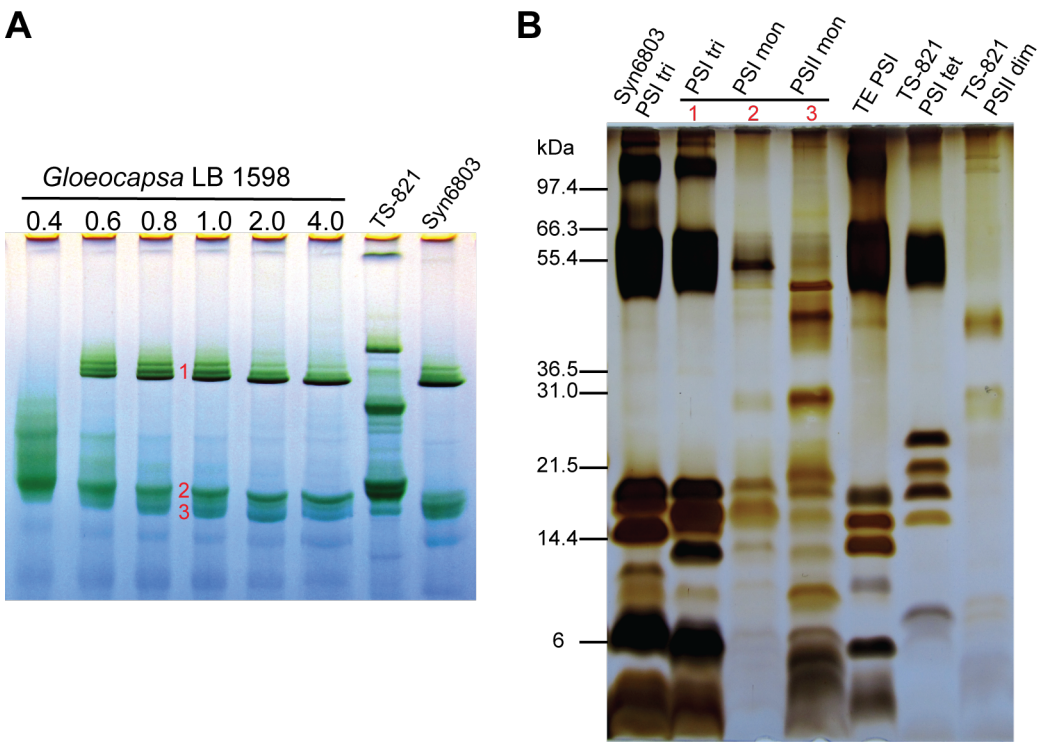

Figure 5- 21 PAGE analysis of PSI oligomeric state in LB 1598

(A) BN-PAGE of solubilized thylakoid membrane from LB 1598 Thylakoid membranes with 0.4 mg/mL Chl from LB 1598 were solubilized in different concentrations of DDM (w/v, %), labeled on top of each lane. Solubilized thylakoid membranes from TS-821 and *Synechocystis* sp. PCC 6803 (Syn6803) with 0.4 mg/mL Chl in 1% DDM were loaded as controls. ~ 2 µg Chl were loaded for each condition. The green bands sliced out for second dimension SDS-PAGE (B) and PSI identification are numbered on the left side of each band.

(B) SDS-PAGE of photosystems from LB 1598 for PSI identification. Syn6803 PSI (tri), TS-821 PSI (tet) and PSII (dim) from BN-PAGE gel, as well as purified TE PSI trimer were used as control for PSI identification. Numbered lanes correspond to numbered bands in (A). PSI oligomeric state interpretations were denoted on top of each lane as well.

were observed as well. These studied strains will be presented in details and the indications will be discussed in a later section.

Chroococcidiopsis sp. PCC 7203 and *Chroococcidiopsis* sp. PCC 6712

Chroococcidiopsis sp. PCC 7203 (PCC 7203) and *Chroococcidiopsis* sp. PCC 6712 (PCC 6712) are both classified as *Chroococcidiopsis* according to their morphology. Phylogenetically, the two strains are placed in different groups, with PCC 7203 closely related to heterocyst-forming cyanobacteria. According to the PSI tetramer distribution hypothesis, PSI tetramer was expected in PCC 7203 and PSI trimer was expected in PCC 6712. PCC 7203 has two copies of *psaL* gene, which may be expressed differently in response to far-red light (*34*). The BN-PAGE and SDS-PAGE analysis showed that PCC 7203 has mainly monomeric PSI with some PSI dimer, while PSI in PCC 6712 is mainly trimeric but may also be hexameric (Figure 5-22). The fact that PSI trimer was not observed in PCC 7203 suggests that two different *psaL* genes do not indicate two forms of PSI oligomers (trimeric PSI and tetrameric/dimeric PSI) are present. To determine whether the potential PSI hexamer is an artifact or native organization, TEM images of isolated PSI hexamer from the sucrose density gradient were taken and analyzed (Figure 5-23). Even though structures of two PSI trimer associated together were observed in the EM images, whether or not those structures are in its native state is still questionable. The BN-PAGE of isolated PCC 6712 PSI trimer and hexamer showed that equilibrium between those two PSI oligomers exist at least *in vitro* (Figure 5-23B).

Figure 5- 22 BN-PAGE of solubilized thylakoid membranes and SDS-PAGE of photosystems from PCC 7203 and PCC 6712 for PSI identification

(A) BN-PAGE of solubilized thylakoid membrane from PCC 7203 and PCC 6712. Thylakoid membranes with 0.4 mg/mL Chl from PCC 7203 and PCC 6712 were solubilized in different concentrations of DDM (w/v, %), labeled on top of each lane. Solubilized thylakoid membranes from TS-821 and Synechocystis sp. PCC 6803 (Syn6803) with 0.4 mg/mL Chl in 1% DDM were loaded as controls. ~ 2 µg Chl were loaded for each condition.
(B) BN-PAGE of solubilized thylakoid membranes of PCC 7203 and PCC 6712 for following SDS-PAGE (C). The green bands sliced out for second dimension SDS-PAGE (C) and PSI identification are numbered.
(C) SDS-PAGE of photosystems from PCC 7203 and PCC 6712 for PSI identification. *Synechocystis* sp. PCC 6803 (PCC 6803) and TS-821 PSI and PSII from BN-PAGE gel were used as control for PSI identification. Numbered lanes correspond to numbered bands in (B). PSI oligomeric state interpretations were denoted on top of each lane as well.

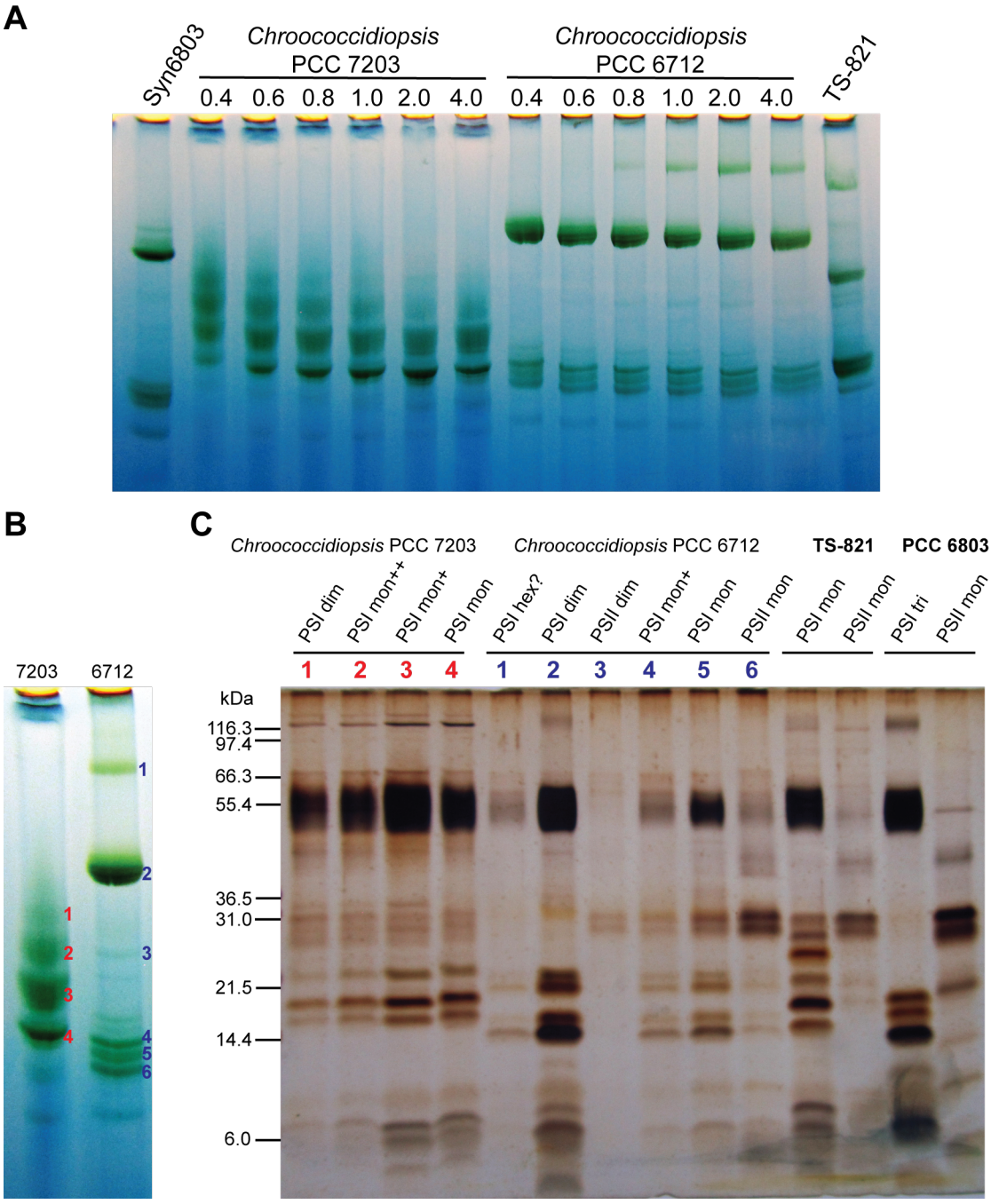

Figure 5-22 continued

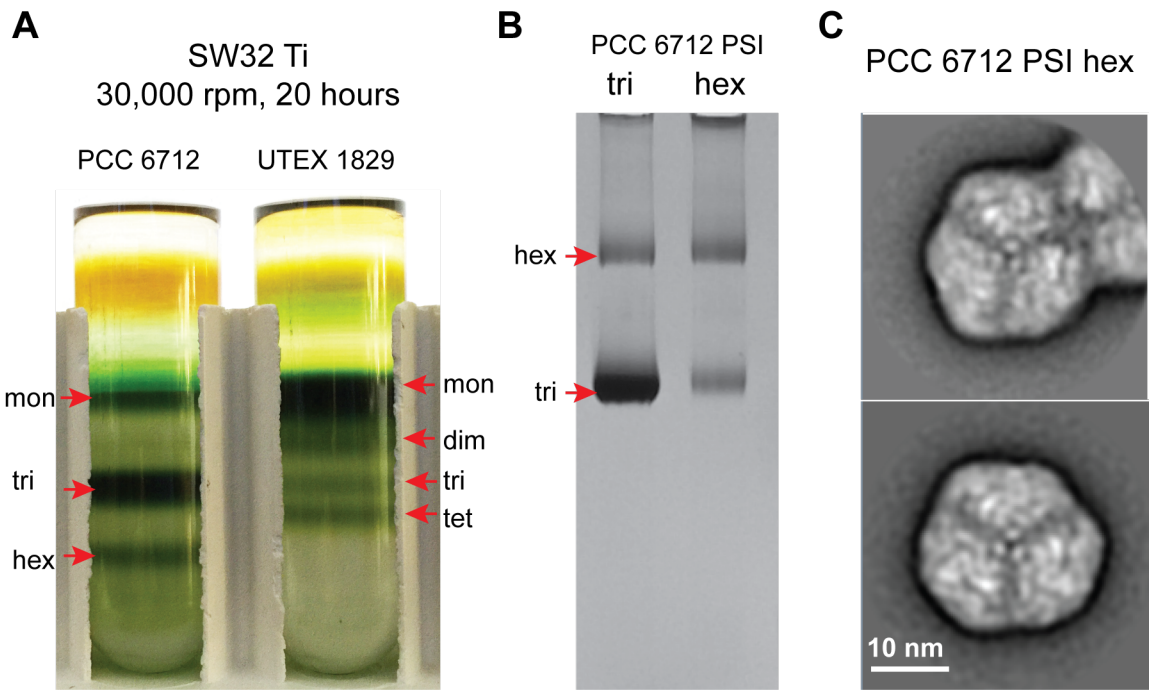

Figure 5- 23 Structure analysis of PCC 6712 potential hexamer

(A) Sucrose density gradient ultracentrifugation of solubilized thylakoid membrane from PCC 6712. Membranes containing 0.4 mg/mL Chl were solubilized in 2% DDM and 0.6% DDM for PCC 6712 and UTEX LB 1829 respectively. LB 1829 was used as control. 1 mg total Chl was loaded on each gradient. The position of PSI monomer (mon), dimer (dim), trimer (tri), tetramer (tet) and hexamer (hex) are pointed out by arrows.

(B) BN-PAGE of PSI trimer and hexamer isolated from (A). The bands corresponding to hexamer and trimer are pointed out. Gel was stained with before imaging.

(C) Single particles analysis images of PSI hexamer sample isolated from sucrose density gradient (A). Two representative species are shown.

EM images were taken and analyzed by Dr. Dmitry A. Semchonok at University of Groningen.

Chlorogloeopsis fritschii PCC 6912

Chlorogloeopsis fritschii PCC 6912 (PCC 6912) is the reference strain for its genus (*61*). PCC 6912 also have two copies of *psaL* gene, which may be differentially expressed.in response to far-red light (*34*). Tetrameric PSI was expected to be present in this heterocyst-forming strain. BN-PAGE and SDS-PAGE showed that PCC 6912 has tetrameric PSI (Figure 5-24). PCC 6912 has multiple green bands that may represent various forms of PSI. A careful analysis of those green bands identified that PSI trimer also present in PCC 6912 (Figure 5-25). The reason for the diversity of PSI oligomers is a very interesting topic to study in the future.

Gloeocapsa sp. PCC 7428

Gloeocapsa sp. PCC 7428 (PCC 7428) is a very close relative to *Chroococcidiopsis* sp. TS-821 (*21*). The BN-PAGE and SDS-PAGE analysis showed the presence of PSI tetramer as well as PSI trimer in PCC 7428 (Figure 5-24). A detailed study of this strain is presented in Chapter Six.

Synechocystis sp. PCC 7509

Synechocystis sp. PCC 7509 (PCC 7509) was named as *Synechocystis* but phylogenetically is more closely related to heterocyst-forming cyanobacteria (*118*). It is expected to have tetrameric PSI considering its close relation with other unicellular cyanobacteria, such as PCC 7428, that are closely related to heterocyst-forming cyanobacteria. As shown in Figure 5-26, PCC 7509 has tetrameric and trimeric PSI, in contrast to PCC 6803.

Figure 5- 24 BN-PAGE of solubilized thylakoid membranes and SDS-PAGE of photosystems from PCC 6912 and PCC 7428 for PSI identification

(A) BN-PAGE of solubilized thylakoid membrane from PCC 6912 and PCC 7428. Thylakoid membranes with 0.4 mg/mL Chl from PCC 6912 and PCC 7428 were solubilized in different concentrations of DDM (w/v, %), labeled on top of each lane. Solubilized thylakoid membranes from TS-821 and Synechocystis sp. PCC 6803 (Syn6803) with 0.4 mg/mL Chl in 1% DDM were loaded as controls. ~ 2 µg Chl were loaded for each condition.
(B) BN-PAGE of solubilized thylakoid membranes PCC 6912 and PCC 7428 for following SDS-PAGE (C). The green bands sliced out for second dimension SDS-PAGE (C) and PSI identification are numbered.
(C) SDS-PAGE of photosystems from PCC 6912 and PCC 7428 for PSI identification. *Synechocystis* sp. PCC 6803 (PCC 6803) and TS-821 PSI and PSII from BN-PAGE gel were used as control for PSI identification. Numbered lanes correspond to numbered bands in (B). PSI oligomeric state interpretations were denoted on top of each lane as well.

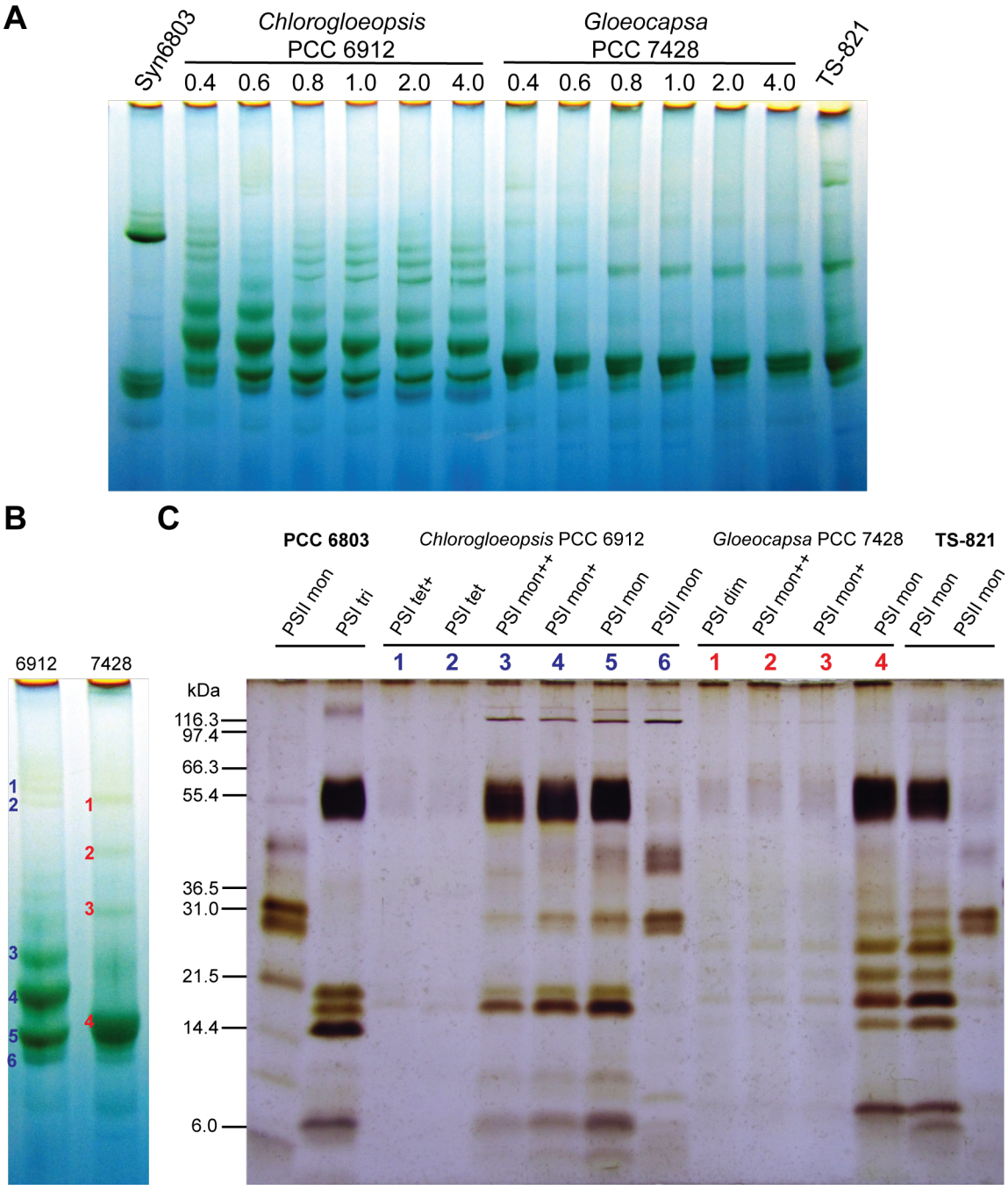

Figure 5-24 continued

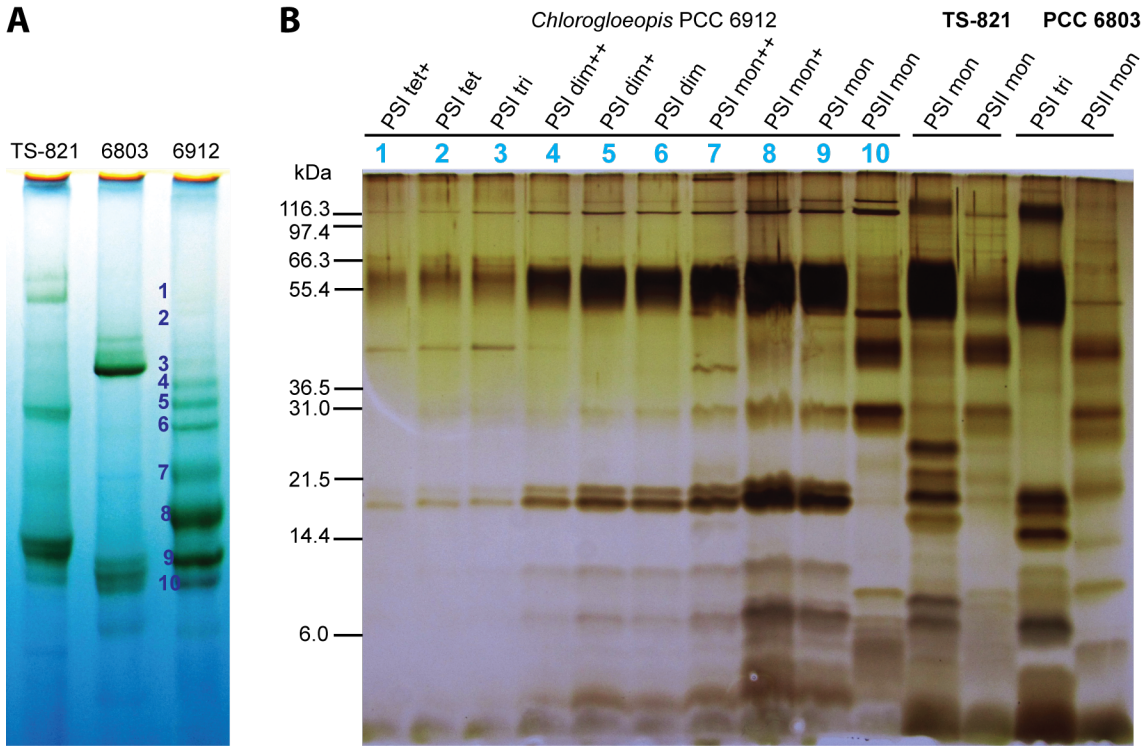

Figure 5- 25 Detailed PAGE analysis of PSI complexes in PCC 6912

(A) BN-PAGE of PCC 6912 solubilized thylakoid membrane. TS-821 and *Synechocystis* sp. PCC 6803 (6803) were shown as controls. Bands sliced out for following SDS-PAGE (B) and PSI identification were numbered.

(B) SDS-PAGE of PCC 6912 green bands isolated from BN-PAGE gel (A) for PSI identification. *Synechocystis* sp. PCC 6803 (PCC 6803) and TS-821 PSI and PSII from BN-PAGE gel were used as control for PSI identification. Numbered lanes correspond to numbered bands in (B). PSI oligomeric state interpretations were denoted on top of each lane as well.

Figure 5- 26 BN-PAGE of solubilized thylakoid membranes and SDS-PAGE of photosystems from PCC 7509 and PCC 73102 for PSI identification

(A) BN-PAGE of solubilized thylakoid membrane from PCC 7509 and PCC 6803. Thylakoid membranes with 0.4 mg/mL Chl from PCC 7509 and PCC 6803 were solubilized in different concentrations of DDM (w/v, %), labeled on top of each lane. Solubilized thylakoid membranes from TS-821 with 0.4 mg/mL Chl in 1% DDM were loaded as controls. ~ 2 µg Chl were loaded for each condition.

(B) BN-PAGE of solubilized thylakoid membrane from PCC 73102.

(C) BN-PAGE of solubilized thylakoid membranes PCC 7509 and PCC 73102 for following SDS-PAGE (D). The green bands sliced out for second dimension SDS-PAGE (D) and PSI identification are numbered.

(D) SDS-PAGE of photosystems from PCC 7509 and PCC 73102 for PSI identification. *Synechocystis* sp. PCC 6803 (PCC 6803) and TS-821 PSI and PSII from BN-PAGE gel were used as control for PSI identification. Numbered lanes correspond to numbered bands in (C). PSI oligomeric state interpretations were denoted on top of each lane as well.

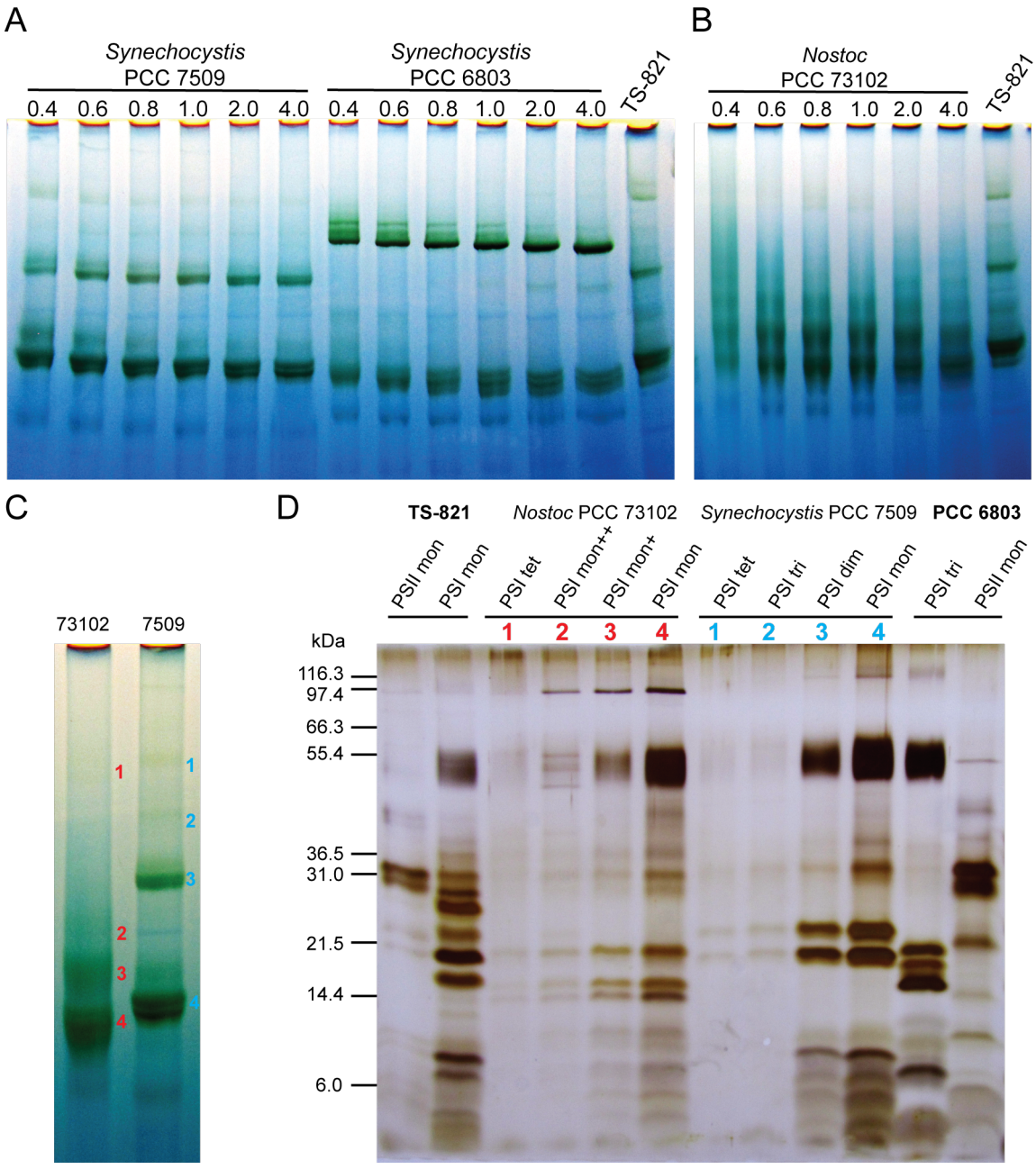

Figure 5-26 continued

Nostoc punctiforme sp. PCC 73102

Nostoc punctiforme sp. PCC 73102 (PCC 73102), also known as *Nostoc punctiforme* ATCC 29133, has been studied for the photosystems in heterocysts (*49*). Even though the initial study showed the potential PSI tetramer on the BN-PAGE gel (*49*), it was interpreted later as tetrameric PSI (*19*). Here PCC 73102 was analyzed again to confirm this interpretation. PCC 73102 was confirmed having tetrameric PSI with low abundance (Figure 5-26), even though monomeric PSI is more predominant in PCC 73102.

Oscillatoria sp. PCC 8926

Oscillatoria sp. PCC 8926 (PCC 8926) is a filamentous cyanobacterium that does not form heterocysts. Little information was known about this strain but it is predicted to form trimeric PSI if the classification of this strain is accurate. As shown in Figure 5-27, PCC 8926 has trimeric PSI as its major PSI oligomer, as expected. At the same time, two obvious green bands (No. 1 and 2 in Figure 5-2A) that are larger in size compared to the trimeric PSI band are also present. Since the top PSI band abundance decreases with the addition more DDM while the amount of No. 4 green band (Figure 5-27A) increases, PCC 8926 may have tetrameric PSI in equilibrium with dimeric PSI, as observed in heterocyst-forming cyanobacteria. The reason why PCC 8926 has tetrameric PS, or additional form of PSI oligomer beside trimeric PSI (if not tetrameric PSI) is interesting to see.

Fischerella sp. PCC 9605 *and Calothrix* sp. PCC 7507

Both *Fischerella* sp. PCC 9605 (PCC 9605) and *Calothrix* sp. PCC 7507 (7507) have two copies of *psaL* genes that may be differentially expressed in

Figure 5- 27 PAGE analysis of PSI complexes in PCC 8926

(A) BN-PAGE of PCC 8926 solubilized thylakoid membrane. Thylakoid membranes with 0.4 mg/mL Chl from PCC 8926 were solubilized in different concentrations of DDM (w/v, %), labeled on top of each lane. Solubilized thylakoid membranes from TS-821 and *Synechocystis* sp. PCC 6803 (Syn6803) with 0.4 mg/mL Chl in 1% DDM were loaded as controls. ~ 2 µg Chl were loaded for each condition. Bands sliced out for following SDS-PAGE (B) and PSI identification were numbered.
(B) SDS-PAGE of PCC 6912 green bands isolated from BN-PAGE gel (A) for PSI identification. *Synechocystis* sp. PCC 6803 (PCC 6803) and TS-821 PSI and PSII from BN-PAGE gel were used as control for PSI identification. Numbered lanes correspond to numbered bands in (B). PSI oligomeric state interpretations were denoted on top of each lane as well. “?” denotes the uncertainty of the oligomeric states.

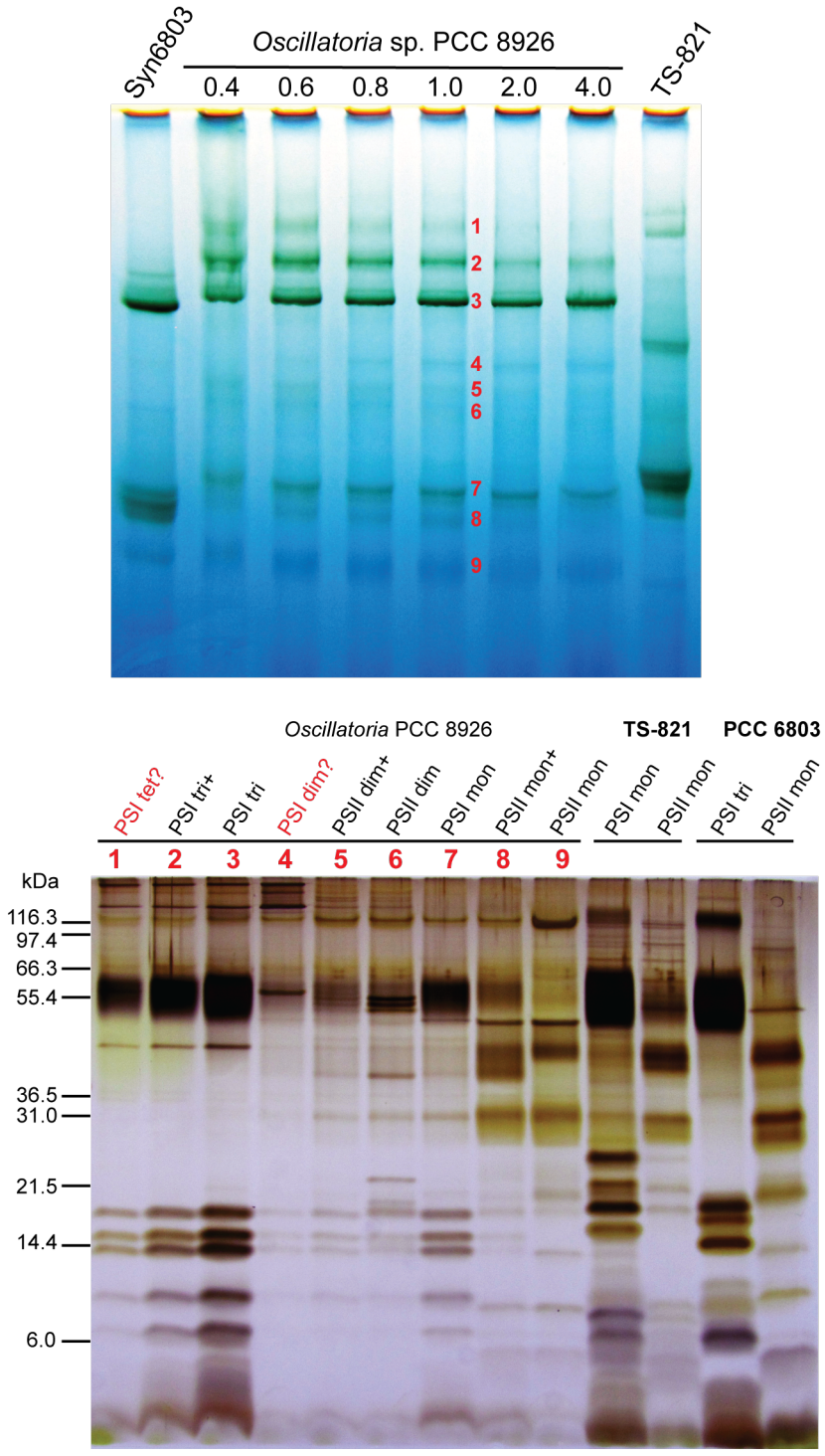

Figure 5-27 continued

response to far-red light (*34*). The BN-PAGE and SDS-PAGE analysis showed that both strains have tetrameric PSI as well as trimeric PSI (Figure 5-28). For PCC 9605, doublets for PSI monomer, dimer, trimer, and tetramer were observed (Figure 5-28A) This pattern has also been observed in other *Fischerella* species presented. Whether this diversity is an artifact of detergent solubilization or it is the result of additional PSI-binding protein attachment is not clear. One explanation could be the IsiA like proteins attachment. The additional subunits to PSI in PCC 9605 and PCC 7507 that look similar to the IsiA protein in size are pointed out by arrows in Figure 5-28 C and D. The IsiA protein in *Leptolyngbya* sp.JSC-1 showed similar migration distance on a SDS-PAGE gel (*56*). It is worth noting that PCC 6912 also has multiple species for PSI oligomers, with possible triplets for some oligomeric states (Figure 5-25). This can be a result of the presence of multiple IsiA like proteins or an outcome of the presence of the far-red light response apparatus. The mechanism of having multiple oligomeric forms of PSI complexes in some of the stains is yet to be investigated.

Chlorogloeopsis fritschii PCC 9212

Chlorogloeopsis fritschii PCC 9212 (PCC 9212), named as same species as PCC 6912, is also phylogenetically very close to PCC 6912. Similar PSI oligomer profile was expected for PCC 9212. As shown in Figure 5-29A, the BN-PAGE analysis of the solubilized membrane of PCC 9212 looks very similar to that of PCC 6912 (Figure 5-24A). The analysis of PCC 9212 thylakoid membranes showed the presence of PSI tetramer, as well as PSI trimer (Figure 5-29).

Figure 5- 28 BN-PAGE of solubilized thylakoid membranes and SDS-PAGE of photosystems from PCC 9605 and PCC 7507 for PSI identification

(A) BN-PAGE of solubilized thylakoid membrane from PCC 9605 and PCC 7507. Thylakoid membranes with 0.4 mg/mL Chl from PCC 9605 and PCC 7507 were solubilized in different concentrations of DDM (w/v, %), labeled on top of each lane. Solubilized thylakoid membranes from *Synechocystis* sp. PCC 6803 (Syn6803) and TS-821 with 0.4 mg/mL Chl in 1% DDM were loaded as controls. ~ 2 µg Chl were loaded for each condition.

(B) BN-PAGE of solubilized thylakoid membranes PCC 9605 and PCC 7507 for following SDS-PAGE (C and D). The green bands sliced out for second dimension SDS-PAGE and PSI identification are numbered.

(C) SDS-PAGE of photosystems from PCC 9605 for PSI identification.

(D) SDS-PAGE of photosystems from PCC 7507 for PSI identification.

For (C) and (D), *Synechocystis* sp. PCC 6803 (PCC 6803) and TS-821 PSI and PSII from BN-PAGE gel were used as control for PSI identification. Numbered lanes correspond to numbered bands in (B). PSI oligomeric state interpretations were denoted on top of each lane as well. Protein bands similar to IsiA protein in size were pointed out by arrows.

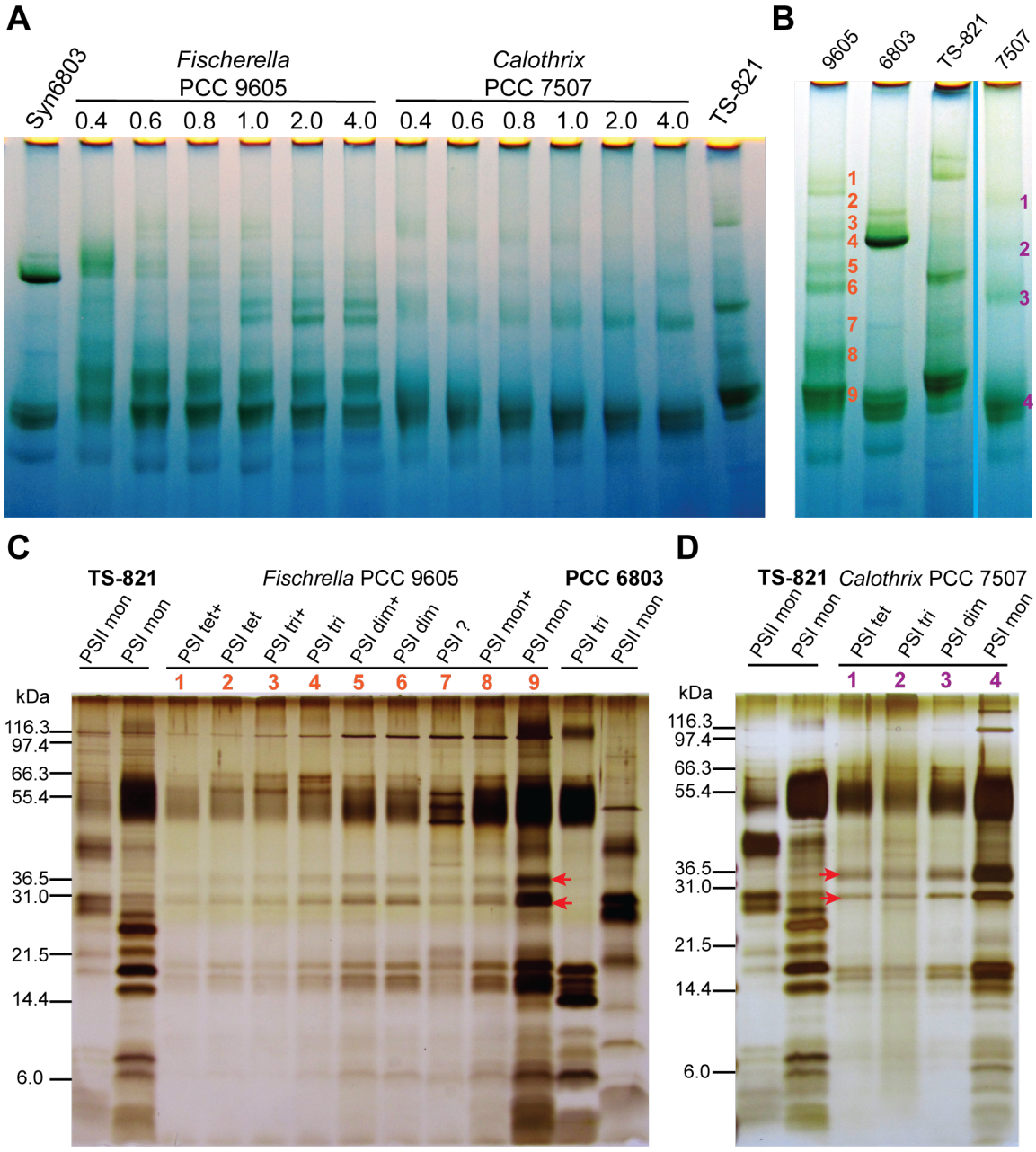

Figure 5-28 continued

Figure 5- 29 BN-PAGE of solubilized thylakoid membranes and SDS-PAGE of photosystems from PCC 9212 and PCC 7103 for PSI identification

(A) BN-PAGE of solubilized thylakoid membrane from PCC 9212 and PCC 7103. Thylakoid membranes with 0.4 mg/mL Chl from PCC 9212 and PCC 7103 were solubilized in different concentrations of DDM (w/v, %), labeled on top of each lane. Solubilized thylakoid membranes from TS-821 and Synechocystis sp. PCC 6803 (Syn6803) with 0.4 mg/mL Chl in 1% DDM were loaded as controls. ~ 2 µg Chl were loaded for each condition.
(B) BN-PAGE of solubilized thylakoid membranes PCC 9212 and PCC 7103 for following SDS-PAGE (C). The green bands sliced out for second dimension SDS-PAGE and PSI identification are numbered.
(C) SDS-PAGE of photosystems from PCC 6912 and PCC 7428 for PSI identification. Purified TE PSI trimer were used as control for PSI identification. Numbered lanes correspond to numbered bands in (B). PSI oligomeric state interpretations were denoted on top of each lane as well.

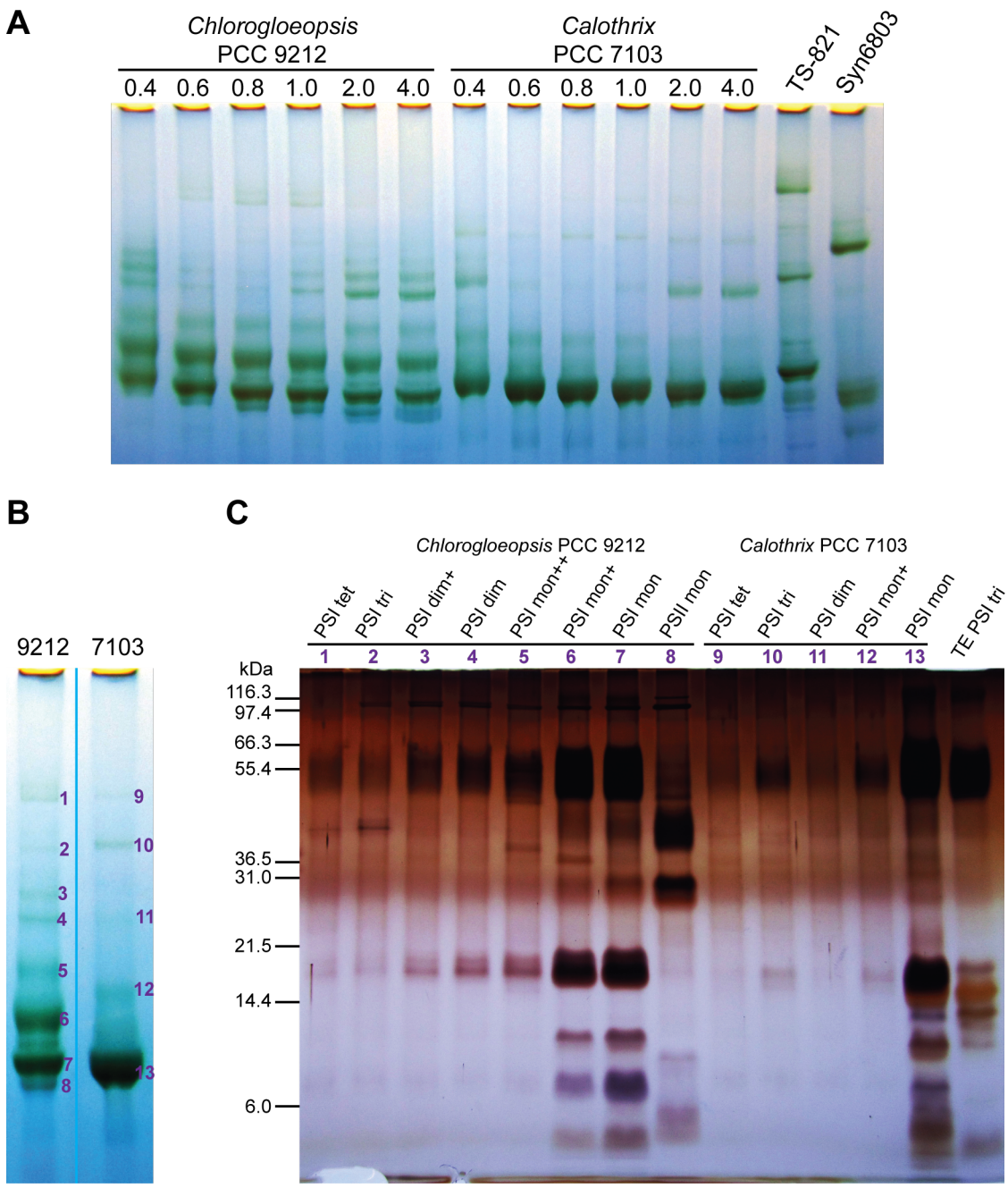

Figure 5-29 continued

Calothrix sp. PCC 7103

Calothrix sp. PCC 7103 (PCC 7103) is another *Calothrix* strain with sequenced genome. In contrast to PCC 7507, only one copy of *psaL* gene is found so far according to published genome data. The analysis of PCC 7103 thylakoid membrane showed the presence of both tetrameric and trimeric PSI (Figure 5-29). The most abundant PSI oligomer is monomeric PSI in PCC 7103.

Scytonema hofmanni PCC 7110

Scytonema hofmanni PCC 7110 (PCC 7110), similar to other two strain in the genus *Scytonema* (UTEX B 2349 and UTEX LB 1556), has tetrameric PSI and trimeric PSI (Figure 5-30). One special property of the PCC 7110 PSI oligomer profile is that the PSI trimer amount decrease dramatically at a high concentration of DDM. Whether this is a result of insufficient solubilization or special trimeric PSI in PCC 7110 is not clear.

Fischerella muscicola PCC 73103

Fischerella muscicola PCC 73103 (PCC 73103), classified as same species as PCC 7414 and LB 1829, does not show the expected tetrameric PSI under our experimental conditions (Figure 5-30). PSI dimers and trivial amount of PSI trimer were observed in PCC 73103. This difference observed in PCC 73104 may be a result of genetic or physiological difference PCC 73104 has, compared with PCC 7414 and LB 1829.

Pseudanabaena sp. PCC 7367

Pseudanabaena sp. PCC 7367 (PCC 7367), similar to B SP48, has trimeric PSI as their major PSI oligomer (Figure 5-30 and Figure 5-31).

Figure 5- 30 BN-PAGE of solubilized thylakoid membranes and SDS-PAGE of photosystems from PCC 7110, PCC 73103 and PCC 7367 for PSI identification

(A) BN-PAGE of solubilized thylakoid membrane from PCC 7110 and PCC 73103. Thylakoid membranes with 0.4 mg/mL Chl from PCC 7110 and PCC 73103 were solubilized in different concentrations of DDM (w/v, %), labeled on top of each lane. Solubilized thylakoid membranes from TS-821 and Synechocystis sp. PCC 6803 (Syn6803) with 0.4 mg/mL Chl in 1% DDM were loaded as controls. ~ 2 µg Chl were loaded for each condition.
(B) BN-PAGE of solubilized thylakoid membranes PCC 7367 (2% DDM, Figure 5-31A), PCC 7110 (0.4% DDM) and PCC 73103 for following SDS-PAGE (C). The green bands sliced out for second dimension SDS-PAGE and PSI identification are numbered.
(C) SDS-PAGE of photosystems from PCC 7367, PCC 7110 and PCC 73103 for PSI identification. Purified TE PSI trimer were used as control for PSI identification. Numbered lanes correspond to numbered bands in (B). PSI oligomeric state interpretations were denoted on top of each lane as well.

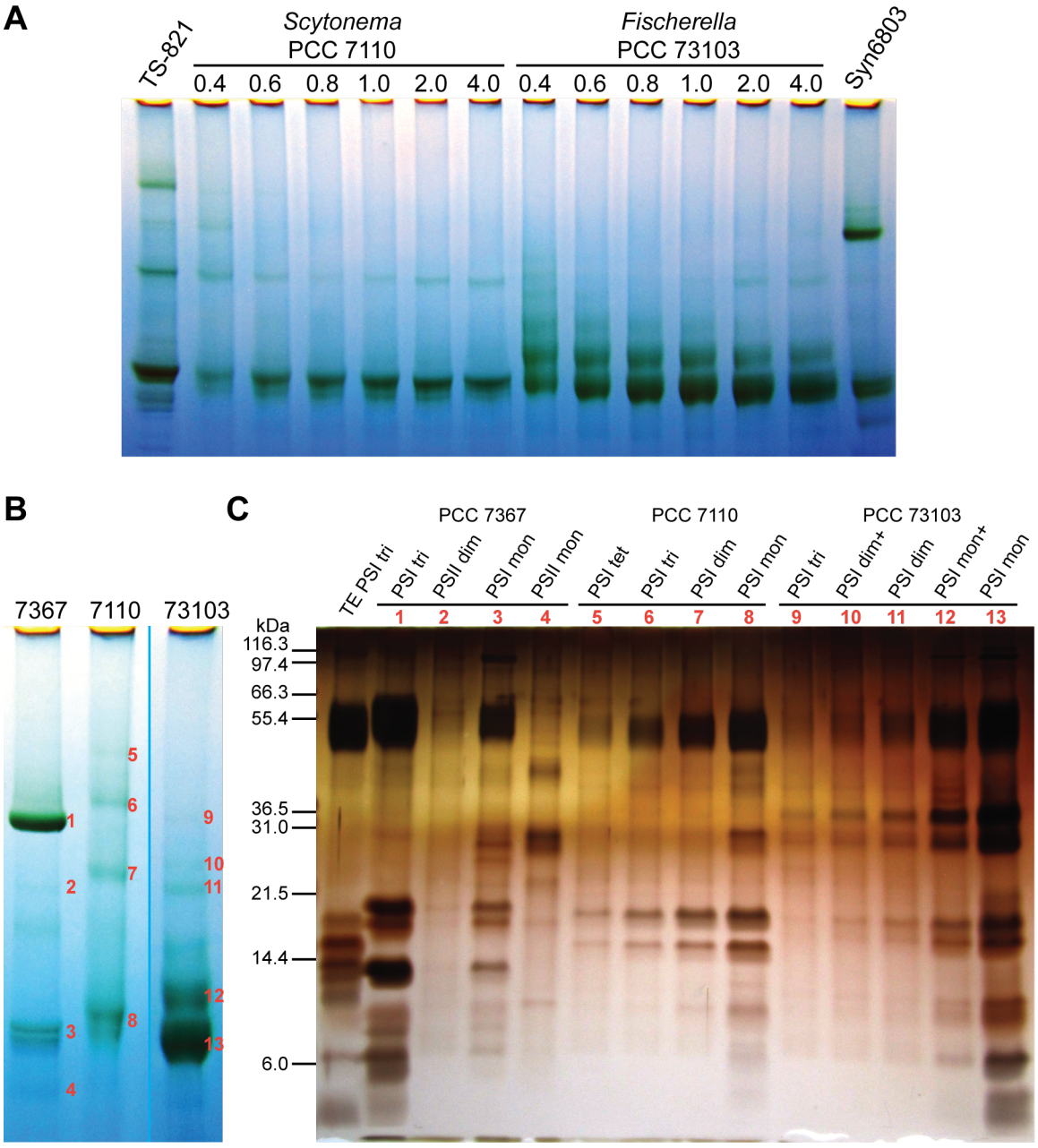

Figure 5-30 continued

Figure 5- 31 BN-PAGE of solubilized thylakoid membranes and SDS-PAGE of photosystems from PCC 7430, PCC 7367, PCC 7107, PCC 7524, and 10914 for PSI identification

(A) BN-PAGE of solubilized thylakoid membrane from PCC 7430 and PCC 7367. Thylakoid membranes with 0.4 mg/mL Chl from PCC 7430 and PCC 7367 were solubilized in different concentrations of DDM (w/v, %), labeled on top of each lane. Solubilized thylakoid membranes from TS-821 and Synechocystis sp. PCC 6803 (Syn6803) with 0.4 mg/mL Chl in 1% DDM were loaded as controls. ~ 2 µg Chl were loaded for each condition.
(B) BN-PAGE of solubilized thylakoid membranes PCC 10914, PCC 7107, PCC 7524 and PCC 7430 for following SDS-PAGE (C). Thylakoid membrane containing 0.2 mg/mL Chl from PCC 10914 was solubilized in 0.6% DDM. The green bands sliced out for second dimension SDS-PAGE and PSI identification are numbered.
(C) SDS-PAGE of photosystems from PCC 10914, PCC 7107, PCC 7524 and PCC 7430 for PSI identification. Purified TE PSI trimer were used as control for PSI identification. Numbered lanes correspond to numbered bands in (B). PSI oligomeric state interpretations were denoted on top of each lane as well.

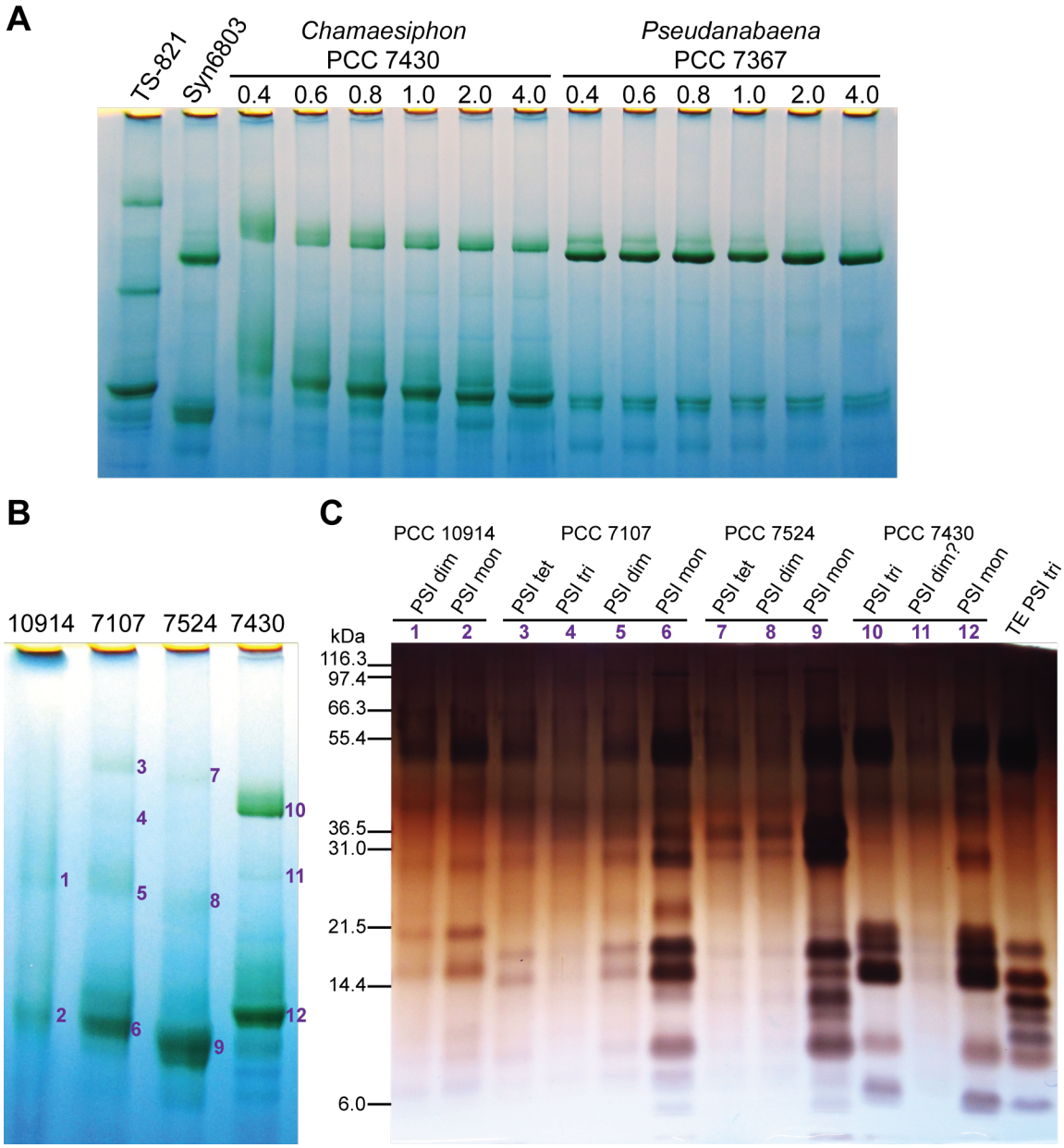

Figure 5-31 continued

Chamaesiphon sp. PCC 7430

Chamaesiphon sp. PCC 7430 (PCC 7430) is a unicellular cyanobacterium strain having trimeric PSI as its major PSI oligomer (Figure 5-31). Even though potential PSI dimer was observed too in PCC 7430 (Figure 5-31), its amount is very low and its structure still needs to be verified.

Mastigocladopsis repens PCC 10914

In this study, a preliminary experiment was done with *Mastigocladopsis repens* PCC 10914 (PCC 10914) using a single condition of membrane solubilization due to limited material. As shown in Figure 5-31, PSI dimer exists in PCC 10914. Considering the low content of Chl in the solubilization condition, the possibility of PSI tetramer in PCC 10914 should not be ruled out.

Nostoc sp. PCC 7107 and *Nostoc* sp. PCC 7524

Nostoc sp. PCC 7107 (PCC 7107) and *Nostoc* sp. PCC 7524 (PCC 7524) are in the same genus and expected to have tetrameric PSI. As shown in Figure 5-31 and Figure 5-32, PSI tetramer was found in both strains. The difference is that PCC 7107 has trimeric PSI as well, while PCC 7524 has no trimeric PSI.

Nostoc sp. PCC 9335

Nostoc sp. PCC 9335 (PCC 9335), a rarely studied strain in the genus of *Nostoc*, showed predominant presence of PSI trimer with significant amount of PSI dimer as well (Figure 5-33 A and Figure 5-34). To understand the PCC 9335 PSI oligomer profile, phylogenetic and genomic studies are necessary to elucidate this special case of *Nostoc*.

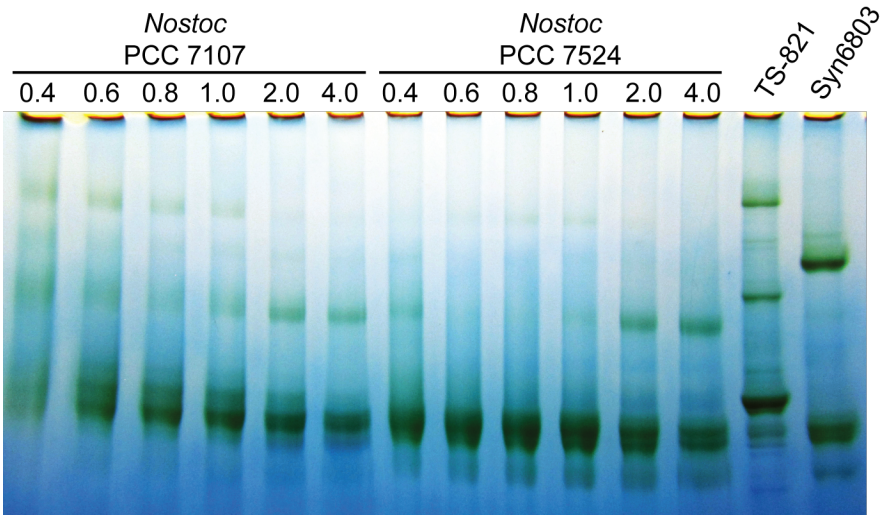

Figure 5- 32 BN-PAGE of solubilized thylakoid membranes from PCC 7107 and PCC 7524.

Thylakoid membranes with 0.4 mg/mL Chl from PCC 7107 and PCC 7524 were solubilized in different concentrations of DDM (w/v, %), labeled on top of each lane. Solubilized thylakoid membranes from TS-821 and *Synechocystis* sp. PCC 6803 (Syn6803) with 0.4 mg/mL Chl in 1% DDM were loaded as controls. ~ 2 µg Chl were loaded for each condition.

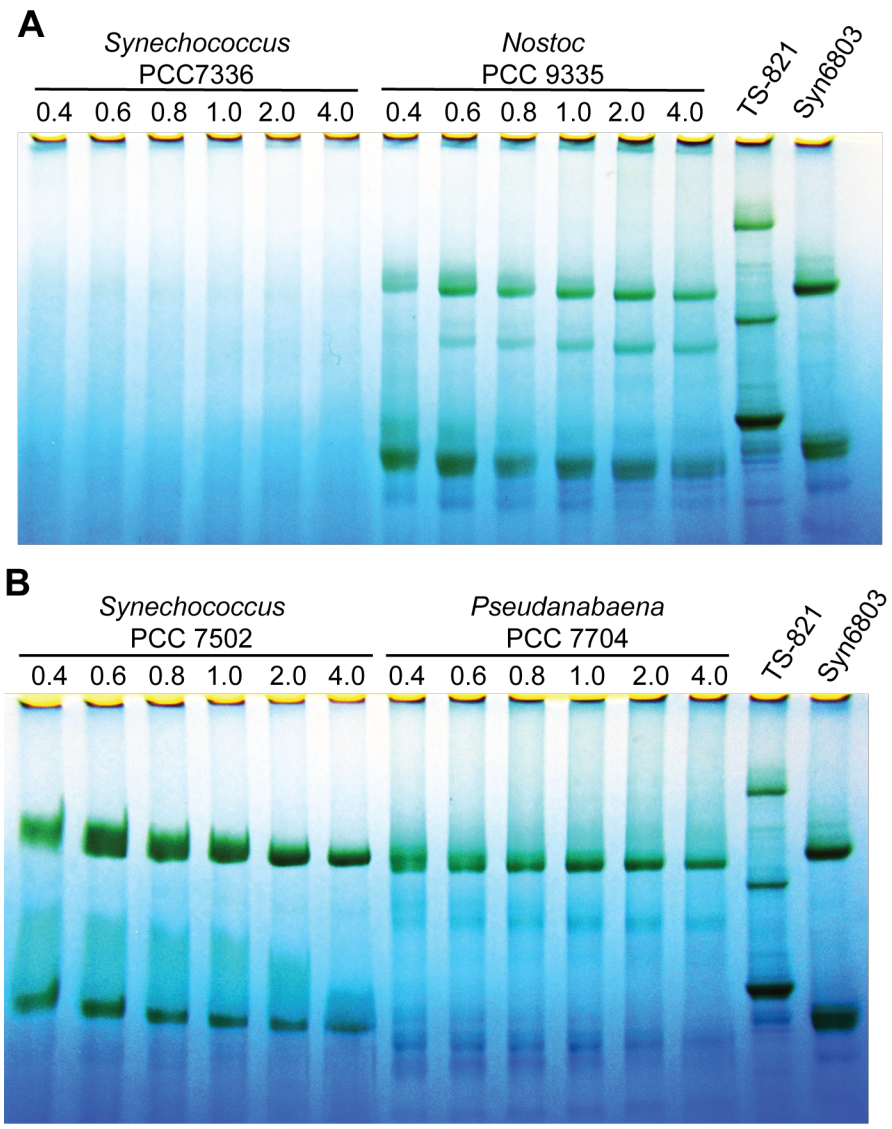

Figure 5- 33 BN-PAGE of solubilized thylakoid membrane from PCC 7336, PCC 9335, PCC 7502 and PCC 7704

(A) BN-PAGE of solubilized thylakoid membrane from PCC 7336 and PCC 9335. (B) BN-PAGE of solubilized thylakoid membrane from PCC 7502 and PCC 7704. Thylakoid membranes with 0.4 mg/mL Chl from each strain were solubilized in different concentrations of DDM (w/v, %), labeled on top of each lane. Solubilized thylakoid membranes from TS-821 and *Synechocystis* sp. PCC 6803 (Syn6803) with 0.4 mg/mL Chl in 1% DDM were loaded as controls. ~ 2 µg Chl were loaded for each condition.

Figure 5- 34 PAGE analysis of PSI complexes in PCC 7336, PCC 9335, PCC 7502, PCC 7704 and PCC 7104

(A) BN-PAGE of solubilized thylakoid membrane from PCC 7336, PCC 9335, PCC 7502, PCC 7704 and PCC 7104. Bands sliced out for following SDS-PAGE (B) and PSI identification were numbered.

(B) SDS-PAGE of green bands isolated from BN-PAGE gel (A) for PSI identification. Purified TE PSI trimer were used as control for PSI identification. Numbered lanes correspond to numbered bands in (A). PSI oligomeric state interpretations were denoted on top of each lane as well.

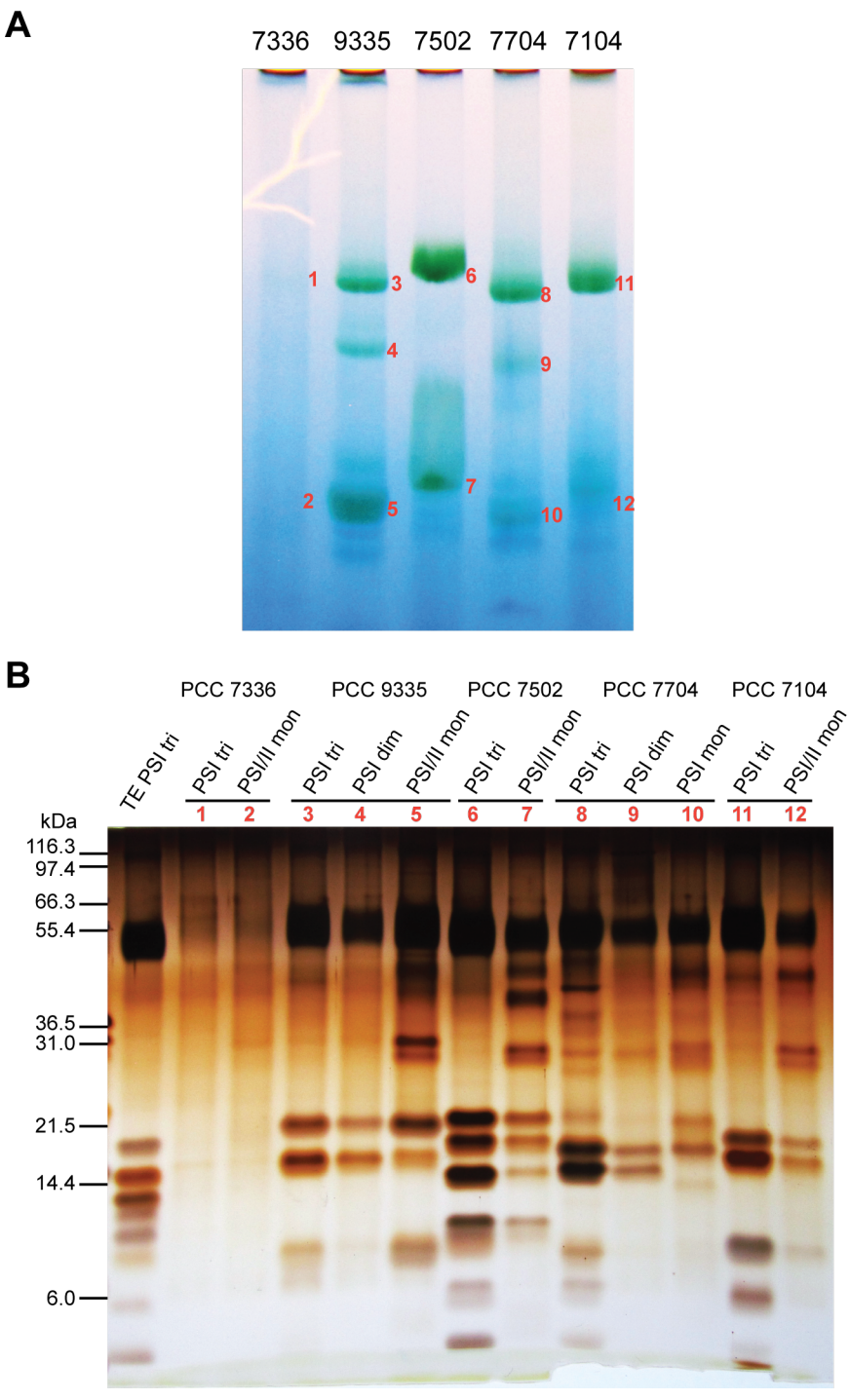

Figure 5-34 continued

Synechococcus sp. PCC 7336, *Synechococcus* sp. PCC 7502, and *Pseudanabaena* sp. PCC 7704.

Synechococcus sp. PCC 7336 (PCC 7336), *Synechococcus* sp. PCC 7502 (PCC 7502), and *Pseudanabaena* sp. PCC 7704 (PCC 7704) are all very basal strains of cyanobacteria. As shown in Figure 5-33 and Figure 5-34, all three strains have trimeric PSI. PCC 7336 thylakoid membrane showed low solubility and PCC 7704 may also have dimeric PSI (Figure 5-33).

Nodosilinea nodulosa PCC 7104, *Leptolyngbya* sp. PCC 6406, and *Leptolyngbya* sp. PCC 7124

Nodosilinea nodulosa PCC 7104 (PCC 7104), is a marine cyanobacterium that is closely related to Leptolyngbya. *Leptolyngbya* sp. PCC 6406 (PCC 6406) and *Leptolyngbya* sp. PCC 7124 (PCC 7124) are close relatives to PCC 7104. One shared feature by those three strains is that their *psaL* gene is placed close to *psaF* and *psaJ*, even though PCC 7124 has another copy of *psaL* placed close to psaI. Even though PCC 7104 and PCC 6406 have mainly trimeric PSI (Figure 5-35A, Figure 5-34 and Figure 5-36), PCC 7124 seem to have dimeric PSI and monomeric PSI (Figure 5-35B and Figure 5-36). The dimeric PSI species in PCC 7124 is yet to be confirmed, as well as the potential PSI dimer in PCC 6406.

Chroococcidiopsis sp. PCC 7434

Chroococcidiopsis sp. PCC 7434 (PCC 7434) is a very close relative to PCC 7203, and the PSI oligomer profile in PCC 7434 (Figure 5-35B and Figure 5-36) is also very similar to what was found in PCC 7203 (Figure 5-22).

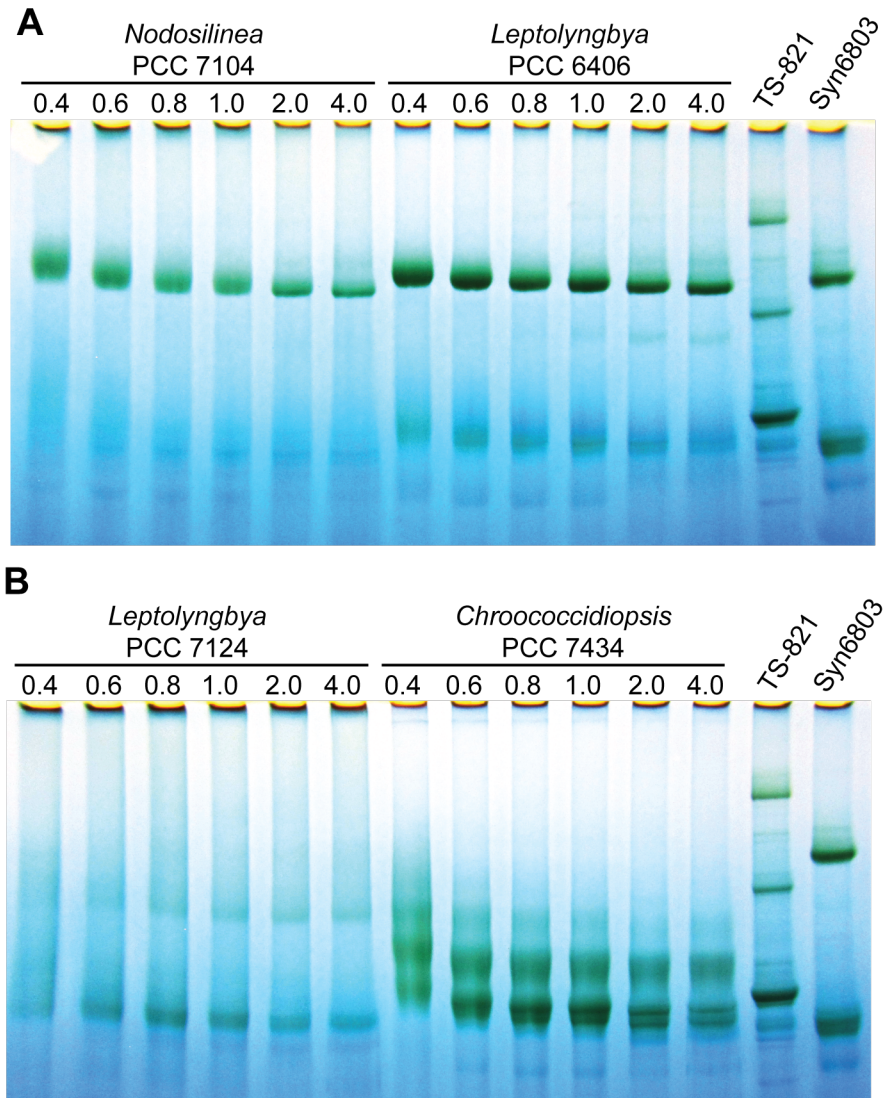

Figure 5- 35 BN-PAGE of solubilized thylakoid membrane from PCC 7104, PCC 6406, PCC 7124 and PCC 7434

(A) BN-PAGE of solubilized thylakoid membrane from PCC 7104 and PCC 6406. (B) BN-PAGE of solubilized thylakoid membrane from PCC 7124 and PCC 7434. Thylakoid membranes with 0.4 mg/mL Chl from each strain were solubilized in different concentrations of DDM (w/v, %), labeled on top of each lane. Solubilized thylakoid membranes from TS-821 and *Synechocystis* sp. PCC 6803 (Syn6803) with 0.4 mg/mL Chl in 1% DDM were loaded as controls. ~ 2 µg Chl were loaded for each condition.

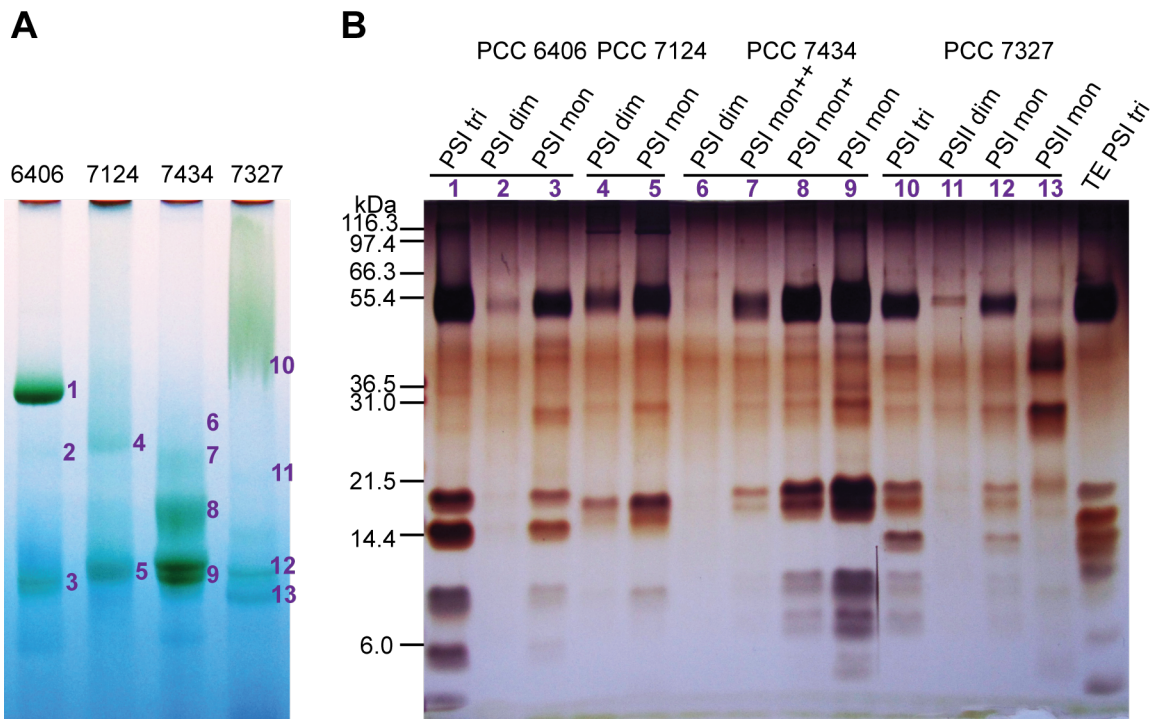

Figure 5- 36 PAGE analysis of PSI complexes in PCC 6406, PCC 7124, PCC 7434, and PCC 7327

(A) BN-PAGE of solubilized thylakoid membrane from PCC 6406, PCC 7124, PCC 7434, and PCC 7327. Bands sliced out for following SDS-PAGE (B) and PSI identification were numbered.

(B) SDS-PAGE of green bands isolated from BN-PAGE gel (A) for PSI identification. Purified TE PSI trimer were used as control for PSI identification. Numbered lanes correspond to numbered bands in (A). PSI oligomeric state interpretations were denoted on top of each lane as well.

Pleurocapsa sp. PCC 7327 and *Oscillatoria* sp. PCC 10802, *Microcystis* sp. PCC 7806 and *Chamaesiphon minutus* PCC 6605

Pleurocapsa sp. PCC 7327 (PCC 7327) and *Oscillatoria* sp. PCC 10802 (PCC 10802) both have *a psaL* gene located in close to *psaF and psaJ.* In PCC 10802, the genomic location of *psaL* is very similar to what has been observed in heterocyst-forming cyanobacteria whose similar *psaL* is also located close to *gmk* gene in most cases, however, PCC 7327 has the *psaL* adjacent to *psaF* also followed by *psaI* which together may be controlled by far-red light (*34*). In addition, PCC 7327 has a second copy of *psaL* that is adjacent to *psaI*. As shown in Figure 5-36 and Figure 5-37A, PCC 7327 has trimeric PSI which does not resolve as a uniform species on BN-PAGE gel. In contrast, both PCC 10802 has a well resolved PSI trimer band on BN-PAGE gel and a minor PSI dimer species as well (Figure 5-37 A and B, Figure 5-38).

Microcystis sp. PCC 7806

Microcystis sp. PCC 7806 (PCC 7806), a strain in the genus of *Microcystis* whose PSI has rarely been studied, was studied as a representative in this genus as well as its close relatives. As shown in Figure 5-37A and Figure 5-38, PCC 7806 has trimeric PSI as its major PSI oligomer, with minor potential dimeric PSI species as well.

Chamaesiphon minutus PCC 6605

Chamaesiphon minutus PCC 6605 (PCC 6605) also has a *psaL* gene located close to *psaF and psaJ,* but without *gmk* gene adjacent. Even though the expected PSI trimer was observed after BN-PAGE analysis (Figure 5-37 B and C,

Figure 5- 37 BN-PAGE of solubilized thylakoid membrane from PCC 7327, PCC 7806, PCC 10802 and PCC 6605

(A) BN-PAGE of solubilized thylakoid membrane from PCC 7327 and PCC 7806.
(B) BN-PAGE of solubilized thylakoid membrane from PCC 10802 and PCC 6605.
(C) Rerun of BN-PAGE of solubilized thylakoid membrane from PCC 6605 compared with PCC 7414.
Thylakoid membranes with 0.4 mg/mL Chl from each strain were solubilized in different concentrations of DDM (w/v, %), labeled on top of each lane. Solubilized thylakoid membranes from TS-821 and *Synechocystis* sp. PCC 6803 (Syn6803) with 0.4 mg/mL Chl in 1% DDM were loaded as controls. For (A) and (B), ~ 2 µg Chl were loaded for each condition. For (C), ~3.2 µg Chl were loaded for each lane.

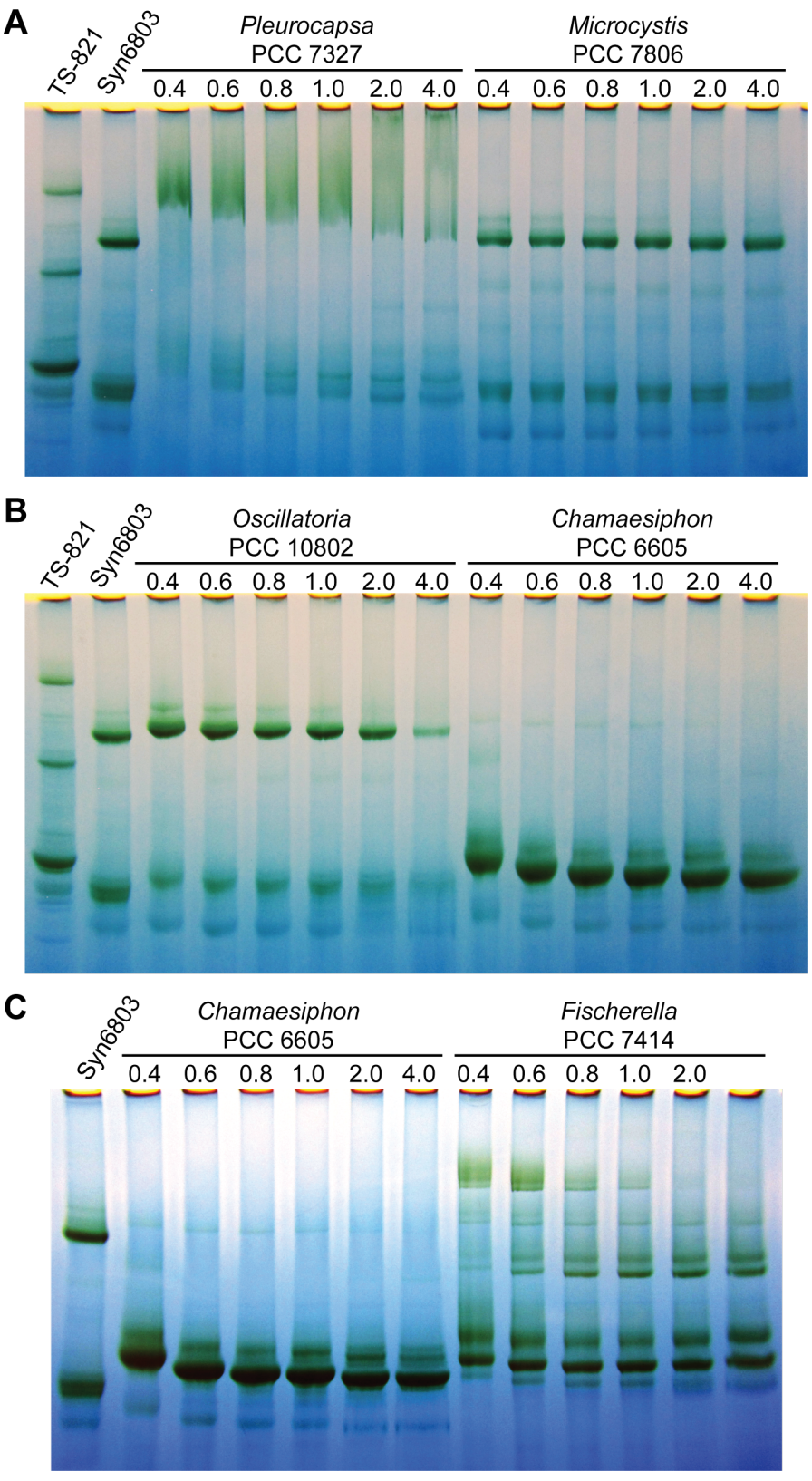

Figure 5-37 continued

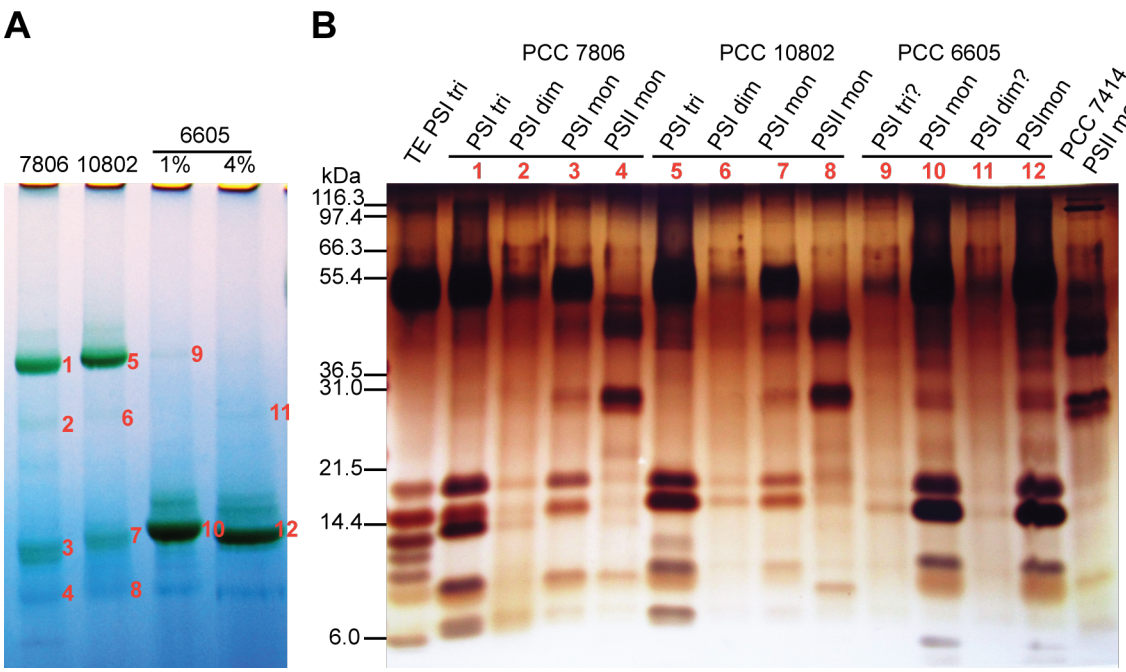

Figure 5- 38 PAGE analysis of PSI complexes in PCC 7806, PCC 10802, and PCC 6605

(A) BN-PAGE of solubilized thylakoid membrane from PCC 7806, PCC 10802, and PCC 6605. For PCC 6605, two solubilization conditions (1% DDM and 4% DDM) were used. Bands sliced out for following SDS-PAGE (B) and PSI identification were numbered.

(B) SDS-PAGE of green bands isolated from BN-PAGE gel (A) for PSI identification. Purified TE PSI trimer and PCC 7414 PSII monomer from BN-PAGE gel were used as control for PSI identification. Numbered lanes correspond to numbered bands in (A). PSI oligomeric state interpretations were denoted on top of each lane as well.

Figure 5-38), the relative abundance is very low compared with the monomeric species. Interestingly, the PSI trimer seems to dissociate into PSI dimer (and monomer) under high detergent concentration (4% DDM) solubilization conditions (Figure 5-37 B and C). This sensitivity to high detergent concentration was only observed for PSI tetramer so far. To confirm the PSI trimer is trimeric, a side by side comparison with PCC 7414 was analyzed (Figure 5-37C). The reason for PCC 6605 having mostly monomeric PSI is yet to be studied.

5.5 Correlation of *psaL* genes and PSI Oligomeric States

Most Heterocyst-forming Cyanobacteria and Their Close Relatives Have Non-trimeric PSI as Their Major PSI Oligomer

As shown in Table 5-1, among the cyanobacteria studied, most heterocyst-forming cyanobacteria and their close relatives have tetrameric PSI. Even though some of the heterocyst-forming cyanobacteria have no known genome sequences, the morphological classification of heterocyst-forming cyanobacteria usually indicates the high possibility of PSI tetramer. In contrast, most cyanobacteria outside this group have trimeric PSI as their major PSI oligomeric form. Among all the strains investigated in this study, three special strains were observed to have exclusively monomeric PSI (UTEX B 379, UTEX B 381, and UTEX B 2014). This indicates the diversity of PSI oligomer in cyanobacteria. PCC 7203 and PCC 7434 also have multiple monomeric PSI species with small amount dimeric PSI observed. The most special case of all the heterocyst-forming cyanobacteria is *Nostoc* sp. PCC 9335, which has both PSI trimer and PSI dimer equally predominant.

Table 5- 1 PSI oligomeric state in cyanobacteria studied

Strains	Genome	Heterocyst-forming	PSI oligomers	Source
Chroococcidiopsis sp. TS-821	unknown	Close relative	**Tet**/Tri/**Dim**/**Mon**	Bruce
Gloeocapsa sp. PCC 7428	known	Close relative	**Tet**/Tri/**Dim**/**Mon**	PCC
Synechocystis sp. PCC 7509	known	Close relative	**Tet**/Tri/**Dim**/**Mon**	PCC
Chroococcidiopsis thermalis PCC 7203	known	Close relative	Dim/**Mon**	PCC
Chroococcidiopsis sp. PCC 7434	known	Close relative	Dim/**Mon**	PCC
Chlorogloeopsis fritschii PCC 6912	known	Y	**Tet**/Tri/**Dim**/**Mon**	PCC
Nostoc punctiforme PCC 73102	known	Y	Tet/**Mon**	PCC
Fischerella sp. PCC 9605	known	Y	**Tet**/Tri/**Dim**/**Mon**	PCC
Calothrix sp. PCC 7507	known	Y	**Tet**/Tri/**Dim**/**Mon**	PCC
Mastigocladopsis repens PCC 10914	known	Y	Dim/Mon	PCC
Chlorogloeopsis fritschii PCC 9212	known	Y	**Tet**/Tri/**Dim**/**Mon**	PCC
Fischerella muscicola PCC 73103	known	Y	Tri/**Dim**/**Mon**	PCC
Nostoc sp. PCC 7107	known	Y	**Tet**/Tri/**Dim**/**Mon**	PCC
Nostoc sp. PCC 7524	known	Y	Tet/Dim/Mon	PCC
Scytonema hofmanni PCC 7110	known	Y	**Tet**/Tri/**Dim**/**Mon**	PCC
Calothrix sp. PCC 7103	known	Y	**Tet**/Tri/**Dim**/**Mon**	PCC
Nodularia spumigena PCC 73104	unknown	Y	Tet/**Dim**/**Mon**	Binder
Fischerella muscicola PCC 7414	known	Y	**Tet**/Tri/**Dim**/**Mon**	Binder
Anabaena cylindrica PCC 7122	known	Y	Tet/Dim/Mon	Binder
Nostoc sp. PCC 7120	known	Y	Tet/Dim/Mon	Binder
Fremyella diplosiphon B 481	known	Y	Tet/Dim/Mon	UTEX
Anabaena flos-aquae B 1444	known	Y	Tet/Dim/Mon	UTEX
Scytonema hofmanni B 2349	known	Y	**Tet**/Tri/**Dim**/**Mon**	UTEX
Fischerella muscicola LB 1829	known	Y	**Tet**/tri/**Dim**/**Mon**	UTEX
Hapalosiphon welwitschii B 1830	known	Y	Tet/Dim/Mon	UTEX
Nodularia harveyana B 2093	unknown	Y	**Tet**/Tri/**Dim**/**Mon**	UTEX
Scytonematopsis contorta 2963	unknown	Y	Dim/**Mon**	UTEX
Spirirestis rafaelensis B 2660	unknown	Y	**Tet**/Tri/**Dim**/**Mon**	UTEX
Fischerella ambigua 1903	unknown	Y	**Tet**/tri/**Dim**/**Mon**	UTEX

Table 5-1 continued

Strains	Genome	Heterocyst-forming	PSI oligomers	Source
Anabaena flos-aquae LB 2558	unknown	Y	Tet/Dim/Mon	UTEX
Calothrix parietina LB 1952	unknown	Y	**Tet**/Tri/**Dim**/**Mon**	UTEX
Gloeotrichia ghosi LB 1920	unknown	Y	Tet/Dim/Mon	UTEX
Mastigocladus sp. B2965	unknown	Y	**Tet**/Tri/**Dim**/**Mon**	UTEX
Tolypothrix distorta B 424	unknown	Y	**Tet**/Tri/**Dim**/**Mon**	UTEX
Scytonema crispum LB 1556	unknown	Y	**Tet**/Tri/**Dim**/**Mon**	UTEX
Calothrix membranacea B 379	unknown	Y	monomeric	UTEX
Cylindrospermum licheniforme B 2014	unknown	Y	monomeric	UTEX
Anabaena inaequalis B 381	unknown	Y	monomeric	UTEX
Nostoc sp. 9335	unknown	Y	Tri/Dim/Mon	PCC
Gloeocapsa alpicola LB 1598	known	N	Trimeric	UTEX
Plectonema boryanum B 482	known	N	Trimeric	UTEX
Spirulina platensis LB 1926	unknown	N	**Tri**/Dim	UTEX
Aphanothece sp. SP25	unknown	N	Trimeric	UTEX
Pseudanabaena sp. B SP48	unknown	N	Trimeric	UTEX
Synechococcus sp. WH 7803	known	N	Trimeric	Bruce
Oscillatoria sp. PCC 8926	unknown	N	**Tri**, Tet?	PCC
Chroococcidiopsis sp. PCC 6712	known	N	**Tri**, hexamer?	PCC
Synechococcus sp. PCC 7336	known	N	Trimeric	PCC
Synechococcus sp. PCC 7502	known	N	Trimeric	PCC
Pseudanabaena sp. PCC 7704	known	N	**Tri**/Dim	PCC
Nodosilinea nodulosa PCC 7104	known	N	Trimeric	PCC
Leptolyngbya sp. PCC 6406	known	N	**Tri**/Dim	PCC
Leptolyngbya sp. PCC 7124	known	N	Dim/Mon	PCC
Oscillatoria sp. PCC 10802	known	N	**Tri**/Dim	PCC
Chamaesiphon minutus PCC 6605	known	N	Tri/Dim/**Mon**	PCC
Pleurocapsa sp. PCC 7327	known	N	Trimeric	PCC
Microcystis sp. PCC 7806	known	N	**Tri**/Dim	PCC
Chamaesiphon sp. PCC 7430	unknown	N	**Tri**/Dim	PCC
Pseudanabaena sp. PCC 7367	known	N	Trimeric	PCC

Major oligomeric states are bolded. “?” denotes the uncertainty.

In contrast to heterocyst-forming cyanobacteria and their close relatives, most cyanobacteria outside this group have trimeric PSI as the major PSI oligomer. Even though potential PSI tetramer was observed in PCC 8926, the major PSI oligomeric state is trimeric. In addition to the special strain of PCC 8926, PCC 6605 has mainly monomeric PSI even though trimeric PSI was observed. Moreover, PCC 7124, a non-heterocyst-forming filamentous cyanobacterium, mainly has potential dimeric PSI and monomeric PSI. This again indicates the diversity of PSI oligomers in cyanobacteria. Some minor PSI dimer species were also observed in multiple species. Whether this PSI dimer is in its native state or an artifact of the BN-PAGE analysis is yet to be studied. Above all, most cyanobacteria outside the heterocyst-forming cyanobacteria clade have trimeric PSI.

Based on the results we observed for PSI oligomeric states in cyanobacteria, one can predict that a heterocyst-forming cyanobacterium very likely has tetrameric PSI. However, the exact PSI oligomeric states should be verified experimentally. In general, non-trimeric PSI is expected in heterocyst-forming cyanobacteria and their close relatives. Also, one should keep an open mind when discussing the PSI structure in cyanobacteria and a general statement of “cyanobacterial PSI is trimeric” should be avoided.

The *psaL* Gene Genomic Location and PSI Oligomeric State

In the initial study of PSI tetramer in TS-821, we observed that the *psaL* gene in TS-821 was located downstream of *psaF* and *psaJ* genes, and also adjacent to *gmk* gene (*21*). It was speculated that this special genomic

arrangement of *psa* genes is related to the PSI oligomeric state. With more available cyanobacterial genome sequences and further extensive investigation, we found that all heterocyst-forming cyanobacteria and their close relatives have a copy of *psaL* gene that is located down stream of *psaF* and *psaJ* (Figure 5-39). In most cyanobacteria in this group, the *psaL* gene is also followed by the *gmk* gene with opposite orientation (Figure 2-6). The cloning results of *psaL* from fourteen heterocyst-forming cyanobacteria without known genome sequences showed similar *psaL* genomic location. Some strains outside this group also have such genomic location for their *psaL* genes, such as PCC 10802 (Figure 5-39). Most cyanobacteria outside the heterocyst-forming group have a *psaL* gene located close to *psaI* (Figure 5-39). This *psaL/I* arrangement was speculated to determine PSI trimeric structure (*21*).

The genomic structure of *psaF/J/L* is probably necessary but not sufficient for forming tetrameric PSI in cyanobacteria. For all the cyanobacteria that have tetrameric PSI, the *psaF/J/L* structure was observed (Figure 5-39); however, not all the cyanobacteria having *psaF/J/L* structure have tetrameric PSI (Figure 5-39). At the same time, strains with single copy of *psaL* gene, such as PCC 7428 and PCC 7103, has both PSI trimer and PSI tetramer, which indicates that *psaF/J/L* structure cannot be used as a single criterion to predict the PSI oligomeric state. Moreover, strains having *psaF/J/L* structure in the heterocyst-forming group can also have exclusively PSI monomer (such as UTEX B381) or with minor PSI dimer (Figure 5-39). For the strains outside the heterocyst-forming group with *psaF/J/L* structure, PSI trimer is the major oligomeric state of PSI.

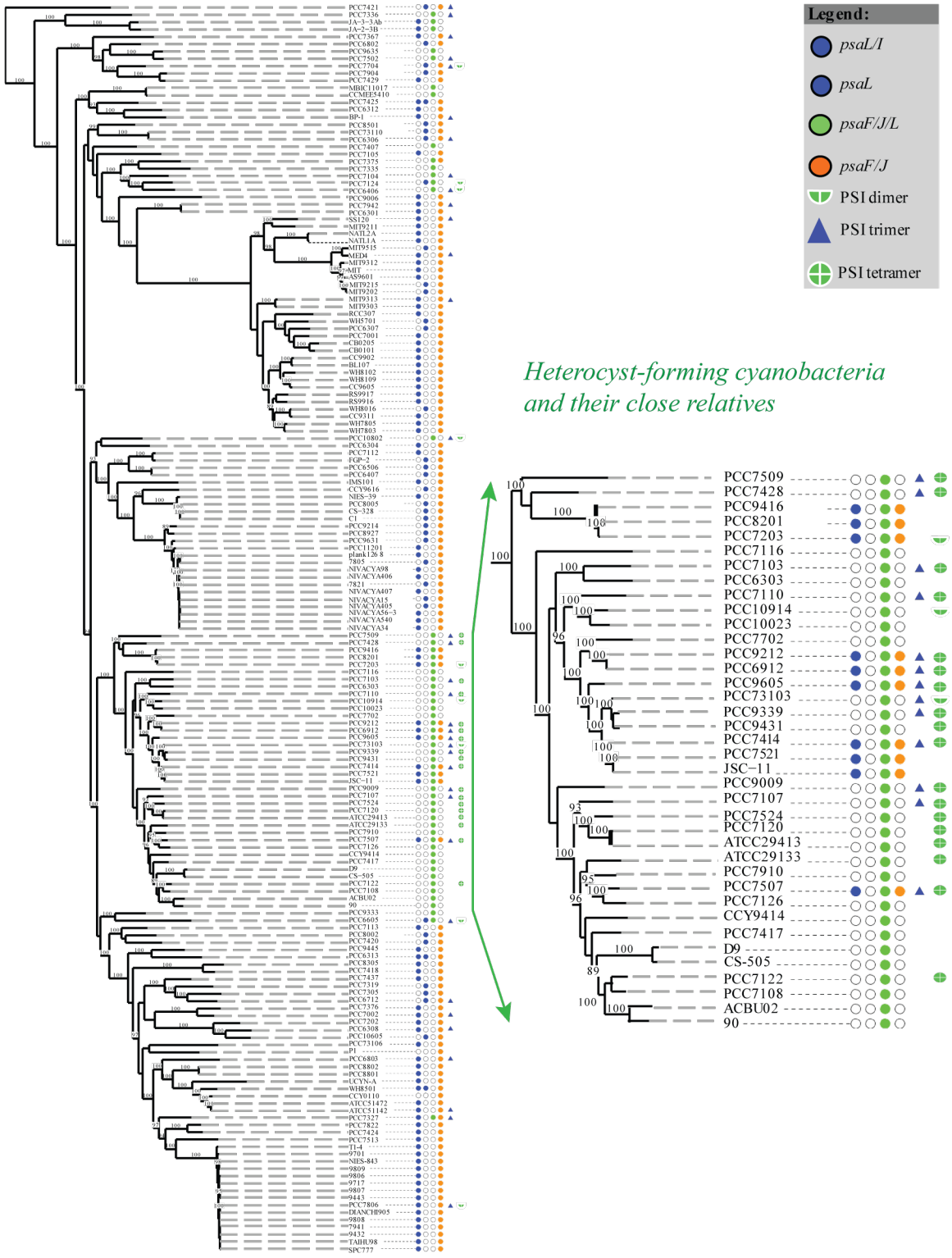

Figure 5- 39 PSI tetramer distribution and *psaL* gene location

The genomic *psaL/I* structure does not predict trimeric PSI in heterocyst-forming cyanobacteria and their close relatives. Even though most cyanobacteria having a single copy of *psaL* gene in *psaL/I* structure have trimeric PSI, this is not the case for heterocyst-forming cyanobacteria and their close relatives. In PCC 7203, there are two copies of *psaL* genes; however, no trimeric PSI was observed. The study of far-red light response of cyanobacteria pointed out that the two copies of *psaL* may be expressed differently in response to far-red light (*34*). Proteomic analyses of PSI trimer and PSI tetramer from PCC 7428, PCC 7414, and TS-821 showed that only one PsaL was detected in both PSI trimer and tetramer, encoded by the *psaL* gene in *psaF/J/L* arrangement. This indicates that the second copy of *psaL* in PCC 7414 is not involved in PSI tetramer/trimer formation under regular culture conditions.

In conclusion, the genomic location of *psaL* cannot be used as single criterion for determining PSI oligomeric state in cyanobacteria. Nevertheless, *psaL/I* is usually expected in cyanobacteria that do not possess PSI tetramer, while *psaF/J/L* structure, as well as PSI tetramer, is highly expected in heterocyst-forming cyanobacteria and their close relative. Strains in this group possessing two copies of *psaL* with both genomic structures may be able to switch on the *psaL* gene in *psaL/I* structure in response to far-red light.

PsaL Structure and PSI Tetramer

PsaL has been known for stabilizing the PSI trimeric structure in cyanobacteria. The fact that PsaL is present in PSI tetramer indicates the structural change in PsaL. Our genetic study also showed that PsaL in TS-821

and *Arabidopsis* do not support the trimeric PSI structure in *Synechocystis* sp. PCC 6803 (Figure 4-12 and Figure 4-14). The diversity of PsaL may results in the diverse PSI oligomeric state.

Phylogenetic analysis identifies the PsaL that may form tetrameric PSI. In consistence with earlier analysis(*21*), most PsaL from heterocyst-forming cyanobacteria and their close relatives are found in one clade (dark green box in Figure 5-40). At the same time, some of the cyanobacteria in this group also have a second copy of *psaL,* all those PsaL are placed in the same group with similar PsaL in PCC 7335 and PCC 7327 (blue box in figure 5-40). The PsaL in this clade (blue box in Figure 5-40) may be involved in photosynthesis under far-red light (*34*). The common PsaL in heterocyst-forming cyanobacteria and their close relative (dark green box in Figure 5-40) may be found in tetrameric PSI, since most studied strains in this group have tetrameric PSI and only have one copy of *psaL* gene. PsaL in this clade have been identified in PSI tetramer in PCC 7414, PCC 7428 and TS-821. One interesting observation is that PCC 6605 has a *psaL* located in *psaF/J/L* structure (pointed out by arrow in Figure 5-41), and have mostly PSI monomer (Figure 5-37 B and C). Considering its close placement to this PsaL to common PsaL in heterocyst-forming cyanobacteria, it indicates that the evolution from trimeric PSI to tetrameric PSI may take a first step by destabilizing the trimeric PSI.

What structural features in PsaL determine PSI tetramer have yet to be studied. Earlier study has speculated the relative short C-termini of PsaL in

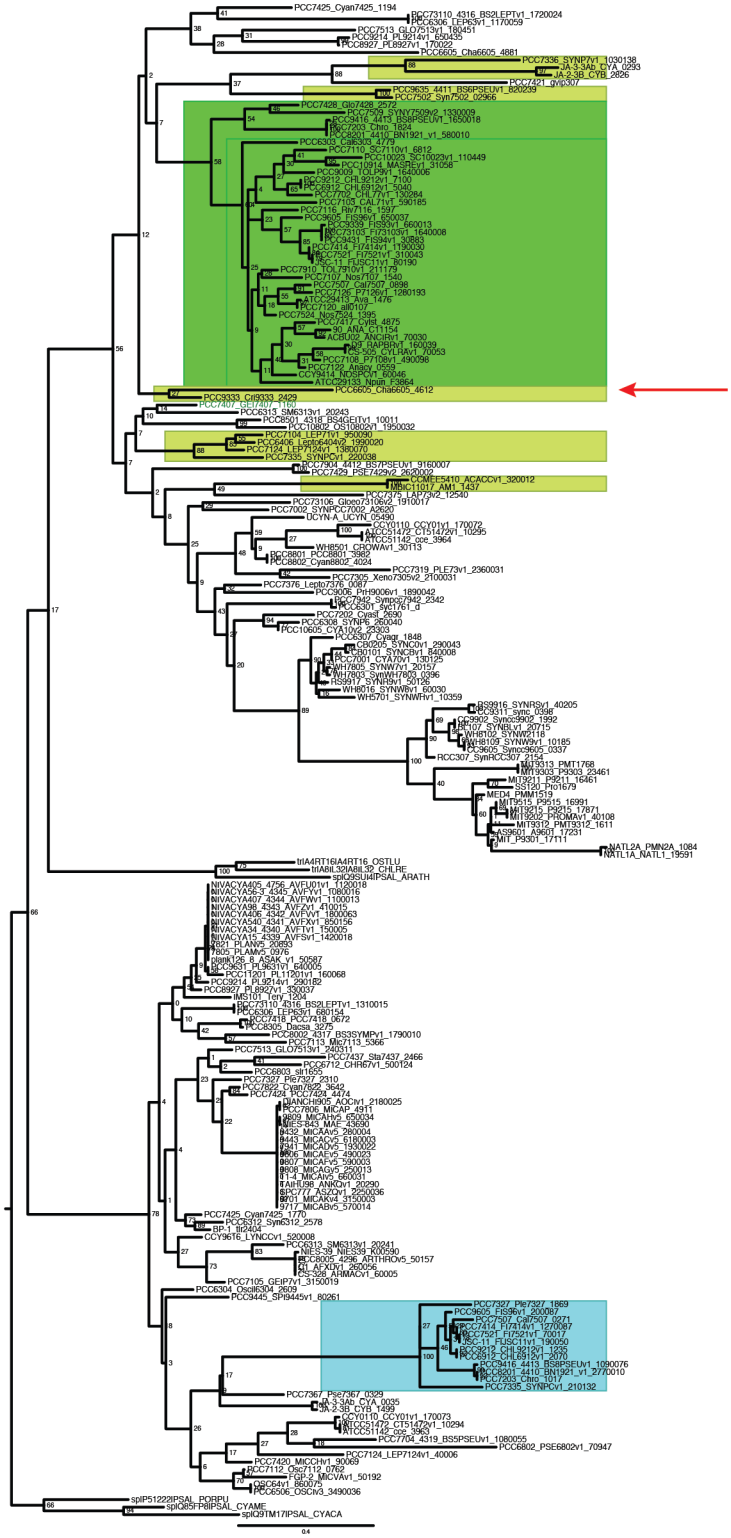

Figure 5- 40 Phylogenetic tree of PsaL

Dark green and light green boxes denote *psaL* in *psaF/J/L* structure, while blue box denotes the potential PsaL for photosynthesis under far-red light.

TS-821 and the longer loop insertion between second and third transmembrane helices may be the key factor for forming PSI tetramer (*21*). While the Cryo-EM study of TS-821 PSI tetramer showed the shorten PsaL C-terminus fits better in the electron density map (Figure 4-4), the loop insertion structure was not resolved. An alignment of the PsaL of studied strains showed that most heterocyst-forming cyanobacteria and their close relatives have multiple prolines in the loop insertion regions (Figure 5-41). The most frequent pattern is PPXP followed by six conserved amino acid residues and then PNPP, with X being polar or charged residues. This multi-proline sequence pattern seems to be involved in protein folding and eventually PSI oligomer formation, considering the slow translation of consecutive prolines (*129*). In the meantime, one should keep in mind that not all PsaL in the tetrameric PSI follow this paradigm. For instance UTEX B 2093 and PCC 7107, whose PsaL do not follow the multi-proline pattern in the loop insertion (Figure 5-41), both have tetrameric PSI. Nevertheless, the high consensus of this linker region in PsaL in tetrameric PSI indicates the evolutionary direction for PsaL in heterocyst-forming cyanobacteria and their close relative. The similar multi-proline pattern in PCC 6605 PsaL (Figure 5-41) indicates this loop insertion may facilitate PSI monomerization.

The *psaL* gene locus, PsaL phylogenetic position and structure, altogether may help predict the PSI oligomeric state in cyanobacteria. Yet, experiments are needed to verify the speculations.

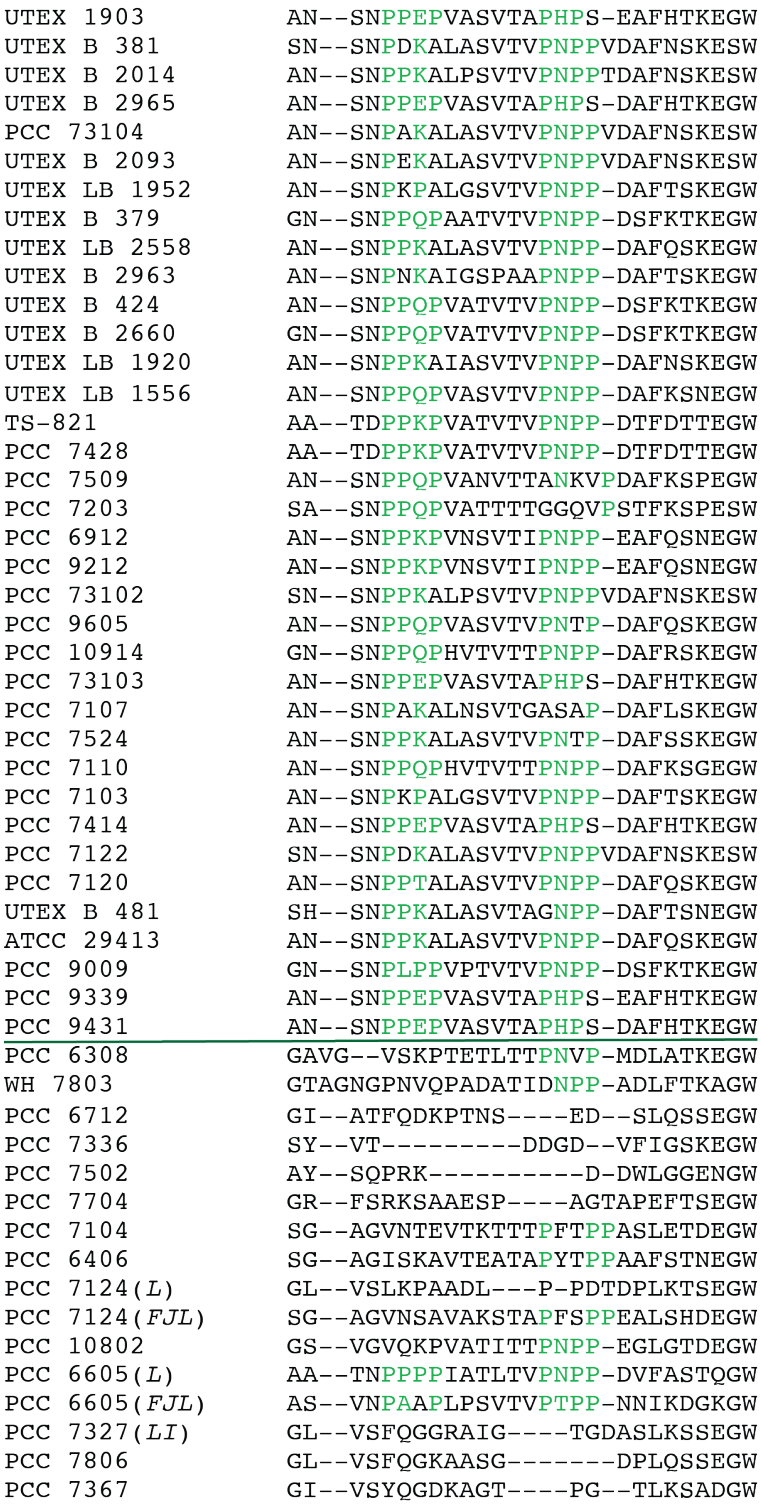

Figure 5- 41 Alignment of PsaL loop insertion between second and third transmembrane helices

Multi-proline pattern is colored green. Different cyanobacteria groups are divided by a green line.

CHAPTER SIX

Physiological and Evolutionary Significance of PSI Tetramer: Tetrameric PSI May be a Primitive Adaptation to High Light Intensity

6.1 Disclosure

This chapter contains mostly unpublished data, even though some of the content have been presented in 12th Workshop on Cyanobacteria and 25th Western Photosynthesis Conference. The initial study of high light response in TS-821 is included in the Cryo-EM structure manuscript, accepted by BBA-Bioenergetics and published as online before print (*50*).

6.2 Abstract

Ever since the discovery of the PSI tetramer in cyanobacteria, a question why some cyanobacteria have tetrameric PSI? Biochemically, the PsaL was the center subunit to investigate; however, physiologically it was an open question what factor selected PSI tetramer over PSI trimer. To investigate physiological influences on the formation of a tetrameric PSI, different environmental factors have been investigated. Our data show that nitrogen source, temperature, and salinity have little effect on the presence of tetrameric PSI. In contrast, the relative abundance of tetrameric PSI increases under high light intensity in at least three different cyanobacteria (TS-821, PCC 7414, and PCC 7428). A detailed study in TS-821 showed that this transition is also accompanied by increased carotenoid accumulation in the PSI tetramer. Moreover, these carotenoids (myxoxanthophyll, canthaxanthan, echinenone, and β-carotene) are released when the tetramer is dissociated into dimers. Together this work suggests that tetrameric PSI may be a primitive adaptation to high light intensity and that tetrameric PSI is the evolutionary intermediate from PSI trimer in cyanobacteria to PSI monomer in chloroplast.

6.3 The Effect of Nitrogen Source on PSI Tetramer

PSI tetramer exists mainly in heterocyst-forming cyanobacteria and their close relatives. One common characteristic shared by those cyanobacteria is their ability of fix nitrogen. Especially in heterocyst-forming cyanobacteria, heterocysts are developed upon removal of combined nitrogen sources. Tetrameric PSI has also been observed in heterocyst, which leads to the question whether or not PSI tetramer is correlated to heterocyst. To answer this question, several heterocyst-forming cyanobacteria were studied under culture conditions with different nitrogen sources. The results showed that nitrogen source has little, if any, effect on the formation of PSI tetramer in heterocyst-forming cyanobacteria.

As shown in Figure 4-3, PCC 7414 does not show difference in terms of PSI tetramer when cultured in BG-11_0 medium, compared with BG-11. In addition, when PCC 7414 was cultured in BG-11 medium supplemented with NH_4^+, its PSI tetramer did not show significant difference when compared with the cells cultured in BG-11_0 (Figure 6-1). These results indicate nitrogen source has little effect on PSI tetramer formation, at least in PCC 7414.

To see if PSI tetramer in other heterocyst-forming cyanobacteria have similar inertia to nitrogen sources, similar experiments have been done in LB 1829, PCC 7122, PCC 7120 and PCC 73104. As shown in Figure 6-2A, when cultured in BG-11_0, no significant difference was observed for the PSI profile in LB 1829 compared with that in BG-11. Similarly, PCC 7120 showed no significant difference in its PSI oligomer profile in thylakoid when utilizing different

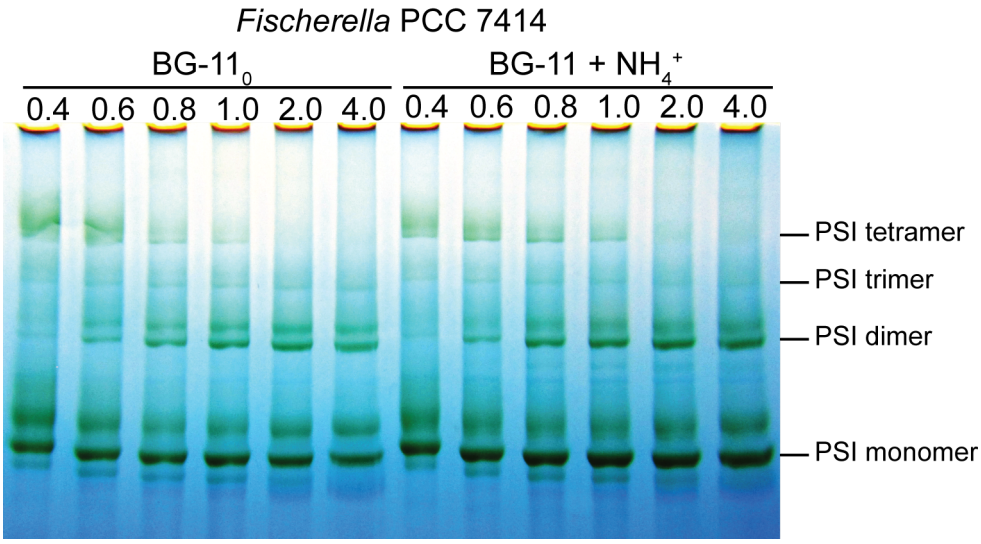

Figure 6- 1 BN-PAGE of solubilized thylakoid membrane from PCC 7414 cultured with different nitrogen sources

Thylakoid membranes with 0.4 mg/mL Chl from PCC 7414, cultured in BG-11$_0$ and BG-11 medium supplemented with NH_4^+, were solubilized in different concentrations of DDM (w/v, %), labeled on top of each lane. ~ 2 µg Chl were loaded for each condition. Bands corresponding to PSI oligomers are denoted.

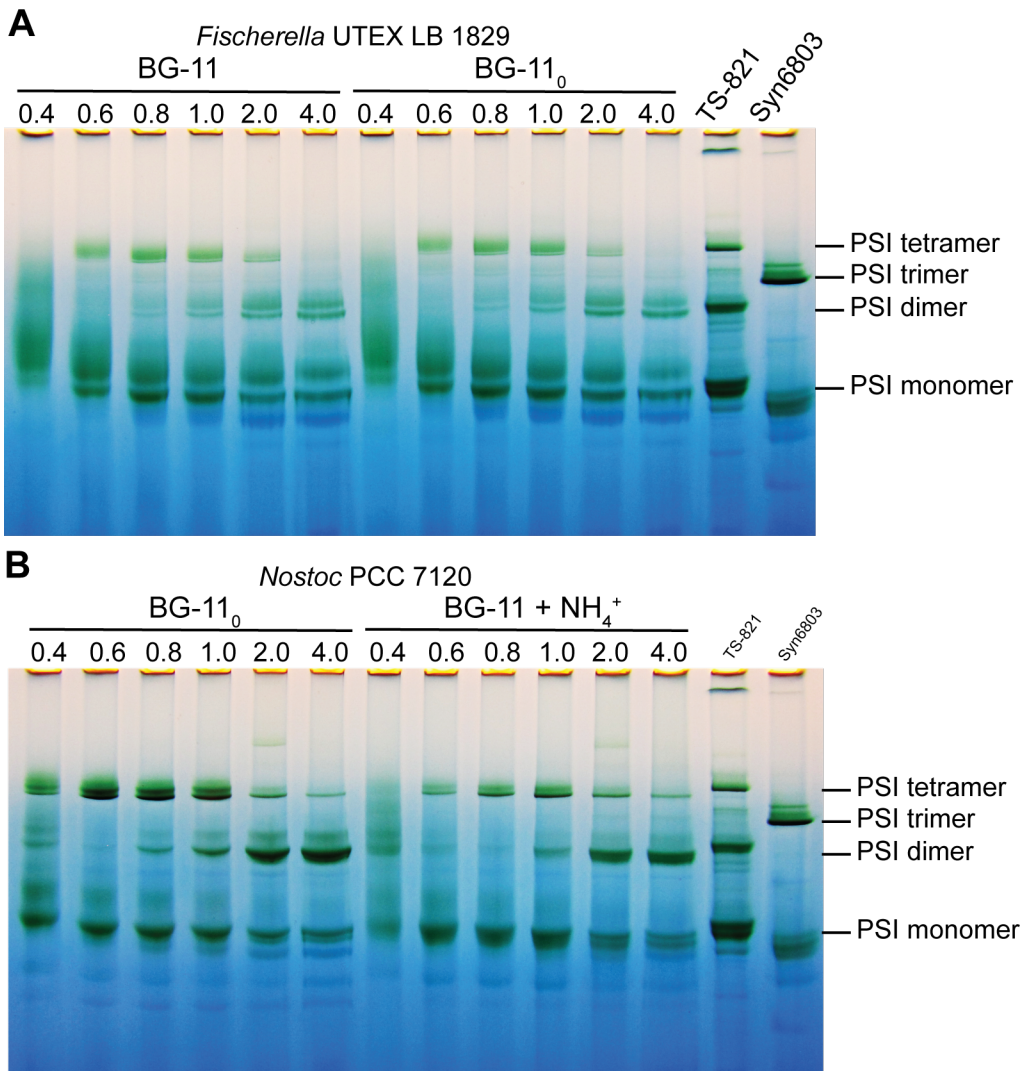

Figure 6- 2 BN-PAGE of solubilized thylakoid membrane from LB 1829 and PCC 7120 cultured with different nitrogen sources

(A) BN-PAGE of solubilized thylakoid membrane from LB 1829

(B) BN-PAGE of solubilized thylakoid membrane from PCC 7120 cultured in BG-11_0 and BG-11 supplemented with NH_4^+.

Thylakoid membranes with 0.4 mg/mL Chl from LB 1829 and PCC 7120 were solubilized in different concentrations of DDM (w/v, %), labeled on top of each lane. Solubilized thylakoid membranes from TS-821 and *Synechocystis* sp. PCC 6803 (Syn6803) with 0.4 mg/mL Chl in 1% DDM were loaded as controls. ~ 2 µg Chl were loaded for each condition. Bands corresponding to PSI oligomers are denoted.

nitrogen sources (Figure 6-2B). In the case of PCC 7122, the effect of nitrogen source on PSI profile (Figure 6-3A) is similar to what was observed in PCC 7120. Moreover, the study of nitrogen source effect on PSI oligomer for PCC 73104 showed that no tetrameric PSI was observed when PCC 73104 was cultured in modified ASNIII medium nor in BG-11 + NH_4^+ medium (Figure 6-3B). PSI tetramer, small amount though, was observed when PCC 73104 was cultured in BG-11 medium (Figure 5-1). This may indicate some subtle physiological changes in PCC 73104 when cultured in different media.

In conclusion, nitrogen sources have little, if any, effect on PSI tetramer formation. The fact that heterocyst-forming cyanobacteria cultured in NH_4^+ have tetrameric PSI indicates PSI tetramer exists in vegetative cells. Combined with the observation of PSI tetramer in heterocysts (*49*), PSI tetramer has no spatial exclusion in heterocyst-forming cyanobacteria. Quantity differences may still exist between vegetative cells and heterocysts.

6.4 The Effect of Salinity on PSI Oligomeric States

In *Nodularia harveyana* UTEX B 2093, very stable PSI tetramer was observed (Figure 5-12A). To study the effect of salinity on PSI tetramer formation, B 2093 cultured in BG-11 was investigated. Even though a slight size shift was observed for PSI in B 2093 cultured in BG-11, the PSI tetramer abundance was not affected (Figure 6-4). This observation and the observation in PCC 73104 (Figure 6-3B) rule out that salinity is a major factor for PSI tetramer formation. Study in *Pseudanabaena* sp. B SP48 also showed no significant effect of salinity on PSI trimer (Figure 5-19A and Figure 5-20A).

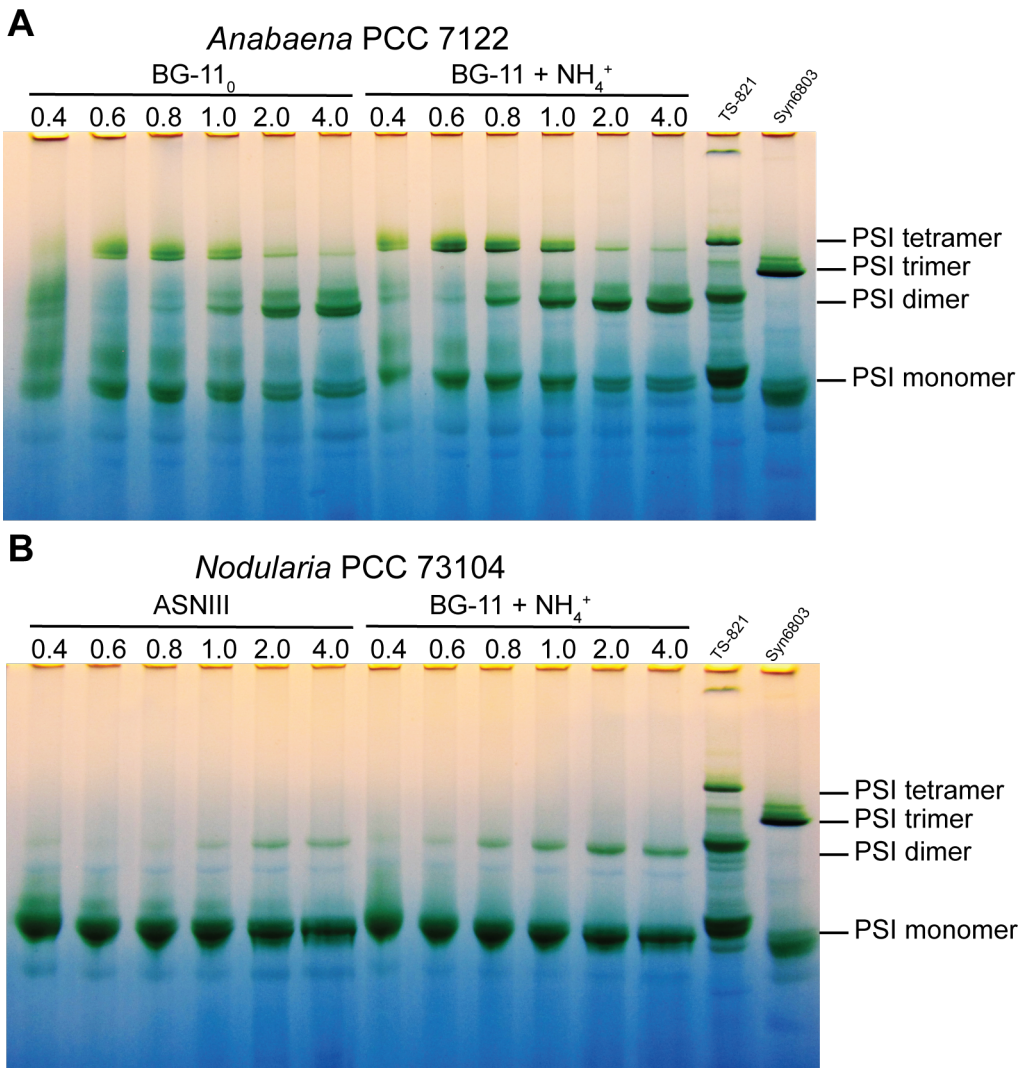

Figure 6- 3 BN-PAGE of solubilized thylakoid membrane from PCC 7122 and PCC 73104 cultured in different media

(A) BN-PAGE of solubilized thylakoid membrane from PCC 7122 cultured in BG-11$_0$ and BG-11 supplemented with NH_4^+.

(B) BN-PAGE of solubilized thylakoid membrane from PCC 73104 cultured in modified ASNIII and BG-11 supplemented with NH_4^+.

Thylakoid membranes with 0.4 mg/mL Chl from PCC 7122 and PCC 73104 were solubilized in different concentrations of DDM (w/v, %), labeled on top of each lane. Solubilized thylakoid membranes from TS-821 and *Synechocystis* sp. PCC 6803 (Syn6803) with 0.4 mg/mL Chl in 1% DDM were loaded as controls. ~ 2 µg Chl were loaded for each condition. Bands corresponding to PSI oligomers are denoted.

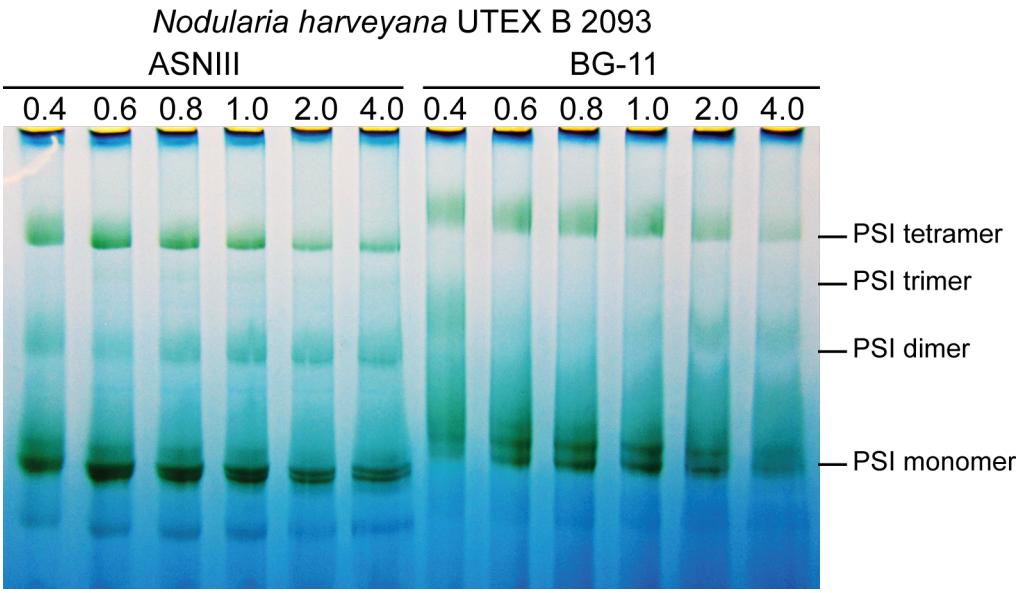

Figure 6- 4 BN-PAGE of solubilized thylakoid membrane from B 2093 cultured in media with different salinity

Thylakoid membranes with 0.4 mg/mL Chl from B2093, cultured in BG-11 and modified ASNIII medium, were solubilized in different concentrations of DDM (w/v, %), labeled on top of each lane. ~ 2 µg Chl were loaded for each condition. Bands corresponding to PSI oligomers are denoted.

6.5 The Effect of Temperature on Cyanobacterial PSI Oligomeric States

Some of the strains studied are thermophilic and known for their survival at different temperatures. Whether the PSI tetramer formation is related to temperature was not known, even though recent report indicates PSI trimer formation was facilitated by elevated temperature in *Synechocystis* sp. PCC 6803 (*36*). Our initial study was done with *Fischerella muscicola* PCC 7414 by incubating PCC 7414 at 24 °C for two days. The BN-PAGE analysis showed no PSI profile difference between 37 °C culture and the 24 °C culture (Figure 6-5A). To confirm that temperature does not affect PSI tetramer formation, PCC 7414 directly cultured in 45 °C was tested for its PSI profile as well. As shown in Figure 6-5B, the PSI profile in PCC cultured at 45 °C is similar to that at 37 °C.

To investigate whether temperature has any effect on PSI tetramer formation in other cyanobacteria, similar study was done with PCC 7203, PCC 7428 and TS-821. In the case of PCC 7203, PSI tetramer has not been observed. At elevation temperature (45 °C), the formation of PSI dimer in PCC7203 seems to be promoted (Figure 6-6A). For PCC 7428, the PSI profiles from cultures at different temperature do not show much difference, with the PSI tetramer slightly more stable against detergent treatment at lower temperature (Figure 6-6B). As the known closest relative to PCC 7428, the PSI tetramer in TS-821 also seems to be more stable when cultured at 37 °C, compared with that at 45 °C (Figure 6-7). At the same time, the PSI trimer is also more abundant at elevated temperature for TS-821 (Figure 6-7).

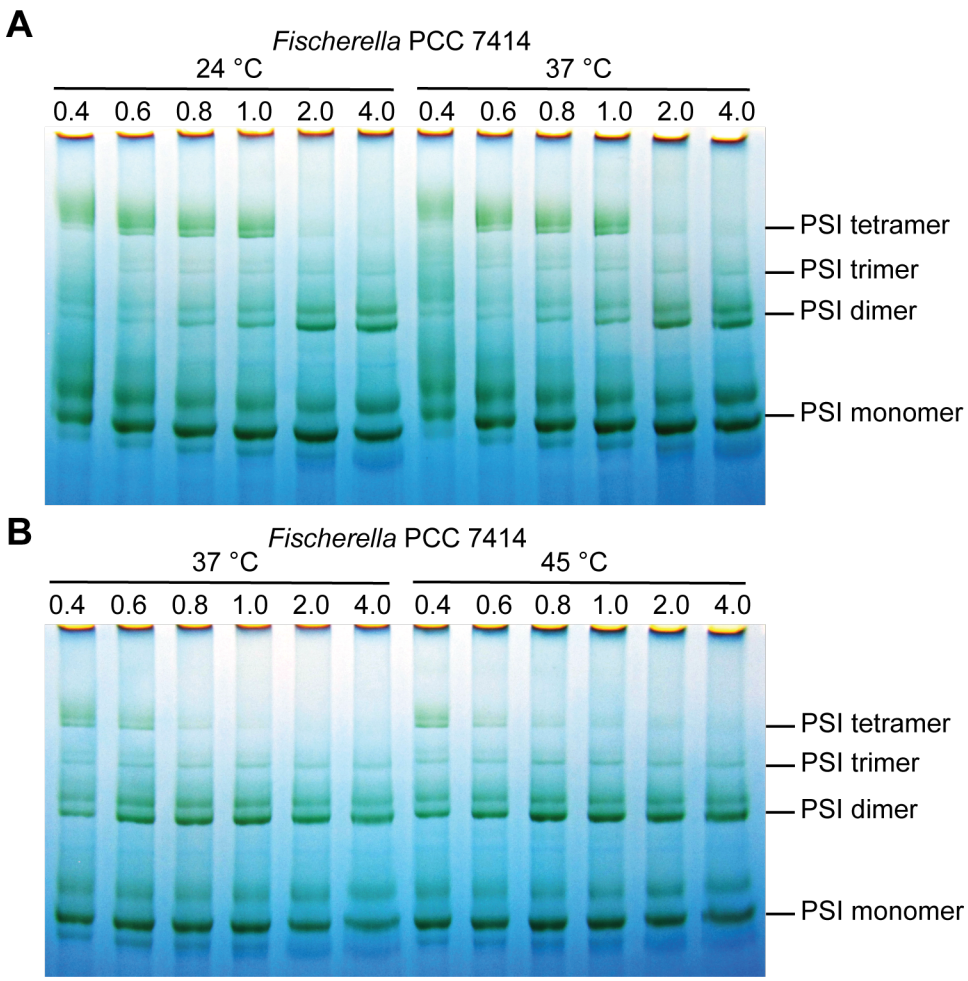

Figure 6- 5 BN-PAGE of solubilized thylakoid membrane from PCC 7414 cultured at different temperatures

(A) Thylakoid membranes with 0.4 mg/mL Chl from PCC 7414 were solubilized in different concentrations of DDM (w/v, %), labeled on top of each lane. ~ 2 µg Chl were loaded for each condition.

(B) Thylakoid membranes with 0.2 mg/mL Chl from PCC 7414 were solubilized in different concentrations of DDM (w/v, %), labeled on top of each lane. ~ 1.6 µg Chl were loaded for each condition.

Bands corresponding to PSI oligomers are denoted.

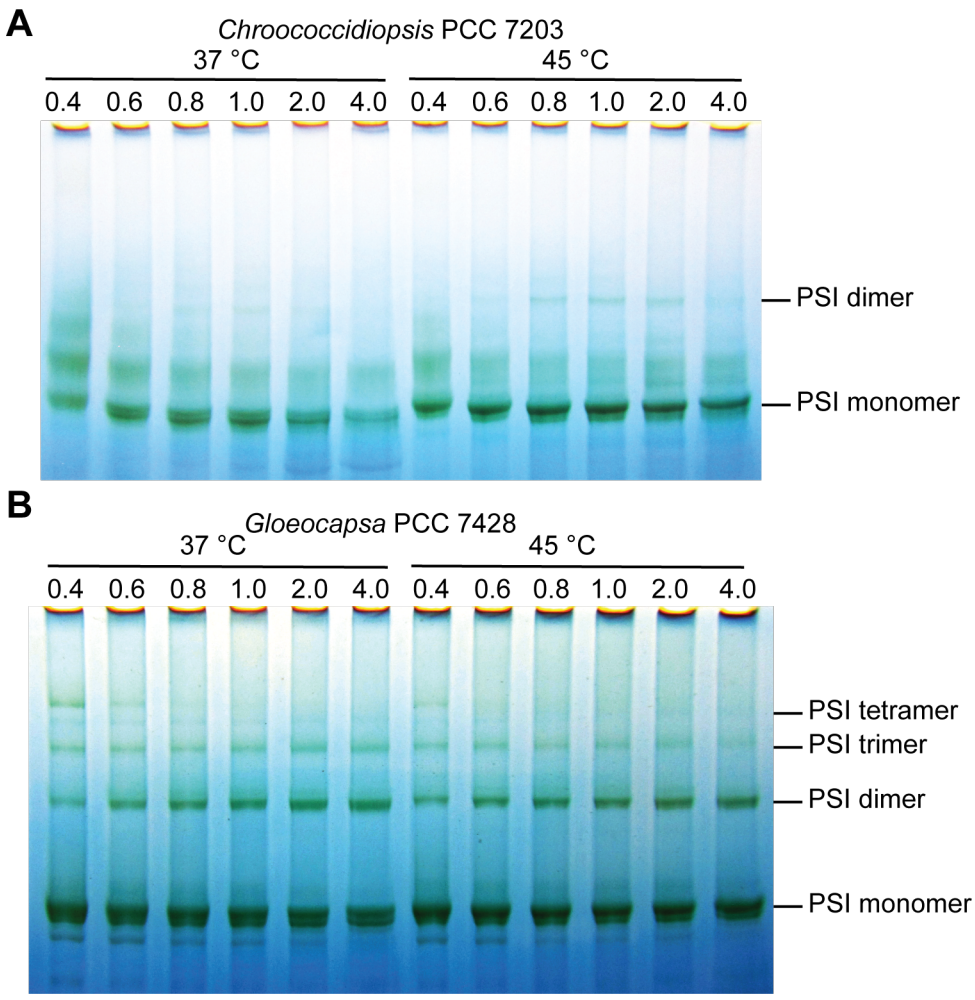

Figure 6- 6 BN-PAGE of solubilized thylakoid membrane from PCC 7203 and PCC 7428 cultured at different temperatures

(A) BN-PAGE of solubilized thylakoid membrane from PCC 7203 cultured at different temperatures.
(B) BN-PAGE of solubilized thylakoid membrane from PCC 7428 cultured at different temperatures.
Thylakoid membranes with 0.2 mg/mL Chl from PCC 7203 and PCC 7428 were solubilized in different concentrations of DDM (w/v, %), labeled on top of each lane. ~ 1.6 µg Chl were loaded for each condition. Bands corresponding to PSI oligomers are denoted.

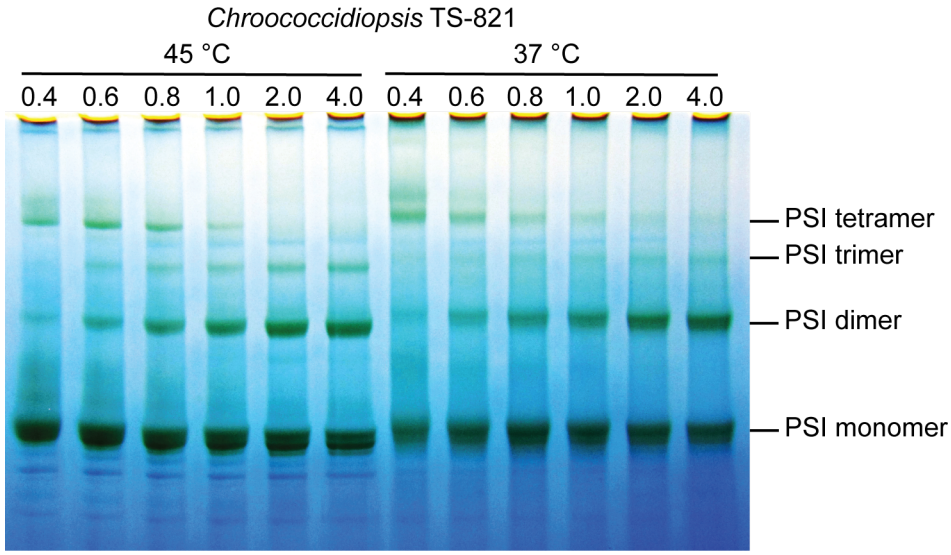

Figure 6- 7 BN-PAGE of solubilized thylakoid membrane from TS-821 cultured at different temperatures

Thylakoid membranes with 0.4 mg/mL Chl from TS-821 were solubilized in different concentrations of DDM (w/v, %), labeled on top of each lane. ~ 2 µg Chl were loaded for each condition. Bands corresponding to PSI oligomers are denoted.

6.6 The Effect of Light Intensity on Cyanobacterial PSI Oligomeric States

More PSI Tetramer is Observed in TS-821 Under High Light

To determine whether cyanobacteria respond to light intensity by changing its PSI oligomeric profile, TS-821 was tested by contrasting culture in low light (LL) intensity with high cell density to culture in high light (HL) intensity with low cell density. Under HL condition, TS-821 showed different absorption spectrum from LL condition (Figure 6-8A). Under LL, TS-821 has less absorption around 500 nm (carotenoids), but more absorption around 600 nm (phycobilisome) and around 720 nm (far-red) (Figure 6-8C). Detailed analysis of the cytosol absorption spectra showed the blue shift of absorption peak, which indicates larger phycobilisome under LL (Figure 6-8B). Comparison of the spectra of solubilized membrane (Figure 6-8D) revealed that difference around 600 nm in whole cell absorption comes from the thylakoid membrane, probably due to elevated content of carotenoids in the membrane under HL. Even though the emission peak of PSI did not change for PSI (Figure 6-8E), the excitation spectra of PSI showed less efficiency around 600 nm (Figure 6-8D), which indicates either less phycobilisome association to PSI or more photo-protection under HL.

To explore the physiological role PSI tetramer plays, the multimeric state was investigated under two different growth conditions: low light (LL, 40 μmol/m^2/s) and high light (HL, 800 μmol/m^2/s). The oligomeric profiles under different light intensities were examined by BN-PAGE analysis after thylakoid membrane solubilization with variable β-DDM concentrations (Figure 6-9A). Under both

Figure 6- 8 Spectra analyses of TS-821 under different light intensities

(A) Normalized whole cell absorption spectra of TS-821.

(B) Normalized absorption spectra of cytosol from TS-821.

(C) Absorption difference spectrum of TS-821 under different light intensities. Spectra in (A) were used for the calculation.

(D) Absorption spectra of solubilized thylakoid membrane from TS-821 under different light intensities. The embedded pictures show the color of solubilized membrane. Red box and black box circle the solubilized membrane isolated from HL and LL conditions respectively.

(E) 77K PSI excitation spectra of TS-821 cells under different light intensities. Spectra were recorded at emission wavelength around 725 nm.

(F) 77 K emission spectra of TS-821 whole cells. Excitation wavelength was around 430 nm.

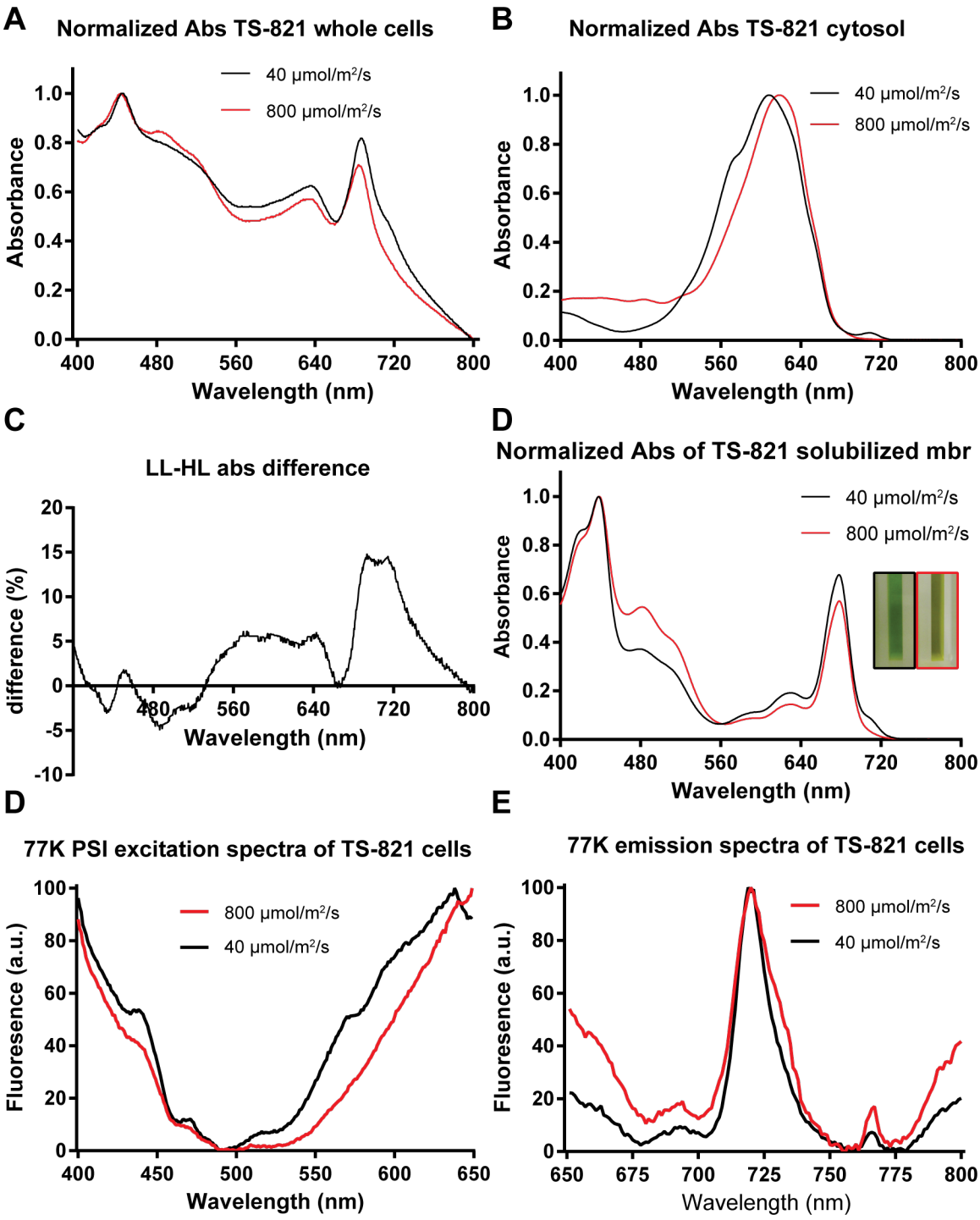

Figure 6-8 continued

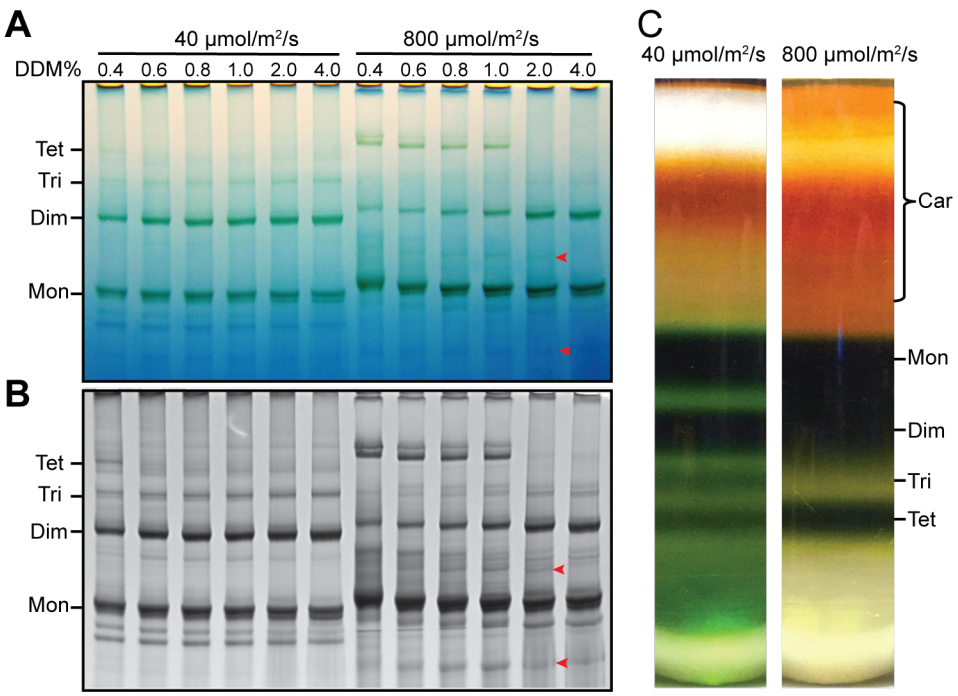

Figure 6- 9 Comparison of TS-821 PSI oligomeric profiles under different light intensities.

(A) The unstained BN-PAGE analysis of TS-821 thylakoid membranes solubilized with the indicated % of DDM. The left lanes are the low light (40 µmol/m^2/s) and the right lanes are the high light (800 µmol/m^2/s).

(B) Same BN-PAGE gel as (A) following staining with CBB to enhance clarity.

(C) Sucrose density gradient centrifugation of solubilized TS-821 thylakoid membrane isolated from cells grown under different light conditions.

Main bands corresponding to carotenoids (Car), PSI monomer (Mon), Dimer (Dim), Trimer (Tri), and Tetramer (Tet) are labeled. Additional changed species of membrane proteins are labeled by arrows.

conditions, PSI monomer, dimer, and tetramer are dominant oligomeric states compared with a less abundant trimeric PSI species. However, under LL, the amount of PSI trimer is higher than that under HL (Figure 6-9A). This is more easily observed after staining with CBB (Coomassie Brilliant Blue) (Figure 6-9B). In contrast, cells grown under high light contain a much higher amount of the PSI tetramer (Figure 6-9 A and B). This difference can also be distinguished without BN-PAGE since the increase in the amount of chlorophyll migrating as a tetramer is easily observed using sucrose density gradient centrifugation (Figure 6-9C). This figure also shows an obvious increase of the trimer under low light conditions as is clear from the new chlorophyll containing band.

At the same time, it seems that under the same detergent concentration, dimeric PSI is less abundant under HL compared to those under LL. PSI tetramer can dissociate into dimers and monomers upon detergent treatment (*21*). Another noticeable difference between LL and HL is that PSI tetramer is more stable under HL, judging by its resistance to higher detergent (β-DDM) concentration (Figure 6-9A). Besides more PSI tetramer and less trimer under HL, more carotenoids can also be found under HL condition in the sucrose density gradient after centrifugation fractioning (Figure 6-9C).

In addition to obvious changes in PSI tetramer, other additional membrane proteins also showed different expression pattern under different light intensities (Figure 6-9 A and B, arrows pointing at examples). A thorough investigation on those proteins is necessary to elucidate how TS-821 coordinate membrane protein complexes under HL.

High Light Also Promotes PSI Tetramer Formation in PCC 7428 and 7414

To investigate if the effect of high light on PSI tetramer formation is universal to other cyanobacteria that may have tetrameric PSI, similar study has been done with PCC 7428, PCC 7414 and PCC 7203. At the same time, to see if high light promotes PSI tetramer formation in *Synechocystis* SCHLLK-12, this mutant was treated with similar high light stress.

Similar to what was shown for TS-821, PCC 7428 showed more abundant and stable PSI tetramer under HL (Figure 6-10). At the same time, the PSI dimer seem to be more abundant under LL (Figure 6-10), similar to what has been described in TS-821. In addition to PSI oligomers, a protein with size between PSI monomer and dimer showed higher abundance under HL (arrows in Figure 6-10). This protein can ATP synthase or NDH-1L according to earlier proteomic studies in heterocyst (*49*). Increase in either protein complex indicates potential increase in cyclic electron transfer around PSI complex.

In the case of PCC 7414, it showed a clearly more stable PSI tetramer under HL (Figure 6-11). Under HL, the abundance of PSI dimer and trimer seem to be lowered at the same time (Figure 6-11), similar to what were observed in both TS-821 and PCC 7428. Meanwhile, the additional more abundant protein under HL with size between PSI monomer and dimer is also observed in PCC 7414, indicating a universal strategy of adapting to high light intensity, probably involving PSI tetramer as well as ATP synthase and/or NDH-1 complex. For PCC 7414, the PSI profile difference is not as dramatic as PCC 7428 and TS-821, probably due to its intrinsic mutual shading among filaments and cell mats.

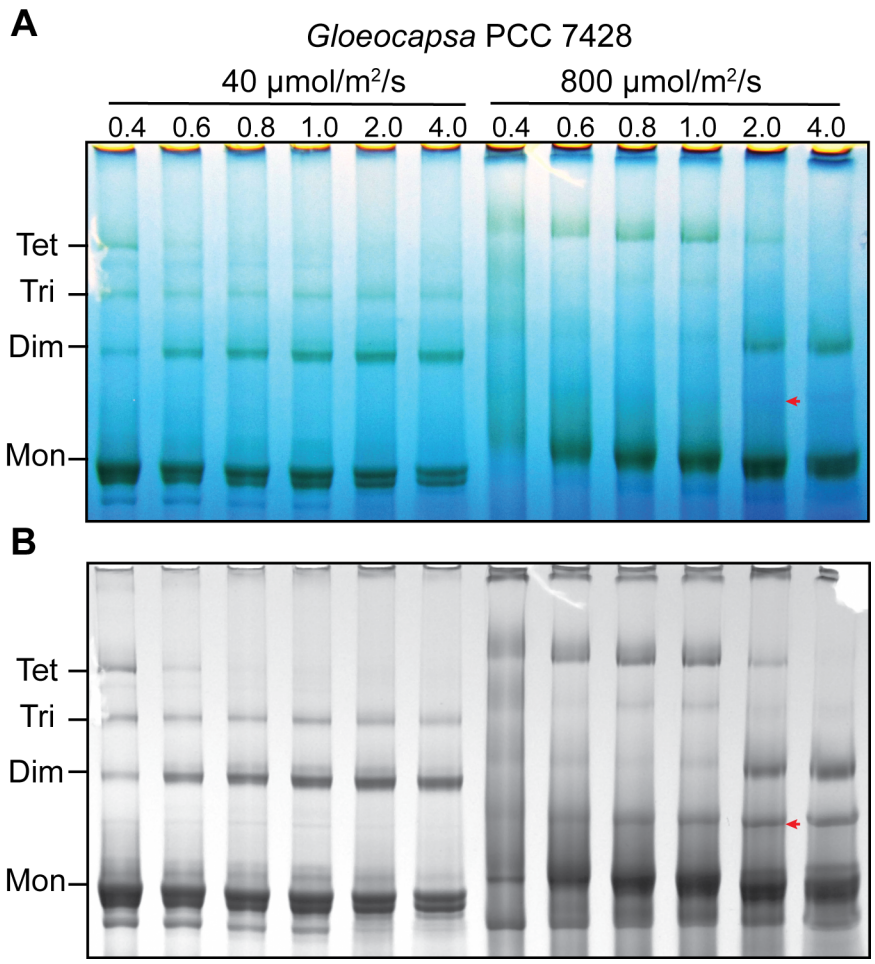

Figure 6- 10 Comparison of PCC 7428 PSI oligomeric profiles under different light intensities.

(A) The unstained BN-PAGE analysis of PCC 7428 thylakoid membranes solubilized with the indicated % of DDM. The left lanes are the low light (40 µmol/m^2/s) and the right lanes are the high light (800 µmol/m^2/s).

(B) Same BN-PAGE gel as (A) following staining with CBB to enhance clarity.

Thylakoid membranes with 0.2 mg/mL Chl were solubilized in different concentrations of DDM (w/v, %), labeled on top of each lane. ~ 1.6 µg Chl were loaded for each condition. Main bands corresponding to PSI monomer (Mon), Dimer (Dim), Trimer (Tri), and Tetramer (Tet) are labeled. Additional changed species of membrane proteins are labeled by arrows.

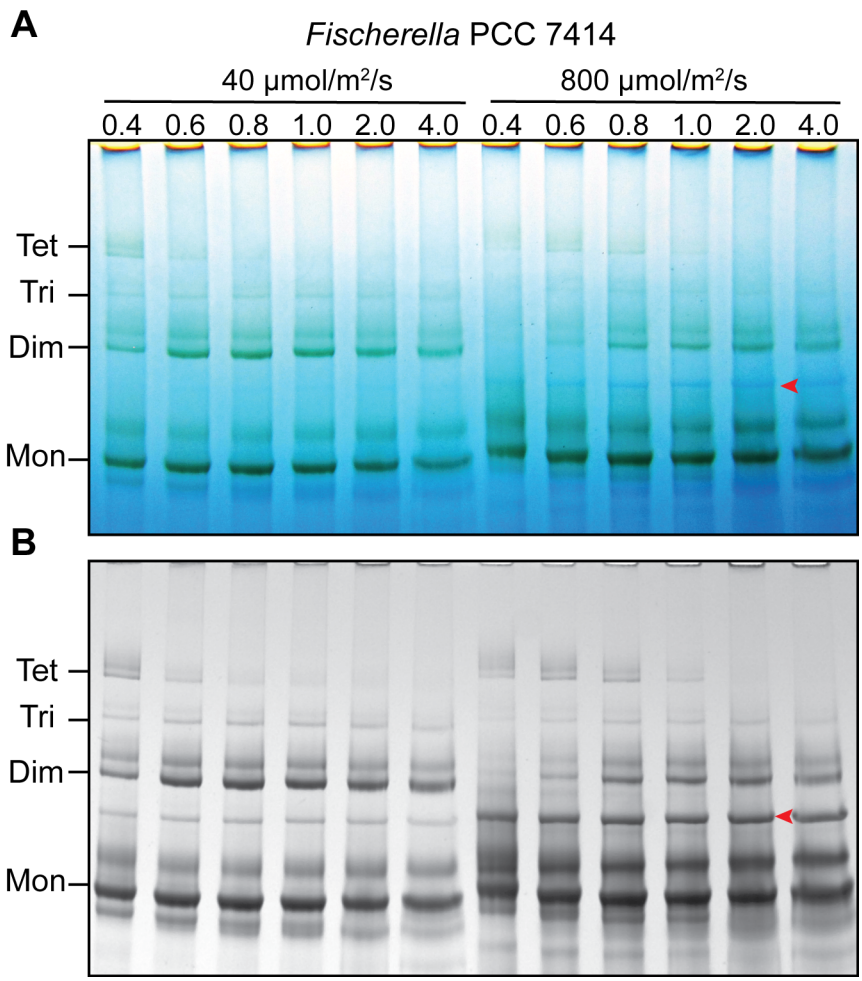

Figure 6- 11 Comparison of PC 7414 PSI oligomeric profiles under different light intensities.

(A) The unstained BN-PAGE analysis of PCC 7414 thylakoid membranes solubilized with the indicated % of DDM. The left lanes are the low light (40 µmol/m^2/s) and the right lanes are the high light (800 µmol/m^2/s).

(B) Same BN-PAGE gel as (A) following staining with CBB to enhance clarity.

Thylakoid membranes with 0.2 mg/mL Chl were solubilized in different concentrations of DDM (w/v, %), labeled on top of each lane. ~ 1.6 µg Chl were loaded for each condition. Main bands corresponding to PSI monomer (Mon), Dimer (Dim), Trimer (Tri), and Tetramer (Tet) are labeled. Additional changed species of membrane proteins are labeled by arrows.

With strains having both PSI tetramer and trimer (PCC 7428, PCC 7414 and TS-821), HL promotes the formation of PSI tetramer. It is interesting to see how strains mainly having PSI monomer and dimer respond to HL. Here PCC 7203 was studied as an example. As shown in Figure 6-12, under both LL and HL, no PSI tetramer was detected. Interestingly, the protein with size between PSI monomer and dimer showed higher abundance under HL (Figure 6-12), similar to what have been observed in other strains studied here. This further indicates a universal mechanism involving this protein in response to HL. In addition, some species of potential PSI oligomers are present under LL but not present (or not as abundant) under HL (triple arrows in Figure 6-12). Those protein bands include PSI dimer, which also showed higher abundance under LL in PCC 7428, PCC 7414 and TS-821.

In the case of SCHLLK-12, PSI tetramer was not observed even under HL condition, even though similar non-photosystem was found with higher abundance under HL (Figure 6-13). This indicates that PSI tetramer formation needs more than the structural change in PsaL. Some other protein as components or chaperon may be needed for PSI tetramer formation.

Fine Tuning of PSI Oligomer Profile in TS-821 in Response Under Different Light Intensities

The experiments for PSI oligomer profile in response to light intensities was done with two extreme conditions: dense culture under low fluorescent light versus dilute culture under high intensity LED light. One can speculate the reason for the observed differences: the light source or the cell density stress.

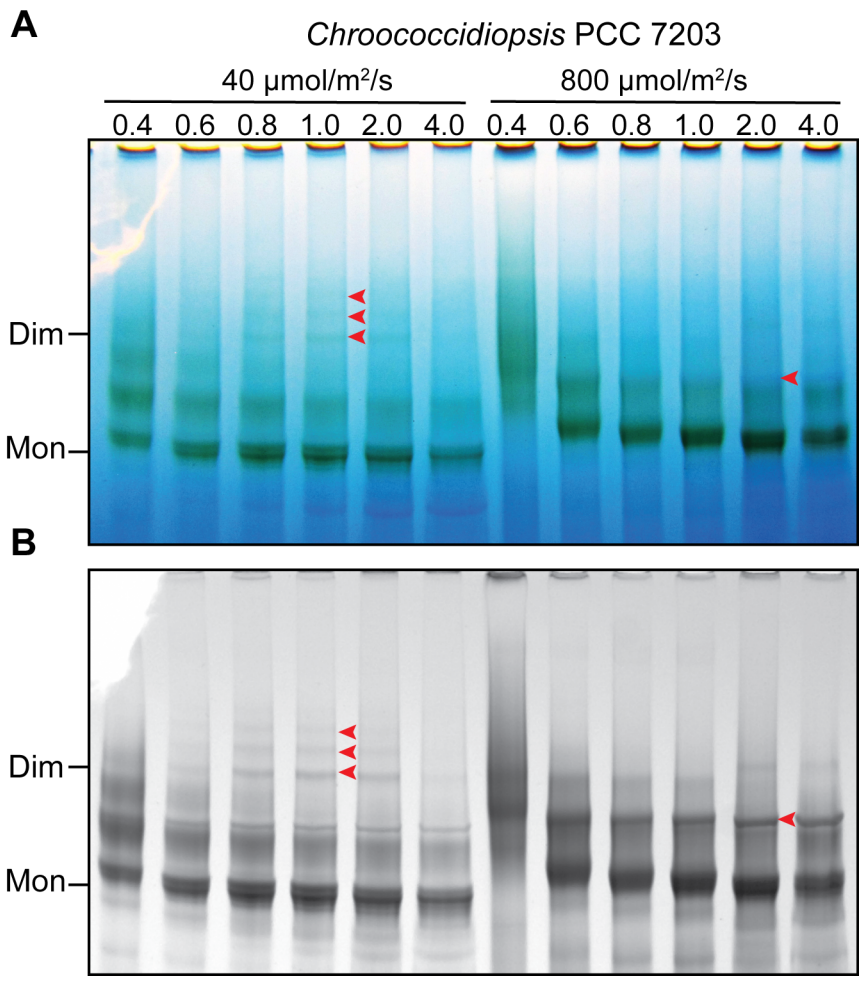

Figure 6- 12 Comparison of PCC 7203 PSI oligomeric profiles under different light intensities.

(A) The unstained BN-PAGE analysis of PCC 7203 thylakoid membranes solubilized with the indicated % of DDM. The left lanes are the low light (40 µmol/m^2/s) and the right lanes are the high light (800 µmol/m^2/s).

(B) Same BN-PAGE gel as (A) following staining with CBB to enhance clarity.

Thylakoid membranes with 0.2 mg/mL Chl were solubilized in different concentrations of DDM (w/v, %), labeled on top of each lane. ~ 1.6 µg Chl were loaded for each condition. Main bands corresponding to PSI monomer (Mon) and Dimer (Dim) are labeled. Additional changed species of membrane proteins are labeled by arrows.

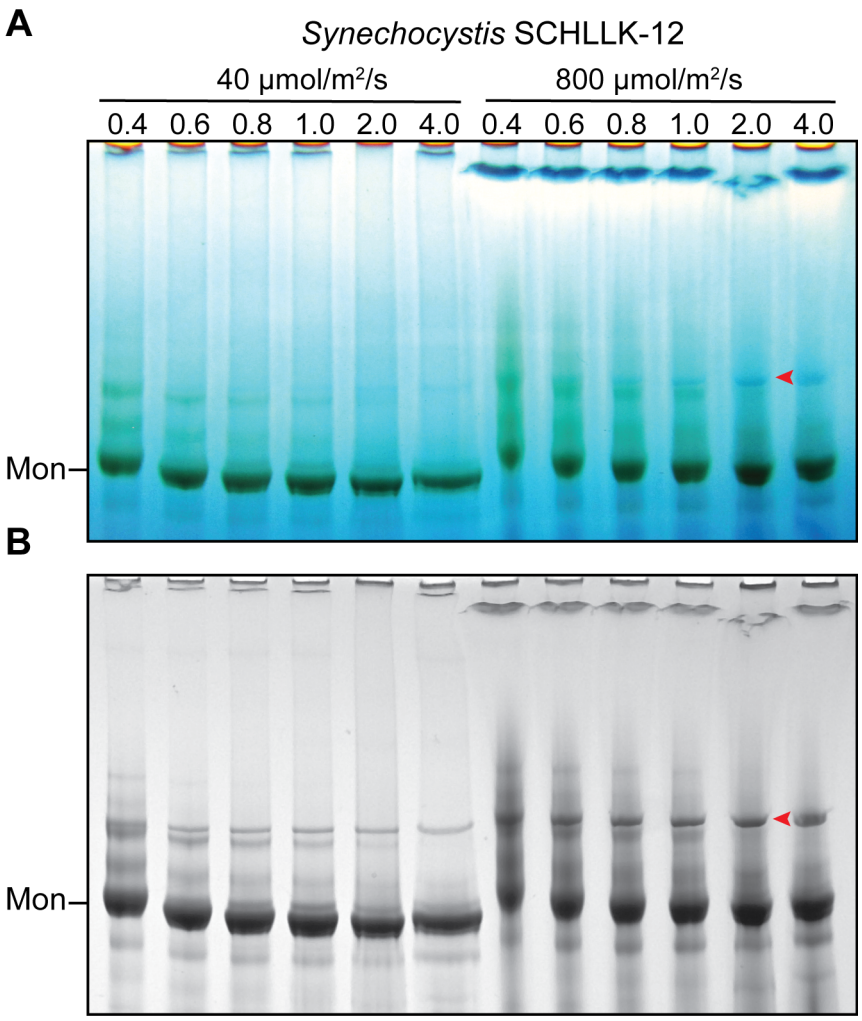

Figure 6- 13 Comparison of SCHLLK-12 PSI oligomeric profiles under different light intensities.

(A) The unstained BN-PAGE analysis of SCHLLK-12 thylakoid membranes solubilized with the indicated % of DDM. The left lanes are the low light (40 µmol/m^2/s) and the right lanes are the high light (800 µmol/m^2/s).

(B) Same BN-PAGE gel as (A) following staining with CBB to enhance clarity.

Thylakoid membranes with 0.2 mg/mL Chl were solubilized in different concentrations of DDM (w/v, %), labeled on top of each lane. ~ 1.6 µg Chl were loaded for each condition. Main bands corresponding to PSI monomer (Mon) are labeled. Additional changed species of membrane proteins are labeled by arrows.

To confirm light intensity is the main environmental factor that tunes the PSI oligomeric state, several different light intensities with the same LED source were tested using TS-821

As shown in Figure 6-14A, the PSI is more stable under HL and less trimer was observed under HL, similar to what have been observed in Figure 6-9. After two-day culture at 50 μmol/m^2/s in PBR, the relative abundance of PSI trimer is not as high as that in dense culture at 40 μmol/m^2/s (Figure 6-9). This indicates the PSI trimer accumulation is favored under extreme low light conditions. As expected, the stability and/or abundance of PSI tetramer increases gradually as the light intensity increases stepwise (Figure 6-14). These results indicating PSI tetramer is favored under high light and cyanobacteria having both PSI tetramer and trimer may have a mechanism fine tuning PSI oligomers under different light intensities.

PSI Tetramer under High Light and Carotenoids between PSI Dimers

When PSI tetramer under HL was separated in a sucrose density gradient, its color is visually distinguishable from the PSI tetramer under LL (Figure 6-9C). To investigate this spectral difference of PSI tetramer under difference light intensities, absorption spectra and 77K emission spectra were obtained (Figure 6-15). As shown in Figure 6-15 A and C, compared with PSI tetramer under LL, PSI tetramer under HL has additional absorption in the range from 470 nm to 570 nm, which corresponds to potential additional carotenoids in PSI tetramer under HL. At the same time, PSI tetramer under LL has similar additional absorption compared with PSI trimer under LL (Figure 6-15 B and C). Even though PSI

Figure 6- 14 Comparison of TS-821 PSI oligomeric profiles under different light intensities with same LED light source

(A) BN-PAGE of solubilized thylakoid membrane from TS-821 cultured two days under light intensities 50 μmol/m^2/s and 800 μmol/m^2/s.
(B) BN-PAGE of solubilized thylakoid membrane from TS-821 cultured two days under light intensities 100 μmol/m^2/s and 200 μmol/m^2/s.
(C) BN-PAGE of solubilized thylakoid membrane from TS-821 cultured two days under light intensities 400 μmol/m^2/s and 800 μmol/m^2/s
Thylakoid membranes with 0.2 mg/mL Chl were solubilized in different concentrations of DDM (w/v, %), labeled on top of each lane. ~ 1.6 μg Chl were loaded for each condition. Main bands corresponding to PSI monomer (Mon) , dimer (Dim), trimer (Tri), and tetramer (Tet) are labeled.

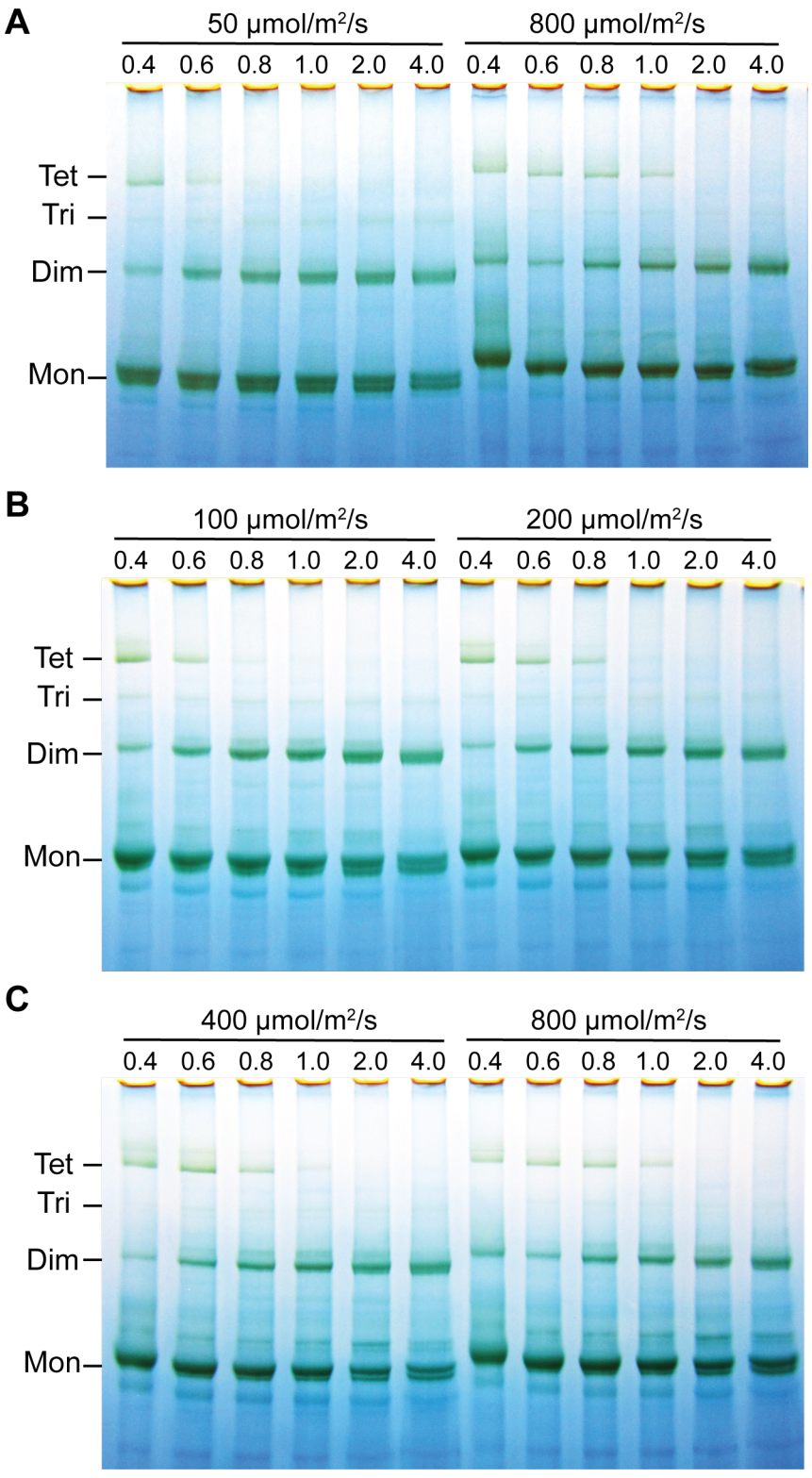

Figure 6-14 continued

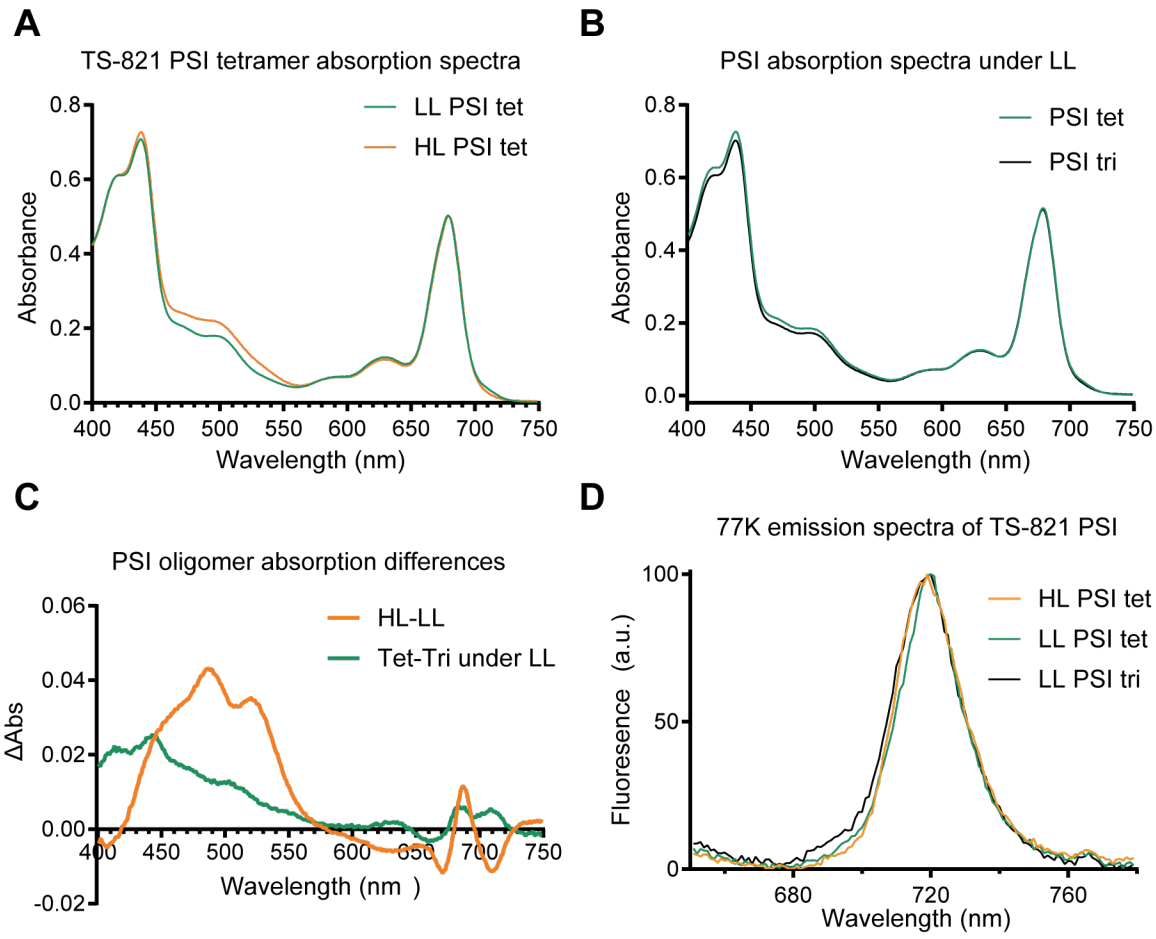

Figure 6- 15 Spectral changes of TS-821 PSI tetramer under high light

(A) Absorption spectra of TS-821 PSI tetramers (tet) under HL and LL.

(B) Absorption spectra of TS-821 PSI tetramer and trimer (tri) under LL.

(C) Absorption spectral differences between TS-821 PSI oligomers. Differences are calculated from (A) and (B). HL-LL denotes the absorption differences between PSI tetramer under HL and PSI tetramer under LL.

(D) 77K emission spectra of TS-821 PSI oligomers.

Samples are harvested from sucrose density gradient (Figure 6-9C).

tetramer showed differences in absorption under different light intensities, the emission spectra of PSI tetramer under both conditions look identical to that of PSI trimer under LL (Figure 6-15D).

PSI tetramer is binding more carotenoids compared with PSI trimer, which may due to special geometry of PSI tetramer. Our structural study showed that PSI tetramer has a central cavity that is not resolved in Cryo-EM study (Figure 4-2), which may provide the additional binding space for carotenoids in PSI tetramer. To test this speculation, isolated PSI tetramer was treated with 5% DDM and loaded on a sucrose density gradient for PSI oligomer separation. Interestingly, after centrifugation, in addition to expected PSI oligomer green bands, a distinct orange band on top of the gradient was observed for the DDM treated sample (Figure 6-16A). This additional orange band was not observed in untreated sample (Figure 6-16A), which indicates the orange species is a result of PSI tetramer dissociation into PSI dimers. The spectral analysis of the orange band showed absorption peaks around 440 nm, 482 nm, and 515 nm with additional minor peak around 675 nm, corresponding free chlorophyll (Figure 6-16B). This indicates that in the inter-dimer space of a PSI tetramer, there are carotenoids and probably chlorophyll as well. The pigment analysis results from HPLC (DHI, Demark) verified this speculation. New PSI-binding carotenoids were identified in addition to known β-carotene and chlorophyll. Those novel PSI-binding carotenoids include myxoxanthophyll, canthaxanthan and echinenone. At the same time, the spectral analysis of PSI oligomers showed that PSI tetramer, compared with PSI dimer and trimer, has additional absorption corresponding

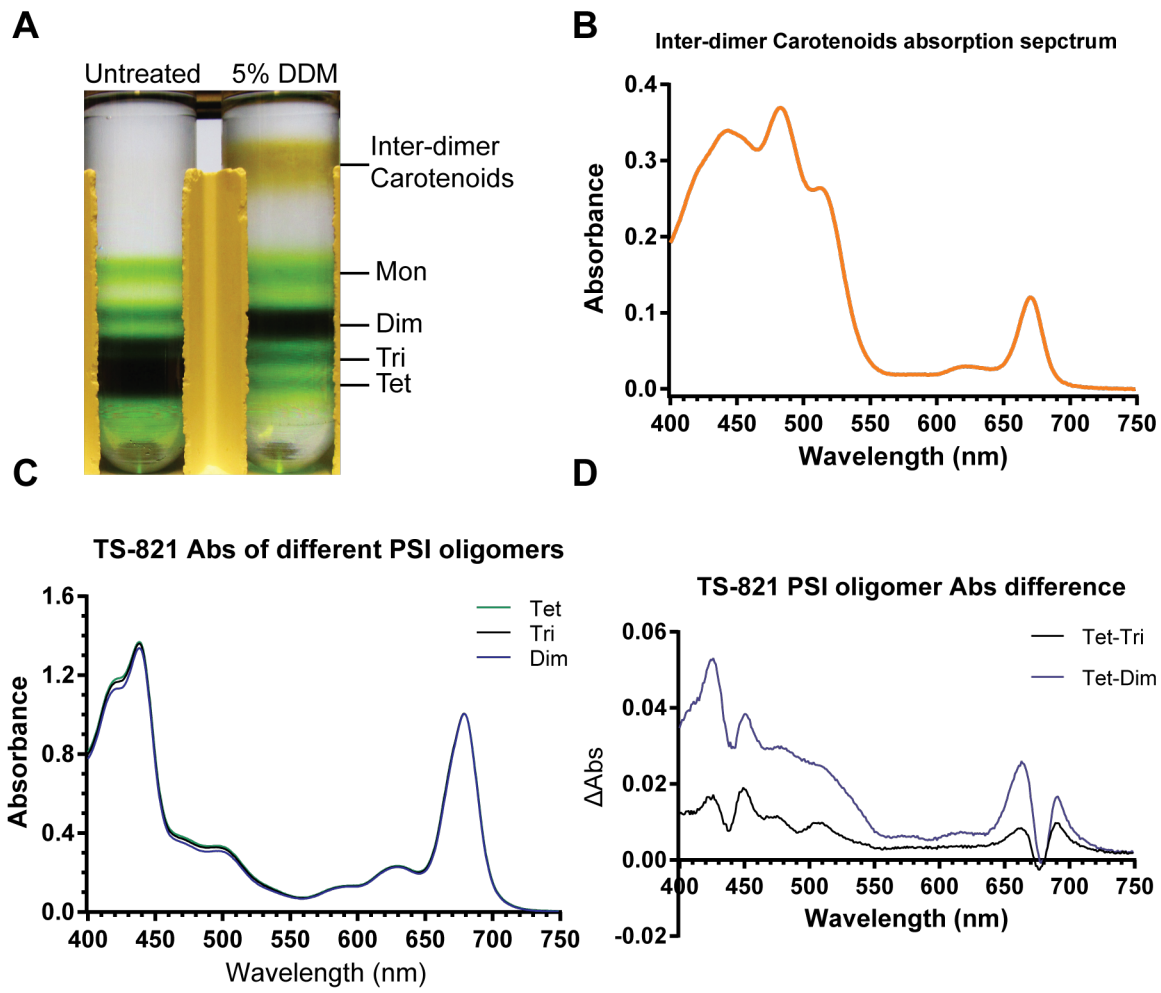

Figure 6- 16 Spectral analysis of TS-821 PSI oligomers and inter-dimer carotenoids

(A) Sucrose density gradient centrifugation of TS-821 PSI tetramers treated with 5% DDM. Untreated PSI tetramer was used as a control. Carotenoids sample and PSI oligomers used for spectral analysis were labeled. Monomer, dimer, trimer, and tetramer are denoted as mon, dim, tri, and tet respectively.

(B) Absorption spectra of TS-821 PSI inter-dimer carotenoids.

(C) Absorption spectra of TS-821 PSI oligomers.

(D) Absorption spectral differences between TS-821 PSI oligomers. Differences are calculated from (C).

to the pigments released (Figure 6-16 C and D). Similar spectral analysis of PSI oligomers in PCC 7414 also revealed that PSI tetramer binds more carotenoids, compared with PSI dimer and trimer (Figure 6-17).

6.7 Speculation on PSI Oligomer Evolution and Plastid Origin from Cyanobacteria

Tetrameric PSI May be a Primitive Adaptation to High Light Intensity

The fact that the abundance and stability of PSI tetramer are increased with elevated light intensities indicates that PSI tetramer is preferred under HL. In other words, PSI tetramer, compared with PSI trimer is more adapted to HL. This speculation is further supported by the fact PSI tetramer under HL contains more carotenoids than PSI tetramer under LL (Figure 6-15 A and C). Moreover, PSI tetramer, compared with other oligomeric states, binds more carotenoids under the same light intensities (Figure 6-16 and Figure 6-17). Carotenoids are known for photo-protection. All these results suggest that tetrameric PSI may be a primitive adaptation to high light intensity, in contrast to PSI trimer, which is enriched under LL.

PSI Monomerization in Plants and Green Algae May be a Result of PsaL Evolution Without Involving PsaH

PSI in plants and green algae are monomeric. At the same time, PsaH, absent in cyanobacteria, is binding to PsaL in eukaryotic PSI monomer. This leads to the speculation on PSI monomerization is due to the introduction of PsaH (*45, 46*). It was a reasonable speculation when the PSI trimer was the only

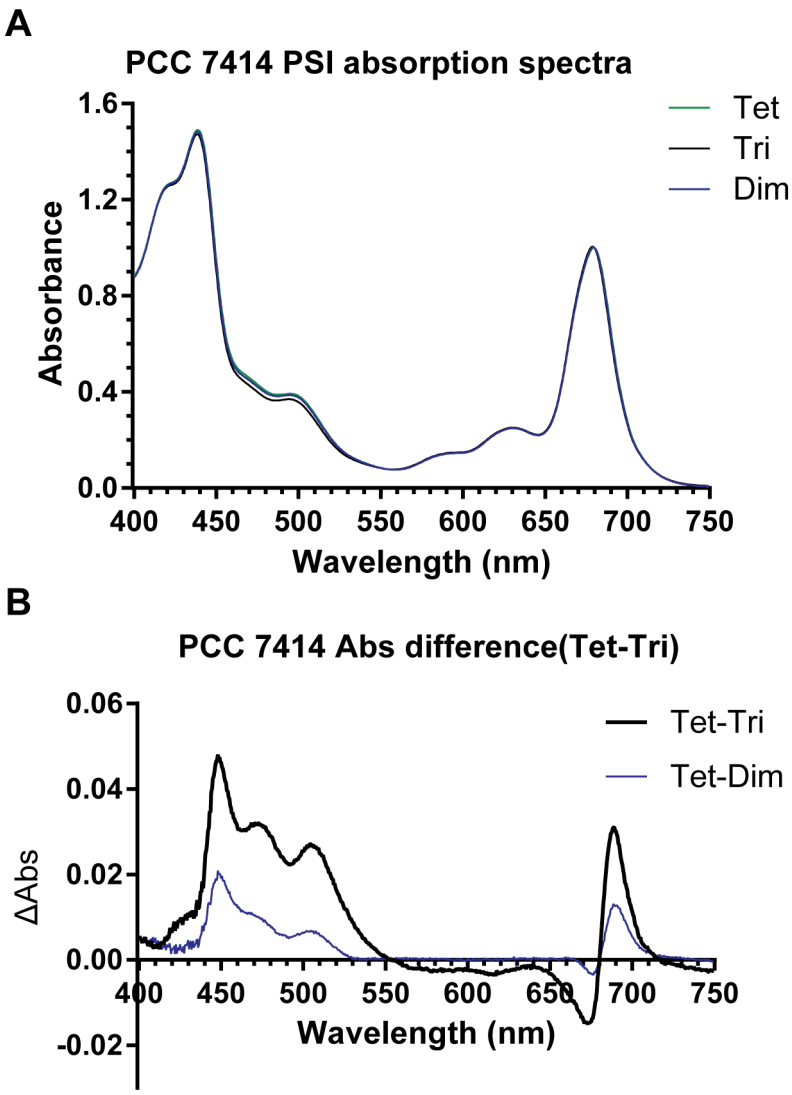

Figure 6- 17 Absorption spectra of PSI oligomers from PCC 7414

(A) Absorption spectra of PCC 7414 PSI oligomers. Dimer, trimer, and tetramer are denoted as dim, tri, and tet respectively

(B) Absorption spectral differences between PCC 7414 PSI oligomers. Differences are calculated from (A).

higher-order PSI oligomer observed in cyanobacteria. The discovery of PSI tetramer should cast doubt on this thought. In our study, we have presented that PSI tetramer can easily dissociate into PSI dimers and monomers. Also there are many species, such as PCC 7203 and UTEX B 381, having mostly or exclusively PSI monomers. This indicates that PSI monomerization does not need PsaH, at least in cyanobacteria. Meanwhile, our transgenic *Synechocystis* showed exclusive monomeric PSI after the replacement of PsaL in the trimeric PSI (Figure 4-12 and Figure 4-14). Altogether, those evidence suggest that PSI monomerization most likely was a result of PsaL structural changes, without the participation of PsaH. The introduction of PsaH in eukaryotic PSI may be an evolutionary step preparing for lateral antenna binding and state transition, since the lack of PsaH leads to the loss of state transition (*121*).

Specific PsaL May Be Needed for the Introduction of PsaH

It was speculated in the initial study of TS-821 PSI tetramer that the loop insertion between second and third tans-membrane helices in PsaL binds to PsaH. This speculation was later supported by the recent refinement of plant PSI monomer structure (*41*). In this structure, the loop insertion in PsaL binds to the N-terminus of PsaH, which suggests that specific PsaL with proper loop insertion between second and third trans-membrane helices is necessary for binding PsaH in PSI. To test this hypothesis, PsaH expressing vectors have been transferred to *Synechocystis* with different PsaL; however, the results is yet to be tested and verified.

CHAPTER SEVEN

Genome of *Chroococcidiopsis* sp. TS-821 and

Proteomic Analyses of PSI Tetramer Versus PSI Trimer

7.1 Disclosure

This Chapter describes the preliminary results of TS-821 genome sequencing and annotation. My primary contribution was providing purified genomic DNA and genome de novo assembly and annotation using publicly available programs and online servers. This proteomic analyses were done by Dr. Julian Whitelegge at UCLA, with PSI samples provided by me. This genome data has not been deposited in any database so far. The results will be combined with content in Chapter five and Chapter six for publication.

7.2 Abstract

To understand why TS-821 has both PSI tetramer and PSI trimer, a careful component analysis is needed to see the difference. Earlier speculation was that TS-821 has two copies of PsaL. With the TS-821 genome sequenced, this hypothesis was easily tested by combining careful proteomic analysis of PSI tetramer and trimer. This comparison may also help identify the key factor in distinguishing PSI tetramer from PSI trimer in TS-821. Similar proteomic analysis was done for PCC 7414 and PCC 7203. Preliminary results are described in this chapter.

7.3 Genome Genome Assembly and Annotation

Genome sequencing of TS-821 in this study generated 3,2161,300 reads with read length 250. With estimated genome size no bigger than 6 Mbp, the coverage of the sequencing is no less than 1340. After de novo assembly, all three programs used generate a genome size in the range of 5.2~5.3 Mb, with GC content around 43.4% (Table 7-1). Among the three de novo assembly

programs, SPAdes generated the longest contig with lowest L50 value, even though it also generated most contigs (Table 7-1). After annotation, SPAdes also generates most CDS (Table 7-1), so the data generated by SPAdes was used for proteomic analysis.

Table 7- 1 Statistics of TS-821 genome de novo assembly

Parameters	SPAdes	A5-miseq	ABySS
Length (bp)	5,256,999	5,232,644	5,259,884
GC%	43.43	43.38	43.45
No. of Contigs	117	60	**59**
Longest Contig (bp)	**1,686,017**	449,707	1,150,472
L50	**3**	8	6
N50 (bp)	**569,273**	267,736	288,245
No. of CDS	**5,103**	5,059	5,064

7.4 PsaL in PSI Tetramer and Trimer Are the Same

PSI oligomer profile changes have been observed in TS-821, PCC 7414, and PCC 7428. To understand whether different PsaL are involved in the shifting of PSI oligomer in cyanobacteria in response to different light intensities, the proteomic comparison between PSI tetramer and PSI trimer was done for all three strains. This analysis also can answer whether PSI tetramer and PSI trimer

have the same PsaL. PSI trimer and PSI tetramer were sliced out from BN-PAGE gel after isolation from sucrose density gradient.

In PCC 7414, two copies of *psaL* coding different PsaL products have been observed. One *psaL* is located in *psaF/J/L* structure, while the other is located adjacent to *psaI*, which was speculated to be expressed in response to far-red light (*34*). The proteomic analysis of PCC 7414 PSI trimer and tetramer revealed that the same PsaL, encoded by the *psaL* located is present in both PSI oligomers. This indicates that additional factors are responsible for determining PSI tetramer or PSI trimer formation. One of the factors can be the carotenoids content in thylakoid membrane.

In the case of PCC 7428 and TS-821, only one copy of *psaL* gene is present in both strains. The proteomic analysis of the PSI trimers and tetramers verified that the single copy of PsaL is present in both forms of PSI, further suggesting that the PSI oligomer shifting in response to different light intensities is not a result of different *psaL* transcription.

In addition to the confirmation of one PsaL for two PSI oligomers, another interesting observation in the proteomic results is that multiple PSII subunits, including PsbO, PsbQ, D2, and CP47, were found in the PCC 7414 PSI trimer band as well. It is possible that this observation comes from contamination of PSI trimer in PCC 7414 PSI trimer, since other components of membrane protein complexes, such as ATP synthase, were observed at the same time. Nevertheless, it is also possible that PSII-Pcb complex, as described previously (*130*), is co-purified with PSI trimer/tetramer, especially in the case of PCC 7414.

Our SDS-PAGE analysis for PSI identification also showed that PSI trimer in PCC 7414 has additional subunits to classic PSI subunits (Figure 5-4). Similar observations in SDS-PAGE analysis were also found in other cyanobacteria such as PCC 6912 and PCC 9212. The identification of a CP43' (CP43-like, IsiA-like) protein (Uniprot: G6FR82) in PCC 7414 trimer supports this speculation. At the same time, a protein containing both CP43-like (IsiA-like) domain and PsaL domain (Uniprot: G6FR83) is identified in PCC 7414 PSI trimer band. This protein can potentially bind both PSI and PSII. A recent report has shown isiA-PsaL protein binds to PSI in Leptolyngbya sp. JSC-1 (*56*). A protein complex with a PSI monomer and a PSII dimer bridged by CP43'-PsaL may exist and migrate similar to PSI trimer. Yet this PSII-(CP43'-PsaL)-PSI supercomplex can be a pure speculation if no further experiments can support this.

Moreover, allophycocyanin has been identified in PSI tetramer from PCC 7428 and TS-821, in agreement with earlier discovery of PSI-PBS supercomplex (*20*).

7.5 Discussion

The sequencing of TS-821 genome provided foundation for PSI tetramer proteomic analysis. It was revealed that TS-821 is closely related to PCC 7428. They both showed single copy of the *psaL* gene, which encodes the PsaL subunit found in both tetrameric PSI and trimeric PSI. Further analysis is needed to elucidate how the PSI tetramer is assembled. Further study can involve filling the gaps between contigs to get the full map of TS-821 genome, as well as gene expression profile changes in TS-821 in response to high light.

CHAPTER EIGHT

Conclusions and Future Directions

8.1 Conclusions

Tetrameric PSI Exists in TS-821

Evidence has shown that tetrameric PSI exists in TS-821.First, the BN-PAGE of solubilized thylakoid membrane showed a green band bigger than the PSI trimer in molecular weight. At the same time, other two major bands have the estimated molecular weights close to half and a quarter of the biggest green protein complex. SDS-PAGE of these green bands identified all as PSI, supporting the idea that they are PSI monomer, dimer and tetramer. Second, potential PSI tetramers, isolated from sucrose density gradient after centrifugation, were imaged using electron microscopy. The tetrameric structure was clearly revealed. Meanwhile, PSI tetramer in TS-821 membrane was also observed by EM analysis. Further structural study using Cryo-EM revealed more structural details about PSI tetramer. Altogether, our study has shown the presence of tetrameric PSI in TS-821.

PSI tetramer, compared with classic PSI trimer from *T. elongatus*, has many unique characteristics. PSI tetramer can be easily dissociated into dimers and monomers when treated with mild detergent (DDM). In contrast, PSI trimer from *T. elongatus* is not disturbed by DDM treatment. PSI trimer is known for its 77K far-red fluorescence emission spectra difference from PSI monomer, but this difference is not present in PSI tetramer. The 77K emission spectra of PSI monomer, dimer, trimer, and tetramer from TS-821 are nearly identical. The association of PSI monomers into tetramer may not involve any far-red

fluorescent Chl. Furthermore, low cooperativity for P700 excitation was observed for PSI tetramer as well.

PsaL Diversity is a Key Reason for the Diversity of PSI Oligomers.

The crystal structure of trimeric PSI from *T. elongatus* showed the central position of PsaL subunits. Previous studies have shown the psaL knockout mutants only have monomeric PSI indicating the central role of PsaL as well. Primary structural differences were observed between the PsaL in tetrameric PSI and trimeric PSI. The structural study showed that the C-terminus of PsaL from *T. elongatus* does not fit in the electron density map of TS-821 PSI tetramer, indicating the necessity of structural change in PsaL for PSI tetramer formation. To test if different PsaL result in different PSI oligomer, the transgenic lines of *Synechocystis* expressing different PsaL showed that PsaL from both TS-821 and *Arabidopsis* do not favor the formation of PSI trimer. These results support that PsaL is the key factor for PSI oligomeric state.

Besides PsaL, other factors are also needed for PSI tetramer formation. The fact that no significant PSI tetramer was observed in *Synechocystis* expressing TS-821 PsaL indicates that PSI tetramer formation needs more than the structural changes in PsaL. Some of the heterocyst-forming cyanobacteria have both PSI trimer and PSI tetramer. Proteomic analysis comparing PsaL subunit in different PSI oligomers identified the same PsaL for both PSI trimer and PSI tetramer. This indicates that one PsaL can be involved in different PSI oligomers and other factors may be involved in determining the PSI oligomeric states. For PSI tetramer, high light is an environmental factor that promotes its

formation. What biochemical factors determine the PSI tetramer formation are yet to be studied.

PSI in Most (If Not All) Heterocyst-forming Cyanobacteria and Their Close Relatives Form Tetramer or Dimer

Using BN-PAGE and SDS-PAGE analyses, thirty-nine heterocyst-forming cyanobacteria and their close relatives have been studied for their PSI oligomeric states. PSI tetramer have been observed in thirty strains. Six stains have dimeric PSI and three strains have exclusive monomeric PSI. Even though special cases have been observed, most heterocyst-forming cyanobacteria and their close relatives have tetrameric PSI. Since PSI tetramer can be easily dissociated into dimers, PSI tetramer and PSI dimer can be classified into similar oligomeric state. PSI dimer may be an assembly intermediate from monomeric to tetrameric PSI, with PSI tetramer binding more carotenoids between two dimers.

PsaL classification correlates well with PSI oligomeric state. PsaL in tetrameric PSI are classified in one clade, consistent with the heterocyst-forming cyanobacteria classification. This PsaL is always encoded by the *psaL* gene located in *psaF/J/*L structure, often followed by *gmk* gene in opposite direction as well. The physiological implication of this genomic structure and how this genomic structure determines PSI tetramer formation are not clear. Some heterocyst-forming cyanobacteria and their close relative have a second copy of PsaL, which is classified in a clade potentially related to far-red light response. This clade PsaL may be found to be monomeric considering initial report on this topic showed monomerization of PSI involving the far-red light PsaL (*34*). PsaL

classified outside the heterocyst-forming clade mostly are found in PSI trimer, even though special cases are also present, such as PCC 7124.

PSI Tetramer, Compared with PSI Trimer, Is More Adapted to High Light

In three strains, PCC 7428, PCC 7414 and TS-821, the relative abundance of PSI tetramer increases under high light intensity. In contrast, the abundance of PSI trimer is decreased under high light but increased under low light. The spectral analysis showed the additional binding of carotenoids in PSI tetramer under high light. PSI tetramer binds carotenoids in the space between two dimers. The preference of PSI tetramer over PSI trimer under high light indicates PSI tetramer is more suitable for coping with high light stress. The additional carotenoids binding also supports this speculation. The fact that we observed this oligomeric state shift in three different cyanobacteria suggest this adaptive mechanism may be universal to most cyanobacteria that have tetrameric PSI.

PSI Evolved from Trimeric to Tetrameric Oligomer *en route* to Monomeric in Plants and Green Algae

In cyanobacteria, PSI evolved from trimeric to tetrameric. Among all the cyanobacteria that have been studied for their PSI oligomeric states, the most primitive cyanobacteria *Gloeobacter* violaceus PCC 7421 has trimeric PSI (*16*). Most cyanobacteria outside heterocyst-forming cyanobacteria and their close relative clades also have trimeric PSI. This indicates that the PSI tetramer evolved from ancestral trimeric PSI. This process possibly involved the PsaL structural changes. From the major PSI trimer clades to PSI tetramer clade,

intermediate strain was identified, *Chamaesiphon minutus* PCC 6605. PCC 6605 has mainly monomeric PSI with trivial amount of trimeric PSI that can be disrupted into probably dimers and monomers by high concentration detergent treatment. At the same time, among the cyanobacteria that have tetrameric PSI, many of them also have the trimeric form of PSI, which has the same PsaL with PSI tetramer. This indicates the evolution to tetrameric PSI has another intermediate stage where both tetrameric and trimeric PSI are present. Furthermore, exclusive tetrameric PSI without forming a trimer, in equilibrium with PSI dimer and monomer, is also observed some cyanobacteria. Altogether, this suggests that trimeric PSI evolved to tetrameric PSI through a less stable PSI trimer (monomerization), an intermediate of simultaneous PSI trimer and tetramer, then the exclusive tetrameric/dimeric PSI.

PSI monomers in plants and green algae may have evolved from PSI tetramer. The structural similarity between PsaL in tetrameric PSI and that in plant PsaL suggests this evolutionary route. The fact that both TS-821 PsaL and *Arabidopsis* PsaL in *Synechocystis* result in PSI monomer indicates their close property similarity. The transgenic experiments also cast doubt on the theory that PSI monomer in plants evolved from trimeric PSI. The monomerization of PSI does not require PsaH. The observation of PSI in glaucophyte *Cyanophora paradoxa (19)* further supports the hypothesis that PSI monomer in plants and green algae evolved from tetrameric PSI. Among the heterocyst-forming cyanobacteria and their close relative, strains have exclusive monomeric PSI or

mainly monomeric PSI have been observed as well. This further points the close evolutionary relation between tetrameric PSI and monomeric PSI.

High light may be the driving force and selection pressure for PSI oligomer evolution. In cyanobacteria, the high light selection for tetrameric PSI has been supported in this study. Other studies of high light response of *Synechocystis* showed that monomeric PSI fraction increases under high light (*33, 119*). These results indicate the evolution of PSI trimer to tetramer and monomer might have been driven by high light stress. Cyanobacteria with monomeric PSI seemed to cope well with high light stress in multiple strains of cyanobacteria. Our results showed that PCC 7203 keeps monomeric PSI under high light. Whether PSI monomer is better than PSI tetramer in coping with high light has yet to be investigated. Nevertheless, it is not hard to imagine that a high light adapted form of PSI was necessary for early endosymbionts to dominant the surface of the continents. Modern plants mostly compete for the availability of sun light. Plastids' ancestor may have had tetrameric PSI or monomeric PSI that is closely related to PSI tetramer in heterocyst-forming cyanobacteria and their close relatives. Our theory of PSI oligomer evolution is consistent with the hypothesis that plastids shared a common ancestor with heterocyst-forming cyanobacteria and their close relatives.

The high light selection theory can also explain the observation that some cyanobacteria have both PSI tetramer and trimer. The significance of keep the PSI trimer is for survival and competition under low light. Strains that have both

forms of PSI can switch the oligomeric form of PSI in accordance to available light intensity.

8.2 Future Directions

The most puzzling question left about PSI tetramer is why biochemically some cyanobacteria have tetrameric PSI and others have trimeric PSI. Initially, the speculation is that different PsaLs make different PSI oligomers. Strains that have two copies of different *psaL* gene may have two forms of PSI oligomer, i.e. PSI trimer and PSI tetramer (*21, 50*). Careful proteomic comparison of PSI tetramer and PSI trimer ruled out this explanation. The existence of two copies of *psaL* in many cyanobacteria may be related to far-red light response (*34*). We have shown that a change in PsaL can result in PSI monomerization, which indicates that PsaL is key but not the only factor that determines PSI oligomeric state. Physiological studies have pointed out that carotenoids are associated between two PSI dimers in a PSI tetramer, suggesting that those carotenoids may be necessary for PSI tetramer formation. To elucidate the mechanism of PSI tetramer formation, further structure study of PSI tetramer is necessary. We have already shown that TS-821 PSI tetramer can be crystallized, but the crystallization condition needs to be optimized for structure determination by X-ray diffraction. Meanwhile, attempt to obtain higher resolution of PSI tetramer structure using Cryo-EM is hopeful as well. In addition to methods in structural biology, comparative genomics combined with genetic studies of some of the cyanobacteria are also promising way to answer the question of PSI tetramer formation mechanism. For instance, PCC 7203 does not show PSI tetramer in

our experimental conditions; however, PCC 7509, PCC 7428 and TS-821, the close relatives to PCC 7203, all have PSI tetramer. A direct comparison of the proteomes may reveal some of the candidate proteins for PSI tetramer formation. Similarly, a proteomes comparison between *Nodularia* strain PCC 73104 and UTEX B 2093 may also reveal some important factors for PSI tetramer formation and stabilization. With identified candidates, genetic studies on some heterocyst-forming cyanobacteria having tetrameric PSI and available genetic tools, such as PCC 7120, will verify the speculations made from comparative genomics. Currently, biochemical comparison between PSI trimer and PSI tetramer hopefully may provide some preliminary information about how PSI form tetrameric oligomer.

Evolutionarily, we speculate that PSI tetramer evolved from PSI trimer and then became exclusively monomeric in plant and green algae. The introduction of PsaH occurred after the monomerization of PSI. Currently, *Synechocystis* mutants with different PsaL have been introduced the PsaH expressing vector to see their PSI oligomeric states as well as component. This study will test if PsaH binding to PSI needs specific PsaL, as well as whether PsaH and block the PSI trimer formation. With cellular materials ready, the results of this experiment is expected before long. In addition to this experiment, *PsaH* knockout mutants in plant or green algae can be tested for their PSI oligomeric states. Moreover, this study on glaucophytes should be more extensive to understand the evolutionary route of PSI oligomer as well as plastid evolution. The genome of *Cyanophora paradoxa* has been sequenced (*131*), however, the *psaL* gene is missing in the

published sequence even though evidence of PsaL protein has been shown (*19*). More genomic and biochemical studies are necessary to help elucidate the evolutionary story of plastid.

Even though most cyanobacterial PSI oligomers are clearly designated as PSI monomer, dimer, trimer and tetramer, many PSI complexes observed do not fall into these categories. Their sizes shown on BN-PAGE gels are intermediates between those oligomeric states. For instance, PCC 6912 and PCC 9212 have more than eight different PSI complexes, indicating additional components, possibly antenna, binding to PSI. Study has shown that multiple IsiA proteins can bind to PSI (*56*). Whether this diversity of PSI complexes is all due to the presence of IsiA-like proteins has yet be to verified. After the extensive study of PSI oligomeric states in cyanobacteria, one should keep an open mind about PSI structure. It is worth mentioning the special strain PCC 7414, whose PSII complex was observed having the same migration property with PSI trimer. This indicates the possibility of the presence of a PSI-PSII complex, bridged by a Cp43'-PsaL protein. More special PSI complexes are expected in future scientific reports.

Finally, last but not the least, how heterocyst-forming cyanobacteria and their close relatives respond to high light stress has yet to be elucidated. The fine tuning of the PSI oligomer profile under different light intensities was shown in this study. In addition to the increase of PSI tetramer abundance under high light, other membrane proteins have also been changed in their relative quantity. A good candidate can be the NDH-1L, which is involved in cyclic electron transfer.

The property of PSI tetramer, compared with PSI trimer, in cyclic electron transfer can also be explored. Commonly, a transcriptomic study is used for elucidating how cyanobacteria strains changed their expression profile under different environments. The similar study on strains (such as TS-821 and PCC 7428) having tetrameric PSI will help understand how those strains respond to high light stress and what stabilizes or facilitate the formation of PSI tetramer. Relatively, tetrameric PSI is still a topic that has not caught much attention nor been well studied. Many more questions about PSI tetramer are yet to be answered. Some of the hypotheses or theories made in this study may be revoked someday, but that also will bring a better understanding about PSI tetramer and PSI in general.

References

1. M. F. Hohmann-Marriott, R. E. Blankenship, Evolution of photosynthesis. *Annual review of plant biology* **62**, 515-548 (2011).
2. S. Demeter, Govindjee, Thermoluminescence in plants. *Physiologia Plantarum* **75**, 121-130 (1989).
3. A. J. Navarro, M. Hervás, A. M. De la Rosa, Co-evolution of cytochrome c6 and plastocyanin, mobile proteins transferring electrons from cytochrome b6f to photosystem I. *JBIC Journal of Biological Inorganic Chemistry* **2**, 11-22 (1997).
4. P. Joliot, A. Joliot, G. Johnson, in *Photosystem I*. (Springer, 2006), pp. 639-656.
5. E. J. Boekema *et al.*, Evidence for a trimeric organization of the photosystem I complex from the thermophilic cyanobacterium *Synechococcus* sp. *FEBS Letters* **217**, 283-286 (1987).
6. V. V. Shubin, I. N. Bezsmertnaya, N. V. Karapetyan, Isolation from Spirulina Membranes of 2 Photosystem I-Type Complexes, One of Which Contains Chlorophyll Responsible for the 77-K Fluorescence Band at 760 Nm. *Febs Letters* **309**, 340-342 (1992).
7. V. Shubin, V. Tsuprun, I. Bezsmertnaya, N. Karapetyan, Trimeric forms of the photosystem I reaction center complex pre-exist in the membranes of the cyanobacterium Spirulina platensis. *FEBS letters* **334**, 79-82 (1993).
8. J. Kruip, E. J. Boekema, D. Bald, A. F. Boonstra, M. Rogner, Isolation and Structural Characterization of Monomeric and Trimeric Photosystem I Complexes ($P700.F_A/F_B$ and $P700.F_X$) from the Cyanobacterium Synechocystis PCC 6803. *Journal of Biological Chemistry* **268**, 23353-23360 (1993).
9. J. Kruip, D. Bald, E. Boekema, M. Rögner, Evidence for the existence of trimeric and monomeric Photosystem I complexes in thylakoid membranes from cyanobacteria. *Photosynthesis Research* **40**, 279-286 (1994).
10. J. Kruip, P. R. Chitnis, B. Lagoutte, M. Rogner, E. J. Boekema, Structural organization of the major subunits in cyanobacterial photosystem 1. Localization of subunits PsaC, -D, -E, -F, and -J. *J Biol Chem* **272**, 17061-17069 (1997).
11. G. Tsiotis, W. Haase, A. Engel, H. Michel, Isolation and structural characterization of trimeric cyanobacterial photosystem I complex with the help of recombinant antibody fragments. *European Journal of Biochemistry* **231**, 823-830 (1995).
12. L. Garczarek, G. W. M. van der Staay, J. C. Thomas, F. Partensky, Isolation and characterization of Photosystem I from two strains of the marine oxychlorobacterium *Prochlorococcus*. *Photosynthesis Research* **56**, 131-141 (1998).
13. T. S. Bibby, I. Mary, J. Nield, F. Partensky, J. Barber, Low-light-adapted *Prochlorococcus* species possess specific antennae for each photosystem. *Nature* **424**, 1051-1054 (2003).
14. E. J. Boekema *et al.*, A giant chlorophyll-protein complex induced by iron defciency in cyanobacteria. *Nature* **412**, 745-748 (2001).

15. D. L. Tucker, L. A. Sherman, Analysis of chlorophyll–protein complexes from the cyanobacterium *Cyanothece* sp. ATCC 51142 by non-denaturing gel electrophoresis. *Biochimica et Biophysica Acta (BBA) - Biomembranes* **1468**, 150-160 (2000).
16. D. Mangels *et al.*, Photosystem I from the unusual cyanobacterium *Gloeobacter violaceus*. *Photosynthesis Research* **72**, 307-319 (2002).
17. O. Almog, G. Shoham, D. Michaeli, R. Nechushtai, Monomeric and trimeric forms of photosystem I reaction center of *Mastigocladus laminosus*: crystallization and preliminary characterization. *Proc Natl Acad Sci U S A* **88**, 5312-5316 (1991).
18. P. Jordan *et al.*, Three-dimensional structure of cyanobacterial photosystem I at 2.5 A resolution. *Nature* **411**, 909-917 (2001).
19. M. Watanabe, H. Kubota, H. Wada, R. Narikawa, M. Ikeuchi, Novel supercomplex organization of photosystem I in *Anabaena* and *Cyanophora paradoxa*. *Plant and Cell Physiology* **52**, 162-168 (2011).
20. M. Watanabe *et al.*, Attachment of phycobilisomes in an antenna-photosystem I supercomplex of cyanobacteria. *Proc Natl Acad Sci U S A* **111**, 2512-2517 (2014).
21. M. Li, D. A. Semchonok, E. J. Boekema, B. D. Bruce, Characterization and evolution of tetrameric photosystem I from the thermophilic cyanobacterium Chroococcidiopsis sp TS-821. *Plant Cell* **26**, 1230-1245 (2014).
22. V. P. Chitnis *et al.*, Targeted inactivation of the gene psaL encoding a subunit of photosystem I of the cyanobacterium Synechocystis sp. PCC 6803. *Journal of Biological Chemistry* **268**, 11678-11684 (1993).
23. V. P. Chitnis, P. R. Chitnis, PsaI Subunit Is Required for the Formation of Photosystem-I Trimers in the Cyanobacterium Synechocystis Sp Pcc-6803. *Febs Letters* **336**, 330-334 (1993).
24. Q. Xu *et al.*, Mutational Analysis of Photosystem I Polypeptides in the Cyanobacterium Synechocystis sp. PCC 6803. TARGETED INACTIVATION OF psaI REVEALS THE FUNCTION OF PsaI IN THE STRUCTURAL ORGANIZATION OF PsaL. *Journal of Biological Chemistry* **270**, 16243-16250 (1995).
25. W. M. Schluchter, G. H. Shen, J. D. Zhao, D. A. Bryant, Characterization of *psaI* and *psaL* mutants of *Synechococcus* sp. strain PCC 7002: A new model for state transitions in cyanobacteria. *Photochem Photobiol* **64**, 53-66 (1996).
26. C. L. Aspinwall, M. Sarcina, C. W. Mullineaux, Phycobilisome mobility in the cyanobacterium *Synechococcus* sp. PCC7942 is influenced by the trimerisation of Photosystem I. *Photosynthesis Research* **79**, 179-187 (2004).
27. S. Naithani, J. M. Hou, P. R. Chitnis, Targeted inactivation of the psaK1, psaK2 and psaM genes encoding subunits of Photosystem I in the cyanobacterium Synechocystis sp. PCC 6803. *Photosynth Res* **63**, 225-236 (2000).

28. H. Tang, P. R. Chitnis, Addition of C-terminal histidyl tags to PsaL and PsaK1 proteins of cyanobacterial photosystem I. *Indian journal of biochemistry & biophysics* **37**, 433-440 (2000).
29. I. Domonkos *et al.*, Phosphatidylglycerol is essential for oligomerization of photosystem I reaction center. *Plant Physiol* **134**, 1471-1478 (2004).
30. Q. Wang, C. L. Hall, M. Z. Al-Adami, Q. He, IsiA Is Required for the Formation of Photosystem I Supercomplexes and for Efficient State Transition in <italic>Synechocystis</italic> PCC 6803. *PLoS ONE* **5**, e10432 (2010).
31. A. G. Ivanov *et al.*, Iron deficiency in cyanobacteria causes monomerization of photosystem I trimers and reduces the capacity for state transitions and the effective absorption cross section of photosystem I in vivo. *Plant Physiol* **141**, 1436-1445 (2006).
32. N. Yeremenko *et al.*, Supramolecular organization and dual function of the IsiA chlorophyll-binding protein in cyanobacteria. *Biochemistry* **43**, 10308-10313 (2004).
33. Q. Wang *et al.*, The high light-inducible polypeptides stabilize trimeric photosystem I complex under high light conditions in Synechocystis PCC 6803. *Plant Physiol* **147**, 1239-1250 (2008).
34. F. Gan *et al.*, Extensive remodeling of a cyanobacterial photosynthetic apparatus in far-red light. *Science* **345**, 1312-1317 (2014).
35. S. Kobayashi, M. Tsuzuki, N. Sato, Sulfite-stress induced functional and structural changes in the complexes of photosystems I and II in a cyanobacterium, Synechococcus elongatus PCC 7942. *Plant & cell physiology*, (2015).
36. K. Klodawska *et al.*, Elevated Growth Temperature Can Enhance Photosystem I Trimer Formation and Affects Xanthophyll Biosynthesis in Cyanobacterium Synechocystis sp PCC6803 Cells. *Plant and Cell Physiology* **56**, 558-571 (2015).
37. Z. Gardian *et al.*, Organisation of Photosystem I and Photosystem II in red alga Cyanidium caldarium: Encounter of cyanobacterial and higher plant concepts. *Biochimica et Biophysica Acta (BBA) - Bioenergetics* **1767**, 725-731 (2007).
38. T. Veith, C. Buchel, The monomeric photosystem I-complex of the diatom *Phaeodactylum tricornutum* binds specific fucoxanthin chlorophyll proteins (FCPs) as light-harvesting complexes. *Biochimica et biophysica acta* **1767**, 1428-1435 (2007).
39. A. Ben-Shem, F. Frolow, N. Nelson, Crystal structure of plant photosystem I. *Nature* **426**, 630-635 (2003).
40. R. Kouril, N. van Oosterwijk, A. E. Yakushevska, E. J. Boekema, Photosystem I: a search for green plant trimers. *Photochemical & Photobiological Sciences* **4**, 1091-1094 (2005).
41. Y. Mazor, A. Borovikova, N. Nelson, The structure of plant photosystem I super-complex at 2.8 A resolution. *Elife* **4**, e07433 (2015).

42. A. Amunts, H. Toporik, A. Borovikova, N. Nelson, Structure Determination and Improved Model of Plant Photosystem I. *Journal of Biological Chemistry* **285**, 3478-3486 (2010).
43. A. Amunts, O. Drory, N. Nelson, The structure of a plant photosystem I supercomplex at 3.4 A resolution. *Nature* **447**, 58-63 (2007).
44. X. C. Qin, M. Suga, T. Y. Kuang, J. R. Shen, Structural basis for energy transfer pathways in the plant PSI-LHCI supercomplex. *Science* **348**, 989-995 (2015).
45. A. Ben-Shem, F. Frolow, N. Nelson, Evolution of photosystem I - from symmetry through pseudosymmetry to asymmetry. *FEBS Letters* **564**, 274-280 (2004).
46. N. Nelson, A. Ben-Shem, The structure of photosystem I and evolution of photosynthesis. *Bioessays* **27**, 914-922 (2005).
47. A. Amunts, N. Nelson, Functional organization of a plant Photosystem I: Evolution of a highly efficient photochemical machine. *Plant Physiology and Biochemistry* **46**, 228-237 (2008).
48. A. Amunts, N. Nelson, Plant Photosystem I Design in the Light of Evolution. *Structure (London, England : 1993)* **17**, 637-650 (2009).
49. T. Cardona *et al.*, Electron transfer protein complexes in the thylakoid membranes of heterocysts from the cyanobacterium Nostoc punctiforme. *Bba-Bioenergetics* **1787**, 252-263 (2009).
50. D. A. Semchonok, M. Li, B. D. Bruce, G. T. Oostergetel, E. J. Boekema, Cryo-EM structure of a tetrameric cyanobacterial photosystem I complex reveals novel subunit interactions. *Biochimica et biophysica acta* **1857**, 1619-1626 (2016).
51. T. S. Bibby, J. Nield, J. Barber, Iron deficiency induces the formation of an antenna ring around trimeric photosystem I in cyanobacteria. *Nature* **412**, 743-745 (2001).
52. J. Vinnemeier, A. Kunert, M. Hagemann, Transcriptional analysis of the isiAB operon in salt-stressed cells of the cyanobacterium Synechocystis sp. PCC 6803. *FEMS Microbiol Lett* **169**, 323-330 (1998).
53. A. K. Singh, H. Li, L. A. Sherman, Microarray analysis and redox control of gene expression in the cyanobacterium Synechocystis sp. PCC 6803. *Physiol Plant* **120**, 27-35 (2004).
54. I. J. Iwuchukwu *et al.*, Self-organized photosynthetic nanoparticle for cell-free hydrogen production. *Nat Nano* **5**, 73-79 (2010).
55. D. R. Baker *et al.*, Comparative Photoactivity and Stability of Isolated Cyanobacterial Monomeric and Trimeric Photosystem I. *J Phys Chem B*, (2014).
56. G. Shen, F. Gan, D. A. Bryant, The siderophilic cyanobacterium Leptolyngbya sp. strain JSC-1 acclimates to iron starvation by expressing multiple isiA-family genes. *Photosynth Res* **128**, 325-340 (2016).
57. R. Kouril *et al.*, Supercomplexes of IsiA and photosystem I in a mutant lacking subunit PsaL. *Biochimica et biophysica acta* **1706**, 262-266 (2005).

58. R. Kouril *et al.*, Photosystem I trimers from Synechocystis PCC 6803 lacking the PsaF and PsaJ subunits bind an IsiA ring of 17 units. *Biochimica et biophysica acta* **1607**, 1-4 (2003).
59. M. Havaux *et al.*, The chlorophyll-binding protein IsiA is inducible by high light and protects the cyanobacterium Synechocystis PCC6803 from photooxidative stress. *Febs Letters* **579**, 2289-2293 (2005).
60. W. Wang *et al.*, Identification of important regions for ethylene binding and signaling in the transmembrane domain of the ETR1 ethylene receptor of Arabidopsis. *Plant Cell* **18**, 3429-3442 (2006).
61. R. Rippka, J. Deruelles, J. B. Waterbury, M. Herdman, R. Y. Stanier, Generic Assignments, Strain Histories and Properties of Pure Cultures of Cyanobacteria. *J Gen Microbiol* **111**, 1-61 (1979).
62. R. Rippka, Isolation and purification of cyanobacteria. *Methods Enzymol* **167**, 3-27 (1988).
63. K. Bodas, C. Brennig, K. R. Diller, J. J. Brand, Cryopreservation of Blue-Green and Eukaryotic Algae in the Culture Collection at the University-of-Texas at Austin. *Cryo-Lett* **16**, 267-274 (1995).
64. M. Watanabe, M. Iwai, R. Narikawa, M. Ikeuchi, Is the photosystem II complex a monomer or a dimer? *Plant and Cell Physiology* **50**, 1674-1680 (2009).
65. T. Iwamura, H. Nagai, S.-E. Ichimura, Improved Methods for Determining Contents of Chlorophyll, Protein, Ribonucleic Acid, and Deoxyribonucleic Acid in Planktonic Populations. *Internationale Revue der gesamten Hydrobiologie und Hydrographie* **55**, 131-147 (1970).
66. H. Schägger, G. von Jagow, Blue native electrophoresis for isolation of membrane protein complexes in enzymatically active form. *Analytical Biochemistry* **199**, 223-231 (1991).
67. I. Wittig, H.-P. Braun, H. Schagger, Blue native PAGE. *Nat. Protocols* **1**, 418-428 (2006).
68. H. Schagger, Tricine-SDS-PAGE. *Nat. Protocols* **1**, 16-22 (2006).
69. M. V. Nesterenko, M. Tilley, S. J. Upton, A simple modification of Blum's silver stain method allows for 30 minite detection of proteins in polyacrylamide gels. *Journal of Biochemical and Biophysical Methods* **28**, 239-242 (1994).
70. E. El-Mohsnawy *et al.*, Structure and function of intact photosystem 1 monomers from the cyanobacterium Thermosynechococcus elongatus. *Biochemistry* **49**, 4740-4751 (2010).
71. G. T. Oostergetel, W. Keegstra, A. Brisson, Automation of specimen selection and data acquisition for protein electron crystallography. *Ultramicroscopy* **74**, 47-59 (1998).
72. E. J. Boekema, H. Van Roon, J. F. Van Breemen, J. P. Dekker, Supramolecular organization of photosystem II and its light-harvesting antenna in partially solubilized photosystem II membranes. *Eur J Biochem* **266**, 444-452 (1999).
73. R. Kouril, E. Wientjes, J. B. Bultema, R. Croce, E. J. Boekema, High-light vs. low-light: effect of light acclimation on photosystem II composition and

organization in Arabidopsis thaliana. *Biochimica et biophysica acta* **1827**, 411-419 (2013).
74. S. J. Toth, J. T. Madden, L. S. Taylor, P. Marsac, G. J. Simpson, Selective imaging of active pharmaceutical ingredients in powdered blends with common excipients utilizing two-photon excited ultraviolet-fluorescence and ultraviolet-second order nonlinear optical imaging of chiral crystals. *Anal Chem* **84**, 5869-5875 (2012).
75. A. S. Kolaskar, P. C. Tongaonkar, A semi-empirical method for prediction of antigenic determinants on protein antigens. *FEBS Lett* **276**, 172-174 (1990).
76. S. Saha, G. P. S. Raghava, Prediction of continuous B-cell epitopes in an antigen using recurrent neural network. *Proteins* **65**, 40-48 (2006).
77. D. Billi, M. Grilli Caiola, L. Paolozzi, P. Ghelardini, A Method for DNA Extraction from the Desert Cyanobacterium Chroococcidiopsis and Its Application to Identification of ftsZ. *Applied and Environmental Microbiology* **64**, 4053-4056 (1998).
78. D. Fewer, T. Friedl, B. Büdel, Chroococcidiopsis and Heterocyst-Differentiating Cyanobacteria Are Each Other's Closest Living Relatives. *Molecular Phylogenetics and Evolution* **23**, 82-90 (2002).
79. J. T. Simpson *et al.*, ABySS: a parallel assembler for short read sequence data. *Genome Res* **19**, 1117-1123 (2009).
80. A. Bankevich *et al.*, SPAdes: a new genome assembly algorithm and its applications to single-cell sequencing. *J Comput Biol* **19**, 455-477 (2012).
81. D. Coil, G. Jospin, A. E. Darling, A5-miseq: an updated pipeline to assemble microbial genomes from Illumina MiSeq data. *Bioinformatics* **31**, 587-589 (2015).
82. A. Gurevich, V. Saveliev, N. Vyahhi, G. Tesler, QUAST: quality assessment tool for genome assemblies. *Bioinformatics* **29**, 1072-1075 (2013).
83. A. R. Wattam *et al.*, PATRIC, the bacterial bioinformatics database and analysis resource. *Nucleic Acids Res* **42**, D581-591 (2014).
84. R. Overbeek *et al.*, The SEED and the Rapid Annotation of microbial genomes using Subsystems Technology (RAST). *Nucleic Acids Research* **42**, D206-D214 (2014).
85. K. Tamura *et al.*, MEGA5: Molecular Evolutionary Genetics Analysis Using Maximum Likelihood, Evolutionary Distance, and Maximum Parsimony Methods. *Molecular Biology and Evolution* **28**, 2731-2739 (2011).
86. C. Notredame, D. G. Higgins, J. Heringa, T-coffee: a novel method for fast and accurate multiple sequence alignment. *Journal of Molecular Biology* **302**, 205-217 (2000).
87. K. Onai, M. Morishita, T. Kaneko, S. Tabata, M. Ishiura, Natural transformation of the thermophilic cyanobacterium Thermosynechococcus elongatus BP-1: a simple and efficient method for gene transfer. *Mol Genet Genomics* **271**, 50-59 (2004).

88. X. Zang, B. Liu, S. Liu, K. K. Arunakumara, X. Zhang, Optimum conditions for transformation of Synechocystis sp. PCC 6803. *J Microbiol* **45**, 241-245 (2007).
89. W. O. Ng, R. Zentella, Y. Wang, J. S. Taylor, H. B. Pakrasi, PhrA, the major photoreactivating factor in the cyanobacterium Synechocystis sp. strain PCC 6803 codes for a cyclobutane-pyrimidine-dimer-specific DNA photolyase. *Arch Microbiol* **173**, 412-417 (2000).
90. N. Nelson, C. F. Yocum, Structure and function of photosystems I and II. *Annual review of plant biology* **57**, 521-565 (2006).
91. M. Brecht, M. Hussels, E. Schlodder, N. V. Karapetyan, Red antenna states of Photosystem I trimers from *Arthrospira platensis* revealed by single-molecule spectroscopy. *Bba-Bioenergetics* **1817**, 445-452 (2012).
92. J. Heinemeyer, H. Eubel, D. Wehmhöner, L. Jänsch, H.-P. Braun, Proteomic approach to characterize the supramolecular organization of photosystems in higher plants. *Phytochemistry* **65**, 1683-1692 (2004).
93. A. Kitmitto, A. O. Mustafa, A. Holzenburg, R. C. Ford, Three-dimensional structure of higher plant photosystem I determined by electron crystallography. *J Biol Chem* **273**, 29592-29599 (1998).
94. N. R. Hayashi *et al.*, Isolation and cultivation of thermophilic cyanobacteria from hot springs of northern thailand. *Journal of Fermentation and Bioengineering* **78**, 179-181 (1994).
95. J. B. Waterbury, R. Y. Stanier, Patterns of growth and development in pleurocapsalean cyanobacteria. *Microbiological reviews* **42**, 2-44 (1978).
96. T. Ishida *et al.*, Growth Characteristics and Dense Culture of a Thermophilic Cyanobacterium, Chroococcidiopsis sp. Strain TS-821. *Journal of Fermentation and Bioengineering* **83**, 571-576 (1997).
97. A. Mershin *et al.*, Self-assembled photosystem-I biophotovoltaics on nanostructured TiO_2 and ZnO. *Scientific reports* **2**, 234 (2012).
98. D. Mukherjee, M. Vaughn, B. Khomami, B. D. Bruce, Modulation of cyanobacterial photosystem I deposition properties on alkanethiolate Au substrate by various experimental conditions. *Colloids and Surfaces B: Biointerfaces* **88**, 181-190 (2011).
99. G. LeBlanc, G. Chen, G. K. Jennings, D. E. Cliffel, Photoreduction of Catalytic Platinum Particles Using Immobilized Multilayers of Photosystem I. *Langmuir* **28**, 7952-7956 (2012).
100. Y. Umena, K. Kawakami, J.-R. Shen, N. Kamiya, Crystal structure of oxygen-evolving photosystem II at a resolution of 1.9 A. *Nature* **473**, 55-60 (2011).
101. N. V. Karapetyan, D. Dorra, G. Schweitzer, I. N. Bezsmertnaya, A. R. Holzwarth, Fluorescence spectroscopy of the longwave chlorophylls in trimeric and monomeric photosystem I core complexes from the cyanobacterium Spirulina platensis. *Biochemistry* **36**, 13830-13837 (1997).
102. R. Kouřil *et al.*, Photosystem I trimers from Synechocystis PCC 6803 lacking the PsaF and PsaJ subunits bind an IsiA ring of 17 units. *Biochimica et Biophysica Acta (BBA) - Bioenergetics* **1607**, 1-4 (2003).

103. R. Kouřil *et al.*, Supercomplexes of IsiA and Photosystem I in a mutant lacking subunit PsaL. *Biochimica et Biophysica Acta (BBA) - Bioenergetics* **1706**, 262-266 (2005).
104. R. Kouřil *et al.*, Structure and functional role of supercomplexes of IsiA and Photosystem I in cyanobacterial photosynthesis. *FEBS Letters* **579**, 3253-3257 (2005).
105. J. A. Ihalainen *et al.*, Aggregates of the Chlorophyll-Binding Protein IsiA (CP43‘) Dissipate Energy in Cyanobacteria. *Biochemistry* **44**, 10846-10853 (2005).
106. P. Kiley *et al.*, Self-Assembling Peptide Detergents Stabilize Isolated Photosystem Ion a Dry Surface for an Extended Time. *PLoS Biol* **3**, e230 (2005).
107. B. Gobets *et al.*, Time-resolved fluorescence emission measurements of photosystem I particles of various cyanobacteria: A unified compartmental model. *Biophys J* **81**, 407-424 (2001).
108. E. Schlodder, M. Hussels, M. Cetin, N. V. Karapetyan, M. Brecht, Fluorescence of the various red antenna states in photosystem I complexes from cyanobacteria is affected differently by the redox state of P700. *Bba-Bioenergetics* **1807**, 1423-1431 (2011).
109. W. Xu, H. D. Tang, Y. C. Wang, P. R. Chitnis, Proteins of the cyanobacterial photosystem I. *Bba-Bioenergetics* **1507**, 32-40 (2001).
110. J. Mareš *et al.*, The Primitive Thylakoid-Less Cyanobacterium Gloeobacter Is a Common Rock-Dwelling Organism. *PLoS ONE* **8**, e66323 (2013).
111. P. J. Keeling, Diversity and evolutionary history of plastids and their hosts. *Am J Bot* **91**, 1481-1493 (2004).
112. O. Deusch *et al.*, Genes of cyanobacterial origin in plant nuclear genomes point to a heterocyst-forming plastid ancestor. *Mol Biol Evol* **25**, 748-761 (2008).
113. L. I. Falcon, S. Magallon, A. Castillo, Dating the cyanobacterial ancestor of the chloroplast. *ISME J* **4**, 777-783 (2010).
114. A. Criscuolo, S. Gribaldo, Large-Scale Phylogenomic Analyses Indicate a Deep Origin of Primary Plastids within Cyanobacteria. *Molecular Biology and Evolution* **28**, 3019-3032 (2011).
115. R. S. Gupta, Protein signatures (molecular synapomorphies) that are distinctive characteristics of the major cyanobacterial clades. *International Journal of Systematic and Evolutionary Microbiology* **59**, 2510-2526 (2009).
116. R. Kern, H. Bauwe, M. Hagemann, Evolution of enzymes involved in the photorespiratory 2-phosphoglycolate cycle from cyanobacteria via algae toward plants. *Photosynthesis Research* **109**, 103-114 (2011).
117. C. Hackenberg *et al.*, Cyanobacterial lactate oxidases serve as essential partners in N_2 fixation and evolved into photorespiratory glycolate oxidases in plants. *Plant Cell* **23**, 2978-2990 (2011).
118. P. M. Shih *et al.*, Improving the coverage of the cyanobacterial phylum using diversity-driven genome sequencing. *Proceedings of the National Academy of Sciences* **110**, 1053-1058 (2013).

119. S. Daddy *et al.*, A novel high light-inducible carotenoid-binding protein complex in the thylakoid membranes of Synechocystis PCC 6803. *Scientific reports* **5**, 9480 (2015).
120. I. Grotjohann, P. Fromme, Structure of cyanobacterial photosystem I. *Photosynth Res* **85**, 51-72 (2005).
121. C. Lunde, P. E. Jensen, A. Haldrup, J. Knoetzel, H. V. Scheller, The PSI-H subunit of photosystem I is essential for state transitions in plant photosynthesis. *Nature* **408**, 613-615 (2000).
122. J. Lehtimaki *et al.*, Characterization of Nodularia strains, cyanobacteria from brackish waters, by genotypic and phenotypic methods. *Int J Syst Evol Microbiol* **50 Pt 3**, 1043-1053 (2000).
123. T. Dagan *et al.*, Genomes of Stigonematalean cyanobacteria (subsection V) and the evolution of oxygenic photosynthesis from prokaryotes to plastids. *Genome Biol Evol* **5**, 31-44 (2013).
124. V. R. Flechtner, S. L. Boyer, J. R. Johansen, M. L. DeNoble, Spirirestis rafaelensis gen. et sp nov (Cyanophyceae), a new cyanobacterial genus from arid soils. *Nova Hedwigia* **74**, 1-24 (2002).
125. L. B. Wiltbank, D. M. Kehoe, Two Cyanobacterial Photoreceptors Regulate Photosynthetic Light Harvesting by Sensing Teal, Green, Yellow, and Red Light. *MBio* **7**, e02130-02115 (2016).
126. R. N. Nordin, J. R. Stein, Taxonomic Revision of Nodularia (Cyanophyceae, Cyanobacteria). *Can J Bot* **58**, 1211-1224 (1980).
127. M. A. Vaccarino, J. R. Johansen, Scytonematopsis contorta sp nov (Nostocales), a new species from the Hawaiian islands. *Fottea* **11**, 149-161 (2011).
128. A. E. Kirkwood, J. A. Buchheim, M. A. Buchheim, W. J. Henley, Cyanobacterial Diversity and Halotolerance in a Variable Hypersaline Environment. *Microbial Ecology* **55**, 453-465 (2008).
129. L. K. Doerfel *et al.*, EF-P Is Essential for Rapid Synthesis of Proteins Containing Consecutive Proline Residues. *Science* **339**, 85-88 (2013).
130. M. Chen, T. S. Bibby, J. Nield, A. W. Larkum, J. Barber, Structure of a large photosystem II supercomplex from Acaryochloris marina. *FEBS Lett* **579**, 1306-1310 (2005).
131. D. C. Price *et al.*, Cyanophora paradoxa genome elucidates origin of photosynthesis in algae and plants. *Science* **335**, 843-847 (2012).

Vita

Meng Li was born in a rural area by Dongting Lake in Hunan Province, China. With parents' support and encouragement, he went to one of the best high schools in his area, Changde No. 1 High School. In his high school biology class, he learned and was fascinated by the fact that biologists can manipulate microbes and get the desired products. As a result, Meng went to college at China Agricultural University where he majored in biological sciences. In college, he was impressed by a description, "cyanobacteria can emit hydrogen gas under anaerobic conditions", from the Plant Sciences textbook. This single piece of information helped Meng in making the decision regarding the direction of his graduate study. In his senior year, he looked around to see who was studying hydrogen production using cyanobacteria. Coincidently, Dr. Barry D. Bruce, his PhD mentor, published a paper in *Nature Nanotechnology* about the hydrogen production using cell free system that year. Meng contacted Dr. Bruce from China for the access to the full text of that publication and Dr. Bruce encouraged him to apply to University of Tennessee. In Fall 2010, Meng started his graduate career in BCMB department. He joined Bruce lab in Summer 2011 after his rotation and around the same time was enrolled in additional curriculum to earn a concentration in Energy Science and Engineering at the Bredesen Center for Interdisciplinary Research and Graduate Education. In Bruce lab, he worked on the novel tetrameric PSI complex in cyanobacteria.